ANALYTICA CHIMICA ACTA

International monthly devoted to all branches of analytical chemistry
Revue mensuelle internationale consacrée à tous les domaines de la chimie analytique
Internationale Monatsschrift für alle Gebiete der analytischen Chemie

ELSEVIER SCIENTIFIC PUBLISHING COMPANY

AMSTERDAM

Anal. Chim. Acta, Vol. 81, No. 2, 231–450, February 1976

Published monthly

Completing Volume 81

ANALYTICA CHIMICA ACTA

Publication Schedule for 1976

Vol. 81, No. 1	January 1976	
Vol. 81, No. 2	February 1976	**(completing Vol. 81)**
Vol. 82, No. 1	March 1976	
Vol. 82, No. 2	April 1976	**(completing Vol. 82)**
Vol. 83	May 1976	**(complete in one issue)**
Vol. 84, No. 1	June 1976	
Vol. 84, No. 2	July 1976	**(completing Vol. 84)**
Vol. 85, No. 1	August 1976	
Vol. 85, No. 2	September 1976	**(completing Vol. 85)**
Vol. 86	October 1976	**(complete in one issue)**
Vol. 87, No. 1	November 1976	
Vol. 87, No. 2	December 1976	**(completing Vol. 87)**

Subscription price for 1976 (covering November '75/December '76, Vols. 80–87): Dfl. 840.00 plus Dfl. 96.00 postage. Subscribers in the U.S.A. and Canada receive their copies by airmail. Additional charges for airmail to other countries are available on request. For advertising rates apply to the publishers.

Subscriptions should be sent to:
Elsevier Scientific Publishing Company, P.O. Box 211, Amsterdam, The Netherlands.

GENERAL INFORMATION

Languages

Papers will be published in English, French or German.

Detailed information

Authors should consult Vol. 73, p. 435 for detailed instructions. Reprints of this information are obtainable from Dr. Macdonald or from: Elsevier Editorial Services Ltd., Mayfield House, 256 Banbury Road, Oxford (Great Britain).

Submission of papers

Papers should be sent to:

Prof. Philip W. West,
Coates Chemical Laboratories,
College of Chemistry and Physics,
Louisiana State University,
Baton Rouge 3,
La. 70803 (U.S.A.)

or to:

Dr. A.M.G. Macdonald,
Department of Chemistry,
The University,
P.O. Box 363
Birmingham B15 2TT (Great Britain)

Reprints

Fifty reprints will be supplied free of charge. Additional reprints (minimum 100) can be ordered at quoted prices. They must be ordered on order forms which are sent together with the proofs.

Methods of Surface Analysis

edited by **A.W. CZANDERNA,** Professor of Physics, Department of Physics and Institute of Colloid and Surface Science, Clarkson College of Technology, Potsdam, N.Y., U.S.A.

METHODS AND PHENOMENA, Volume 1

1975. 496 pages. US $62.50/Dfl. 150.00. ISBN 0-444-41344-8

This book elucidates the methods and procedures used to obtain the elemental composition of surfaces and of the underlying bulk and to identify species attached to a surface. The composition-in-depth profile, which depends on using ion etching with surface analysis, is also treated.
First, the effect of sputtering on the results obtained by the most widely used methods of surface analysis is considered. Then an overview is presented of the strengths and weaknesses of the various methods as related to the multiplicity of important parameters such as the influence of the sample on the results, detection sensitivity, resolution, matrix effects, signal to noise, time to obtain the data, the potential for quantitative analysis, etc. The following chapters present details on ion scattering (ISS), X-ray photoelectron spectroscopy (ESCA), Auger spectroscopy (AES), secondary ion mass spectrometry (SIMS), AES combined with SIMS, the atom probe field ion microscope, field ionization mass spectrometry and infrared reflection-absorption spectroscopy. Although the emphasis is on experimental methods and procedures, a generous presentation of typical results and applications is also given.
The book not only provides an overview to prospective scientists and technologists who plan to use surface analytical techniques, but also presents refreshing ideas to active workers in the fields of physics, chemistry, materials, electronic devices, engineering science, catalysis and corrosion. The volume is particularly timely since instruments for SIMS, XPS, AES, ISS and the atom probe have become commercially available in recent years and the application of these methods is expanding rapidly.

ELSEVIER SCIENTIFIC PUBLISHING COMPANY

P.O. Box 211, Amsterdam, The Netherlands

Distributed in the U.S.A. and Canada by:
AMERICAN ELSEVIER PUBLISHING COMPANY, INC.,
52 Vanderbilt Ave., New York, N.Y. 10017

The Dutch guilder is definitive. US $ prices are subject to exchange rate fluctuations.

Analytica Chimica Acta, 81 (1976) 231—263

Review

METHODS FOR THE DETERMINATION OF WATER IN POLYMERS

JOHN MITCHELL, Jr.

Plastics Department, E. I. du Pont de Nemours & Co., Inc., Experimental Station, Wilmington, Delaware 19898 (U.S.A.)

(Received 9th June 1975)

SUMMARY

Water may be "weakly" or "strongly" bound to other substances by physical or chemical forces. Knowledge of the amount of water and the type of bonding in polymeric materials is very important in control of many polymerization processes and in the physical behavior of the polymer. Hundreds of methods have been proposed for the determination of water in concentrations ranging from p.p.b. to high percentages. Some are direct; others require preliminary concentration or chemical reaction. The most useful methods of analysis for water in polymers are based on chemical, spectroscopic, gravimetric, thermal, electrical, and physical techniques. Chemical methods are represented by Karl Fischer titration, acylation, and nitride reactions. Infrared, nuclear magnetic resonance, and mass spectrometry are the principal spectroscopic approaches. Other useful methods include direct weight loss, thermogravimetry, differential thermal analysis, thermal evolution analysis, dielectric constant, conductance, coulometry, chromatography, azeotropic distillation, piezoelectric, manometric, and volumetric procedures. Recent developments are described with emphasis on applications of these techniques.

Water is the most abundant substance on earth and in living matter, but often its remarkable properties tend to be overlooked. Water remains a liquid over a conveniently wide temperature range and is often referred to as the nearly universal solvent. Water is an "ionizing solvent," probably because of its high dielectric constant. Water can contribute to acid—base equilibria over a range of 16 pH units and participate in redox equilibria over a range in excess of 2 V. Its decrease in density on formation of ice is critical to maintenance of life in the seas. The water molecule contains two protons and two lone pairs of electrons which occupy nearly tetrahedrally-spaced, hybridized orbitals.

Water may exist in many forms, readily bonding with itself or other polar substance. In fact, each body of water can be described as a macromolecule or lattice having the structure $(H_2O)_n$. Pauling proposes that the structure of liquid water is similar to those of the gas hydrates consisting of a framework of ordered water. The framework may be considered from the basis of a pentagonal dodecahedron of 20 water molecules, each participating in three hydrogen bonds.

Spectroscopic data strongly suggest that the amount of nonhydrogen-

bonded water monomer in liquid water is less than 1 % between 0 °C and 100 °C. Also, some polymeric water exists in slightly polar organic solvents. However, in nonpolar materials such as hydrocarbons and halides, water is present as a monomer. In the presence of other species, water may be "weakly" or "strongly" bound as represented by loosely adsorbed water or constitutional water. Usually water held stoichiometrically in crystals is referred to as water of hydration. Water also may be associated in crystals in a nonstoichiometric manner as described by Barrer [1].

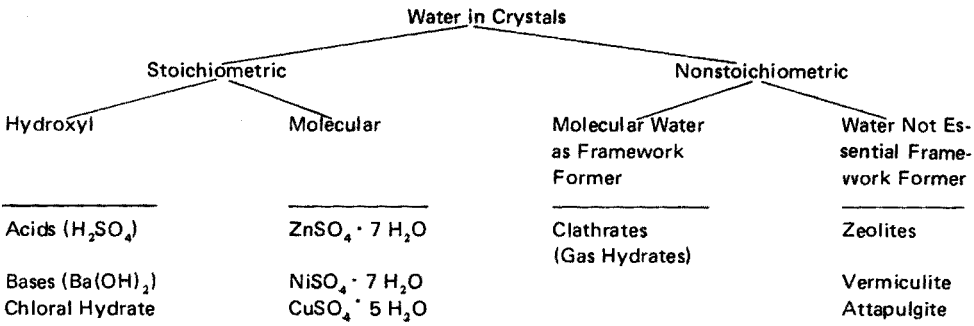

Bonding strengths vary considerably. Some hydrates are quite stable even at elevated temperatures, e.g., hydrated zinc and nickel sulfates become anhydrous only above 280 °C. Others effloresce in air, e.g., cyanuric acid dihydrate rather quickly becomes anhydrous in normal atmosphere. Water is sometimes so firmly combined that the hydrate is regarded as a primary valency compound, e.g., sulfuric acid which is the hydrate of sulfur trioxide, and barium hydroxide, the hydrate of barium oxide. In chloral hydrate the intramolecular bonding appears to be between hydroxyl hydrogens and chlorine atoms. For most analytical purposes the determination of water does not include hydroxyl water but rather molecular water as such. In crystals where water is held nonstoichiometrically, the water is often considered "bound" and is usually thought of as that which is occluded within a crystal lattice or cell.

The clathrate compounds are unusual in the way that water is held in their crystals; the "gas hydrates" offer examples. In these compounds the hydrate formers do not exceed one molecule per cavity and cannot escape without destruction of the cage.

Substances such as the crystalline zeolites represent quite a different type of structure in which the framework does not involve water. Molecules of water per intercrystalline cavity may exceed one. Spacings are sufficiently large for water to pass from one cavity to another, and water may leave the lattice without affecting the framework. The physical dimensions of the cavities and the windows between cages control the ease with which water can be removed from these materials. Crystalline zeolites can be used for drying and separations of gases and liquids, as well as for ion exchange. Numerous synthetic zeolites, e.g. aluminum silicates, which have controlled

cavity sizes and, thus, the ability to separate molecules by size, have been developed. Small molecules, such as water, are accommodated by these molecular sieves while larger molecules are excluded.

The structure of water adsorbed on any surface is probably different from that of bulk water. On glass water is adsorbed mainly as OH groups; three different states of OH-group bonding are known. On aluminas the amount of sorbed water is proportional to the surface area, corresponding to the binding of one molecule of water to 2 O atoms at the surface. Additional water is adsorbed on the monolayer by physical means. Bound water continues to be lost from γ-alumina even after heating to 1000 °C.

Infrared and thermogravimetric data distinguish between water of constitution and adsorbed water on silica gel. These results when combined with chemical methods for determining surface hydroxyl groups permit distinction between adsorbed water, inner hydroxyls and surface hydroxyls. Loss of water from silica gel may begin at temperatures as low as 50 °C, reaching a maximum rate of desorption at about 140 °C. Complete loss of water, however, requires temperatures above the critical temperature.

Water has marked effects on the physical behavior of many plastics; it may cause swelling, dissolve or leach certain additives, act as a plasticizer, or cause hydrolysis of some species. Braden [2] reported that the absorption and desorption of water by many plastics is a predictable diffusion process involving only a diffusion coefficient (D) and equilibrium uptake. He showed that during the initial stages of absorption, a simplified relationship may apply,

$$M_t/M_\infty = 2(Dt/\pi l^2)^{1/2}$$

where M_t is the mass absorbed after time t, M_∞ is the amount absorbed at equilibrium, and l is the thickness of the specimen. For a given plastic in the early stages of adsorption, D can be determined at constant temperature from a simple plot of M_t vs. $t^{1/2}$. Applicability was demonstrated for poly(methyl methacrylate) (PMMA), poly(vinyl chloride) (PVC), and polystyrene (PS). With these materials the sorption/desorption process is reproducible through successive cycles. This behavior indicates little or no structural change of the plastic during the process. However, polymers susceptible to hydrogen bonding do not show this reversible behavior.

Extensive reports on the physical behavior of water are available. Kirshenbaum [3] provided one of the more nearly complete listings of the physical constants of water. Structural features, chemical behavior, and many physical constants of water serve as the basis of analytical methods for its determination. The need for reliable qualitative and quantitative analytical methods for water touches on essentially all industrial process work involving synthetic and natural products, biochemical and biological investigations, and meteorology. Water enters directly or indirectly into most chemical reactions. In some media traces of water may have a primary effect on the nature or extent of reaction.

In response to the widespread need for reliable methods, a wide array of procedures is now available, covering the range from fractional parts-per-million to pure water. Some are applicable to many systems; others have limited applicability to specific substances or to certain types of bonding. In this review, discussion is limited to those techniques which have been of particular value in determining water in polymer systems. Included are gravimetric, separation and thermal procedures, spectrometric, electrical and physical measurements, as well as chemical reactions.

GRAVIMETRIC METHODS

Methods based on weight loss represent the oldest approaches for determining water in nonvolatile materials. Usually they are oven drying procedures in which (a) the weight loss is measured after the sample has been heated at atmospheric or reduced pressure, or (b) the weight of water released from the heated sample is measured after condensation or absorption by a desiccant. Thermogravimetric analysis and freeze-drying represent special approaches. The former permits heating under programmed temperature conditions and provides a means of distinguishing between free and bound water. The latter is particularly valuable for partial drying of biological specimens, foods and other thermally unstable materials. Various other gravimetric methods are now available for special systems. For example, an infrared heat source may reduce drying time on many materials.

Usually in conventional drying procedures the weighed sample is heated in an oven at atmospheric pressure; the total weight loss is taken as a measure of the water in the sample. Temperature and time of heating are usually established empirically, based on attainment of "constant" weight. Accuracy then depends on the requirements that (a) constant weight be due to complete removal of water and (b) total weight loss be due only to water. Where applicable, oven drying techniques can be very useful. However, in establishing conditions for meaningful analyses, many variables must be controlled. Movement of water from the sample will take place as long as the vapor pressure of water in the sample exceeds that of water in the surrounding environment. Thermodynamic, kinetic and operational factors associated with dehydration must be considered. Actually these factors apply to all methods for removing water thermally including absorption, desiccation and distillation as well as oven drying.

From physical considerations alone the removal of water is favored by high temperatures and indeed, all moisture would be removed at 365 °C, the critical temperature of water. However, with most organic materials at high temperatures complications arise from loss of volatiles other than water and from chemical reactions. (Vapor pressure data for water and several organic materials have been reported by Stull [4].)

For some materials, infrared lamps offer distinct advantages as sources of heat. About 15 % of the energy emitted by the infrared lamp at about

2000 K penetrates 2—3 mm below the surface of a water layer. This effect offers an increase in evaporating surface, since the radiation is directly absorbed into the sample. Heating of the surrounding air is not required as it is in conventional oven drying techniques. Forced ventilation in the infrared drier helps to keep water vapor at a low level. Zimmermann [5] designed a simple apparatus for drying dates and other foods. With the infrared drier there is no crust formation during drying.

Several devices have been proposed for special cases, including hinged electrically heated plates between which thin (ca. 2 mm) samples of paper or textiles are dried in a few minutes at 140—160 °C, or pressed pellets of cellulose are dried in 9 min at 195—210 °C. Heidbrink [6] briefly described a "Planwägeglas" for rapid determinations of water in a wide variety of emulsions, oils and other relatively nonvolatile liquids or pastes. The unit consists of two flat circular ground-glass plates, 6 cm in diameter; the top plate can be placed directly on the lower one or hung on a hook, providing separation between the plates. For analysis, 100—200 mg of sample is placed on the lower plate and the upper plate is used as a cover. After the sample weight has been determined, the plates are rubbed together to attain a thin evenly distributed film and the upper plate is moved to the hanging position. The complete unit is placed in an oven at 50—100 °C or in a vacuum desiccator over concentrated sulfuric acid. After drying is complete, usually within 20 min, the top plate is replaced on the lower one and the unit reweighed.

Application of oven drying methods to natural products is subject to significant errors from loss of volatile substances in addition to water. Such errors may be due to direct loss of other volatiles or to thermal degradation. The behavior of leather illustrates the latter source of error. Degradation of components from tanning material leads to evolution of carbon dioxide and water, as illustrated by oxidative decomposition of the pyrogallol group of tannins,

$$4\ C_6H_6O_3 + 3\ O_2 \rightarrow 2\ C_{11}H_8O_5 + 2\ CO_2 + 4\ H_2O$$

Kanagy and Charles [7] studied the effects of time and temperature on volatiles by absorbing water in magnesium perchlorate and carbon dioxide in Ascarite, their results on Chestnut-Tanned leather are shown in Fig. 1.

Schenker et al. [8] used a weight loss method for determining water and residual monomer in polycaprolactam. The sample is weighed into the sample tube, which is then connected to the apparatus as shown in Fig. 2; the pressure is reduced to < 20 mm Hg, and the block temperature is set at 200 ± 5 °C and bridge temperature at 225 ± 15 °C. At the end of a predetermined time, the condensate is dissolved in water and its volume adjusted to 5.00 ml. Measurement of refractive index of the diluted condensate is a measure of monomer content. Total weight loss corrected for monomer is calculated as water. Sixteen analyses each at two different volatiles levels gave standard deviations of 0.26 and 0.25 %, respectively, for

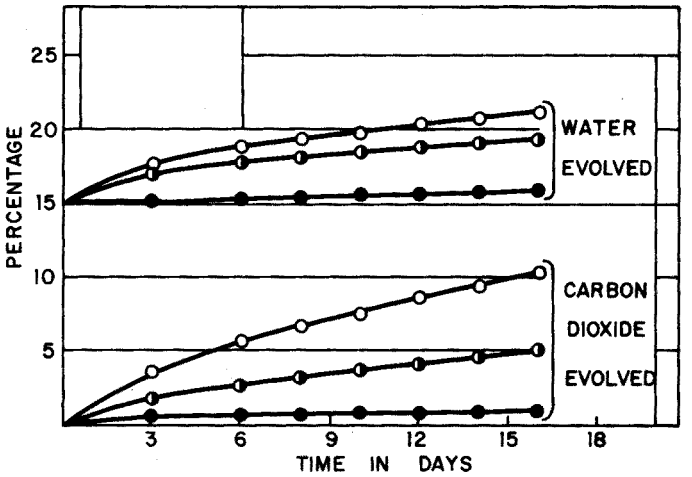

Fig. 1. Rates of evolution of CO_2 and H_2O from chestnut-tanned leather heated at 120 °C in (○) oxygen, (◑) air or (●) helium.

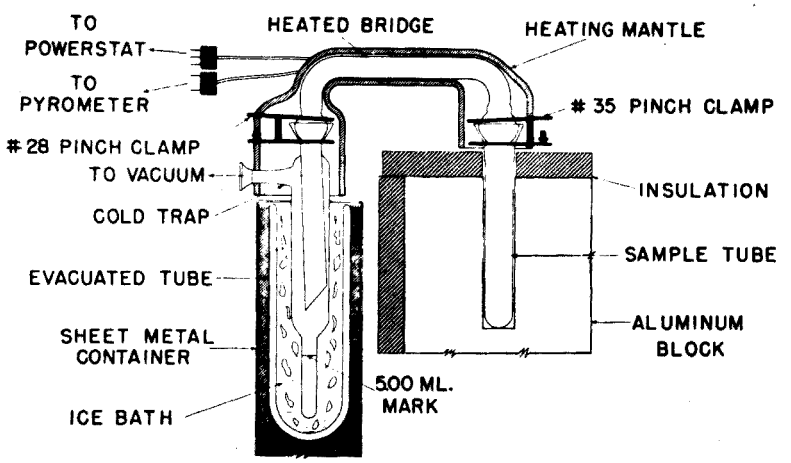

Fig. 2. Apparatus for moisture and monomer in polycaprolactam.

about 8 % monomer and 1.70 % moisture; at an average level of 0.53 % monomer and 0.47 % moisture, standard deviations were 0.03 and 0.06%, respectively. When only water content is desired, the condensate can be titrated with Karl Fischer reagent. Studies have been reported comparing vacuum oven methods with vacuum distillation to determine water in nylon 66 and nylon 6 moldings. For example, Mears and Palmer [9] heated a sample of molding at 105 °C and 3 torr, and reported that this method gave results close to the true values; but a determination took 2—3 months. For inspection purposes they proposed a distillation method.

Thermogravimetry

Thermogravimetric analysis (TGA) allows weight loss to be followed as functions of time and temperature. Ovens with built-in balances, of course, provide weight loss data as a function of time at constant temperature. Temperature programming and continuous recording of weight loss during drying and decomposition results in curves which often permit selective measurement of free and bound water; inflections in the curve represent changes in composition [10].

TGA, differential thermal analysis (DTA) and other thermal techniques usually can discriminate between "free" and "bound" water, and are particularly valuable for determining water of hydration. This is illustrated by observing the thermal behavior of pyromellitic acid dihydrate, a polymer intermediate. Chiu [11] reported on its behavior on heating from room temperature to several hundred degrees. Figure 3 provides TGA, DTA, differential thermogravimetry (DTG) and electrothermal analysis (ETA) on

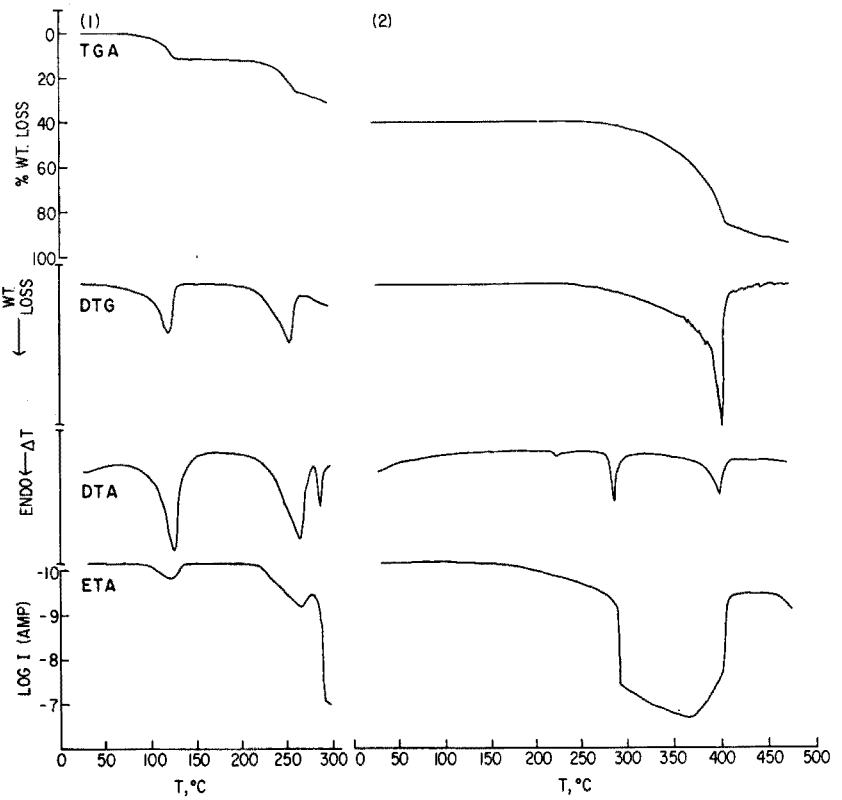

Fig. 3. Simultaneous TGA—DTG—DTA—ETA of pyromellitic acid (dihydrate). (1) Preliminary heating. (2) Reheating.

(1) preliminary heating to 300 °C and after cooling, reheating to 500 °C. The transitions are consistent with the sequence shown. On recycling the residue, now the anhydride, the dehydration steps are eliminated. A small DTA endotherm appears at about 225 °C, indicating a crystalline transition in the dianhydride. After melting at about 290 °C, the anhydride is almost completely volatilized near 400 °C, as shown by the final step of the weight loss curve, the sharp endotherm, and the rapid decrease in electrical conductivity.

SEPARATION METHODS

Distillation

With the exception of the older conventional oven drying procedures, the distillation method has been used more widely than any other technique for determining water. It has found extensive application in the food and petroleum industries for analyses of solids, greases, and other relatively non-volatile materials. Normally, these procedures depend on entrainment distillation with carriers in which water is only slightly soluble under normal conditions. In most cases hydrocarbons or organic halides are used which form minimum boiling azeotropes or which boil above 100 °C and, therefore, act as carriers for water during the distillation process. The sample is dispersed in a relatively large volume of the entraining agent, the temperature is raised to ebullition and the vapor is condensed into a graduated receiver. The condensate separates into two phases and the aqueous phase is measured volumetrically. Some widely used heterogeneous entraining agents are noted in Table 1.

Entrainment distillation offers a broadly applicable means for removing water from relatively nonvolatile substances. When it is used strictly as a separation step, many chemical and instrumental techniques become better suited than volumetric measurement to the determination of water. This approach usually permits the use of homogeneous azeotropes for separation. Typical binary and ternary systems are shown in Table 2; with these

TABLE 1

Heterogeneous entraining agents

Entrainer			Azeotrope with water	
Compound	b.p. (°C)	d	b.p. (°C)	% H_2O
Iso-octane	99.2	0.69	80	11
Benzene	80.2	0.88	69.25	8.8
Toluene	110.7	0.86	84.1	19.6
Carbon tetrachloride	76.75	1.59	66.0	4.1
Chlorobenzene	132.1	1.11	90.2	28.4

TABLE 2

(a) Homogeneous binary systems with water

Entrainer		Binary	
Compound	b.p. (°C)	b.p. (°C)	% H_2O
Ethanol	78.3	78.15	4.43
n-Propanol	97.2	87.72	28.31
1,4-Dioxan	101.32	87.82	18
Propionitrile	97.0	81.5	24
Pyridine	115.5	92.6	43

(b) Ternary azeotropes with water

Component A		Component B		Azeotrope	
	b.p. (°C)		b.p. (°C)	b.p. (°C)	Wt. % H_2O
Benzene	80.2	Ethanol	78.3	64.86	7.4
n-Heptane	98.4	Pyridine	115.5	78.6	14.0
Chloroform	61.2	Ethanol	78.3	55.4	3.5

compositions, there is little likelihood of hold-up of water as may be encountered in heterogeneous systems. Also, homogeneous azeotropes can be chosen with higher concentrations of water than heterogeneous carriers and also offer a wider choice of agents.

Volumetric determinations of water, with a heterogeneous entrainer, have been reported for a number of polymers containing several percent water, and particularly for natural textile fibers. However, a considerable improvement in the limit of detection and in selectivity can be achieved by chemical or spectroscopic analysis of a homogeneous distillate. The benzene—ethanol—water ternary mixture has been used to remove small quantities of water from GR-S rubber stock; water in the homogeneous condensate is determined by titration with Karl Fischer reagent. Several physical and chemical methods have been used in attempts to determine water in phenol—formaldehyde resols (phenol—alcohol intermediates formed initially during the alkali-catalyzed condensation of phenol with formaldehyde). Volatiles in addition to water are distilled with xylene or tetrachloroethane. The results are variable because of further condensation of the resol which polymerizes to a solid state, trapping part of the water. Distillation with isoamyl alcohol gives high results. Carriers such as xylene, toluene and benzene are unsatisfactory. To maintain a homogeneous solution during distillation, Bentz and Neville [12] used a mixture of 90 g of cinnamyl alcohol and 30 g of toluene for 30 g of resol. The aqueous layer contains, principally, water, formaldehyde, formic acid with small amounts of phenol, methanol and carrier. The water content, usually about 70 % of the aqueous layer, is determined by direct titration with Karl Fischer reagent.

Mears and Palmer [9] compared vacuum distillation at 1 torr at just below the melting points of nylon 66 and 6 with heating at 105 °C and 3 torr. They suggested that the former method is suitable for inspection purposes, particularly in the range 2—4 % water. However, White [13] preferred vacuum distillation at 1 torr at about 30 °C above the melting point of the polymer. They determined water from the weight loss or by Karl Fischer titration of the distillate.

Gas chromatography

Before the development of Porapak as a column packing, direct separation of water in organic systems usually was not very reliable, because of extensive tailing. Consequently, much of the early work on water determinations by g.c. was indirect. Prior selective chemical reaction was used and a volatile reaction product determined, e.g.

$$CaC_2 + 2\,H_2O \rightarrow HC \equiv CH + Ca(OH)_2$$

$$CaH_2 + 2\,H_2O \rightarrow 2\,H_2 + Ca(OH)_2$$

$$(CH_3O)_2C(CH_3)_2 + H_2O \rightarrow CH_3COCH_3 + 2\,CH_3OH$$

$$Pb(OOCCH_3)_4 + 2\,H_2O \rightarrow PbO_2 + 4\,CH_3COOH$$

These reactions usually are not stoichiometric, and require empirical calibration, on the system used in the actual analysis. In most cases involving solid samples, it is desirable to extract water into a suitable inert solvent. The applicability of the calcium carbide reaction in determinations of water in hydrocarbons was reported by Knight and Weiss [14] for benzene and butadiene.

For determining water in inert, noncondensable (at —78 °C) gases, Turkel'taub et al. [15] used calcium hydride as reagent, the hydrogen formed being determined by gas chromatography. The applicability of the technique is shown by the determination of residual water in nitrogen after passage through various drying agents (Table 3).

In another approach, Martin and Knevel [16] used the acid-catalyzed reaction between 2,2-dimethoxypropane and water to form acetone and methanol as the basis for a gas chromatographic method; the unreacted 2,2-dimethoxypropane serves as a convenient internal standard, and acetone as a measure of water. Mary [17] applied this method to natural products, after extraction of the water into dry methanol.

Direct separation of water has become increasingly reliable as improved liquid and solid column packing materials are developed. A major breakthrough was made on introduction of Porapak porous polymer beads. Hollis [18] reported that gas—solid chromatography over porous polyaromatic polymer beads is suitable for analysis of a variety of volatile materials. These interesting supports were derived from the porous polymer

TABLE 3

Residual water in nitrogen after drying

($CaH_2 + 2\ H_2O \rightarrow 2\ H_2 + Ca(OH)_2$)

Drying agent	Sample (ml)	Residual water ($mg\ l^{-1}$)
None	25	0.87
Silica gel (dried at 350 °C, 5 mm)	500, 500, 486	0.06, 0.04, 0.04
$Mg(ClO_4)_2$	470, 250, 450	0.08, 0.05, 0.06
Molecular sieve	500, 400, 400	0.054, 0.052, 0.046
P_2O_5	420, 360, 420	0.009, 0.001, 0.010
$Mg(ClO_4)_2 + P_2O_5$	660, 660, 660	0.005, 0.004, 0.008

beads developed for gel-permeation chromatography. For example, Hollis found that dried polymer beads of styrene and divinylbenzene retain their size and apparently much of their physical structure within the wet bead. The Porapak porous polymer beads represent a family of materials with a range of separation capabilities. Data on determinations of water in polymer systems with Porapak and other column packing materials are summarized in Table 4.

Slanski et al. [19] used Porapak Q in their gas-chromatographic procedure for determining water in plasticizer—pigment formulations; the water contents varied from 0.2 to 0.7 % with standard deviations of about ±0.15 %, and recovery of 2-mg quantities of water added to 1-g samples were about 90—110 %.

Rice and Trowell [20] used a vaporizer to remove volatiles from polymers before gas chromatographic analysis. The volatiles may be collected at the head of a column or collected in a cryogenic trap for subsequent separation. On-column trapping is best suited to analysis of loosely divided solids,

TABLE 4

Direct g.c. methods for water in polymers

Substance	Packing	Water, range
Polymers	DOP on Porapak Q	%
Acrylics, PVA, NC	DOP on Chromosorb	%
	Carbowax on teflon	%
NC	Carbowax on Chromosorb	Tenths %
Phenolics	Triton on Gas-Pak	p.p.m.-%
Polyolefins, Polyesters, Cellulosics	Carbowax on Haloport	p.p.m.-%
Cotton fabric	Porapak T	low %
Dextran	Porapak QS	%
PVC	Theed on Chromosorb	p.p.m.—%
Plast.—TiO_2	Porapak T	low %

high-boiling liquids, and thermally stable materials from which water and other volatiles can be removed fairly quickly. Acetone, ethanol and water can be determined in nitrocellulose by the on-column trapping technique. Heptane, acetone, isopropanol and water evolved from nitrocellulose are collected in a liquid nitrogen trap and then separated on the column. Data for 0.2—0.6 % water by the gas chromatographic procedure compare favorably (usually within 0.04 %) with data from Karl Fischer titrations. The subambient trapping method is suitable in determinations of water and phenol in phenolic resins.

Kurasaki and Murano [21] found Porapak Q a suitable column material in their vaporization method for water in certain polymer films. The sample is placed in a pyrolyzer and heated in a flowing gas stream and the volatiles are carried into the gas chromatograph. Figure 4 shows the water recovery, on a relative basis, from several polymers. Most materials show a leveling effect at temperatures of about 70—160 °C; at higher temperatures, some of the condensation polymers indicate further polymerization.

In assessing analyses for water in a hydrophilic macromolecular substance

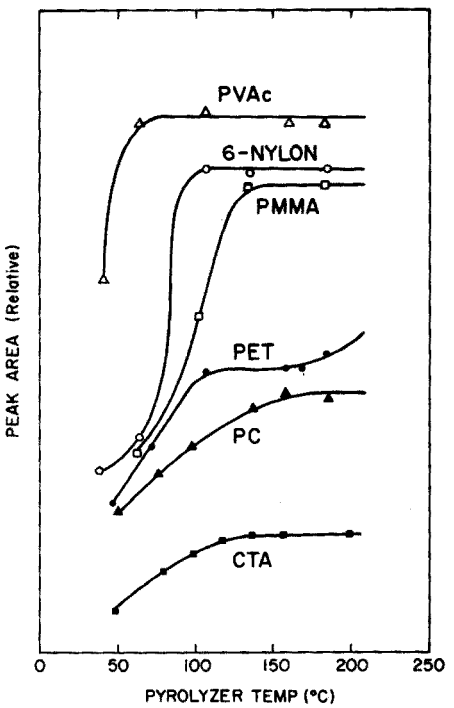

Fig. 4. Peak area of water in various polymer films as a function of pyrolyzer temperature under 5 minutes of heating time: PVAc = poly(vinyl acetate); PMMA = poly(methyl methacrylate); PET = poly(ethylene terephthalate); PC = polycarbonate; CTA = cellulose triacetate.

such as dextran, Pasika and West [22] found that direct injection of a solution of the sample was unsatisfactory. The injection syringe and column became partially covered with gum, leading to prolonged bleeding during subsequent analyses. They proposed a solution—precipitation system with subsequent analysis of the clear liquid phase through a column packed with Porapak QS. In a typical determination, wet dextran is dissolved in dry dimethylsulfoxide (DMSO) and diluted to volume with dry dimethylformamide (DMF), the precipitated polymer is allowed to settle, with centrifuging if necessary to provide a clear supernate, and a portion is separated on Porapak QS at 225 °C. A sample of dextran, which contained 16.9 % water by direct injection of a DMSO solution (with subsequent gum problems), gave a value of 16.9 % by the solution—precipitation method. Vacuum drying at 65 °C gave only 13.0 % water with an additional 3.9 % found by the solution—precipitation procedure on the "dried" sample. The gas chromatographic procedure is calibrated by use of DMSO—DMF mixtures containing known amounts of water.

An extraction procedure was recommended by Berni et al. [23] for determining moisture in cotton fabric. The sample is placed in a bottle with septum cap, a known volume of acetone is added containing methanol as internal standard, and a portion of the solution is removed and separated through a Porapak T column. Average recoveries were within 95 % of those obtained by the standard ASTM oven drying method.

Water in polyolefins and other polymers may be estimated by passage of volatiles from the molten polymer through a column packed with Carbowax on Haloport. Keister and Harrington [24] found the method well-suited to pigmented polyethylene used in paper coating. The sample is placed in a furnace at 316 °C through which helium is flowing; the sample melts rapidly and is swept into the column. The effluent from the column is carried through a thermal conductivity detector at 100 °C and the signal is amplified and integrated. Figure 5 illustrates the procedure for handling the sample weighed into the platinum boat and placed in the position shown by means of an external magnet and magnet M2. After removal of moisture and oxygen

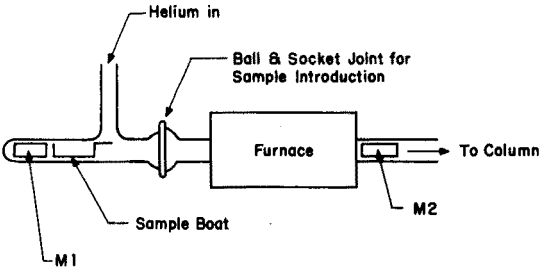

Fig. 5. Sample handling system for water in polymers: polypropylene — 343 °C; polyesters — 288 °C; polyamide — 288 °C; cellulosics — 204 °C.

introduced during placement of the sample boat by means of a helium stream, the boat is moved into the furnace by manipulation of magnet M1. The sample remains in the hot zone for about 2 min and is then removed with magnet M2. A single analysis requires about 10 min. A standard deviation of 0.003 % was reported from 6 determinations on polyethylene containing about 0.04 % water, and of 0.019 % on a sample containing about 0.8 % water. The method was also reported to be suitable for analyses of other solids such as carbon black, titanium dioxide and aspirin.

COLORIMETRY

Of the colorimetric methods for determining water, those based on the use of cobalt(II) chloride and bromide are most widely applied. The solid anhydrous chloride is pale blue, progressing through violet, purple, magenta to red-brown for the di-, tri-, tetra-, and hexahydrates, respectively. The anhydrous bromide is brilliant green and its hexahydrate, red.

There are significant shifts in the absorption spectra of cobalt(II) chloride solutions with the nature of the solvent. Marked differences are observed between spectra in water and in organic liquids, but the spectra for alcohols above methanol are nearly identical in shape and differ only in absorptivity. Ethanol and isopropanol are popular solvents for cobalt chloride; a 2 % solution of $CoCl_2 \cdot 6H_2O$ in absolute ethanol shows an absorption maximum at 640 nm, which shifts to a maximum at 520 nm with increasing water level. The method is applicable to several organic solvents, including alcohols, acetone and acetic acid.

Many procedures are available for colorimetric determinations of water in solids, liquids and gases. For solids, a suitable water-miscible liquid is usually employed to extract water, and the colorimetric measurement is made on the extract. In addition to their use in solution, cobalt(II) chloride and bromide commonly serve as visual indicators for estimating moisture in the atmosphere and are used in many relative humidity devices. Paper or other porous solid support impregnated with the anhydrous chloride or bromide can be used (a) to determine water vapor transmission rates through films, (b) to indicate evaporation rates of water from liquids or through monolayers, such as cetyl alcohol on a quiescent water surface, and (c) to test for water in such substances as halogenated refrigerants, gasoline and other poor solvents. Paper containing cobalt(II) chloride also can be used in a micro test for water liberated from solids by heat. Silica gel, treated with cobalt chloride and phosphoric acid, is used for semiquantitative determinations of water in powders as well as a humidity indicator.

A sensitive hygrophotographic test has been reported by Sivadjian and coworkers, based on the effects of light and moisture on photographic emulsions impregnated with the double iodide of silver and mercury. The yellow emulsion turns black in the light but becomes yellow again in the presence of water. Sivadjian and Corral [25] used the method for studying

the permeability of packaging materials to moisture. In applying the technique to plastic films, the sensitized photographic plate is sealed in a plastic bag. The bag is exposed to known humidity or liquid water in the dark and the time to develop a given yellow color is noted. Data were given for the effects of plasticizers, film thickness, and irradiation on the permeability of polyethylene and polyvinyl chloride to moisture. Permeabilities of several plastics to water and water vapor at room temperature were reported. Sivadjian and Ribeiro [26] found that the permeability of polymers such as polyethylene, polypropylene and polyvinyl fluoride at room temperature, is slightly higher for liquid water than for water vapor. Fluorinated resins, such as polytrifluorochloroethylene, showed approximately equal permeability to water and water vapor over the range from room temperature to 95 °C.

INFRARED SPECTROMETRY

Where applicable, infrared spectrometry provides sensitive, very selective methods for water in many solids, liquids and gases. These procedures are particularly well-suited to small concentrations of water in relatively small samples. They are usually nondestructive, permitting recovery of samples.

Both the fundamental and near infrared regions contain bands suitable for determining water. The 4000—1600 cm^{-1} (2.5—6 μm) fundamental region has been studied extensively. The near infrared between 14300 and 5000 cm^{-1} (0.7—2 μm) is particularly important for quantitative analysis. Overtone and combination bands occur in this region. The stronger combination bands are essentially specific for water. Table 5 summarizes reported applications to analyses for water in polymers.

Jones [27] found a linear relationship for acrylic resins between the absorptivity at 5260 cm^{-1} and percent water in the range 0—1.2 % water. At higher water levels, the relationship was nonlinear but reproducible. He assumed, for calibration, that samples stored at 0 % relative humidity

TABLE 5

Analysis for water in polymers by infrared spectrometry

Polymer	Frequency (cm^{-1})	Water range %	Reference
Acrylic resins	5260 (~1.9 μm)	0.1—1.2	27
Cellophane	5260	Several	28
Cellulose	3500 (~2.8 μm)	0.1—>1	29
Polyamides	5260	0.0—0.3	30
PET	3400—3700 (2.94—2.70 μm)	Tenths	31
Polyols	5260	0.1—0.3	32
Polypeptides	3500	Tenths	33

contained no absorbed water. Weight increases were used to determine the water contents of the dried samples after storage at higher relative humidities. The indicated accuracy was about 0.05 %.

Jeffries [28] found an approximately linear relationship between the amorphous fraction of cellulose and moisture regain. Infrared studies in the hydroxyl-stretching region indicated strongly that sorption of water by cellulose occurs almost completely in the amorphous regions. He defined "crystalline" regions of cellulose as those areas which are hydrogen-bonded in a sufficiently regular and ordered way as to give sharp well-defined peaks for the OH vibrations; and "amorphous" as those regions in which hydrogen bonding is not regular and thus give a broad, featureless OH stretching band.

Bly and Dulz [29] used near-infrared measurement for determining water in molten 6/10 nylon. They found that at temperatures above 200 °C only free water is present, showing an absorption maximum at 1.88 μm. (Bonded water absorbs at 1.91 μm and is found at temperatures below 200 °C.) A cell containing the sample is placed in an aluminum block heater at a temperature up to 320 ± 3 °C. After melting, the sample is scanned from about 2.0 to 1.8 μm, and the absorbance is measured at 1.88 μm. Water content is taken from a calibration curve prepared from a model amide, such as n-hexylcaproamide or pentylhexanamide, which has been treated with steam to achieve varying amounts of water. The absolute water contents of the model amide were determined by titration with Karl Fischer reagent. Samples of 6/10 nylon equilibrated with steam at 239, 267 and 293 °C contained 0.15, 0.12, and 0.09 % water, respectively. The technique is applicable to 6/6 nylon, but 6 nylon could not be analyzed; bonded water was observed even at 40 °C above the melting point.

Illustrative of applications of the infrared method to determination of water in polymer films is the method of Langbein and Seufert [30] for polyethylene terephthalate (PET). Measurements in the range 3300—4100 cm^{-1} (3.0—2.4 μm), give the spectra shown in Fig. 6. The shaded area from about 3400 to 3700 cm^{-1} indicates the absorption spectrum of water in PET. (The strong and weak bands at lower frequencies are probably from a $-\overset{|}{C}=O$ overtone and O — H vibration, respectively.) Quantitative analysis for water requires measurement of $\log (I_0/I) = K$, where I_0 is the intensity of the incident radiation and I is the intensity of the transmitted radiation at 3630, 4080 and 3750 cm^{-1}. The intensity of the absorption K at 3630 cm^{-1} (ca. 2.755 μm) is determined primarily by the water, and that at 4080 cm^{-1} (ca. 2.45 μm) by the PET; the absorption at 3750 cm^{-1} (ca. 2.667 μm) is caused mainly by scattering losses resulting from internal inhomogeneities. (The influence of reflection and scattering at the film surfaces is eliminated by immersing the films in a mixture of carbon tetrachloride and carbon disulfide.) However, at each of the three frequencies there is overlap of all three absorptions. Measurements on films showing different intensities of scattered light (variation in crystallinity) and different water contents give the following relation between the measured K value and the K' which would be obtained

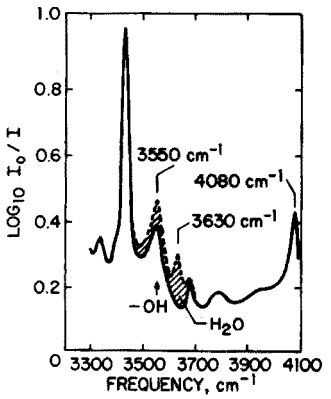

Fig. 6. Infrared spectra of polyethylene terephthalate containing water (---) and dry (—).

if only one of the factors mentioned determined the light absorption

$$\frac{K'_{3630}}{K'_{4080}} = \frac{K_{3630} - 0.19\,K_{4080} - 0.14\,K_{3750}}{K_{4080} - 0.31\,K_{3750}}$$

The ratio is proportional to the mass concentration ratio of water and PET, i.e.,

$$C\frac{K'_{3630}}{K'_{4080}} = \frac{[H_2O]}{[PET]} = \frac{\text{Weight with water} - \text{weight without water}}{\text{weight without water}}$$

From experiments with samples containing known amounts of water, the factor C varies between 0.008 (at a H_2O/PET ratio of 10^{-4}) and 0.004 (at a H_2O/PET ratio of $4 \cdot 10^{-3}$). Figure 7 is a logarithmic presentation of the correlation between K'_{3630}/K'_{4080} and H_2O/PET. The 45 ° line corresponds to a linear correlation between the two magnitudes, that is, to a

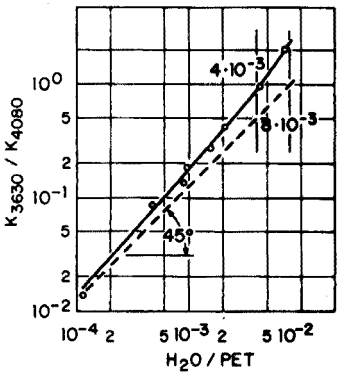

Fig. 7. Water content of polyethylene terephthalate and intensity of infrared absorption at 3630 cm^{-1}

concentration-independent value for C. At higher water concentrations, the factor C diminishes. This is attributed to association of water molecules at higher water concentrations which is not significant at low concentrations.

Then, to determine water in films of PET, the absorption coefficient, $K = \log I_0/I$, of the films is measured at 3630, 3750, and 4080 cm^{-1}. The relation K'_{3630}/K'_{4080} is determined from the above formula and yields the ratio of water concentration to PET concentration via the unbroken standard curve of Fig. 7.

Malcolm [31] reported on studies of water adsorbed on poly-*D*-alanine, poly(γ-ethyl-*L*-glutamate), and poly(γ-methyl-*L*-glutamate) in the 2000—4000 cm^{-1} region. In all three polymers, the center of OH absorption is at 3500 cm^{-1} rather than at 3400 cm^{-1} as in liquid water. He demonstrated that water molecules are adsorbed at specific sites and orientations relative to the matrix.

Molecular processes involved in hydration of polyelectrolytes, particularly cation-exchange resins, were reported by Zundel [32], who described infrared studies made at the University of Munich. Ackerman and Zivernemann [33] described infrared absorption measurements on anion-exchange resins as films and as solutions with small amounts of water in organic solvents.

For some substances, direct infrared scanning is impractical or subject to interferences. Both extraction and azeotropic distillation can be employed for many solid materials. Dioxane is a particularly convenient entrainer for distillation. Preliminary chemical reaction also has been used in special cases, e.g., calcium carbide and dimethoxypropane. The carbide, of course, reacts with water to release acetylene which may be measured in the vapor phase. The dimethoxypropane reacts with water to form acetone (1 mole) and methanol (2 moles); Critchfield and Bishop [34] measured the acetone formed at 5.87 μm.

NUCLEAR MAGNETIC RESONANCE SPECTROMETRY

In studies involving liquid water, both high-resolution and wide-line resonance techniques have been employed. The former for all practical purposes is limited to solutions and provides a means of differentiating among protons associated with different groups. Wide-line n.m.r. provides a rapid, nondestructive method of analysis for water in a variety of solids and relatively nonvolatile liquids. Spectra are relatively broad with line widths related to the mobilities of the protons. The more mobile protons tend to give sharper lines than those which are bound by physical and chemical forces. Thus, water loosely adsorbed on solids is more mobile, and signals have narrower line widths, than those for water of crystallization.

Most reported applications of n.m.r. to determinations of water have been based on the wide-line technique, for analyses of agricultural and food products.

Golling [35] used the wide-line technique for determinations of 0.09—8 %

water in polyamides and epoxy resins. Typical proton signals are shown in Fig. 8. The distance between maxima, $\Delta\nu_s$, is not identical with the half-width but indicates the distance between the reversal points of the absorption signal. A_m represents the maximum signal amplitude. With these resins, the contribution of the water protons can be distinguished clearly from the protons of the plastic. The nuclear resonance signal is proportional to water content and appears to be independent of the particular resin used.

Rakos [36] observed three kinds of adsorbed water on sodium polymethacrylate: (a) below 5 %, water provides a monolayer of water essentially localized at the hydrophilic group; (b) from 5 to about 35 %, the adsorbed water is adjacent to the monolayer and is partially oriented, impeding motion of these molecules; (c) above 35 % the water molecules move much more freely. These three types provide significant differences in relaxation times.

Moisture can be measured from 1.5 to over 20 % in a variety of textiles. Calibration curves of n.m.r. signal versus weight percent water (as determined by oven drying at 105—110 °C) have been reported for rayon and nylon tow, wool tow, silk and raw lint cotton. In studies of rayon fibers, Dehl [37] observed two types of lines in the wide-line spectrum; he concluded that in the magnetic field, molecules of water reorientate rapidly about all possible axes but maintain a small resultant orientation along the fiber axis.

High-resolution studies on native cellulose (mulberry paper) indicate two types of sorbed water, both of which are mobile. These appear to change in state at about 20 % water. Ogiwara et al. [38] classified the types as bound and free water. The former is characterized as tightly bound to cellulose molecules and apparently is involved directly in fiber swelling. The amount

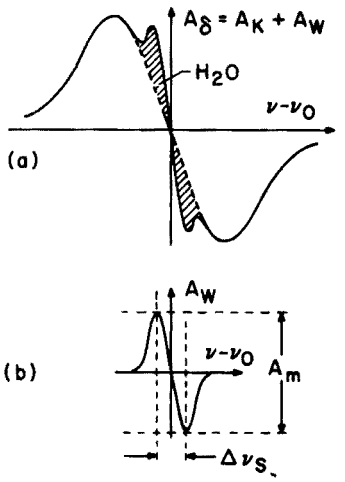

Fig. 8. Nuclear magnetic resonance signals on differential scanning; (a) total signal; (b) contribution of the protons of the absorbed water.

of bound water in cotton cellulose is about 15 %. Determination of the amount of bound water is made with improved accuracy; the lower the temperature of measurement. Also, the technique permits determination of the temperature at which water molecules become bound to the cellulose. Free water is present on the surface or in the capillaries of fiber structures; it can be removed by centrifugation or similar mechanical means. With unbeaten softwoods dissolving pulp the width at half value of the n.m.r. absorption spectrum of water decreases with increase in water.

Pittman and Tripp [39] studied wide-line spectra of various cellulose preparations in the dry state and containing 7 % water. Figure 9 shows a typical derivative curve of the n.m.r. spectrum of moist cellulose. The narrow component, W, represents protons of adsorbed water and the broad component, C, cellulose. These investigators proposed the following interpretations of these and similar spectra to support five states in moist cellulose; (1) protons in crystalline regions, characterized by a second moment of about 17 gauss; (2) protons in amorphous areas, with second moment of about 14 gauss; (3) protons showing rapid exchange between water and cellulose with spin—spin relaxation times of ca. 10—35 μs; (4) protons of water having spin—lattice relaxation times ca. 2.5—11 μs; (5) protons of more tightly bound water having shorter spin—lattice relaxation times than those in the mobile state.

Kimura et al. [40] used wide-line n.m.r. in studies of the effects of temperature on adsorbed water in linter cellulose. Based on first derivative curves and second moments, they concluded that marked changes in proton

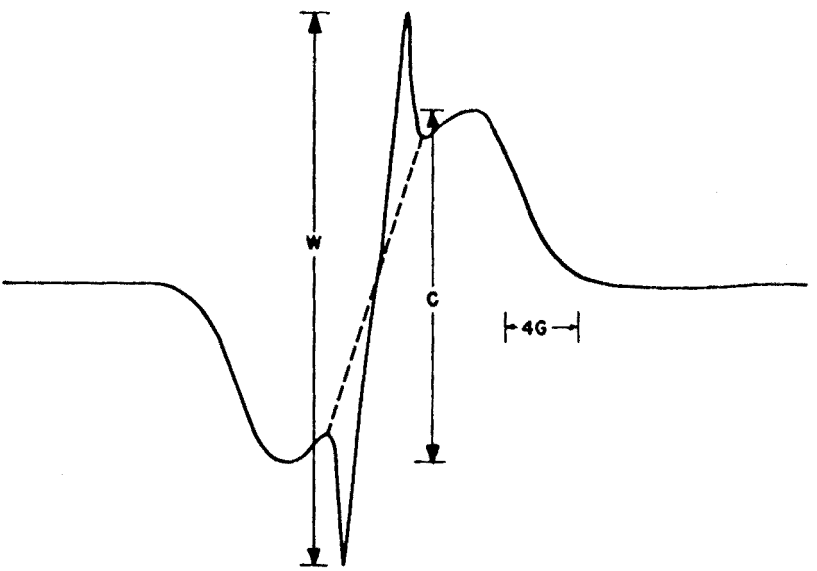

Fig. 9. Typical n.m.r. spectrum of moist cellulose.

movement of adsorbed water occur over the temperature range 180—200 K and that adsorbed water reduces the glass transition to room temperature.

N.m.r. can be used effectively in studies of the physical state of water in membranes, an area of particular interest to biochemists. Krishnamuthy et al. [41] and Shporer et al. [42] studied membranes of cellulose acetate, and found partial ordering of water near the surface of the films, resulting in splitting of the n.m.r. spectrum.

In some cases ^{19}F n.m.r. provides a broadly useful means of determining water and other active protonated species. Ho and Kohler [43] utilized the reaction of hexafluoroacetone to form adducts of active protic compounds. Applications to water and hydroxyl end-group determinations in Carbowax 200 were reported. Since the chemical shifts differ markedly for different types of protonated functional groups the HFA technique usually permits simultaneous analysis for each species.

ELECTRICAL METHODS

Various electrical measurements can be employed for the determination of moisture. Often they require separation of water from a solid sample by vaporization or extraction, the subsequent detection of water being made in the vapor or liquid phase. However, with many granular materials capable of uniform compaction direct electrical measurements may be feasible.

Dielectric techniques

Included in the category of dielectric methods are measurements for dielectric constant, dielectric loss, and often capacitance. Direct determination of dielectric constant is usually the most reliable because of the high constant for water, ca. 80, compared to most other materials. Paper, for example, has a dielectric constant of about 2.5.

Under ideal conditions the dielectric constant of a binary mixture, ϵ_m, can be calculated from the linear relation

$$\epsilon_m = \epsilon_1 p_1 + \epsilon_2 p_2$$

where p_1 and p_2 are the relative concentrations of each component. In this case $p_1 + p_2 = 1$, and p_2 can be expressed as $1 - p_1$. A substance containing 1 % water would then have a calculated ϵ_m of $0.8 + \epsilon_2$ or $\Delta\epsilon = \epsilon_m - \epsilon_2 = 0.8$ ($\epsilon_1 p_1 = 80 \times 0.01$, and $\epsilon_2 p_2 = \epsilon_2 \times 0.99 \approx 1$). Theoretically, therefore, the presence of 1 % water in any substance will lead to an increase in dielectric constant of the substance by 0.8 unit. Oehme [44] found, however, that most systems did not behave ideally and, hence, calibration curves are required for each system to be analyzed. Figure 10 shows the effect of increasing concentrations of water on the dielectric constants of methanol, dioxane, and octanol at constant temperature; only the methanol—water system gives a linear relationship. In the Figure, for illustrative purposes, the

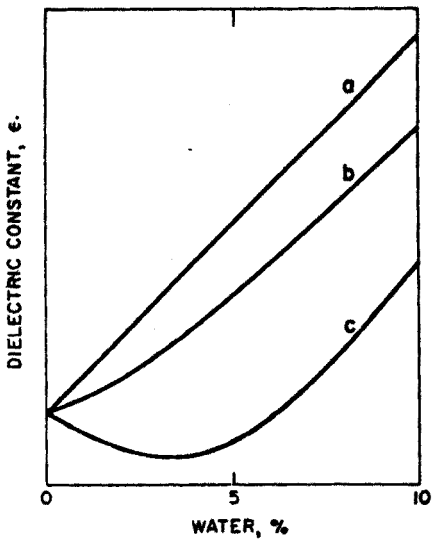

Fig. 10. Effect of water on the dielectric constants of (a) methanol, (b) dioxane and (c) n-octanol.

three organic compounds are expressed in terms of identical dielectric constants, but actually they differ considerably, the ϵ values being 2.3 and 33.8 for dioxane and methanol, respectively. Deviations from theory appear to be associated with decreased precision of measurement as the dielectric constant of the substance increases and with the nature of the molecular association in solution.

The dielectric methods have been applied to determinations of water in liquids and solids. The sample is placed in a suitable measuring cell, the instrument is tuned, and a reading is taken. The equipment and type of measurement vary with the nature of the material to be analyzed. Dielectric measurements also have been used for determining water in leather, paper, textiles, powders, meat products, and salts.

Analysis of extracts from solids often has been preferred to direct analysis, particularly on materials which are difficult to pack uniformly or on which the water may be distributed unevenly. Dioxane is one of the most useful extraction solvents because of its low dielectric constant and complete miscibility with water. For extraction of some materials, for example, meats, a mixture of dioxane and ethylene glycol has been found superior to dioxane alone.

In some instances dielectric loss angle measurements may be superior to dielectric constant measurements. For a given frequency, ω, the loss angle, δ, can be calculated from the relation $\tan \delta = k\sigma/\omega\epsilon$ where k is a constant ($1.13 \cdot 10^{13}$) and σ is the conductivity. With the method of grid current maximum, $\tan \delta$ also can be calculated from the effective capacity and the

damping of the measuring cell containing the sample. For determinations of small amounts of water (up to 1 %) in C_1—C_5 alcohols, dielectric loss angle measurements may be more reliable than dielectric constant measurements. However, small amounts of impurities interfere seriously in the loss angle method.

Conductivity, resistance

Among the electrical techniques, those based on conductivity measurements are probably the most widely used. Applications to solids, liquids, and gases require that (1) an electrolyte be present, and (2) components other than water in the sample be essentially nonconducting materials. Under these conditions, when electrodes at a fixed potential are placed in the sample, the current is proportional to the water content. Analyses are made either directly on a measured amount of the sample or indirectly on an inert water-miscible liquid used to extract water from the sample. The former method requires rather simple compact apparatus and is well suited for rapid analyses of solid materials containing several percent water. Each system must be calibrated, however, since the physical form and density of the material affect the results. Instruments have been described for the direct determination of water in grains, paper, textiles, plastics, tobacco, sand, concrete mix, wood, leather, soils and oil. The indirect approach, with an inert liquid, gives more versatility if the water can be extracted reproducibly; acetone, methanol, and ethanol have been used as extractants. Oxalic acid, sodium chloride, and lower fatty acids are typical of electrolytes which have been added when necessary.

Electrical conductivity measurements of solid or liquid absorbents can be used directly or indirectly for determining water in gases. Thus lithium salts have been employed for measuring the relative humidity of gases above 5 %. A mixture of sulfuric and phosphoric acids is a suitable absorbent in rapid determinations of low concentrations of water in small samples. The method also can be used for determining water in liquids and solids by employing a dry inert gas to elute the water. Alternatively, the water content of air in equilibrium with a liquid sample may serve as a measure of water in the sample.

Electrolysis

Of the electrical methods available for determining water in gases, that based on electrolysis is probably the most versatile. Keidel [45] devised a unique system based on quantitative absorption of water in a suitable hygroscopic material followed by electrolysis of the water to oxygen and hydrogen. The electrolysis current serves as a direct indication of water content. The technique is particularly appropriate for continuous determination of about 1—1000 p.p.m. water in gases. It also can be used as a batch analyzer.

In the special cell used absorption is combined with electrolysis. The absorbent (phosphorus pentoxide) is distributed as a thin viscous film in contact with two platinum electrodes. Water vapor in the gas flowing through the cell is absorbed by the hygroscopic electrolyte. The absorbed water is quantitatively electrolyzed at the electrodes by application of a d.c. voltage greater than the decomposition potential of water. According to Faraday's law, the electrolysis of 0.5 g-mole of water requires 96,500 coulombs. The electrolysis current is proportional to the number of moles of water absorbed per unit time. This not only provides a continuous measure of water concentration but also maintains the film in an active condition. Usually a flow rate of 100 cm^3 min^{-1} is suitable. Under these conditions the electrolysis current is 13.2 μA/p.p.m by volume.

The method has been applied successfully to determinations of water in a variety of gases, including air, nitrogen, hydrogen, carbon dioxide, argon, helium, hydrocarbons, and Freon fluorinated hydrocarbon refrigerants and propellants. Successful applications also have been made to analyses for water in many liquids. Materials boiling below 100 °C can often be handled as vapors. Others in which water is only slightly soluble have been analyzed indirectly by sparging with a stream of dry, inert gas such as air or nitrogen. Compounds which interfere include hydrogen fluoride, ammonia and other basic materials, and high concentrations of alcohols or acetone. The basic materials react with the phosphoric acid electrolyte. In many cases, potassium carbonate or hydroxide can be substituted for the phosphorus pentoxide absorbent in analyses for several hundred parts per million water in the presence of volatile bases.

Units based on electrolysis are available from several commercial sources. Usually at least 1 l of gas sample is required for an analysis. A maximum error of 5 % in the reading can be achieved easily with commercially available components.

An interesting variation in the electrolysis technique was described by Capuano [46]. In contrast to coulometric measurements on which previous instrumentation has been based, Capuano eliminated the time factor in the electrolysis, by maintaining steady-state conditions and depending on principles of mass transfer. Thus the new approach becomes in effect an amperometric method rather than a coulometric procedure. Application of the method was illustrated with samples of chlorine gas of differing water contents flowing through an electrolysis cell at rates from 100 to 250 cm^3 min^{-1}.

Applications of the electrolytic method to determinations of water in polymers have been described for nylon [47], polyester [48], polyolefin [49], and ionomer resin [50].

PHYSICAL METHODS

Numerous physical properties form the basis of rapid analyses for water. Like electrical methods they are most useful for gases and liquids. Some are applicable only to narrowly defined systems; included in this category are cryoscopy, density, displacement, and refractive index. Others are quite broadly applicable, such as chemical reaction—gasometric measurement, dew point, hygrometry, piezoelectric sorption and vapor pressure. The more general procedures are limited to gases.

Turbidity

Turbidity or cloud point is useful in several applications. In this technique the homogeneous liquid sample is titrated with a water-immiscible liquid in which other components of the sample are soluble until the solution becomes turbid. The amount of liquid producing turbidity, i.e., phase separation, depends on the nature and temperature of the system, and the relative amounts of the various components. Alternatively, the critical solution temperature, i.e. the temperature at which a mixture of two liquids immiscible at ordinary temperature just ceases to separate into two phases, may be determined. This technique has only limited applicability in polymer systems.

Vapor pressure

Direct and indirect methods for vapor pressure measurements are used on a variety of gases and solids. A gas, such as moist air, is usually drawn into an evacuated flask. The pressure is then measured manometrically before and after removal of the water. The water may be removed by freezing or by absorption into a suitable desiccant such as phosphorus pentoxide or sulfuric acid.

Direct measurement

For water in sugar and other finely divided solids, a sealed ampoule of the sample may be placed in a flask which is then evacuated. The ampoule is broken and the sample heated. Evolved moisture is condensed in a second evacuated flask of known volume. The condensate is evaporated and the vapor pressure measured. The condensation step permits compensation for adsorbed gases released with the water during heating of the sample. This, of course, requires accurate measurements of the residual pressure after condensation of the water and of the total pressure after re-evaporation of the water. Equipment for these measurements is available commercially.

David et al. [51] used a modification of a commercially available apparatus to determine water in several polymers as a means of correcting

for volatiles other than water. Pressure is measured for volatiles in the sample before and after passage through calcium hydride. The difference is due to water provided that no other compounds are present which react with the hydride. The authors [51] reported an average of 78 p.p.m. water with a standard deviation of 3 p.p.m. for six 10-g samples of polycarbonate. Comparative data between this method and the Karl Fischer reagent titration on samples of poly(ethylene adipate) having a molecular weight of about 2000 were good. David et al. reported that the vapor pressure method requires from 30 to 90 min for each analysis, depending on whether moisture plus other volatiles are required or moisture only. The reproducibility is ±0.001 % absolute and the accuracy is ±0.002 % absolute, based on an original sample of 10 g; the minimum amount of water that can be detected is 0.001 %. The times and temperatures of the heating cycle must be determined for each different polymer.

Illing and Hobe [52] used differential pressure measurements in estimating small amounts (>0.01 %) water in polymers; they used a simple vacuum bench in which the finely ground sample is heated to 150—200 °C (set empirically by type of polymer) in an evacuated system. At equilibrium (usually 15—20 min), the increase in pressure is measured in the range 0.1—1 torr, and the amount of water is calculated from a calibration curve prepared from known weights of water. The results compare favorably with those by Karl Fischer reagent methods. Table 6 gives results on some polymers.

Direct measurement of steam volume can be used in the field for estimating water in 66 and 610 nylon resins [53]. The sample is placed in a hypodermic syringe and heated. The displacement of the syringe plunger is related directly to water content. The apparatus consists of a 50-ml hypodermic syringe; a cylindrical glass sleeve resting on the upper flanged surface with which the displacement of a fixed mark on the plunger surface can be read; a

TABLE 6

Analytical data on polymers

Polymer	Sample wt., (g)	Pressure diff., (mm)	Water found (Wt. %)
Nylon 6 (m.p. 212 °C)	0.46	20	0.21
Nylon 66, 6 + Polyethylene (PE) (m.p. 260—265 °C)	0.99	26	0.125
Nylon 66, 6 + PE	0.97	40	0.20
(m.p. 210—215 °C)	1.00	40.5	0.195
Nylon 66, 6 + PE	1.00	45	0.22
(m.p. 255—260 °C)	0.96	41	0.20
Polycarbonate (m.p. 223 °C)	0.98	12	0.06

cylindrical aluminum heating block provided with a central hole for insertion of the syringe assembly, and two smaller holes, respectively for a thermoregulator and a 50—400 °C mercury thermometer; a 500-W, 120-V band heater, 12.7-cm long, fitted snugly to the aluminum heater block; insulation, provided by supporting the block on a disc of "Transite" in a metal can and packing the annular space with glass wool. Commercial equipment is available which provides space for four syringes.

The standard deviation of the method was 0.04 % based on 60 determinations on 10-g samples containing 0.2—0.3 % water. Although designed specifically for analysis of 66 and 610 nylon resins, the steam-volumetric method appears to be applicable to moisture determinations for other sparingly soluble solid materials, provided that they are thermally stable at 200 °C.

Indirect measurement

Calcium hydride and calcium carbide have been used effectively in determining moisture in inert solids such as cellulose, leather and polyorganosiloxanes.

Piezoelectric sorption hygrometry

Piezoelectric quartz crystals have a variety of applications from radiofrequency control to highly sensitive detection of weight changes. King [54] described a novel detector for moisture in gases based on a quartz crystal coated with a hygroscopic material; vibration changes are measured as the coated crystal gains or loses weight. King used quartz discs of about 12-mm diameter and about 0.2-mm thickness with a frequency of 9 MHz. Such crystals are readily available. With these crystals, frequency change (ΔF in c.p.s.) is closely proportional to mass added or subtracted (ΔM in g) as follows: $\Delta F = K\Delta M$, where $K = 2.3 \cdot 10^8$ c.p.s./g for a 9-MHz unit.

In practice, the coated quartz crystal is placed in an oscillator circuit. As the hygroscopic coating absorbs water, the change in radiofrequency signal from the oscillator is measured with a digital frequency counter or similar device. A change of 0.1 c.p.s. can be measured readily. From the previous equation, it is easily shown that a quantitative relationship exists between the oscillator signal and the adsorption isotherm of the hygroscopic coating

$$\Delta F = \frac{\Delta W}{\Delta W_0} \Delta F_0$$

where ΔF is the frequency change caused by absorbed water; ΔW, the water absorbed in g; ΔF_0, the frequency change caused by the dry coating; and ΔW_0, the weight of the dry coating. Since the weight gain of the hygroscopic absorbent is a function of water partial pressure, the sorption detector signal (ΔF) is also a function of water partial pressure. Molecular sieves are

particularly sensitive as water detectors for low partial pressures. Polar liquids, such as polyethylene glycol, make rapid linear detectors. King used a single detector for the range from 0.1 p.p.m. to 3 % water in air, which gave a net signal of from 0.5 to 3900 c.p.s.

Since this quartz hygrometer measures weight change, other substances which are absorbed or which affect water absorption may interfere; usually the interference is quite small. Often correction can be made by analyzing the gas before and after passage through an efficient drying agent.

A commercially available instrument achieves high sensitivity and fast response, as it compares the changes in frequency of two coated quartz crystals. Moisture is adsorbed and desorbed alternately on each crystal, resulting in a mass difference and thus a corresponding change in the frequency of vibration. Two coated crystals together with a system for flow switching provides a unique means for measuring dynamic changes of decreasing water vapor concentration. Each crystal is exposed alternately to the sample gas and then to a dry reference gas. Moisture in the range 0—25,000 p.p.m. can be determined in atmospheric gases, petroleum hydrocarbons such as methane, ethylene and benzene, fluorocarbons, alcohols, and corrosive gases including sulfur dioxide, sulfur trioxide, hydrogen sulfide, ammonia and mercaptans.

The piezoelectric technique is suitable only for determining moisture in gases, so that its applicability to polymers depends on the volatilization of the water. A variety of inert carrier gases may be used to carry water to the cell.

In an interesting variation, Kennerly [55] measured the water absorption by hygroscopic materials. The dry substance is deposited on the quartz crystal and water sorption is measured by following the change in frequency of the crystal. Applicability was demonstrated for the water absorption isotherm of polyglycine.

CHEMICAL METHODS

Magnesium nitride

Water reacts with magnesium nitride to form ammonia,

$$Mg_3N_2 + 6\ H_2O \rightarrow 3\ Mg(OH)_2 + 2\ NH_3$$

In 1931 Dietrich and Conrad [56] reported on the use of this reagent in a titrimetric method for determining water in alcohol, but the method has been used only sparingly in recent years. However, it appears worth examining in some detail because of the wide variety of procedures available for ammonia. Conventional titration with acid is the only approach which seems to have been reported in the literature. Colorimetry, electrical conductivity and chromatography are alternative, sensitive approaches suitable for batch or continuous analysis. For some plastics extraction or volatilization might be

used to isolate water for subsequent reaction with nitride. Dietrich and Conrad reported satisfactory results by titrimetry for from 40 p.p.m. to 10 % water in ethanol, benzene, diethyl ether and acetone. Thus, several organic solvents are suitable for the isolation step. Alternatively, often water vapor can be removed by an inert carrier gas which might be carried through the magnesium nitride reagent.

Acylation

The reaction of water with acyl halides and anhydrides provides the basis for several procedures for determining water, e.g.

$$RCOX + H_2O \rightarrow RCOOH + HX$$

$$(RCO)_2O + H_2O \rightarrow 2\ RCOOH$$

Possibilities for use of such reagents should be considered for polymers and intermediates. There are a variety of methods now available for determining end products or unreacted reagent. Essentially all reported procedures employ acidimetric titration, but alternative detection systems should be considered, recognizing that several alkyl and aryl halides and anhydrides are now available in high purity.

Karl Fischer reagent

The most widely applicable method for determining water is based on the Karl Fischer reagent. Since its discovery in 1935, the reagent has been applied successfully to analyses of an increasing number of materials. The very selective nature of this reagent, together with the rapidity with which analyses can be performed, has led to hundreds of applications. Many of the reported studies have presented an inaccurate picture of the method, often because of inadequate recognition of safeguards required during its use and neglect of interferences. Effective use of the reagent requires a thorough understanding of its potential and limitations.

Major developments in the Karl Fischer methods over the last several years have been associated with stabilized reagent and with improved procedures of end-point detection. The original reagent was composed of iodine, sulfur dioxide, pyridine and methanol. In this system reaction with water involves the two-step reaction,

$$C_5H_5N \cdot I_2 + C_5H_5N \cdot SO_2 + C_5H_5N + H_2O \rightarrow 2\ C_5H_5N \cdot HI + C_5H_5N \cdot SO_3$$

$$C_5H_5N \cdot SO_3 + CH_3OH \rightarrow C_5H_5N(H)SO_4CH_3$$

Most modifications of the reagent to achieve better stability have involved replacement of the methanol by cellosolve, glycol or formamide, or by introduction of certain salts. The methanol-based reagent becomes quite stable when the water equivalent is no greater than 1 mg H_2O/ml reagent.

End-point detection can be based on the following techniques: visual, dead-stop, potentiometric, coulometric, photometric and thermometric titrations. Visual titration is useful only at water equivalent concentrations exceeding 2 mg H_2O/ml reagent with an optimum of 3—3.5 mg H_2O/ml. The dead-stop technique is the basis of most automatic titrimeters. Recent improvements in instrumentation have made the coulometric approach reliable and highly sensitive.

In applying the Karl Fischer procedure it must be remembered that for highest sensitivity moisture in the atmosphere must be rigorously excluded. A convenient titration flask is shown in Fig. 11. This small sealed vessel employs serum bottle stoppers which permit transfer of solutions via hypodermic needles in a closed system. The flasks may have sealed-in electrodes or wire electrodes may be inserted through one neck of the 3-necked vessel.

Both visual and electrometric titrations have been used successfully for determining water in polymers. In addition to its laboratory use for determining several percent water by the visible titration method, the technique can also be adapted to field use. (A precision of better than 0.5 mg of water is readily obtainable in spite of the many skeptics who claim otherwise.) A field kit has been used with considerable success for determining water in acrylic resins and other organic solvent soluble polymers [57, 58]. Compact kits are available containing stabilized Karl Fischer reagent, screw-cap bottles with polyethylene seals containing chloroform or other solvent, similar bottles containing permanent color standards, hypodermic syringes and needles, and calibrated glass vials for volumetric sampling. The technique has been used successfully for cube-cut acrylic molding powder and granular resin covering the range 0.08—1 % water. For molding powders

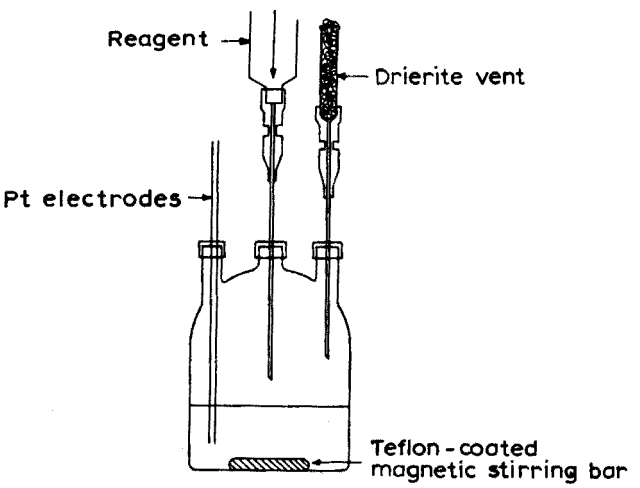

Fig. 11. Small sealed vessel for Karl Fischer titrations.

Fig. 12. Field kit for use with acrylics.

or granules of low solubility, the so-called hot block is often suitable. Special solvents include hexafluoroisopropanol (HFIP) and trifluoroethyl alcohol (TFE) for use with polyamides (see Table 7) [59].

Where a precision of 0.5 mg is inadequate, electrometric titration is essential. Instruments based on the dead-stop end-point readily detect microgram amounts of water. Similar sensitivity is observed in many procedures based on coulometric generation of the active reagent. Fairly realistic limits of detection are about 300 μg and 100 μg of water, respectively, by the dead-stop and coulometric techniques.

Typical applications of the Karl Fischer method to analyses for water in polymers are shown in Table 7.

TABLE 7

Karl Fischer procedures for water in polymers

Polymer	Procedure	Range (%)	Comments
Acrylic	Solution	0.05—1	σ = 0.006
Cellulose acetate	Extraction	0.2—2	Reflux (CH_3OH)
GRS	Extraction	0.04—0.5	Dist. (C_2H_5OH—C_6H_6)
Melamine	Solution		Titration — 35 °C
Paraform	Solution	0.4—2	Free and combined
Polycarbonate	Vaporiz.	~0.01	
Polyester	Vaporiz.	0.004—0.08	170 °C
PET	solution-dist.	0.05	C_6H_5OH—$Cl_4C_2H_2$ + Alcohol
Polyamide			
6 Nylon	Solution	0.02—3	C_6H_5OH—CH_3OH, *m*-Cresol
	vaporiz.	0.01—0.1	170 °C (σ = ± 0.0037)
66 Nylon	Solution	0.2—3	*m*-Cresol
	vaporiz.	0.01—3	260 °C
6, 66, 610 Nylon	Solution	0.1—0.5	HFIP, TFE
Polyethers	Solution	~0.5	Glycol
Polyolefins	Solution-precip.	0.02—0.2	Xylene
PE	vaporiz.	0.0006—0.5	120 °C
Polyoxymethylene	Solution	0.4—3	Free and combined
Phenol-formaldehyde	Extraction	3—5	CH_3OH Reflux
Urea-formaldehyde		5—15	

REFERENCES

1 R. M. Barrer, XVIth International Congress of Pure and Applied Chemistry, Paris, July 18—24 (1957), Plenary Lectures, Birkauser Verlag, Basel and Stuttgart, 1957, p. 113.
2 M. Braden, Trans. Plastics Inst., 31, (94) (1963) 83.
3 I. Kirshenbaum, Natl. Nuclear Energy Ser., Div. III, 4-A (1951).
4 D. R. Stull, Ind. Eng. Chem., 39, (1947) 517.
5 G. Zimmermann, J. Sci. Food Agri., 12, (1961) 240.
6 W. Heidbrink, Fette, Seifen Anstrich., 53, 291 (1951).
7 J. R. Kanagy, and A. M. Charles, J. Amer. Leather Chemists Assoc., 36, (1941) 609.
8 H. H. Schenker, C. C. Casto and P. W. Mullen, Anal. Chem., 29, (1957) 825.
9 P. R. Mears and G. L. Palmer, Mem. Chemical Insp., No. 157, 1965.
10 C. Duval, Chim. Anal. (Paris), 36, (1954) 61.
11 J. Chiu, J. Polym. Sci., C8, (1965) 27; Anal. Chem., 39, (1967) 861.
12 R. W. Bentz and H. A. Neville, J. Polym. Sci., 4, (1949) 673.
13 J. S. White, Mem. Chem. Insp., No. 211, 1967.
14 H. S. Knight and F. T. Weiss, Anal. Chem., 34, (1962) 749.
15 N. M. Turkel'taub, B. M. Luskina and N. A. Palamarchuk, J. Anal. Chem. (USSR), Engl. Transl., 22, (1967) 917.
16 J. H. Martin and A. M. Knevel, J. Pharm. Sci., 54, (1965) 1464.
17 N. Y. Mary, J. Chromatogr., 42, (1969) 411.
18 O. L. Hollis, Anal. Chem., 38, (1966) 309.
19 J. M. Slanski, H. Jacin and R. J. Moshy, J. Appl. Polym. Sci., 13, (1969) 1169.
20 D. D. Rice and J. M. Trowell, Anal. Chem., 39, (1967) 157.

21 K. Kurosaki and J. Murano, Kobunshi Kagaku, 29, (1972) 411.
22 W. M. Pasika and A. C. West, III, Anal. Chem., 43, (1971) 275.
23 R. J. Berni, D. M. Soignet, J. V. Beninate and M. W. Pilkington, Text. Res. J., 42, (1972) 576.
24 D. C. Keister and R. C. Harrington, Jr., Tappi, 50, (3), (1967) 81A.
25 M. J. Sivadjian and F. Corral, Anal. Chim. Acta, 26, (1962) 185; J. Appl. Polym. Sci., 6, (1962) 561.
26 M. J. Sivadjian and D. Ribeiro, J. Appl. Polym. Sci., 8, (1964) 1403.
27 E. R. S. Jones, J. Sci. Instrum., 30, (1953) 132.
28 R. Jeffries, J. Appl. Polym. Sci., 8, (1964) 1213.
29 D. D. Bly and G. Dulz, Paper presented at Pittsburgh Conference on Analytical Chem. and Applied Spectroscopy, March 1966.
30 G. Langbein and W. Seufert, Kolloid-Z Z. Polym., 193, (1963) 37.
31 B. R. Malcolm, Nature (London), 227, (1970) 1358.
32 G. Zundel, Hydration and Intermolecular Interaction, Academic Press, New York, 1970.
33 T. Ackerman and Zivernemann, Ber., Bunsenges. Phys. Chem., 73, (1969) 446.
34 F. E. Critchfield and E. T. Bishop, Anal. Chem., 33, (1961) 1034.
35 E. Golling, Z. Angew. Phys., 14, (1962) 717.
36 M. Rakos, Czech. J. Phys., 16, (1966) 864.
37 R. E. Dehl, J. Chem. Phys., 48, (1968) 831.
38 Y. Ogiwara, H. Kubota, S. Hayashi and N. Mitomo, J. Appl. Polym. Sci., 13, (1969) 1689.
39 R. A. Pittman and V. W. Tripp, J. Polym. Sci., Part. A-2, 8, (1970) 969.
40 M. Kimura, H. Hotakeyama, M. Usuda and J. Nakano, J. Appl. Polym. Sci., 16, (1972) 1749.
41 S. Krishnamusthy, O. McIntyre, E. R. Santee, Jr. and C. W. Wilson, J. Polym. Sci., Polym. Phys. Ed., 11, (1973) 427.
42 M. Shporer, A. J. Vega, and M. A. Frommer, J. Polym. Sci., Polym. Phys. Ed., 12, (1974) 645.
43 F. F-L Ho and R. A. Kohler, Anal. Chem., 46, (1974) 1302.
44 F. Oehme, Angew. Chem., 68, (1956) 457.
45 F. A. Keidel, U.S. Pat. 2,830,945 (1958); Anal. Chem., 31, (1959) 2043.
46 I. A. Capuano, U.S. Pat. 3,799,846 (1974).
47 P. S. Gill, Du Pont Company, Instrument Products Division, Application Brief SMA-3.
48 R. L. Blaine, Du Pont Company, Instrument Products Division, Application Brief SMA-4.
49 K. F. Daly, Du Pont Company, Instrument Products Division, Application Brief SMA-5.
50 R. L. Blaine, Du Pont Company, Instrument Products Division, Application Brief SMA-2.
51 D. J. David, G. F. Baumann and S. Steingeiser, Soc. Plastics Engineers, SPE Trans., (1962) 231.
52 G. Illing and D. V. Hobe, Z. Anal. Chem., 230, (1967) 418.
53 N. K. J. Symons and E. C. McKannan, Anal. Chem., 31, (1959) 1990.
54 W. H. King, Jr., Res./Dev., April 1969, p. 28.
55 M. G. Kennerley, Polymer, 10, (1969) 833.
56 K. R. Dietrich and C. Conrad, Angew. Chem., 44, (1931) 532.
57 C. F. Roth and J. Mitchell, Jr., Anal. Chem., 28, (1956) 1502.
58 J. Mitchell, Jr., Water, in Treatise on Analytical Chemistry, Pt. II, Vol. 1, Interscience, 1961.
59 G. E. Kellum and J. D. Barger, Anal. Chem., 42, (1970) 1428.

Analytica Chimica Acta, 81 (1976) 265—271

MEASUREMENT OF SULFUR DIOXIDE IN AUTOMOBILE EXHAUSTS AND INDUSTRIAL STACK GASES WITH A COATED PIEZOELECTRIC CRYSTAL DETECTOR

K. H. KARMARKAR, L. M. WEBBER and G. G. GUILBAULT

Department of Chemistry, University of New Orleans, New Orleans, Louisiana 70122 (U.S.A.)

(Received 11th July 1975)

SUMMARY

A portable instrument operating on a car battery and based on a quadrol-coated piezoelectric crystal detector has been successfully used for monitoring sulfur dioxide in auto exhausts and refinery stack gases. The concentrations of sulfur dioxide in the auto exhausts lie in the range 20—50 p.p.m. Up to 300 p.p.m. of sulfur dioxide occurs in the refinery stack gases.

There is an ever-increasing demand for new, simple, and inexpensive methods for measurement and control of sulfur dioxide pollution. Oil refineries, pulp mills, and effluents from a number of other industrial stacks constitute a prime source of emission of SO_2 into the atmosphere. Burning of high sulfur fuels in automobiles is another cause of pollution at the ground level. Coated piezoelectric quartz crystals have recently been used as selective and sensitive air pollution sensors. The principle of such a detector is that the frequency of vibration of the oscillating crystal is decreased by the adsorption of a foreign material on its surface. A gaseous pollutant is selectively absorbed by a coating on the crystal surface, thereby increasing the weight on the crystal and decreasing the frequency of vibration. The decrease in frequency is related to the amount of gas absorbed. King [1] developed sensitive piezoelectric sorption detectors for monitoring hydrocarbons in the atmosphere. Janghorbani and Freund [2] have described the use of these crystals as digital sensors for the sulfur compounds commonly found in pulp mill effluents. Frechette and Fasching [3] have proposed their use in a static system for the detection of sulfur dioxide. Karmarkar and Guilbault [4, 5] developed a sensitive crystal cell design and coatings for the detection of SO_2, NO_2, and NH_3 in the p.p.b. range. In a recent paper, Cheney and Homolya [6] have described a systematic approach for the evaluation of triethanolamine as a crystal coating for sulfur dioxide detection; this coating was reported earlier [4].

The results of field tests of the piezoelectric crystal SO_2 detector developed earlier [4, 5] are described in this paper.

EXPERIMENTAL

Apparatus

Figure 1 shows the experimental set-up for a piezoelectric crystal detector in a flow system for auto exhaust monitoring. The cell design (Fig. 1, F) is similar to the one described earlier [4] and is the most sensitive one for use in a flow system. For monitoring oil refinery effluents, an insensitive cell design was used (Fig. 1, G). The crystals used were 9-MHz AT-cut quartz crystals with silver-plated electrodes on both sides (International Crystal Manufacturing Co., Oklahoma). A low-frequency OX transistor oscillator was built from an oscillator kit obtained from the same company. The oscillator was powered by a Heathkit 1-30-V d.c. variable power supply, Model 1P-28. The applied voltage was kept constant at 9 V. A Systron—Donner frequency meter, Model 8050, with a range of 0—30 MHz and a resolution of 0.1 Hz, was used for a digital read-out of frequency. For monitoring automibile exhaust, commercial nitrogen at a rate of 15 ml min^{-1} was used as the carrier gas. A small fish tank pump was used to supply ambient air (20 ml min^{-1}) for the carrier gas for monitoring oil refinery effluents. A Micronta (Model 22-130) 12-V d.c.—115-V a.c. power inverter connected to a 12-V car battery was used to operate the frequency meter, power supply, and the pump.

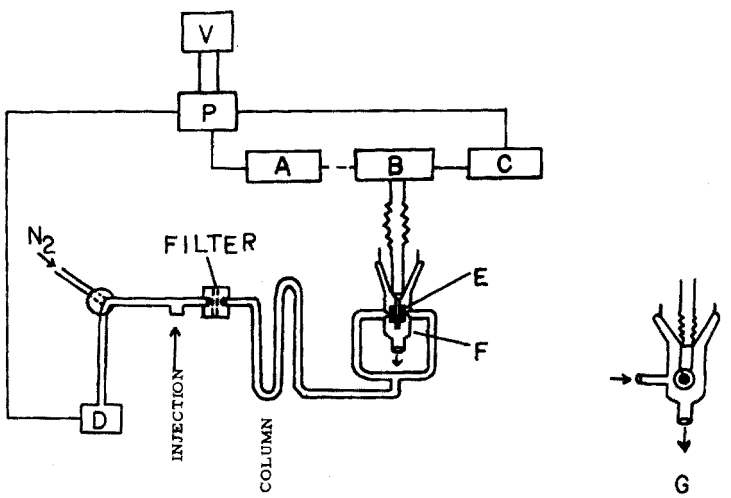

Fig. 1. Experimental set-up with a piezoelectric crystal detector. (A) Frequency meter. (B) Oscillator. (C) Power supply. (D) Fish tank pump. (E) Crystal coating. (F) Detector cell. (G) Insensitive cell. (V) 12-V car battery and (P) 12-V d.c.—115-V a.c. power inverter.

Materials

Two layers of a hydrophobic membrane filter (type ANH 200 pore size 0.2 μm; Gelman Instrument Co., Ann Arbor, Michigan) were placed in the flow system between the injection port and the empty column with the help of a swagelok union.

Sulfur dioxide (Matheson Co., Inc., lecture bottles) was used for calibration purposes.

Crystal coating

Quadrol (Applied Science Lab., Inc.) was used as a crystal coating. A solution of quadrol in chloroform was applied over the entire surface of the electrode, on both sides, with a tiny brush. Chloroform evaporated quickly, leaving the quadrol coating on the crystal. The amount of coating corresponded to a decrease of 11000 Hz in the basic frequency (9 MHz) of the crystal.

RESULTS AND DISCUSSION

The most important drawback with the quadrol-coated piezoelectric crystal detector is that a small response is obtained with atmospheric moisture. In an earlier preliminary report [5], it was shown that a hydrophobic membrane filter (pore size 0.45 μm) was successful in reducing greatly the moisture response of such a piezoelectric crystal detector. Each additional filter layer further reduces the moisture response, and with 4 layers the response for air (moisture) is completely suppressed. Figure 2 shows how the moisture response decreases as the number of filter layers increases. The small

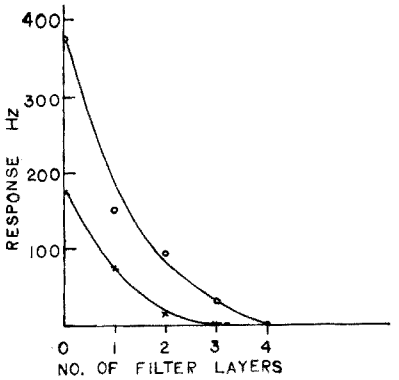

Fig. 2. Effect of number of filter layers on the response of piezoelectric detector to moisture. New cell design; N_2 carrier 15 ml/min^{-1}. (O) 10 ml air injected. (X) 5 ml air injected.

response observed even with 4 filter layers is due to the pressure differential and is observed even with dry air. There is one disadvantage, however, with increasing the number of filter layers: the response for sulfur dioxide also decreases. Thus the response for 10 p.p.m. SO_2 in lab air (10-ml injection) reduced from 375 Hz without any filter to 90 Hz with 4 filter layers. The SO_2/H_2O response ratio may be optimized by using filters of smaller pore size (e.g., 0.2 μm) and two filter layers instead of 4.

Sulfur dioxide in automobile exhaust

The instrument designed operates on a car battery and is portable; the instrument and a small nitrogen tank were mounted on an instrument cart. In studies in a University parking lot, the instrument and the carrier flow were allowed to stabilize for 10—15 min. Two filter layers (pore size 0.2 μm) were used and nitrogen at a rate of 15 ml min^{-1} served as carrier gas. Each car was started, and with the engine idle for 5 min, a 5-ml sample was sucked directly from the exhaust with a syringe, and injected into the instrument; the decrease in frequency was noted for several such injections. The value for the concentration of sulfur dioxide in the exhaust for each car (in p.p.m.) was then obtained from a calibration plot (e.g. Fig. 3). Responses for the exhausts from the cars, A, B, C, and D and the corresponding sulfur dioxide values are given in Table 1. Different qualities of gasoline were used in these cars and that may be a cause of the different sulfur dioxide levels observed in

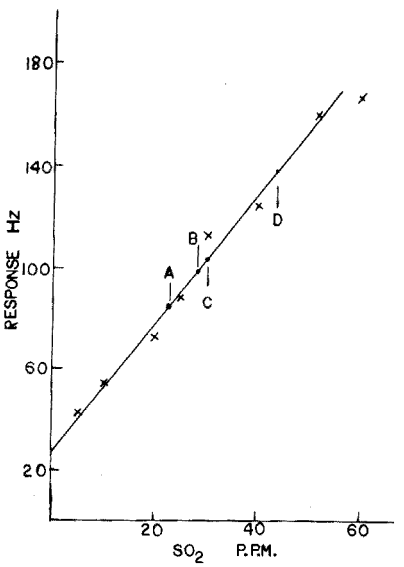

Fig. 3. Calibration plot for SO_2 (5-ml sample injection) on quadrol coated detector. Assay of auto exhausts. A, B, C, and D are the response for the exhausts of 4 cars in Table 1. N_2 carrier, 15 ml min^{-1}. Sensitive cell design (Fig. 1, F).

TABLE 1

Sulfur dioxide concentrations for various auto exhausts

Car	Description	Exhaust Response (Hz)	(p.p.m.) SO_2
A	Dodge Swinger (1973) V8 — pollution control device	84	22.5
B	Opel Kadette (1970) L4 — pollution control device	98	28
C	Plymouth Valiant (1971) S6 — pollution control device	104	30
D	VW Truck (1965) O4 — no pollution control device	138	43.5

the exhausts. The level of sulfur dioxide emission may also depend on the type and the age of the engine and whether or not pollution control devices are present. This method proved to be very fast, sensitive and reproducible.

Stack gas monitoring

The detector cell used for auto exhaust monitoring is very sensitive for sulfur dioxide and the detector response levels off at concentrations larger than 60 p.p.m. For stack gas monitoring, where high concentrations of sulfur dioxide are expected, an insensitive cell design was used (one inlet and one outlet, Fig. 1, G). In earlier work [4, 5], nitrogen served as the carrier gas; this was not practical for field work, and ambient air was therefore used, being provided at a rate of 20 ml min^{-1} by a fish tank pump. Two filter layers (pore size 0.2 μm) helped to reduce the moisture response and also to exclude particulates in the stack gas. These filters lasted for at least a month, and were very easy to replace. The crystal and crystal coating used were the same as for the auto exhaust monitoring. A linear response for sulfur dioxide was obtained for the range of 50—700 p.p.m. (Fig. 4). Two oil refineries in Louisiana were chosen for stack gas monitoring with this detector. Stack effluents were brought to ground level through pipes by an air aspirator, and then were sucked out by rubber bulbs and ultimately by a syringe. A portion (2 ml) of this effluent was injected directly into the instrument and the response observed. The values for sulfur dioxide were simultaneously obtained with a Gastec Bendix pump, SO_2 analyzer for comparison; this method is based on the length of color change (pink to yellow) of phenolphthalein granules in a glass tube as a measure of the sulfur dioxide in stack gas. The results (Table 2) indicate reasonable agreement.

At one refinery there was no burning of fuel and at the other there were two fuel-burning units but there was no provision to bring the effluents to the ground level for our purpose. Fuel burning stacks generally show higher concentrations of sulfur dioxide.

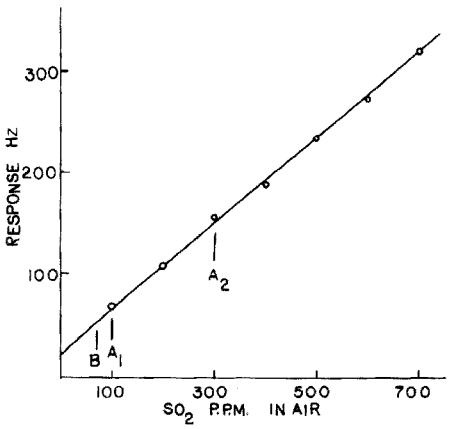

Fig. 4. Calibration plot for SO_2 (2-ml sample injection) for quadrol coated detector. Insensitive cell design (Fig. 1, G) used for refinery stack gas analysis. Samples, A_1, A_2, and B refer to samples of Table 2. Two filters (0.2 μm) used to block moisture. Air carrier gas 20 ml $min.^{-1}$.

TABLE 2

Comparison of results for sulfur dioxide at two refineries with the piezoelectric detector and a color detector

Refinery	Nautre of stack	SO_2 level (p.p.m.)	
		Piezoelectric crystal detector	Gastec bendix pump
A	Vacuum heater stack (A_2)	300	200—300[a]
	Preheater to gas burning (A_1)	100	95
B	CO boiler flue gas	None	—
	Catalyst absorber of gas	70	—

[a]The exact value was not obtainable.

The above results show that a piezoelectric crystal coated with quadrol can be successfully used as a sulfur dioxide sensor for stack gas and auto exhausts analysis. However, effluents from one of the refinery stacks contained a very high concentration of hydrogen sulfide. Unlike sulfur dioxide, the response for this gas was only slowly reversible. From the size of the response, the concentration of hydrogen sulfide was predicted as about 15000 p.p.m. The coulometric method at the refinery had given a value of 1.5 % (v/v) H_2S in the stack gas, which closely corresponds with the crystal detector results. At such high concentrations of hydrogen sulfide, small

concentrations of sulfur dioxide would go undetected by the piezoelectric crystal.

The authors gratefully acknowledge the financial assistance of the Army Research Office (Grant No. DAHCO4-75-G-0098) in carrying out this research project, as well as a free sample supply of hydrophobic membrane filters from the Gelman Instrument Co., Ann Arbor, Michigan.

REFERENCES

1 W. H. King, Jr., Res. Develop., 20 (1969) 28, Environ, Sci. Technol., 4 (1970) 1136.
2 M. Janghorbani and H. Freund, Anal. Chem., 45 (1973) 325.
3 M. W. Frechette and J. L. Fasching, Environ. Sci. Technol., 7 (1973) 1135.
4 K. H. Karmarkar and G. G. Guilbault, Anal. Chim. Acta, 71 (1974) 419; 75 (1975) 111.
5 K. H. Karmarkar, L. M. Webber and G. G. Guilbault, Environ. Lett., 8 (4) (1975).
6 J. L. Cheney and J. B. Homolya, Anal. Lett., 8 (1975) 175.

Analytica Chimica Acta, 81 (1976) 273—295

ELECTROCHEMICAL REDUCTION OF 5,5′-DICHLOROHYDURILIC ACID. MECHANISM AND ANALYTICAL APPLICATIONS

B. M. VISINSKI and GLENN DRYHURST

Department of Chemistry, University of Oklahoma, Norman, Okla. 73069 (U.S.A.)

(Received 14th July 1975)

SUMMARY

The electrochemical reduction of 5,5′-dichlorohydurilic acid has been studied at the dropping mercury electrode (DME) and the pyrolytic graphite electrode (PGE). At the DME the single polarographic reduction wave observed at pH 6—11 involves a direct 4e—$2H^+$ reduction of the carbon—halogen bond to give hydurilic acid and chloride. The state of hydration or ionization of the 5,5′-dichlorohydurilic acid has no effect on the electrochemical reaction. At the PGE, 5,5′-dichlorohydurilic acid shows two voltammetric peaks. Peak I_c, observed between pH 5 and 7, arises from an overall 4e—$2H^+$ reduction of 5,5′-dichlorohydurilic acid via a mechanism that involves initial electron attack at a carbonyl group alpha to a carbon—halogen bond with simultaneous elimination of chloride ion. The peak II_c process involves an initial 2e—$1H^+$ reduction of a partially hydrated form of 5,5′-dichlorohydurilic acid with only one unhydrated halocarbonyl moiety available for reaction. Attack is again via the carbonyl group with simultaneous elimination of chloride and formation of 5-chlorohydurilic acid. A chemical dehydration step then occurs with a rate constant of ca. 0.24 s^{-1} at pH 8.2, with formation of a further reducible halocarbonyl group. This is again reduced in an overall 2e—$2H^+$ reaction to give hydurilic acid and chloride ion. The peak II_c process hence proceeds via an ECE mechanism. The different mechanisms observed for reduction of 5,5′-dichlorohydurilic acid at mercury and pyrolytic graphite electrodes are unusual. Analytical methods have been developed for the polarographic determination of 5,5′-dichlorohydurilic acid via its reduction wave at the DME, and for the voltammetric determination of hydurilic acid via its first oxidation peak at the PGE.

During recent investigations of the electrochemical oxidation of barbituric acid and hydurilic acid at the pyrolytic graphite electrode (PGE) it was found that, in the presence of chloride ion, a major product was 5,5′-dichlorohydurilic acid [1, 2] which is electrochemically reducible at both the dropping mercury electrode (DME) and the PGE. Both the mechanism and analytical utility of the polarographic and voltammetric reduction of 5,5′-dichlorohydurilic acid have been investigated, and the results are reported here.

EXPERIMENTAL

Chemicals

5,5′-Dichlorohydurilic acid was conveniently synthesized by electrochemical oxidation of barbituric acid at the PGE at pH 1 in the presence of chloride ion [1]. Approximately 1 g of barbituric acid (Cyclo Chemical) was dissolved in ca. 200 ml of a chloride buffer (9.5 ml of 12 M hydrochloric acid plus 24.82 g potassium chloride dissolved in 1 l of deionized water) and electrolyzed at several plates of pyrolytic graphite (area $\approx$ 110 cm^2) at 1.00 V with continuous stirring and de-aeration with nitrogen [3]. 5,5′-Dichlorohydurilic acid was formed as a white precipitate which adhered to the electrode surface and was periodically scraped off so that the electrolysis could proceed. After completion of the electrolysis (typically ca. 56—72 h) the 5,5′-dichlorohydurilic acid was recovered by filtration and recrystallized from hot aqueous ethanol as pure 5,5′-dichlorohydurilic acid dihydrate.

The more tedious chemical syntheses of 5,5′-dichlorohydurilic acid and 5,5′-dichloro-1,1′,3,3′-tetramethylhydurilic acid were done by the methods of Biltz and Hamburger [4]. 5-Chlorobarbituric acid and 5,5′-dichlorobarbituric acid were prepared as described by Bock [5]. Hydurilic acid was prepared by the method of Korte et al. [6].

Chloride-free buffer solutions, prepared with an ionic strength of 1.0, were constituted as follows: pH 2.0—8.0, citric acid—NaH_2PO_4—K_2SO_4 (McIlvaine); pH 8.0—9.0, $Na_2B_4O_7$—H_2SO_4—K_2SO_4; pH 10—10.8, $Na_2B_4O_7$—NaOH—K_2SO_4; pH 11—13, NaOH—K_2SO_4. Argon and nitrogen for deoxygenating test solutions were equilibrated with water and used without further purification.

Apparatus

Polarographic curves and voltammograms were obtained with an instrument of conventional operational amplifier design [7] based on a function generator patterned after that of Myers and Shain [8, 9], and were recorded on a Hewlett-Packard Model 7001A X-Y recorder. Fast-sweep voltammograms were recorded on a Tektronix Model 5031 Dual-Beam Storage Oscilloscope equipped with a Tektronix Model C-70 camera. A.c. polarograms utilized a Princeton Applied Research Corporation Model 121 Lock-In Amplifier/Phase Detector as described previously [10]. For a.c. polarography, a frequency of 100 Hz and an amplitude of 10 mV peak-to-peak were employed. A mechanical drop dislodger in conjunction with a dual timing circuit [11] was used to achieve a known and reproducible drop time, normally, 2.00 s.

Cathodic stripping voltammetry at the hanging mercury drop electrode

(HMDE; Metrohm A. G. Model 3 M 503 Microburet Electrode) was performed with a Princeton Applied Research Corporation Model 174 Polarographic Analyzer in the differential pulse mode.

A water-jacketted three-compartment cell, maintained at 25 ± 0.1 °C, with each compartment separated by a medium-porosity sintered glass frit, was used for polarography and voltammetry. Salt bridges, inserted on the counter and reference sides of the frits, were prepared by suspending 4 g of agar (Difco Laboratories) in 90 ml of hot water and then adding 8.5 g of K_2SO_4. A mercury(I) sulfate reference electrode and a platinum foil counter electrode were used. For convenience, all potentials are reported versus the saturated calomel electrode (SCE) at 25 °C on the basis [12] that $E_{SCE} = + 0.4 + E_{MSE}$.

Pyrolytic graphite was obtained from Super-Temp Company, Santa Fe Springs, California. Preparation of the PGE for micro electrodes and for coulometry and mass electrolysis has been described previously [3].

Controlled potential electrolyses were carried out with a Princeton Applied Research Corporation Model 173 Potentiostat. Current integration during controlled potential coulometry was performed with a Hewlett-Packard Model 2212A voltage-to-frequency converter and two Hewlett-Packard Model 5321A electronic counters connected in series. Controlled potential coulometry utilized either a stirred mercury pool electrode (area ca. 3.8 cm^2) or a pyrolytic graphite electrode (area ca. 10.4 cm^2) in a small three-compartment cell with a platinum gauze counter electrode, saturated mercury(I) sulfate reference electrode and a working electrode compartment volume of 25 ml. The usual volume of the electrolysis solution was 15 ml. Macroscale electrolyses were carried out in a large three-compartment cell with the working electrode compartment having a volume of 300 ml. The working electrode was a stirred mercury pool (area ca. 38.5 cm^2). Platinum foil dipping into supporting electrolyte served as the counter electrode. The reference electrode was a Coleman Fiber Tip SCE. The volume of the electrolysis solution was normally 150—200 ml. In all cells, argon or nitrogen was bubbled through the solution. Solutions were stirred magnetically.

Infrared spectra (KBr discs) were recorded on a Beckman IR—8 Spectrophotometer; u.v. spectra were obtained on a Perkin-Elmer Hitachi Model 124 Spectrophotometer using 1.00 cm quartz cells, and mass spectra were recorded on a Hitachi RMU-6E spectrometer.

Polarographic and voltammetric procedure

Test solutions were prepared by dissolving 5,5′-dichlorohydurilic acid directly into the appropriate diluted buffer solution (10.0 ml, ionic strength 0.5). The resultant solution was then transferred to the polarographic cell and de-aerated with nitrogen or argon for 5—10 min.

Coulometric and macroscale electrolysis procedure

For controlled potential coulometry both at the mercury pool and pyrolytic graphite electrodes, 15 ml of ca. 0.5—1.0 mM 5,5′-dichlorohydurilic acid in pH 6 or 7 McIlvaine buffer was placed in the working electrode compartment of the coulometric cell. The solution was stirred and de-aerated with argon until all 5,5′-dichlorohydurilic acid dissolved (ca. 20—30 min). To prevent excessive chemical reaction between 5,5′-dichlorohydurilic acid and mercury, the mercury pool working electrode was added only after dissolution was complete and immediately prior to initiation of the electrolysis. Completion of the electrochemical reaction was confirmed by decrease of the current to a very low level and by the absence of either the 5,5′-dichlorohydurilic acid voltammetric peaks or polarographic wave.

Macroscale electrolysis usually involved reduction of ca. 40 mg of 5,5′-dichlorohydurilic acid in 150—200 ml of 0.5 M KCl, and dissolution was not normally complete before initiation of the electrolysis. A glass electrode was inserted into the solution in the working electrode compartment to monitor the pH change as the electrolysis proceeded, and the pH was maintained at ca. 5.0 by the addition of 0.1 M HCl.

Isolation and characterization of electrolysis product

After complete electroreduction of 5,5′-dichlorohydurilic acid in 0.5 M KCl, the solution was lyophilized to give a tan colored residue. This was dissolved in ca. 5 ml of deionized water and passed through a Dowex 50W-X8 (65 × 3 cm) cation-exchange column in the H^+ form, and eluted with water. The eluate, which exhibited a u.v. absorption peak at 258—259 nm (pH < 4), was collected and again lyophilized. The solid, free of KCl, was redissolved in ca. 5 ml of 0.1 M acetic acid and passed through a Sephadex G-10 column (120 × 2.5 cm) which has been previously washed with deionized water (2 l) and 0.1 M acetic acid (2 l). Fractions (4 ml) were collected and those showing a u.v. absorption peak at 258—259 nm were combined and lyophilized to give a white, fluffy solid. This material was identified as hydurilic acid by comparison of its u.v., mass, and i.r. spectra with those of the authentic compound, and by comparison of its voltammetric behavior with that of hydurilic acid over the pH range 1.9—8.15.

Determination of hydurilic acid

Quantitative analysis for hydurilic acid was carried out at the completion of coulometric experiments at pH 6—7 by transferring a known volume of the electrolysis solution to a polarographic cell and recording three replicate voltammograms at a PGE between 0.15 V and 1.05 V at a sweep rate of 5 mV s^{-1}. The average value of the peak current for peak I_a of hydurilic acid, corrected for background, was used to determine the concentration of

hydurilic acid from a calibration curve prepared with the authentic material over the concentration range 0.2—2 mM.

The voltammetric determination of hydurilic acid was checked by use of a u.v. absorption method, based on its absorption peak at 263 nm at pH 6—7. At pH 6 and 7, $\epsilon_{max} = 3.0 \pm 0.1 \cdot 10^4$ l mole^{-1} cm^{-1}. Typically, a 0.1—0.4 ml aliquot of the coulometric electrolysis product was diluted to 10.0 ml with the appropriate buffer. The u.v. absorbance of at least three test solutions of varying concentration and two standard hydurilic acid solutions were measured for each determination.

Determination of chloride ion

Chloride ion was determined by a modification of the cathodic stripping method of Wilson et al. [13]. A 2.5 or 3.0-ml aliquot of a coulometric electrolysis product solution was diluted to 25.0 ml with 1.8 M H_2SO_4. Chloride ion was oxidized at the HMDE (area 2.22 mm^2) for 2 min at 0.33 V (vs. SCE), the solution being stirred at a fixed rate. At the end of this period both the stirring and electrolysis were stopped. After 10.0 s, the electrolysis potential (0.33 V) was again applied for a further 20.0 s without stirring. Then a cathodic stripping sweep, under differential pulse voltammetric conditions, was initiated at a voltage sweep rate of 2 mV s^{-1}. The average peak current of at least three replicate voltammetric traces was compared with a calibration curve prepared with 0.05—0.2 mM KCl solutions under identical conditions. The counter electrode compartment of the electrochemical cell used in these analyses contained a saturated solution of K_2SO_4, and a saturated mercury(I) sulfate reference electrode was used.

RESULTS AND DISCUSSION

Stability of 5,5'-dichlorohydurilic acid

In order to ascertain whether 5,5'-dichlorohydurilic acid undergoes any hydrolytic dehalogenation, a series of fresh solutions in chloride-free buffers between pH 6—9 were prepared. After 20 min at room temperature, the solutions were acidified with dilute nitric acid, followed by the addition of a few drops of 0.1 M $AgNO_3$. At pH values above 8, a white precipitate of AgCl was observed, indicating loss of chloride ion from 5,5'-dichlorohydurilic acid. Buffer solutions alone gave no reaction with silver(I) under identical conditions. Most of the subsequent electrochemical data was therefore obtained at pH values below 8.

pK_a Values of 5,5'-dichlorohydurilic acid

Between pH 5 and 7, 5,5'-dichlorohydurilic acid exhibits a hypsochromic shift in λ_{max} from 259 nm to 256 nm. Below pH 5 the extreme insolubility

of 5,5′-dichlorohydurilic acid precludes meaningful measurements of λ_{max}. Accordingly pK_{a_1} has a value of 5—7. By analogy with other 5,5-substituted barbituric acids [14, 15] pK_{a_1} corresponds to dissociation of neutral 5,5′-dichlorohydurilic acid to its monoanion. At pH 7—11, λ_{max} for 5,5′-dichlorohydurilic acid occurs at 256 nm, but at higher pH shifts to ca. 280 nm (pH 12—14). By plotting λ_{max} versus pH for pH 6—14 according to the method of Shugar and Fox [14, 16], pK_{a_2} was found to be ca. 11.2 and corresponds to dianion formation.

D. c. polarography

In the pH range 6—10.4, 5,5′-dichlorohydurilic acid (I) exhibits a single polarographic reduction wave at rather positive potentials, the $E_{1/2}$ of which shifts linearly more negative with increasing pH (Fig. 1(A)) according to the equation: $E_{1/2} = 0.458—0.050$ pH. The diffusion current constant for this polarographic wave has an average value of 5.31 ± 0.17 between pH 6 and 10.4 (Fig. 1(B)). The theoretical diffusion current constant for a 4e process

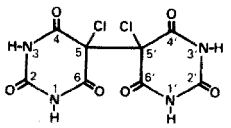

(I)

is 4.44, assuming a value* for the diffusion coefficient of $3.35 \cdot 10^{-6}$ cm^2 s^{-1}. Above pH 8, polarograms of 5,5′-dichlorohydurilic acid decrease in height with time and a second wave appears at very negative potentials (e.g., $E_{1/2} = -1.63$ V at pH 9.23). The rate of decrease of the first wave increases with increasing pH. At times when the second wave is observed, chloride can be detected in solution, which indicates some decomposition of 5,5′-dichlorohydurilic acid. The nature of the product formed by base-catalyzed decomposition of 5,5′-dichlorohydurilic acid was not examined.

The extreme insolubility of 5,5′-dichlorohydurilic acid below pH 6, and its increasing instability at pH values above 8 limited detailed studies to the pH 6—7 range. Between pH 6 and 7 the limiting current is diffusion-controlled as shown, for example, by the constancy of $i_l h_{corr}^{-1/2}$. The temperature coefficient of the limiting current at pH 7, for example is 1.9 % per °C, again typical of a diffusion controlled process [17]. At pH 7 the limiting current for the polarographic wave is linearly proportional to the concentration of 5,5′-dichlorohydurilic acid between 0.025 and 1 mM.

Linear and cyclic sweep voltammetry at the HMDE was not possible because of the reaction between 5,5′-dichlorohydurilic acid and mercury

*This is the value of the diffusion coefficient of hydurilic acid measured in an earlier investigation [2].

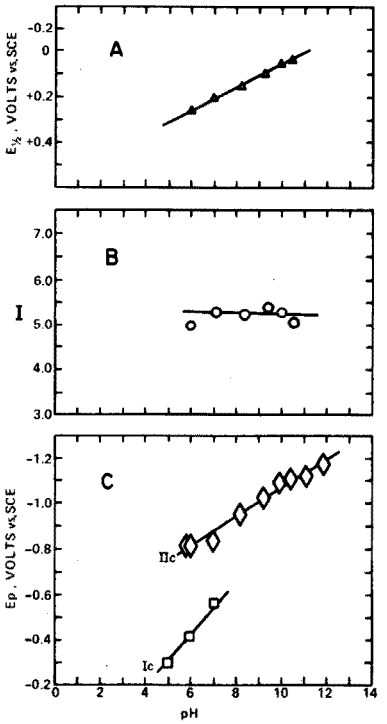

Fig. 1. (A) Variation of the polarographic $E_{1/2}$ with pH. (B) Variation of the diffusion current constant I (= $i_1 / Cm^{2/3} t^{1/6}$) with pH. (C) Variation of the voltammetric peak potentials (E_p) with pH at the PGE for 5,5′-dichlorohydurilic acid. For voltammetry at the PGE the sweep rate was 5 mV s^{-1}; for polarography the sweep rate was 2.5 mV s^{-1}.

(see below). Cyclic voltammograms, for example, at the HMDE gave a number of spiky, irreproducible peaks, none of which appeared to correlate with the polarographic wave observed at the DME.

A.c. polarography

5,5′-Dichlorohydurilic acid shows a single small a.c. peak (E_s = + 0.1 V at pH 6.0) corresponding to the d.c. polarographic wave. Base current depression is evident at potentials more positive than the a.c. peak, indicating that 5,5′-dichlorohydurilic acid is adsorbed at the DME [18].

Controlled potential coulometry

Controlled potential coulometry at a mercury pool electrode was complicated by a rapid reaction of 5,5′-dichlorohydurilic acid with mercury even in the absence of any externally applied potential. Thus, in a chloride-

free McIlvaine buffer at pH 7, a 0.6 mM solution of 5,5′-dichlorohydurilic acid in contact with a stirred pool of mercury turned grey within about 5 min, and after a few more minutes a fine grey precipitate formed. D.c. polarography of this solution showed a small anodic wave caused by the oxidation of chloride [19]. Cyclic voltammetry of the solution at the PGE showed on the initial positive-going sweep, a small oxidation peak, with E_p = 0.41 V,which value corresponds to that expected for hydurilic acid [2]. The u.v. spectrum of a centrifuged solution indicated the presence of a species with λ_{max} = ca. 263 nm which corresponds closely to the value expected for hydurilic acid (263 nm at pH 7). This behavior may be interpreted as a direct reaction of 5,5′-dichlorohydurilic acid with mercury to form an insoluble complex salt along with some further reduction to give hydurilic acid and chloride ion. Hydurilic acid under similar conditions does not react with mercury. Because of this reaction, coulometry was always carried out with a minimal contact time before initiation of electrolysis.

Coulometry of 5,5′-dichlorohydurilic acid at mercury at pH 6—7 gave faradaic *n*-values close to 4 (Table 1). The u.v. spectrum and linear sweep voltammetry of the reduction product were identical with that of hydurilic acid (Table 2).

Macroscale electrolysis of 5,5′-dichlorohydurilic acid at a mercury pool electrode was carried out in 0.5 M KCl (see Experimental) because of the ease of separating the organic electrochemical reaction products from supporting electrolyte. The voltammetric behavior of 5,5′-dichlorohydurilic

TABLE 1

Coulometric *n*-values for the electrochemical reduction of 5,5′-dichlorohydurilic acid (The last two columns give the mole ratio for hydurilic acid/5,5′-dichlorohydurilic acid found by linear sweep voltammetry and u.v. spectrometry at 263 nm)

pH[a]	Electrolysis potential (V vs. SCE)	Initial concn. (mMl^{-1})	*n*-Value	Mole ratio found	
				Voltammetry at PGE	U.v.
6[b]	—0.05	0.616	3.62	1.12	0.95
6[b]	—0.05	0.650	3.53	0.94	0.97
6[b]	—0.05	0.500	3.62	1.08	0.93
6[c]	—0.35	0.493	3.72	0.85	—
6[c]	—0.45	0.460	3.90	0.91	—
6[c]	—0.65	0.500	3.49	0.94	0.99
7[b]	—0.05	0.628	3.72	1.07	0.96
7[b]	—0.05	0.626	3.97	0.99	0.96
7[c]	—0.85	0.974	3.65	0.92	0.94

[a] McIlvaine buffer.
[b] Stirred mercury pool electrode; area = 3.8 cm^2.
[c] Pyrolytic graphite electrode; area = 10.4 cm^2.

TABLE 2

Comparison of the u.v. spectra and voltammetric oxidation peak potentials for hydurilic acid and the product of electrochemical reduction of 5,5′-dichlorohydurilic acid at pH 6 and 7 at mercury

pH	Electrochemical product			Hydurilic acid		
	Peak potential, (V vs. SCE)		λ_{max} (nm)	Peak potential, (V vs. SCE)		λ_{max} (nm)
	I_a	III_a[a]		I_a	III_a[a]	
6	0.44	0.97	263	0.45	0.98	263
7	0.42	0.90	263	0.41	0.89	263

[a] Very close to background discharge.

acid in this medium was the same as that observed in McIlvaine buffers of pH ca. 6. After completion of the electrolysis, KCl was removed by ion-exchange chromatography. The product was then purified by column chromatography on Sephadex G-10 (see Experimental). The u.v., i.r. and mass spectra (Fig. 2) of the isolated reduction product were identical with those of authentic hydurilic acid.

Analysis of product solutions obtained after coulometry of 5,5′-dichlorohydurilic acid (Table 1) indicated an almost quantitative formation of hydurilic acid. The amount of chloride ion produced during electrolysis was determined by cathodic stripping voltammetry [13] at the HMDE; 95 % of the theoretical amount of chloride ion (2 moles Cl^-/mole of 5,5′-dichlorohydurilic acid) was found.

Linear and cyclic sweep voltammetry at the PGE

Linear sweep voltammetry of 5,5′-dichlorohydurilic acid at the PGE indicates the presence of two reduction peaks (Fig. 3). Peak I_c appears between pH 5 and 7 (E_p = 0.3—0.12 pH) (Fig. 1(C)). At pH 6 and above, peak II_c appears, and this grows in height at the expense of peak I_c between pH 6 and 7. The peak potential for peak II_c is pH-dependent; E_p (pH 6—11.9) = —0.423—0.064 pH. Above pH 7, only peak II_c is observed. The insolubility of 5,5′-dichlorohydurilic acid precluded voltammetric studies below pH 5.

The experimental peak current function, $i_p/ACv^{1/2}$, for peak I_c of 5,5′-dichlorohydurilic acid at pH 7 had a value of 868.4 ± 64 μA cm^{-2} (mM l^{-1}) $V^{-1/2}$ s$^{1/2}$ which was independent of sweep rate between 0.01 and 1.0 V s^{-1}. This experimental peak current function is close to that expected for a totally irreversible 4e diffusion-controlled process (1091 μA cm^{-2} mM^{-1} l $V^{-1/2}$ s$^{1/2}$) calculated from the equation [20]

$$\frac{(i_p)_{irrev}}{ACv^{1/2}} = 2.98 \times 10^5 \; n \; (\alpha n_a)^{1/2} D^{1/2} \qquad (1)$$

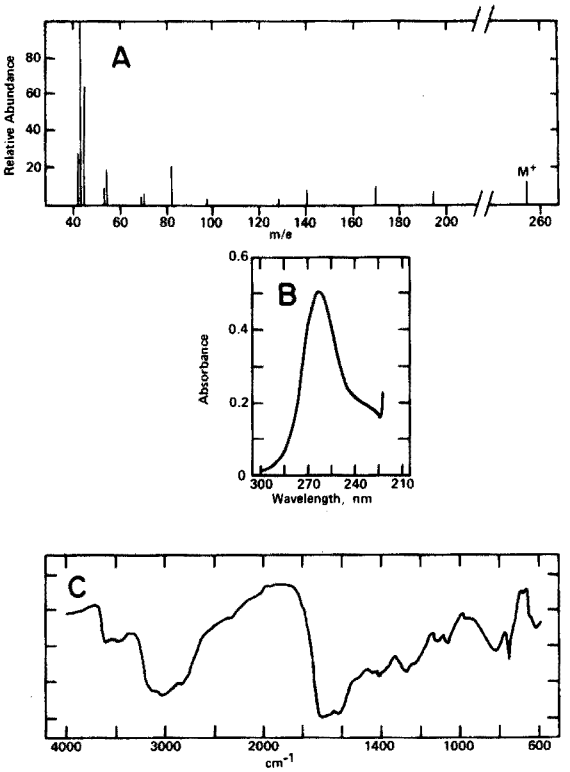

Fig. 2. Mass (A), u.v. (B) and i.r. (C) spectra of hydurilic acid formed on electrochemical reduction of 5,5′-dichlorohydurilic acid. Mass spectrum obtained at 240 °C and an ionizing voltage of 70 eV. I.r. (KBr disc). U.v. spectrum obtained at pH 7.0 (McIlvaine buffer).

where all terms have their usual electrochemical significance. The value of αn_a was computed from the expression [21]

$$E_p - E_{p/2} = -0.048/\alpha n_a \quad (2)$$

Between pH 6 and 7 the experimental value of αn_a varied from 0.17 to 0.27 with an average value of 0.25.

The invariance of the experimental peak current function for peak I_c with voltage sweep rate and the reasonably close agreement with the theoretical peak current function are strong evidence that the peak I_c process is an uncomplicated, totally irreversible diffusion-controlled 4e reaction at pH 6–7.

Cyclic voltammetry of 5,5′-dichlorohydurilic acid at the PGE at pH 6 and 7 shows two reduction peaks (peaks I_c and II_c) on the initial sweep toward negative potential. On the reverse sweep, three oxidation peaks are observed (peaks I_a, II_a and III_a) (Fig. 4(A, B)). Under no conditions did

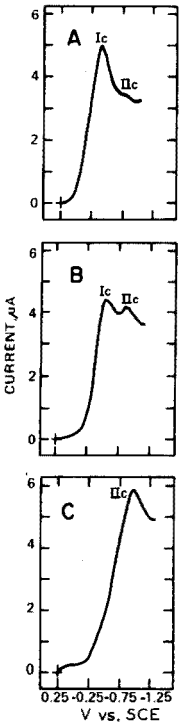

Fig. 3. Linear sweep voltammograms of ca. 0.5 mM solutions of 5,5′-dichlorohydurilic acid at the PGE. (A) pH 6.0, (B) pH 7.0 and (C) pH 8.2. All solutions were chloride-free McIlvaine buffers. Sweep rate in all cases 5 mV s^{-1}.

peaks I_c or II_c exhibit any corresponding reversible oxidation peak under cyclic voltammetric conditions. Oxidation peaks I_a, II_a and III_a were not observed unless reduction peaks I_c and II_c had first been scanned, i.e., peaks I_a, II_a and III_a are due to oxidation of the products of the peak I_c and II_c processes.

The peak potentials for peaks I_a and II_a were pH-dependent. Under cyclic voltammetric conditions at a sweep rate of 50 mV s^{-1} the peak potential for peak I_a is given by E_p (pH 5—12) = 0.595—0.032 pH; while for peak II_a, E_p (pH 6—9.5) = 0.96—0.028 pH. Peak III_a was generally observed as an inflection very close to background discharge (see Fig. 4 A, B) and hence precise peak potential data could not be obtained. Nevertheless, at pH 6, E_p for peak III_a was = ca. 1.07 V, and, at pH 7, E_p = ca. 0.99 V.

Under cyclic voltammetric conditions, peak I_a showed a small, reversible reduction peak (peak I_c', Fig. 4 (A, B)). This peak increased in height relative to peak I_a with increasing sweep rate.

Comparison of the cyclic voltammetric curves of hydurilic acid (Fig. 4 (C)) with that of 5,5′-dichlorohydurilic acid (Fig. 4 (B)) showed that peaks

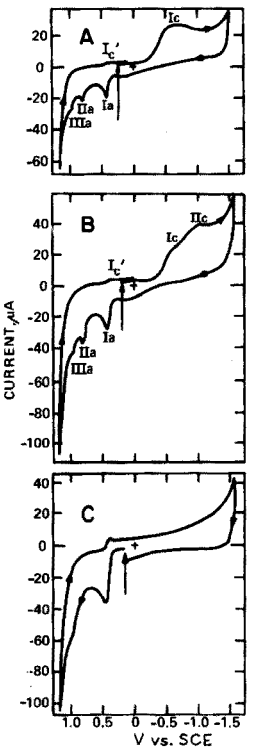

Fig. 4. (A, B): Cyclic voltammograms of ca. 0.5 mM 5,5'-dichlorohydurilic acid at the PGE in (A) McIlvaine buffer pH 6.0, (B) McIlvaine buffer pH 7.0, (C) 0.5 mM hydurilic acid in McIlvaine buffer pH 7.0. Arrow indicates starting potential. Initial sweep direction towards negative potentials for (A) and (B) and towards positive potentials for (C). Sweep rate 200 mV s^{-1} ; PGE area 0.122 cm^2 .

corresponding to oxidation peaks I_a and III_a are present on the first positive-going sweep of hydurilic acid and a small reduction peak corresponding to peak I'_c is observed on the reverse sweep. This behavior confirms that hydurilic acid is a major product of the peak I_c and/or II_c processes. (The mechanisms associated with the various voltammetric peaks of hydurilic acid will be discussed elsewhere [2]).

Constant potential electrolysis and cyclic voltammetric studies of 5,5'-dichlorohydurilic acid at a micro PGE were carried out to determine the relationship between peaks I_a, II_a and III_a and the peak I_c and II_c processes. At pH 7, for example, a constant potential of —0.45 V was applied at the PGE for 3s. This potential corresponds to the rising portion of peak I_c. After this electrolysis time a voltage sweep towards positive potentials was applied when peak I_a is clearly present (Fig. 5 (A)). Peak III_a could often be observed under these conditions but only as a very poorly defined inflection on background discharge. If a constant potential of —1.10 V

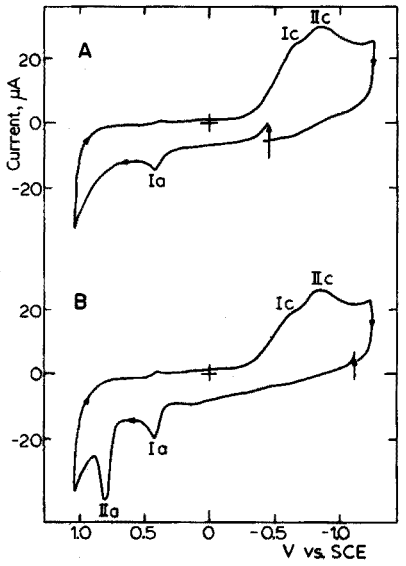

Fig. 5. Constant potential electrolysis of 0.5 mM 5,5'-dichlorohydurilic acid in McIlvaine buffer pH 7 at (A) −0.45 V and (B) −1.10 V for 3s, followed by a positive-going voltage sweep at 200 mV s^{-1}. Large arrow indicates initial 3s electrolysis potentials.

was initially employed, where both peaks I_c and II_c processes can occur, then peaks I_a, II_a and often III_a were observed on the subsequent voltage sweep with peak II_a larger than peak I_a (Fig. 5 (B)). Accordingly, the species giving rise to peak II_a must be formed in the peak II_c process. Similar behavior to that reported above at pH 7 was observed at pH 6.

Potentiostatic studies

In order better to understand the nature of the peak I_c and peak II_c processes, potentiostatic current—time curves were measured between pH 6 and 9. Under potentiostatic conditions, the expression for the instantaneous current, i_t, in microamperes, at a plane electrode under semi-infinite linear diffusion control is given by the Cottrell equation [22]

$$i_t = \frac{nFAD^{1/2}C}{\pi^{1/2}t^{1/2}} \tag{3}$$

where all terms have their usual electrochemical significance. This equation predicts that $i_t t^{1/2}/C$ should be a constant for a simple diffusion-controlled process. At pH 6, where peak I_c is the predominant process, the value of $i_t t^{1/2}/C$ at a constant potential of −0.60 V was essentially constant (49.7 μA $s^{1/2}$ (mM l^{-1})$^{-1}$) and of the same magnitude as that predicted for a 4e process (48.6 μA $s^{1/2}$ (mM l^{-1})$^{-1}$). At pH values 8—9, where the peak II_c

process is predominant, at potentials more negative than peak II_c, the value of $i_t t^{1/2}/C$ at short time periods (ca. 0.5 s) was close to that expected for a 2e process, while at longer times $i_t t^{1/2}/C$ increased and approached that expected for a 4e process. One possible explanation for such current–time behavior for the sum of the peak I_c and II_c processes at pH 8–9 is a process in which a chemical reaction is interposed between two charge transfer steps, i.e., an ECE mechanism (see below).

Hydration of 5,5′-Dichlorohydurilic acid

In view of the measured pK_{a_1} of 5,5′-dichlorohydurilic acid (ca. 6) it was suspected that peak I_c might be due to reduction of the neutral compound and peak II_c to reduction of its monoanion. The potentiostatic behavior at, for example, pH > 7 at potentials more negative than peak II_c however, suggested an ECE process which is not easy to rationalize on the basis of simple acid–base equilibria. The possibility that acid–base processes were responsible for the peak I_c–II_c behavior was eliminated by a brief study of 5,5′-dichloro-1,1′,3,3′-tetramethylhydurilic acid at the PGE. This compound gives two voltammetric peaks: peak I_c with E_p (pH 6–7) = −0.40 ± 0.03 V, and peak II_c with E_p (pH 6–10) = 0.86 ± 0.03 V at a sweep rate of 5 mV s^{-1}. Such behavior is very similar to that observed for the non-methylated compound except for the pH-independence of the peaks. Above pH 7, 5,5′-dichloro-1,1′,3,3′-tetramethylhydurilic acid decomposed to some extent within ca. 20 min since chloride was detected in solution. Since 5,5′-dichloro-1,1′,3,3′-tetramethylhydurilic acid cannot exhibit acid–base dissociation or, for that matter, keto–enol tautomerism, it was concluded that such processes were not responsible for the observed voltammetric behavior of 5,5′-dichlorohydurilic acid. The possibility of any tautomeric keto–enol equilibria of the latter compound is also unlikely since the keto form of barbiturates is always predominant [23, 24]. In addition the u.v. absorption spectrum of 5,5′-dichlorohydurilic acid (e.g. λ_{max} = 256 nm at pH 9.2) is essentially the same as that of 5,5′-dichloro-1,1′,3,3′-tetramethylhydurilic acid (λ_{max} = 258 nm at pH 9.2) indicating the presence of the same chromophore system in both molecules.

Accordingly, it was concluded that hydration processes are responsible for the observed voltammetry of 5,5′-dichlorohydurilic acids*. Molecules with chloro substituents alpha to a carbonyl group undergo extensive hydration of the carbonyl group [25, 26] The electron-withdrawing ability of the chloro group adjacent to the carbonyl appears to increase the positive charge on the carbonyl carbon, making it more susceptible to nucleophilic attack by water [27].

The existence of carbonyl hydration can often be demonstrated by comparing the values of ϵ_{max} and of λ_{max}, corresponding to the weak

*Subsequently 5-chloro- and 5,5-dichlorobarbituric acid have been shown to exhibit similar hydration effects.

$n \rightarrow \pi^*$ absorption band at 280 nm ($\epsilon \approx 50$ l mole^{-1} cm^{-1}), measured in non-aqueous solvents and in aqueous solution as described by Bell [28]. Unfortunately, sufficiently concentrated solutions of 5,5′-dichlorohydurilic acid could not be prepared to observe the $n \rightarrow \pi^*$ band at 280 nm. In addition, the intense band at ca. 256 nm ($\epsilon_{max} \approx 10^4$ l mole^{-1} cm^{-1}), presumably from a $\pi \rightarrow \pi^*$ or $n \rightarrow \sigma^*$ transition, would mask the weak band at 280 nm.

Nevertheless, in the absence of acid—base or keto—enol processes and on the basis of further information (see below) it was concluded that carbonyl hydration is important in understanding the voltammetry of 5,5′-dichlorohydurilic acid.

Coulometry and macroscale electrolysis at the PGE

Controlled potential coulometry of 5,5′-dichlorohydurilic acid at the PGE at pH 6—7 gave faradaic n-values close to 4 (Table 1). The products formed, accounting for $\geqslant 90$ % of the starting material, were hydurilic acid and chloride ion (Table 1).

REACTION SCHEME

The behavior of 5,5′-dichlorohydurilic acid at mercury and graphite electrodes is different. Thus, at the DME, only a single reduction wave at positive potentials is observed and this decreases in height only when some decomposition of the compound has taken place. Hydration does not appear to be important in the electrochemical behavior of 5,5′-dichlorohydurilic acid at mercury. There is also a direct reaction between 5,5′-dichlorohydurilic acid and mercury which results in formation of chloride ion and hydurilic acid even without any applied potential at the mercury.

At the PGE, two voltammetric peaks are observed. Peak I_c occurs at ca. —0.5 V to —0.6 V negative of the wave observed at the DME. The formation of two peaks is pronounced at pH 6—7, a pH value where little or no decomposition of 5,5′-dichlorohydurilic acid occurs for several hours.

At both mercury and pyrolytic graphite electrodes the overall reaction involves 4e with virtually quantitative formation of hydurilic acid and chloride ion.

Because of the differences in potentials for the electrochemical reduction of 5,5′-dichlorohydurilic acid at the DME and PGE and the obvious effects of hydration processes at the latter electrode, different reaction schemes are proposed to occur at mercury and graphite.

Reduction scheme at mercury electrodes

5,5′-Dichlorohydurilic acid clearly gives a single, 4e, pH-dependent polarographic reduction wave at the DME. An experimental plot of

E_{DME} vs. log $i/i_d - i$ gives an average slope of −0.0216 V compared with a value of −0.0148 V expected for a reversible 4e process; i.e., the wave is irreversible.

The proposed electrochemical reaction scheme therefore involves a straightforward 4e—2H$^+$ reduction of 5,5′-dichlorohydurilic acid (I, Fig. 6) below pH 7 or its monoanion (I_a, Fig. 6) above pH 7 to the monoanion of hydurilic acid (II_a, Fig. 6) along with formation of chloride ion [2]. This reaction hence assumes a direct attack on the carbon—halogen bond regardless of the state of hydration or dissociation of 5,5′-dichlorohydurilic acid. The observed interaction between 5,5′-dichlorohydurilic acid and mercury might in some way facilitate direct carbon—halogen bond fission.

Kinetic studies and reduction scheme at the PGE

The electrochemical reduction of 5,5′-dichlorohydurilic acid to hydurilic acid and chloride ion at the PGE at pH 6—9 is, overall, an irreversible 4e reaction. The pH-dependent peak I_c is observed at pH 5—7 and is the predominant peak over this pH range. Above pH 6, pH-dependent peak II_c appears, and above pH 7, becomes the only reduction peak of 5,5′-dichloro-

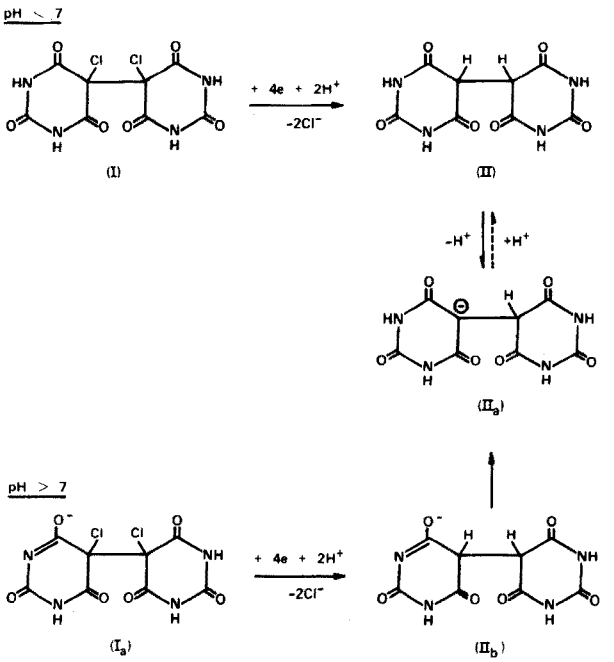

Fig. 6. Proposed reaction scheme for the electrochemical reduction of 5,5′-dichlorohydurilic acid at mercury electrodes.

hydurilic acid. Below pH 7, potentiostatic experiments showed that peak I_c is a straightforward, diffusion controlled 4e process. However, similar experiments above pH 7 at potentials more negative than peak II_c, showed that the observed current is close to the value expected for a 2e reaction at short time (ca. 0.5 s) and gradually increases to the value expected for a 4e reaction. Comparison of the voltammetry and spectra of 5,5′-dichlorohydurilic acid with those of 5,5′-dichloro-1,1′, 3,3′-tetramethylhydurilic acid suggests that hydration phenomena influences the observed behavior. The known facile hydration of other α-halocarbonyl compounds supports this conclusion.

Hydration of a carbonyl group alpha to a chloro substituent could affect the electrochemical reduction of 5,5′-dichlorohydurilic acid only if the carbonyl group is directly involved in the electrode reaction. The electrochemical reduction of some 2-halocyclohexanones [29] and α-bromoketosteroids [30] has been proposed to proceed by an initial electron attack at the carbonyl groups with simultaneous elimination of halide ion.

Of the many possible hydrated forms of 5,5′-dichlorohydurilic acid, the three structures below (IV, V, VI) might be expected to have a direct effect on the electrode reaction at pH 7—11 (where the compound exists as a monoanion).

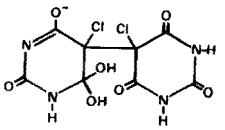

(IV)

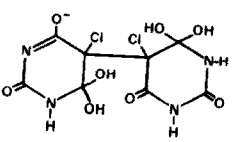

(V)

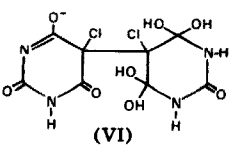

(VI)

Below pH 7, the peak I_c process probably arises from a direct $4e—2H^+$ reduction of unhydrated 5,5′-dichlorohydurilic acid (neutral or monoanionic species) (I, Fig. 7) at the carbonyl group located at the 4,4′,6 or 6′-positions with simultaneous elimination of chloride to give the enolic form of hydurilic acid (III, Fig. 7). This would rapidly rearrange to the more stable keto form [30] (II, Fig. 7).

The peak II_c process may arise from reduction of a hydrated form of 5,5′-dichlorohydurilic acid. It is not possible to specify the exact forms of the hydrated compound, but, for illustrative purposes, structure IV will be employed. Electrochemical reduction of the hydrated form of 5,5′-dichlorohydurilic acid (peak II_c) below pH 7 takes place at more negative potential than for the non-hydrated species (peak I_c) and this may result

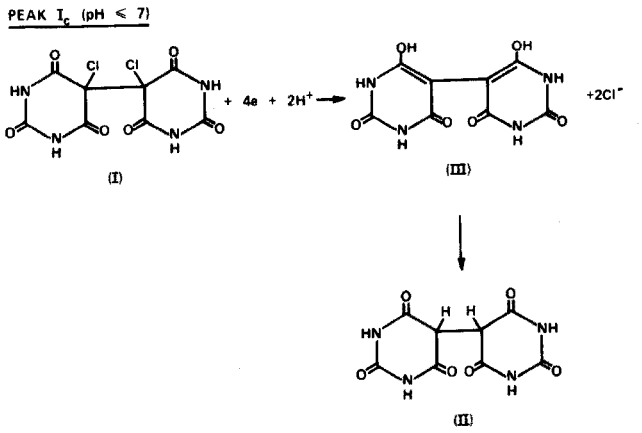

Fig. 7. Proposed electrochemical reduction scheme for 5,5′-dichlorohydurilic acid peak I_c process at the PGE.

from decreased accessibility of the non-hydrated α-halocarbonyl moiety through the introduction of a gem diol group on carbonyl hydration. This could make it more difficult for the hydrated molecule to obtain a proper orientation at the electrode surface for reduction to occur.

The basic reaction scheme proposed for the peak II_c process is an initial $2e—1H^+$ reduction of the hydrated monoanion of 5,5′-dichlorohydurilic acid (e.g., IV, Fig. 8) to the enolate VII followed by rearrangement to a hydrate of 5-chlorohydurilic acid (VIII, Fig. 8). This compound is not reducible since both carbonyl groups alpha to the chloro group are removed by ionization or hydration. Further electrochemical reduction requires dehydration of VIII to the non-hydrated form of 5-chlorohydurilic acid (IX, Fig. 8). This is then further reduced in an overall $2e—H^+$ reaction to the enol X, which rapidly rearranges to the monoanion of hydurilic acid (XI ⇆ XII, Fig. 8). The pK_{a_1} of hydurilic acid is 4.1 [ref. 2]. Assuming that the enolization step (VII → VIII, Fig. 8) is very rapid, the reaction scheme proposed is a typical ECE process. That such a reaction scheme takes place is clearly demonstrated by potentiostatic experiments.

In general terms, the ECE process can be represented as

$$A + n_1 e \rightarrow B \overset{k_f'}{\rightarrow} C \xrightarrow{+n_2 e} D \qquad (4)$$

At a plane electrode, regardless of whether the coupled chemical reaction (B → C, eqn. 4 or VIII → IX, Fig. 8) is reversible or irreversible, the normalized instantaneous current is given by the equation [31]

$$i/FAD^{1/2}C = \frac{n_1 + n_2\ (1—e^{-k_f t})}{t^{1/2}\pi^{1/2}} \qquad (5)$$

where k_f is the homogeneous rate constant for the interposed chemical

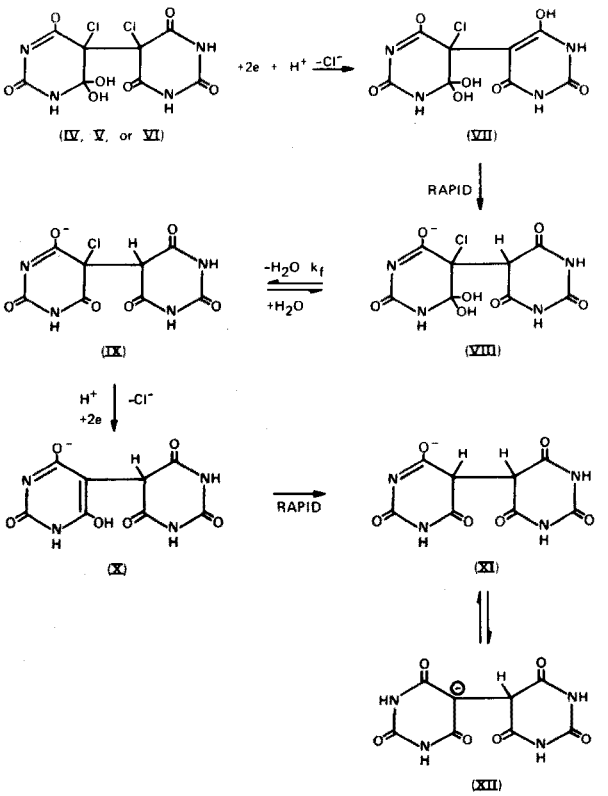

Fig. 8. Proposed electrochemical reduction scheme for 5,5′-dichlorohydurilic acid peak II_c process at the PGE.

reaction, s^{-1}, and all other terms have their usual or obvious electrochemical significance. By measuring the current versus time curves at a PGE under potentiostatic conditions at a potential more negative than peak II_c a plot of $i/FAD^{1/2}C$ vs. $t^{-1/2}$ can be obtained. A typical curve obtained at, for example, pH 8.21 is shown in Fig. 9. At short times the observed current corresponds closely to that expected for a 2e diffusion controlled process, but at longer times there is a transition to a current corresponding to a 4e process, i.e., to both 2e charge transfer steps (Fig. 8, eqn. 4). The homogeneous rate constant, k_f, was calculated from the slope of a plot of $\frac{\ln 1-i\sqrt{\pi t}}{FAD^{1/2}c/n_2} - n_1$ vs. t. At pH 8.21 the k_f value so computed had a value of 0.24 s^{-1} (Fig. 8). Such potentiostatic results clearly support an ECE reaction such as that shown in Fig. 8.

The cyclic voltammetry of 5,5′-dichlorohydurilic acid (Figs. 4 and 5) can also be rationalized adequately on the basis of the reaction schemes presented

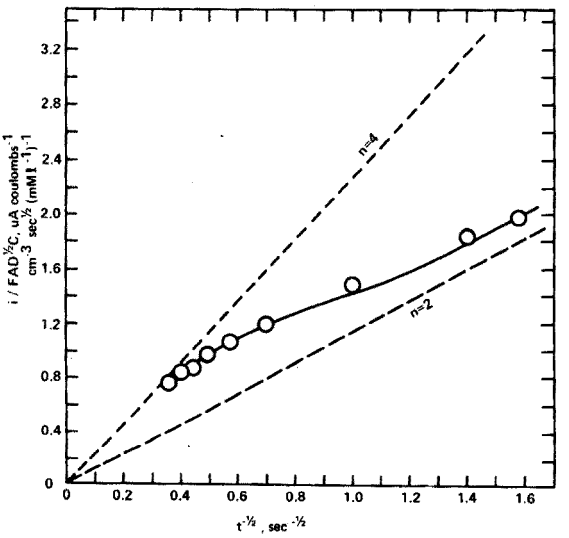

Fig. 9. Comparison of the experimental and theoretical normalized current—time curves for the peak II_c electrochemical reduction of 5,5'-dichlorohydurilic acid at the PGE at pH 8.21. Open circles represent experimental values. Solid line is the theoretical curve for $k_f = 0.24\ s^{-1}$. Dotted lines represent theoretical curves for diffusion-controlled 2e and 4e processes calculated from the Cottrell equation.

in Figs. 7 and 8. Thus, provided that the electrode potential is such that only peak I_c can occur (Fig. 5A), then on sweeping towards positive potentials only peaks I_a and III_a are observed through the oxidation of hydurilic acid (II, II_a Fig. 6). Electrolysis at potentials where both the peak I_c and II_c processes can occur simultaneously (Fig. 5B) results in the appearance of the hydurilic acid oxidation peaks (peaks I_a and III_a) and peak II_a. If the reaction scheme shown in Fig. 8 is correct, some 5-chlorohydurilic acid (VIII, Fig. 8) should remain for a short period at the electrode surface. It is proposed that peak II_a is due to electrochemical oxidation of the latter compound. We were unable to synthesize 5-chlorohydurilic acid chemically [2]. However, a very closely related compound, 5-chlorobarbituric acid (XIII), which would be expected to exhibit very similar behavior to 5-chlorohydurilic acid has been examined [1]. This compound

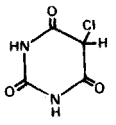

(XIII)

shows a single oxidation peak at the PGE, E_p (pH 6—9.2) = 0.91—0.023 pH, at very similar potential to peak II_a observed on cyclic voltammetry of

5,5′-dichlorohydurilic acid, E_p (pH 6—9.2) = 0.96—0.028 pH. These peak potentials were obtained at a sweep rate of 50 mV s^{-1}.

Analytical utility of the electrochemical behavior of 5,5′-dichlorohydurilic acid and hydurilic acid

One of the reasons for studying the electrochemistry of 5,5′-dichlorohydurilic acid was to develop methods for its determination and for the determination of hydurilic acid, for which methods were not available. These compounds are of interest in studies of the electrochemistry of barbiturates [1, 2, 32].

5,5′-Dichlorohydurilic acid is best determined by its single polarographic wave at the DME at pH 6—7. Typical i_l vs. C curves are linear between ca. $2.5 \cdot 10^{-5}$ and 10^{-3} M 5,5′-dichlorohydurilic acid. Because of the rather positive half-wave potential for this compound, the other chlorobarbituric acid derivatives examined do not interfere with the polarographic determination of 5,5′-dichlorohydurilic acid. The voltammetric reduction peaks of 5,5′-dichlorohydurilic acid at the PGE are not sufficiently reproducible for analytical purposes.

Between pH 1 and 12, hydurilic acid shows up to four oxidation peaks at the PGE [2], but only the first peak (peak I_a, see Fig. 4 (C)) is suitable for analytical purposes. The analytical methodology for hydurilic acid has been described earlier (see Experimental). Linear peak current (for peak I_a) versus concentration curves were obtained for hydurilic acid solutions over the entire pH range. Some typical data at pH 6 and 7 are shown in Fig. 10.

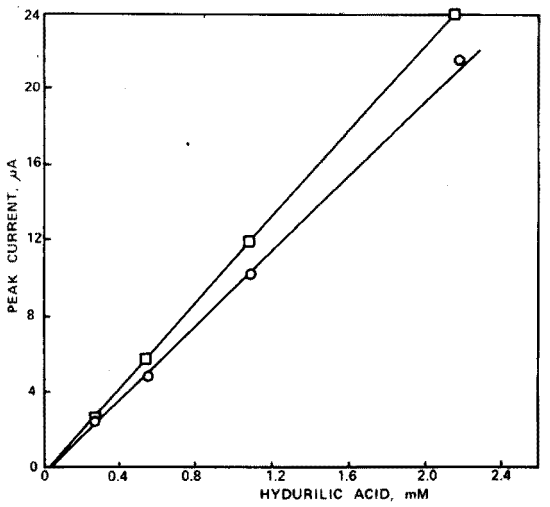

Fig. 10. Linear peak I_a current versus concentration relationship for hydurilic acid at the PGE. Open circles refer to results in McIlvaine buffer pH 6, squares refer to McIlvaine buffer pH 7. PGE area: 0.122 cm^2. Voltage sweep rate: 5 mV s^{-1}.

Hydurilic acid can be determined quantitatively from its u.v. absorption spectrum, (λ_{max} = 259 nm below pH 4 and 263 nm above pH 4), Beer's Law being obeyed for solutions more dilute than ca. 3×10^{-5} M. The electroanalytical method has one major advantage over the u.v. method, since 5,5′-dichlorohydurilic acid interferes in the u.v. absorptiometric determination of hydurilic acid. Thus, λ_{max} for 5,5′-dichlorohydurilic acid below pH 6 is 262.5 nm; at pH 6—11, λ_{max} is 256 nm. However, the latter compound does not interfere with the voltammetric determination of hydurilic acid. Correspondingly, hydurilic acid does not interfere in the polarographic determination of 5,5′-dichlorohydurilic acid. The reproducibility of the polarographic determination of 5,5′-dichlorohydurilic acid at the DME and the voltammetric determination of hydurilic acid at the PGE is ca. ±5 %.

The authors acknowledge the assistance of Mr. Henry F. Nichols, Mr. James L. Owens and Dr. S. Kato in some aspects of this study. The authors also thank the National Science Foundation for partial financial support of this work.

REFERENCES

1 S. Kato and G. Dryhurst, J. Electroanal. Chem. Interfacial Electrochem. 62 (1975) 415.
2 S. Kato, B. Visinski and G. Dryhurst, J. Electroanal. Chem. Interfacial Electrochem. in press.
3 D. L. McAllister and G. Dryhurst, J. Electroanal. Chem. Interfacial Electrochem., 47 (1973) 479.
4 H. Biltz and T. Hamburger, Chem. Ber., 49 (1916) 655.
5 W. Bock, Chem. Ber., 56 (1923) 1222.
6 F. Korte, W. Paulus and K. Störiko, Ann. Chem., 63 (1958) 619.
7 G. Dryhurst, M. Rosen and P. J. Elving, Anal. Chim. Acta, 42 (1968) 143.
8 R. L. Myers and I. Shain, Chem. Instr., 2 (1969) 203.
9 D. L. McAllister and G. Dryhurst, Anal. Chim. Acta, 64 (1973) 121.
10 D. L. McAllister and G. Dryhurst, Anal. Chim. Acta, 58 (1972) 273.
11 E. R. Brown, T. E. McCord, D. E. Smith and D. D. Deford, Anal. Chem., 38 (1966) 1119.
12 J. J. Lingane, Electroanalytical Chemistry, Interscience, New York, 2nd edn., 1966, p. 363.
13 G. Colovos, G. S. Wilson and J. L. Moyers, Anal. Chem., 46 (1974) 1051.
14 J. J. Fox and D. Shugar, Bull. Soc. Chim. Belg., 61 (1952) 44.
15 L. A. Gifford, W. P. Hayes, L. A. King, J. N. Miller, D. T. Burns and J. W. Bridges, Anal. Chem., 46 (1974) 94.
16 D. Shugar and J. J. Fox, Biochim. Biophys. Acta, 9 (1952) 199.
17 L. Meites, Polarographic Techniques, Wiley, New York, 2nd edn., 1965, pp. 132—133, 140.
18 B. Breyer and H. H. Bauer, Alternating Current Polarography and Tensammetry, Interscience, New York, 1963, pp. 267—269.
19 L. Meites, Polarographic Techniques, Wiley, New York, 2nd edn., 1965, pp. 213—214.
20 R. S. Nicholson and I. Shain, Anal. Chem., 36 (1964) 706.
21 R. N. Adams, Electrochemistry at Solid Electrodes, Dekker, New York, 1969, p. 136.

22 P. Delahay, New Instrumental Methods in Electrochemistry, Interscience, New York, 1954, p. 51.
23 J. March, Advanced Organic Chemistry: Reactions, Mechanisms and Structure, McGraw—Hill, New York, 1968, pp. 59, 457.
24 A. R. Katritzky and J. M. Lagowski, in A. R. Katritzky (Ed.), Advances in Heterocyclic Chemistry, Vol. 1, Academic Press, New York, 1963, pp. 375—376.
25 D. Quoc-Quan, Compt. Rend., 251 (1960) 2927.
26 P. J. Elving and C. E. Bennett, J. Electrochem. Soc,, 101 (1954) 520.
27 J. Hine, Physical Organic Chemistry, McGraw-Hill, New York, 1962, p. 249.
28 R. P. Bell in V. Gold (Ed.), Advances in Physical Organic Chemistry, Vol. 4, Academic Press, 1966, pp. 1—29.
29 A. M. Wilson and N. L. Allinger, J. Amer. Chem. Soc., 83 (1961) 1999.
30 V. Delaroff, M. Bolla and M. Legrand, Bull. Soc. Chim. Fr., (1961) 1912.
31 G. S. Alberts and I. Shain, Anal. Chem., 35 (1963) 1859.
32 S. Kato and G. Dryhurst, work in progress.

Analytica Chimica Acta, 81 (1976) 297—303

THE DETERMINATION OF CADMIUM IN GEOLOGICAL MATERIALS BY FLAMELESS ATOMIC ABSORPTION SPECTROMETRY

HENRY GONG and NORMAN H. SUHR

Mineral Constitution Laboratories, Pennsylvania State University, University Park, Pa. 16802 (U.S.A.)

(Received 30th June 1975)

SUMMARY

The use of graphite-furnace atomic absorption spectrometry for the determination of cadmium in rocks and sediments by direct atomization from the solid state is described. At the 10—1000 p.p.b. level, the relative standard deviation is ± 10—20 %. Samples were ground to 100 mesh and, if necessary, 325 mesh before analysis. Two resonance lines were employed: 228.8 nm for less than 5 p.p.m. cadmium and 326.1 nm for levels above 5 p.p.m. Instrumental parameters were optimized to produce maximum peak heights. Results are given for a series of standard rocks and for stream sediment samples.

Flame atomic absorption spectrometry (a.a.s.) has proved to be ideally suited for many types of determinations, but the determination of cadmium in geological materials by a.a.s. has often called for lengthy preconcentration, separation, and digestion steps before a suitably concentrated solution could be obtained. Despite this, various investigators have used the flame for a limited number of samples, especially in regions with high cadmium levels, caused either by natural mineralization and/or pollution [1—7]. In uncontaminated, unanomalous rock samples, however, the levels of cadmium are such that many workers have turned to alternative techniques such as neutron activation [8—16] and mass spectrometry [17—18]. Others [19, 20], meanwhile, have used flameless atomic absorption spectrometry, which is relatively simple and inexpensive compared to some of the other techniques, and allows cadmium to be determined in the p.p.m., as well as the p.p.b. range. In addition, there tends to be less need for preconcentration of the sample and in some cases, such as those encountered in this work, direct analysis of solid samples is possible, thus precluding any dissolution or concentration steps.

Many flameless a.a.s. devices are currently available; the unit used in this work was the Perkin-Elmer furnace-type device [21], which permits analyses of both liquid and solid samples. Some early drawbacks in the instrument were the existence of blank problems caused by absorbance effects in the form of smoke and by the intensity of the furnace emission during the atomization step. These barriers have since been largely overcome by the substitution of a continuous background reference beam (deuterium

arc) [22] for the normal reference beam and by the introduction of an optical baffle system [23] which screens out excessive radiation from the furnace.

The flameless atomic absorption technique described here is sensitive enough to detect the low concentrations of cadmium which occur in natural materials, yet is neither overly time-consuming nor prone to contamination, which is often a problem in trace element determinations.

EXPERIMENTAL

A Perkin-Elmer HGA-2000 graphite furnace attachment was used with a Perkin-Elmer 305A spectrophotometer equipped with a deuterium arc background corrector and a Model 56 recorder (Perkin-Elmer). The scale expansion and gas interrupt facilities were not used.

Weighed (2—4 mg), powdered samples were introduced into the furnace via a tantalum solid sampling spoon (Perkin-Elmer), while liquids were injected with Eppendorff micropipettes. In both cases, the tube was heated after the introduction stage and the sample was dried (if necessary), charred and atomized as indicated in Table 1.

The technique was found to be so sensitive for cadmium that two resonance lines had to be used. For the low range of values encountered in most rocks (0—5 p.p.m.), the 228.8-nm wavelength was employed. For higher values of cadmium (> 5 p.p.m.), the less sensitive, secondary resonance line at 326.1 nm was used. However, when the 228.8-nm line was used for the analysis of samples containing 0.5—5 p.p.m. cadmium, it was sometimes necessary to dilute the samples with a blank to bring the signal on scale.

All the results presented here were obtained by the above procedure, but a variable millivolt recorder (Kipp and Zonen, Model BD12) used with the 326.1-nm wavelength also overcame the problem of determining 0.5—5 p.p.m. of cadmium; when the full scale was changed from 10 mV to 5 or 2 mV, the

TABLE 1

Instrumental parameters for cadmium determinations on the HGA furnace (powdered samples)

Parameter	Setting
Wavelength(s) (nm)	228.8, 326.1
Slit	0.7 nm
Purge gas	Nitrogen, 2 l min^{-1}
Damping	1 (lowest value)
Charring time and temp.	60 s/200 °C
Atomizing time and temp.	10 s/2650 °C
D_2 arc backgd. corrector	Used only at 228.8 nm
Chart speed	40 mm min^{-1}

range could be extended to 0.5 p.p.m. without adversely affecting the precision. Of course, the scale expansion on the spectrophotometer could have been used, but the variable millivolt recorder introduced considerably less noise into the system.

For evaluation, the peak heights were measured, and the results were read from a calibration graph obtained with a series of liquid standards.

Sample preparation

In preliminary tests, it was found that at the lower wavelength, stream sediment samples had to be ground to pass a 325-mesh sieve for optimal response. At the higher wavelength, however, grinding had little or no effect on the readings, thus, only 100-mesh material was required. This probably happens because at relatively low values the bulk of the cadmium is in the lattices of minerals, while at the high values, most has been adsorbed from solution onto surfaces. One would expect adsorbed cadmium to be more readily atomized (i.e. less grinding would be needed for liberation). In general, the analytical and preparation steps were as follows:

(1) stream sediment samples were sieved to 100 mesh and rocks were ground to pass a 100-mesh sieve before all determinations at 326.1 nm;

(2) all samples containing less than 5 p.p.m. Cd were ground in a tungsten-carbide ball mill to pass a 325-mesh sieve and analyzed at the more sensitive 228.8-nm line.

RESULTS AND DISCUSSION

The results for various rock standards are presented in Table 2 along with literature values. All values presented for this work were obtained by direct analysis, i.e. no dissolution of preconcentration steps were taken.

The use of liquid standards for solid analyses has been shown to be acceptable [20, 27]. When the peaks are sharp, measurement of peak heights is satisfactory [20] and precision is not significantly improved when peak areas are used [28] but there is some disagreement on this point [29]. When peak heights are measured, the experimental parameters must be optimized to produce as immediate a liberation of free atoms from the sample as possible. Accordingly, the atomization temperature was set at a higher value (2650 °C) than that used in other work based on peak area (e.g. 1700 °C [ref. 20]); damping was also reduced to its lowest setting in order to provide as rapid a pen response as possible, and maximize the peak heights. These measures resulted in very sharp peaks (Fig. 1).

A plot of the values obtained in this work against literature values is shown in Fig. 2; the dotted diagonal represents a one-to-one equivalence between the two sets of values. Except for AGV-1, the values obtained here most closely correspond to the isotope dilution mass spectrometric values [17]. This correspondence may indicate the relative accuracy of the flame-

TABLE 2

Cadmium content of U.S. G.S. rock standards and the ASK Schist

Standard	Cd content (p.p.b.)	Ref.	Standard	Cd content (p.p.b.)	Ref.
AGV-1	115	11[a]	GSP-1	50	11[a]
	75 ± 7	13[a]		64	12[a]
	17	24[b]		61 ± 19	13[a]
	57	17[c]		16	24[b]
	90	25[d]		78	19[e]
	16 ± 2	This work[e,f]		52 ± 3	20[e]
				51	17[c]
				60	25[d]
BCR-1	82	12[a]		52 ± 4	This work[e,f]
	148 ± 59	13[a]			
	99	10[a]			
	128 ± 16	14[a]	PCC-1	195	11[a]
	135	15[a]		17	12[a]
	136	16[a]		23 ± 16	13[a]
	140 ± 10	20[e]		1	24[b]
	122	17[c]		35	19[e]
	120	25[d]		15	17[c]
	93 ± 10	This work[e,f]		100	25[d]
				14 ± 1	This work[e,f]
DTS-1	110	11[a]			
	10	12[a]	W-1	151	11[a]
	9.6 ± 1.1	13[a]		155	12[a]
	5	24[b]		330	8[a]
	12	20[e]		146 ± 34	13[a]
	9	17[c]		270 ± 30	9[a]
	120	25[d]		220 ± 30	24[b]
	8 ± 1	This work[e,f]		80	26[g]
				160 ± 30	20[e]
				139	17[c]
G-2	27	12[a]		150	25[d]
	26 ± 5	13[a]		130 ± 10	This work[e,f]
	10	24[b]			
	16	17[c]			
	39	25[d]	ASK		
	18 ± 1	This work[e,f]	Schist	880	20[e]
				750	18[c]
				860 ± 130	This work[e,f]

[a]Neutron activation. [b]Polarography. [c]Mass spectrometry. [d]Compiled results. [e]Flameless a.a.s. [f]The standard deviation based on 4 results is given. [g]Anion-exchange and spectrophotometry.

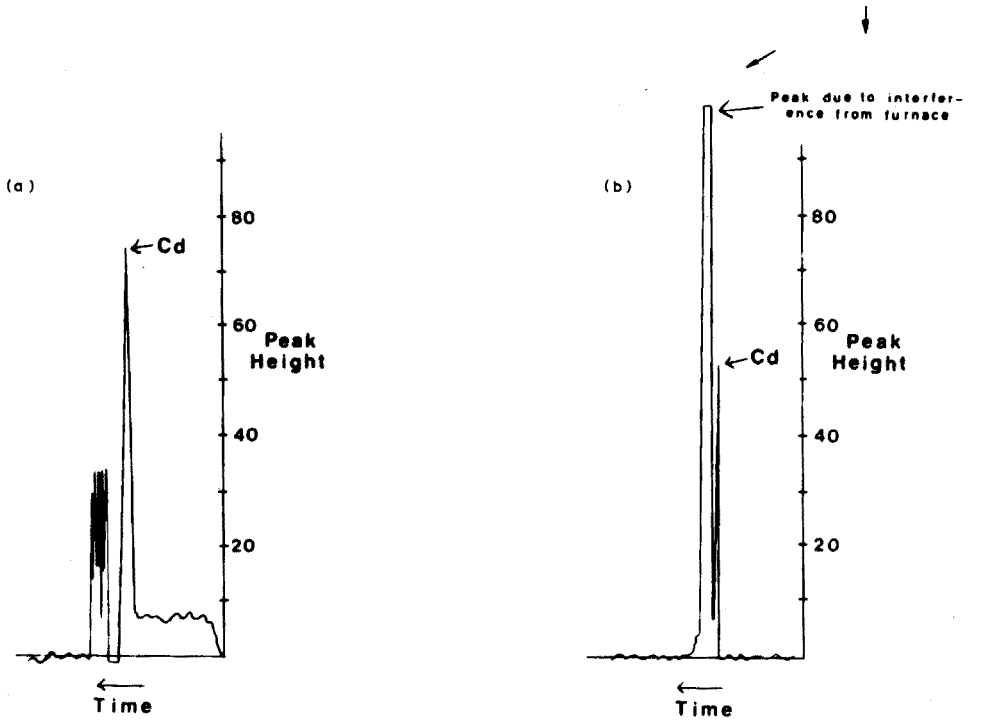

Fig. 1. Typical chart recordings. (a) At 228.8 nm with deuterium arc background correction. (b) At 326.1 nm without deuterium arc.

less a.a.s. technique, because values obtained by isotope dilution mass spectrometry are generally considered highly reliable. If this is indeed the case, then it would appear that most of the literature values now available on the cadmium content of rock standards tend to be somewhat high.

The relatively low values for samples AGV-1 and BCR-1 may have been caused by slow atomization of the cadmium in these rocks, which would reduce the peak height. Experiments based on peak area, however, were inconclusive, and the values obtained from peak heights were kept.

Some values obtained at the 326.1 nm wavelength on stream sediments from a polluted area near a zinc smelter, were checked by comparison with a hydrofluoric—perchloric acid digestion technique [30]; in the latter method, 20-μl aliquots of the digested solutions were introduced into the furnace with a micropipette. The results are presented in Table 3.

We wish to acknowledge Dr. F. J. Langmyhr of the University of Oslo, Oslo, Norway, for his helpful comments in the early stages of this work and for his help in obtaining a sample of the ASK Nordic Schist.

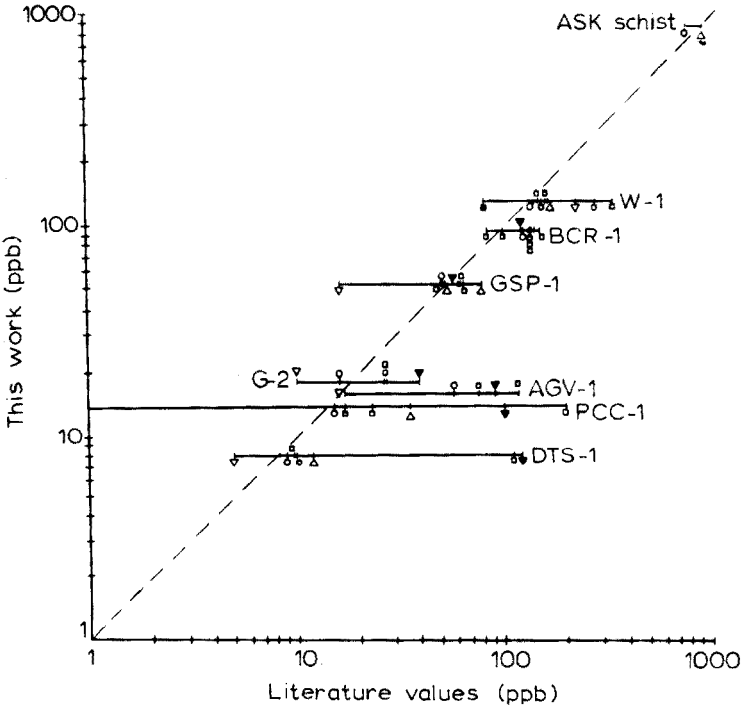

Fig. 2. Comparison plot of cadmium values from U.S.G.S. standard rocks and ASK Schist obtained in this work versus values in the literature obtained by: (○) mass spectrometry; (□) neutron activation; (■) emission spectroscopy; (△) flameless a.a.s.; (▽) polarography; (▼) a compilation.

TABLE 3

Comparison of cadmium values obtained for stream sediments

Sample	Cadmium (p.p.m.)	
	HGA	$HF—HClO_4$ digestion
4706	3	6
4705	21	22
4712	15	13
4701	8	7
4717	15	13

REFERENCES

1 N. Yamagata and I. Shigematsu, Bull. Inst. Pub. Health, Tokyo, 19 (1970) 1.
2 A. S. G. Jones, Mar. Geol., 14 (1973) M1.
3 M. J. Buchauer, Environ. Sci. Technol., 7 (1973) 131.
4 D. H. Klein and P. Russell, Environ. Sci. Technol., 7 (1973) 357.
5 J. V. Lagerwerff, D. L. Brower and G. T. Biersdorf, in D. D. Hemphill (Ed.), Trace Substances in Environmental Health V1, Univ. Miss. Press, 1973, p. 71.
6 E. Bolter, D. Hemphill, B. Wixson, D. Butherus and R. Chen, in D. D. Hemphill (Ed.), Trace Substances in Environmental Health V1, Univ. Miss. Press, 1973, p. 79.
7 C. W. Holmes, E. A. Slade and C. J. McLernan, Environ. Sci. Technol., 8 (1974) 255.
8 E. A. Vincent and L. I. Bilefield, Geochim. Cosmochim. Acta, 19 (1960) 63.
9 J. R. Butler and A. J. Thompson, Geochim. Cosmochim. Acta, 31 (1967) 97.
10 R. Ganapathy, R. R. Keays, J. C. Laul and E. Anders, Proc. Apollo 11 Lunar Sci. Conf., Geochim. Cosmochim. Acta Suppl. 1, Vol. 2, Pergamon, Oxford, 1970, p. 117.
11 G. Marowsky, Z. Anal. Chem., 253 (1971) 267.
12 P. A. Baedecker, R. Schaudy, J. L. Elzie, J. Kimberlin and J. T. Wasson, Proc. Second Lunar Sci. Conf., Geochim. Cosmochim. Acta Suppl. 2, Vol. 2, M.I.T. Press, Cambridge, Mass., 1971, p. 1037.
13 P. A. Baedecker, C. L. Chou and J. T. Wasson, Proc. Third Lunar Sci. Conf., Geochim. Cosmochim. Acta Suppl. 3, Vol. 2, M.I.T. Press, Cambridge, Mass., 1972, p. 1343.
14 U. Krahenbuhl, J. W. Morgan, R. Ganapathy and E. Anders, Geochim. Cosmochim. Acta, 37 (1973) 1353.
15 J. C. Laul and R. A. Schmitt, Geochim. Cosmochim. Acta, 37 (1973) 927.
16 J. W. Morgan, U. Krahenbuhl, R. Ganapathy and E. Anders, Geochim. Cosmochim. Acta, 37 (1973) 953.
17 K. J. R. Rosman and J. R. DeLaeter, Chem. Geol., 13 (1974) 69.
18 E. Steinnes, private communication as reported in [ref. 20].
19 H. Heinrichs and J. Lange, Z. Anal. Chem., 265 (1973) 256.
20 F. J. Langmyhr, J. R. Stubergh, Y. Thomassen, J. E. Hanssen and J. Dolezak, Anal. Chim. Acta, 71 (1974) 35.
21 D. C. Manning and F. J. Fernandez, At. Absorption Newslett., 9 (1970) 65.
22 H. L. Kahn, At. Absorption Newslett., 7 (1968) 40.
23 J. D. Kerber, A. J. Russo, G. E. Peterson and R. D. Ediger, At. Absorption Newslett., 12 (1973) 106.
24 W. Wahler, Neues Jahrb. Mineral Abh., 108 (1968) 36.
25 F. J. Flanagan, Geochim. Cosmochim. Acta, 37 (1973) 1189.
26 R. R. Brooks, L. H. Ahrens and S. R. Taylor, Geochim. Cosmochim. Acta, 18 (1960) 162.
27 E. L. Henn, Anal. Chim. Acta, 73 (1974) 273.
28 R. B. Cruz and J. C. Van Loon, Anal. Chim. Acta, 72 (1974) 231.
29 P. Schramel, Anal. Chim. Acta, 72 (1974) 414.
30 A. W. Rose, Bull. Earth Miner. Sci. Exp. Sta. Pa. State Univ., 86 (1971) 3.

Analytica Chimica Acta, 81 (1976) 305—312

DETERMINATION OF CADMIUM, ZINC, AND LEAD BY NON-DISPERSIVE ATOMIC FLUORESCENCE SPECTROMETRY WITH A NEW GRAPHITE FURNACE ATOMIZER

K. KUGA and K. TSUJII*

Central Research Laboratory, Hitachi, Ltd., Kokubunji, Tokyo (Japan)

(Received 30th June 1975)

SUMMARY

A new graphite furnace atomizer has been developed and applied to the determination of cadmium, zinc, and lead by non-dispersive atomic fluorescence spectrometry. A solar-blind photomultiplier, a lock-in amplifier, and microwave-excited electrodeless discharge lamps are used. The detection limits for cadmium, zinc, and lead in the non-dispersive atomic fluorescence mode are $1 \cdot 10^{-13}$g, $2 \cdot 10^{-13}$g, and $2 \cdot 10^{-11}$g, respectively, which are 20-, 10-, and 2-fold better than those in the atomic absorption mode. The analytical working curves are linear over about three decades of concentration from the detection limits.

The advantages and disadvantages of non-dispersive atomic fluorescence spectrometry have been discussed by many workers [1—10]. This system offers improved signal levels, because of the large optical aperture and simultaneous detection of multiple lines for the element of interest. However, the noise level will also increase if atom reservoirs which emit high background radiation are used. Up to now background radiation has been reduced by: (1) combination of a solar-blind photomultiplier with a u.v. filter, and (2) the use of an inert gas separated flame.

In previous papers, an argon—hydrogen—entrained air flame combined with a gas sampling technique was used for sensitive determinations of arsenic [11] and antimony [12]. However, flame atomization techniques have mainly been employed for the production of atomic vapours in non-dispersive atomic fluorescence spectrometry of solution samples.

Since the report by Massmann [13], various types of non-flame atom reservoirs have been used in atomic fluorescence studies [14, 15], but these devices have been used mostly with detection systems for dispersed fluorescence radiation. Only the West carbon filament atom reservoir has been applied to a non-dispersive system [16]. The principal difficulty in the application to non-dispersive systems seems to be the intense continuum radiation emitted from the heated graphite furnace, which increases the noise level.

*Author for reprint requests.

In this paper the construction of a new graphite furnace atomizer and its application to the determination of cadmium, zinc, and lead by non-dispersive atomic fluorescence spectrometry are described. In parallel with the detection of fluorescence radiation, atomic absorption was measured and the results wer compared.

EXPERIMENTAL

Apparatus

The arrangement of the apparatus and the graphite furnace atomizer used are shown in Figs. 1 and 2. The graphite tube was made from high purity graphite (Japan Carbon Co. Ltd.). The internal and external diameters and the length of the tube are 2.5 mm, 4.5 mm, and 50 mm, respectively. Tube temperature and time of the heating were established by controlling the power supply and the time controller which were made in this laboratory. These devices can provide a furnace temperature of up to 2500 °C (2.5 kW at 10 V) and a heating interval up to 180 s. By circulating a stream of cooling water, the temperature of the graphite tube can be lowered from the maximum to room temperature in about 50 s.

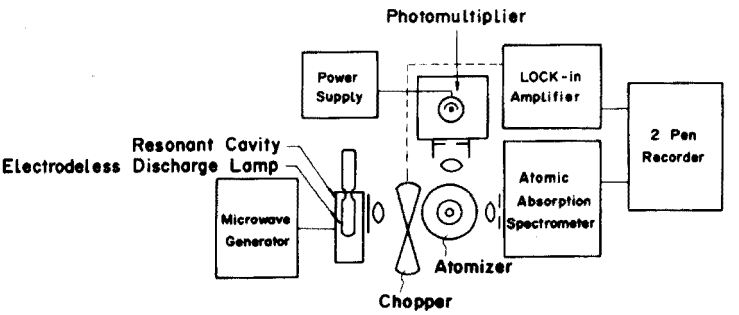

Fig. 1. Schematic diagram of the apparatus.

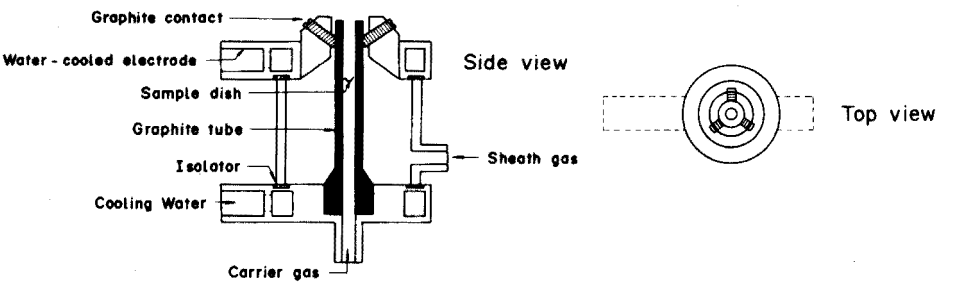

Fig. 2. The new graphite furnace atomizer.

The outer mantle which protrudes slightly beyond the graphite tube, prevents the intense background radiation emitted by the heated graphite tube from reaching the detector. This screening out of the unwanted background radiation results in increased sensitivity, and is particularly desirable in non-dispersive atomic fluorescence measurement.

The light sources used were microwave-excited electrodeless cadmium, zinc, and lead discharge lamps (EMI Electronics Ltd.); they were maintained with a Microtron 200 Microwave Generator (2450 ± 25 MHz) and a Model 214 L Resonant Cavity (Electro-Medical Supplies, Ltd.). The optimal incident power for the operation of these lamps was 40 W (Zn), 50 W (Cd), and 50 W (Pb). The light beam from a light source was mechanically modulated at 110 Hz and focused immediately above the graphite tube. It was then refocused on the entrance slit of the monochromator (Hitachi atomic absorption spectrophotometer, Model 207).

The fluorescence radiation was observed at right angles to the excitation beam by a solar-blind photomultiplier (HTV R166), which was housed in the detector box of a Hitachi Model 139 Spectrophotometer. A John Fluke Model 412B power supply was used to provide high voltage (500 V) for the photomultiplier, the signals from which were fed into a lock-in amplifier (Princeton Applied Research Corp., Model HR-8) tuned to the modulating frequency.

Atomic clouds produced by heating the graphite tube were transported to the light path by argon carrier gas. To prevent combustion of the graphite tube and to minimize any recombination reactions of atoms, another argon flow was employed as a gas sheath.

Atomic fluorescence and atomic absorption signals were recorded, simultaneously, on a Hitachi two-channel recorder (Model 056). Atomic absorption lines used for measurements were 228.8 nm (Cd), 213.8 nm (Zn), and 217.0 nm (Pb).

Reagents

All the stock solutions used were 1000 p.p.m. in metal ion, prepared from commercially available standard cadmium chloride, zinc chloride, and lead nitrate solutions (Kanto Chemical Corp. Inc.). More dilute standard solutions were prepared as required.

Procedures

The flow rates of argon carrier and sheath gases were adjusted to the optimal settings. When the graphite tube was newly installed, the graphite was heated repeatedly until no appreciable signals from light scattering effects caused by carbon particles, could be observed.

Before the atomic fluorescence measurements, the program for the control of the drying and atomization temperatures and the duration of the heating

was set. A 10-μl sample solution was placed on a graphite dish located in the middle of the graphite tube by means of a Eppendorf micropipette with a plastic tip.

By supplying a low voltage (1—1.5 V) for 10—20 s, the tube was heated to about 150 °C and the solvent was vaporized. Subsequently, the graphite was heated to incandescence and the sample was atomized. Atomic fluorescence and atomic absorption signals were recorded, simultaneously, on a recorder and the peak heights were measured.

RESULTS AND DISCUSSION

Effect of the atomization voltage on fluorescence intensity

The effect of the atomization voltage on the fluorescence intensities of cadmium, zinc, and lead is shown in Fig. 3. Fluorescence intensities for the three elements increased and leveled off with increase of the voltage. However, a higher voltage was needed for the production of lead atomic vapours than for those of cadmium and zinc. This may be partly related to the higher dissociation energy of PbO (3.9 eV) than those of CdO (< 3.8 eV) and ZnO (2.8 eV) [17]. The atomization voltages employed in the following measurements were 5.5 V for cadmium and zinc, and 7.5 V for lead. The temperatures at the exit orifice of the graphite tube for these two voltage settings were about 1500 °C and 2000 °C, respectively, measured with an optical pyrometer.

Effect of the flow rates of argon carrier and sheath gases

As mentioned above, two argon flows are provided in the graphite furnace atomizer. With the flow rate of argon carrier gas at 0.2 l min^{-1}, the effect of

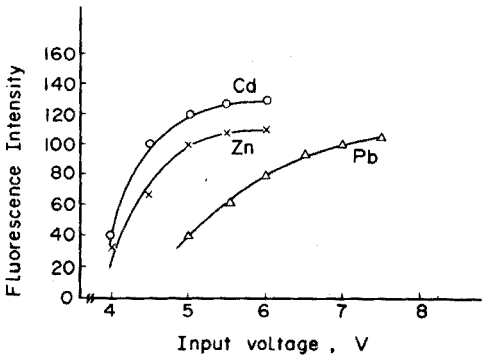

Fig. 3. Effect of the input voltage supplied to the graphite furnace atomizer on fluorescence intensity.

the flow rate of argon sheath gas on the atomic fluorescence intensity was examined. The fluorescence intensity for each element went through a maximum and then decreased with increase in the argon flow rate (Fig. 4). The increase of fluorescence intensity at low flow rates of argon is possibly due to decreasing entrainment of air, and the decrease of fluorescence intensity beyond the maximum to a cooling effect. The following measurements were carried out at argon flow rates of 0.4 l min^{-1} (Cd and Zn) and 0.7 l min^{-1} (Pb).

The dependence of the fluorescence intensity on the flow rate of argon carrier gas is shown in Fig. 5; relatively high fluorescence signals can be observed even in the absence of argon carrier flow. However, the maximal fluorescence intensities were observed for a low flow rate of argon (ca. 0.1 l min^{-1}). The decrease in the fluorescence signals beyond the maxima is probably due partly to the reduced residence time of the atoms in the light path, and partly to a cooling effect. Subsequent measurements were made with the argon carrier gas flow rate at 0.1 l min^{-1}.

Effect of the distance between the light path and the top of the graphite furnace atomizer

The diameter of the light beam immediately above the graphite tube was about 3 mm. The variation of the atomic fluorescence signals with the height above the graphite furnace atomizer was examined for each element. The results indicate that the fluorescence intensity decreases strikingly with increased distance (Fig. 6). However, a more marked decrease in the fluorescence intensity was observed for lead, probably because of the stronger affinity of lead for oxygen. The data from the height profiles were used to select optimal conditions, and the top of the furnace atomizer was situated 2 mm from the center of the light beam in all subsequent work.

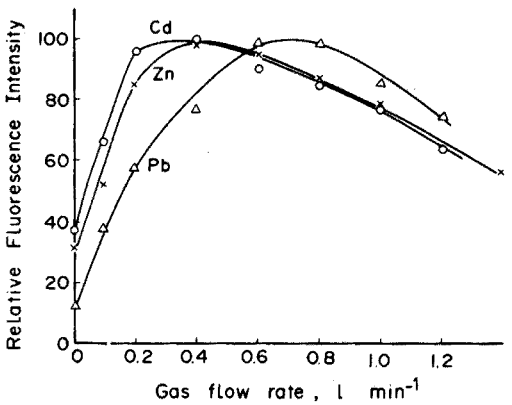

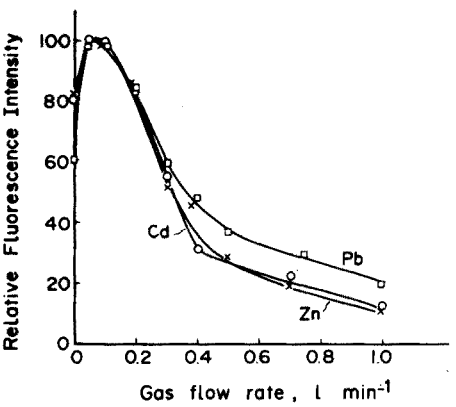

Fig. 4. Effect of the flow rate of argon sheath gas on fluorescence intensity.

Fig. 5. Effect of the flow rate of argon carrier gas on fluorescence intensity.

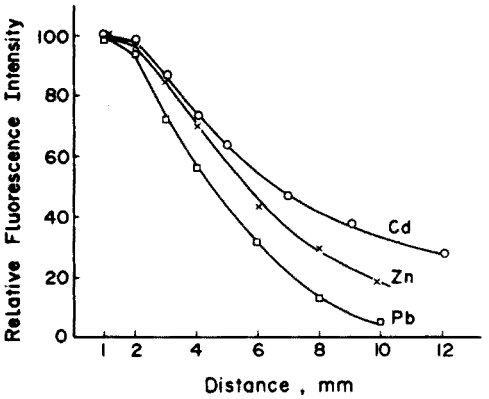

Fig. 6. Effect of the atomizer height on fluorescence intensity.

Detection limits and analytical working curves

The detection limit is defined as the amount of the element at which the peak height is equal to twice the background noise. The detection limits for cadmium, zinc, and lead were $1 \cdot 10^{-13}$g, $2 \cdot 10^{-13}$g, and $2 \cdot 10^{-11}$g, respectively, in a non-dispersive atomic fluorescence mode and $2 \cdot 10^{-12}$g, $2 \cdot 10^{-12}$g, and $4 \cdot 10^{-11}$g in an atomic absorption mode. For cadmium and zinc, the detection limits in the former mode were 20- and 10-fold better than those in the latter mode. For lead, however, the improvement was only 2-fold. The marginal improvement in the detection limit for lead is partly related to the light source intensity. However, the principal reason is that the most sensitive fluorescence line of lead (405.8 nm) [18—20] is out of the spectral response sphere of the detector (160—320 nm).

The analytical working curves for the three elements in atomic fluorescence measurements are shown in Fig. 7. The curves are linear over nearly three decades of concentration from the detection limits.

To verify that the output signals were due to atomic fluorescence radiation and not to scattering effects, the light sources were changed from cadmium and zinc to tellurium, and from lead to cadmium, respectively, and the atomic fluorescence measurements were repeated. The latter light sources radiate emission spectra as strong as the former ones in the spectral response of the detector. In all cases, however, no appreciable signals were observed even in the presence of 10 p.p.m. of each solution. This showed that the output signals measured in this work can be safely ascribed to fluorescence radiation.

A typical recorder tracing of cadmium atomic fluorescence and atomic absorption signals obtained with a 0.001 p.p.m. cadmium solution is shown in Fig. 8. The relative standard deviation calculated from the six peak measurements of the cadmium fluorescence signals was 3.8 %.

Throughout the experiment, no appreciable memory effects were experienced even when 100 p.p.m. solutions of each element were used.

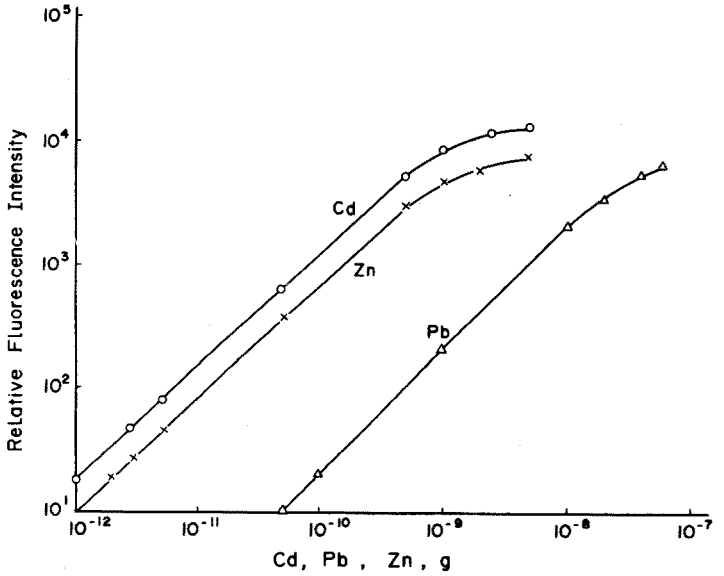

Fig. 7. Analytical working curves for Cd, Zn, and Pb.

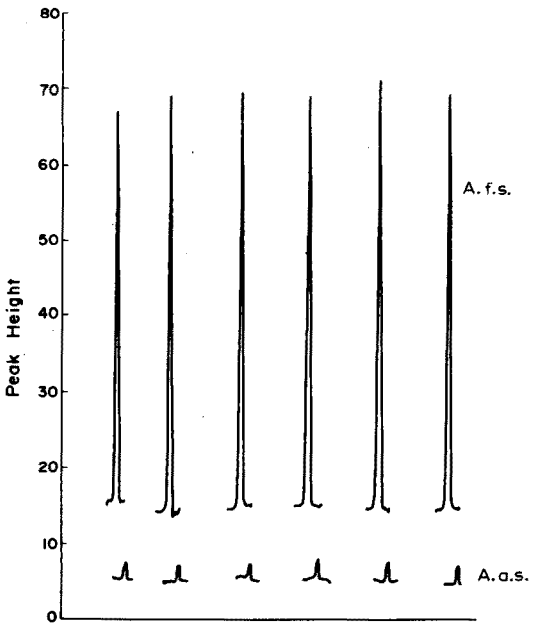

Fig. 8. Typical recorder tracings of cadmium a.a.s. and a.f.s. signals. 10 μl of 0.001 p.p.m. Cd solution.

Conclusion

A graphite furnace atomizer can be successfully applied to nondispersive atomic fluorescence spectrometry if incandescent radiation emitted from the heated graphite furnace is prevented from reaching the detector. The memory effect which is caused by the incomplete vaporization of the elements is insignificant, and progress is being made in the application of the graphite furnace to practical analysis.

The authors are grateful to Dr. Kazuo Yasuda, Dr. Norio Shibata, and Dr. Shinya Iida for valuable discussions, to Dr. Teruo Tsunoda for encouragement and helpful criticism, and to Mr. Masahiro Takahashi for his contribution in the construction of the time controller used.

REFERENCES

1 P. L. Larkins, R. M. Lowe, J. V. Sullivan and A. Walsh, Spectrochim. Acta, Part B, 24 (1969) 187.
2 T. J. Vickers and R. M. Vaught, Anal. Chem., 41 (1969) 1476.
3 P. D. Warr, Talanta, 17 (1970) 543.
4 D. G. Mitchell and A. Johansson, Spectrochim. Acta, Part B, 25 (1970) 175.
5 P. L. Larkins, Spectrochim. Acta, Part B, 26 (1971) 477.
6 P. L. Larkins and J. B. Willis, Spectrochim. Acta, Part B, 26 (1971) 491.
7 R. C. Elser and J. D. Winefordner, Appl. Spectrosc., 25 (1971) 345.
8 T. J. Vickers, P. J. Slevin, V. I. Muscat and L. T. Farias, Anal. Chem., 44 (1972) 930.
9 R. F. Browner, Analyst (London), 99 (1974) 617.
10 V. I. Muscat, T. J. Vickers, W. E. Rippetoe and E. R. Johnson, Appl. Spectrosc., 29 (1975) 52.
11 K. Tsujii and K. Kuga, Anal. Chim. Acta, 72 (1974) 85.
12 K. Tsujii, K. Kuga and I. Sugaya, Chem. Lett., to be published.
13 H. Massmann, Spectrochim. Acta, Part B, 23 (1968) 215.
14 G. F. Kirkbright, Analyst (London), 96 (1971) 609.
15 T. S. West and M. S. Cresser, Appl. Spectrosc. Rev., 7 (1973) 79.
16 T. S. West, Analyst (London), 99 (1974) 886.
17 A. G. Gaydon, Dissociation Energies and Spectra of Diatomic Molecules, Chapman and Hall, London, 1968.
18 R. F. Browner, R. M. Dagnall and T. S. West, Anal. Chim. Acta, 50 (1970) 375.
19 V. Sychra and J. Matoušek, Talanta, 17 (1970) 363.
20 B. W. Bailey, Anal. Chim. Acta, 54 (1971) 537.

Analytica Chimica Acta, 81 (1976) 313—318

THE FLAMELESS ATOMIC ABSORPTION SPECTROMETRIC DETERMINATION OF ALUMINUM WITH A CARBON ATOMIZATION SYSTEM

TOSHIHISA MARUTA, KEIICHI MINEGISHI and GIICHI SUDOH

Central Laboratory of Research and Development, Chichibu Cement Co., Ltd., Ohmiya, Chichibu-shi, Saitama-ken (Japan)

(Received 20th June 1975)

SUMMARY

The atomic absorption spectrometry of aluminum with a carbon tube atomizer is described, with particular reference to the heating cycle, argon flow rate and amplifier time constant. Interferences are eliminated by pre-atomization heating or with a hydrogen—argon—entrained air flame. Under optimal conditions, the sensitivity (1 % absorbance) is $5 \cdot 10^{-11}$ g, and the relative standard deviation is 2.3 for 2.5 ng Al.

In recent years, many flameless atomizers for atomic absorption spectrometry have been developed and used for the determination of trace amounts of elements, including aluminum. Brodie and Matoušek [1] reported that a carbon rod atomizer could be used in the determination of aluminum in lubricating oils. Heinrichs and Langer [2] described the analysis of rock standards for aluminum with a heated graphite furnace. Welz and Wiedeking [3] reported the determination of aluminum in natural and waste waters with a heated graphite furnace, from the point of view of environmental protection. In these papers, the applications of flameless atomic absorption to practical samples were the main concern, and there has been little fundamental research on the determination of aluminum and interferences.

In this paper, fundamental aspects of the use of a carbon tube atomizer in the determination of aluminum are evaluated and discussed, and the effects of foreign cations are described.

EXPERIMENTAL

Apparatus

A Varian-Techtron Model 63 carbon rod atomizer was mounted in place of the burner assembly in a Nippon Jarrell-Ash AA-1E atomic absorption and flame emission spectrophotometer. A Westinghouse aluminum hollow-cathode lamp was employed as light source. A Rikadenki Kogyo strip-chart

recorder (1/5-s full scale deflection) Model B-18 Mark II was used at a speed of 60 cm min^{-1}. Unless otherwise stated, argon was employed as sheathing gas. A hydrogen—argon—entrained air flame was also used with the carbon tube for comparison; hydrogen (2 l min^{-1}) was introduced into the argon stream, and ignited spontaneously when the carbon tube reached a high enough temperature. The hydrogen flow was stopped at the end of the atomization cycle. Samples (5-μl) were added with Eppendorf micropipettes with disposable plastic tips. The atomic absorption of aluminum was monitored at 309.3 nm. The amplifier used had a time constant of 0.1 s.

Reagents

The 1000-p.p.m. stock aluminum solution was made by dissolving aluminum metal plate (99.9 % purity) in the minimum amount of hydrochloric acid. All others solutions were made from analytical-grade materials.

Procedures

Before use, the carbon tube was heated at high temperature until no absorption signal was observed.

Aliquots (5 μl) of sample solutions were introduced into the carbon tube atomizer and then heated to about 120 °C for 45 s to remove the solvent. The temperature was increased to about 1200 °C for 20 s for the pre-atomization heating, and atomization was done at 1850—2400 °C for 10 s.

The temperature attained by the carbon tube atomizer was measured with a thermistor or an optical pyrometer.

RESULTS AND DISCUSSION

Effects of different temperatures in the heating cycle

The drying cycle, in which the solvent was completely vaporized at 120 °C for 45 s without vaporization of sample salt, had no effect on the absorbance.

Generally, when only inorganic matter was present in the sample solution, the pre-atomization heating cycle was unnecessary. However, this cycle was used to obtain better reproducibility and to eliminate the interference of volatile foreign elements. The effect of the pre-atomization temperature on the absorbance of aluminum is shown in Fig. 1. The decrease in absorbance above 1350 °C can be attributed to some aluminum chloride being evaporated or converted to oxide before the atomization. Fuller [4] reported a loss of copper during the preatomization heating with a 50 % reduction in concentration within 30 s at 1100 °C. For 10 determinations of aluminum, the relative standard deviation was found to be 4.8 for a preatomization temperature of 25 °C but only 2.3 for a temperature of 1200 °C.

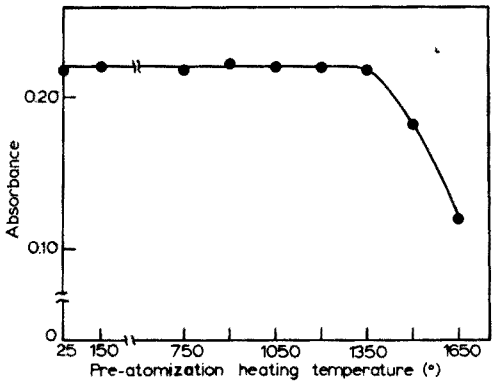

Fig. 1. Variation of absorbance with pre-atomization heating temperature. 2.5 ng Al; 20-s pre-atomization heating time. Atomization at 2400 °C for 10 s.

The aluminum absorbance showed a linear relationship with the atomization temperature, increasing from 0.04 at 1850 °C to 0.22 at 2400 °C, for 10-s heating periods. Thus the effect of atomization temperature on the aluminum absorbance is very different from that on chromium [5]. The absorbance signal for an atomization time of 10 s at 2400 °C is shown in Fig. 2. It is interesting that the two peaks were observed during the atomization cycle. The first large peak (I) can be attributed to atomization of the aluminum chloride molecule, or of the oxide formed during the pre-atomization heating. The second peak may arise from atomization of a thermally stable oxide formed during the initial atomization in this carbon tube; it was not found at atomization temperatures below 2400 °C. The tests indicate that the decrease in absorbance with decreasing atomization temperature is due to a decrease in the atomization of the oxide.

Unless otherwise noted, the results discussed below are based on the absorbance signal of the first peak.

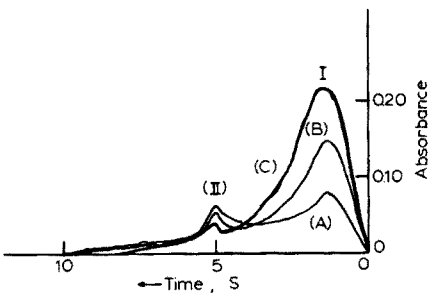

Fig. 2. Variation of absorbance signal with argon flow rate. 2.5 ng Al. Argon flow rate: (A) 0.9 l min^{-1}, (B) 1.9 l min^{-1}, (C) 3.4 l min^{-1}. Atomization temperature, 2400 °C. Chart speed: 60 cm min^{-1}.

Effect of argon flow rate

Absorbances were measured for argon flows varying from 0.3 l min^{-1} to 4.4 l min^{-1}. The absorbance increased with increasing flow rate, and reached a plateau value for flows above 3.2 l min^{-1}. The signals obtained at different flow rates are shown in Fig. 2. For peak II, the width and height decreased with increasing argon flow rates. The reproducibility of the analysis was better at 3.4 l min^{-1} than at lower flow rates. These results indicate that more oxide is formed at low flow rates because of inefficient sheathing from oxygen.

Effect of amplifier time constant

The effect of the time constant on the absorbance of aluminum at various atomization temperatures was measured. The peak height decreased and the peak width increased with increasing time constants, irrespective of temperature. When a time constant of 1.1 s was used with an atomization temperature of 2400 °C, the aluminum peak height was 50 % less than that obtained with a 0.1-s constant (Fig. 3). The small peak II (Fig. 2) was found only with the 0.1-s time constant, probably because of sluggish response to transient signals at higher time constants. The results obtained with a hydrogen—argon—entrained air flame sheath instead of an argon sheath were similar.

Calibration curves

Figure 4 shows typical calibration curves. The curvature of the graph with a 1.1-s time constant is mainly due to insensitivity to the transient signal. With the 0.1-s time constant, the sensitivity, defined as the amount of aluminum producing a 1 % change in absorbance was $5 \cdot 10^{-11}$ g.

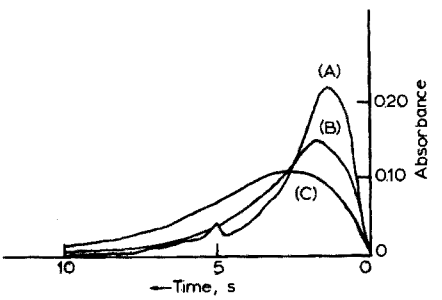

Fig. 3. Variation of absorbance signal with amplifier time constant. 2.5 ng Al. Time constant: (A) 0.1 s, (B) 0.6 s, (C) 1.1 s. Atomization temperature, 2400 °C.

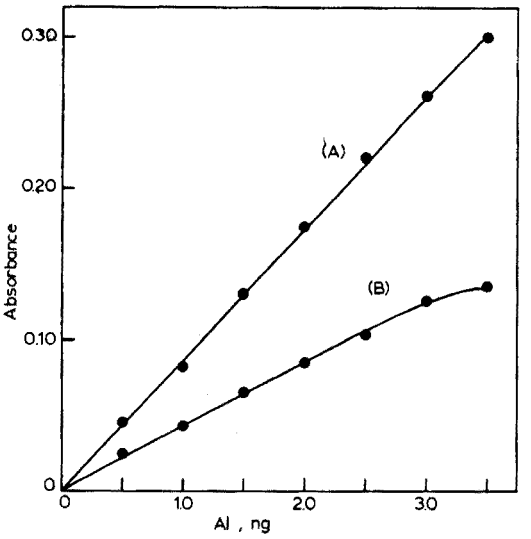

Fig. 4. Calibration curves for aluminum. Amplifier time constant: (A) 0.1 s, (B) 1.1 s. Atomization temperature: 2400 °C.

Interferences of cations

The effects of 300-fold weights of calcium, strontium, iron, zinc, cadmium and lead were examined. The results obtained with and without the pre-atomization heating at 1200 °C are shown in Table 1; ions causing variations less than twice the standard deviation were regarded as non-interfering. There was no interference from volatile elements such as zinc, cadmium and lead whether or not pre-atomization heating was used. Without the pre-atomization heating, calcium, strontium and iron depressed the absorbance of aluminum, but when pre-atomization heating was used, the interferences of calcium and strontium were completely eliminated because the metal chlorides were removed from the carbon tube during the cycle. The interference of iron was only partly removed; this interference

TABLE 1

The suppression of the aluminum absorbance by interfering cations (2.5 ng Al. Atomization temperature, 2400 °C)

Element	% Change in signal	
	Pre-atomization heating	
	None	At 1200°
Ca	16	0
Sr	19	0
Fe	42	23

may be attributed to the formation of a solid solution such as $Fe_2O_3 \cdot Al_2O_3$ in the carbon tube at the high temperature.

In order to eliminate the interference of iron, a hydrogen—argon—entrained air flame around the carbon tube was examined. No interference was then observed, probably because of the reducing environment caused by the flame, but the aluminum absorbance was small. Thus both pre-atomization heating and the hydrogen—argon—entrained air flame are effective in eliminating interferences. The interferences of cations at low atomization temperatures were essentially the same as at 2400 °C.

The authors wish to thank Mr. H. Mori, Director of Central Laboratory of Research and Development, Chichibu Cement Co., Ltd., for his interest in this work.

REFERENCES

1 K. G. Brodie and J. P. Matoušek, Anal. Chem., 43 (1971) 1557.
2 H. Heinrichs and J. Lange, Z. Anal. Chem., 265 (1973) 256.
3 B. Welz and E. Wiedeking, Z. Anal. Chem., 264 (1973) 110.
4 C. W. Fuller, Anal. Chim. Acta, 62 (1972) 442.
5 T. Maruta and T. Takeuchi, Anal. Chim. Acta, 66 (1973) 5.

Analytica Chimica Acta, 81 (1976) 319—324

THE APPLICATION OF ELECTRODEPOSITION TECHNIQUES TO FLAMELESS ATOMIC ABSORPTION SPECTROMETRY PART III. THE DETERMINATION OF CADMIUM IN URINE

WALTER LUND and BJØRN VIGGO LARSEN
Department of Chemistry, University of Oslo, Blindern, Oslo 3 (Norway)
NILS GUNDERSEN
Institute of Occupational Health, Gydas vei 8, Oslo 3 (Norway)
(Received 8th August 1975)

SUMMARY

Cadmium in urine can be determined by a simple flameless atomic absorption technique, in which the metal is electrolyzed onto a thin platinum wire, followed by electrical heating of the wire. The technique is compared with the well-established flame procedure, involving extraction with APDC into MIBK. The data obtained by the two techniques are in good agreement. Large individual variations occur in the urinary concentration of cadmium for workers suspected of cadmium exposure. The group mean values for these workers lie in the range 4—5 p.p.b.; mean values for unexposed control groups are around 1 p.p.b. On a group basis, the results indicate a significantly higher urinary excretion of cadmium for the workers than for the control groups.

The cadmium exposure of workers in certain factories is recognized as a serious health hazard. From a toxicological point of view, there is considerable interest in studies of the urinary excretion of cadmium, although there does not appear to be a simple relationship between the exposure and urinary excretion of this metal. The cadmium values for unexposed persons, and frequently also for exposed workers, are very low, usually around 1 p.p.b., although large individual variations have been reported. Most data on urinary cadmium have been obtained by using the atomic absorption technique, after extraction with ammonium 1-pyrrolidine carbodithioate (APDC) into methyl isobutyl ketone (MIBK).

In previous Parts of this series [1, 2], the use of electrochemical deposition as a separation and preconcentration technique in flameless atomic absorption spectrometry has been discussed. In the present paper, this reagent-free technique is used for the determination of cadmium in urine, and the results are compared with data obtained by the usual flame technique, after extraction with APDC into MIBK. The comparison of results obtained by different methods is very valuable in determining the accuracy of a given analysis, and this is particularly important in ultra-trace analysis, where systematic errors will frequently occur.

EXPERIMENTAL

Apparatus

The APDC—MIBK extracts were analyzed with a Perkin-Elmer 403 atomic absorption spectrometer, using an air—acetylene flame. For the experiments based on flameless atomization, a Perkin-Elmer 300 instrument and a Perkin-Elmer 56 recorder were used. The burner head was here replaced by a cell made of glass, with quartz windows. The filament electrode was positioned in the centre of the cell. Details of the electrode and cell have been published previously [1]. In the present experiments, the tungsten filament was replaced by a platinum spiral, made from a 0.2-mm platinum wire. The cell was flushed with nitrogen, and the filament was heated electrically from a simple 30-W power supply, consisting of a Variac and an a.c. transformer.

The equipment used for the controlled potential electrolysis was the same as that described previously [1].

Samples and solutions

Urine samples were collected in 100-ml polyethylene bottles which had been thoroughly cleaned with acids; 0.1 g of EDTA (disodium salt) was added to each bottle before the collection of the samples, to minimize adsorption and deposition of heavy metals during transport and storage. The EDTA salt was added instead of an acid, mostly for practical reasons. The bottles were stored in a refrigerator until they were analyzed.

Unless otherwise stated, all the reagents used were of analytical grade. The 2 % (w/v) ammonium 1-pyrrolidine carbodithioate (APDC) solution, which was prepared daily, was filtered through glass wool. Methyl isobutyl ketone (MIBK) was saturated with water before use. The cadmium stock solution was prepared from the sulphate salt. Standard solutions with a concentration below 10^{-3} M were prepared just before use, by diluting the stock solution. The water used was demineralized with an ion-exchange resin and then distilled.

Procedure I

Acidify 25 ml of the urine sample to pH $\leqslant$ 2 with nitric acid (Suprapur, Merck), and then carry out the electrodeposition at —1.0 V vs. Ag/AgCl for 5 min, while the solution is stirred by a nitrogen flow of 140 cm^3min^{-1} through the solution. Remove the filament electrode from the electrolytic cell without disconnecting the electrical circuit, rinse with distilled water and dry with acetone before placing the electrode in the atomization cell. Record the atomic absorption signal during the application of a voltage of 4 V (1650 °C) to the filament for 5 s.

Add 20 μl of a 10^{-5} M cadmium solution to the urine sample, and repeat

the deposition and atomization steps. Calculate the concentration of cadmium by the usual equation for the standard addition technique.

Procedure II

Add 2 ml of 18 M sulphuric acid, 3 ml of 16 M nitric acid and 1 ml of 70 % perchloric acid to 20 ml of the urine sample, and heat on a hot plate until the sulphuric acid is seen to condense on the glass walls. Then cool, add 5 ml of 100-vol. hydrogen peroxide and heat once more. After cooling, add 20 ml of water and adjust the pH to 3.5 ± 0.2 with ammonia or sulphuric acid. Add 1 ml of APDC solution, wait for 5 min before adding 4 ml of MIBK, and then shake for 70 s. Finally centrifuge the organic solution for 10 min and analyze it by atomic absorption in an air-acetylene flame. Calculate the concentration of cadmium from a calibration curve, after correcting for the blank value.

RESULTS AND DISCUSSION

Urine is a complex matrix, where the presence of salts and complex-for forming compounds may give rise to various interference effects in the determination of cadmium by the atomic absorption technique. Thus, the sodium chloride present in urine will give rise to non-specific absorption, unless background correction is used. For this reason, and also because of the low concentration levels of cadmium in urine, a separation and pre-concentration step is frequently employed. This is usually achieved by ex extraction with APDC into MIBK. Recently, Ross and Gonzales [3] showed that cadmium in urine may be determined directly by selective volatilization in a graphite furnace, provided that background correction is used. As an alternative to this technique, an electrochemical preconcentration on a metal wire followed by flameless atomization may be used. The electrochemical approach, which does not necessitate the use of expensive equipment for the flameless atomization, effectively removes interferences from salts, and represents also a powerful preconcentration step. However, it was found that a platinum filament was to be preferred to the previously used tungsten filament, owing to the deactivation of tungsten in acidic solution [1]. An increased sensitivity was obtained when the urine samples were acidified to pH $\leqslant$ 2. This increase in sensitivity was probably due to the dissociation of cadmium complexes, particularly the EDTA complex, which results in a higher concentration of uncomplexed cadmium in solution. Separate experiments showed that the cadmium—EDTA complex was not reduced under the present conditions. Because of the low pH value, the negative reduction potential, and the low overvoltage for hydrogen on platinum, a marked evolution of hydrogen was observed at the platinum filament during the deposition step. However, this did not have any noticeable effect on the results.

The sensitivity of this technique is a function of the deposition time chosen. For deposition times below 30 min, the amount deposited, and thus the sensitivity, increases linearly with the deposition time. By successive additions of a standard cadmium solution to urine samples it was ascertained that there was a linear relationship between the amount deposited and the concentration of cadmium, in the concentration range 0—25 p.p.b. The reproducibility of the method was found to be of the order of 10—20 %. Typically, the relative standard deviation of 15 % was obtained for 15 repeated analyses on the same urine sample, which contained ca. 5 p.p.b. cadmium.

Analysis of urine samples

The results of the analyses of samples from six persons are shown in Table 1. The concentrations, which vary from 1.5 to 12.4 p.p.b., were determined by the standard addition technique. The peak heights before and after the addition of the cadmium standard, and also the amount added are indicated in the Table. As may be seen, the sensitivity varies markedly from one urine sample to another, indicating significant differences in the chemical composition of the samples. The presence of complex-forming ligands and surface-active compounds may have a marked effect on the concentration of free cadmium and its electrochemical deposition rate, and consequently also on the amount of cadmium deposited during the electrolytic step. However, the results obtained by using the standard addition technique were in good agreement with the data obtained by procedure II, as may be seen by comparing the last two columns in Table 1.

Procedure II requires both an acid digestion and an extraction step. The method is time-consuming and the many reagents added result in relatively high blank values, which are frequently of the order of 1—2 p.p.b. For the analysis of sub-p.p.b. levels of cadmium, the electrochemical preconcentration technique therefore appears to be the more suitable method. The good

TABLE 1

Determination of cadmium in urine
(p_1 and p_2 represent the peak heights before and after the addition of standard. Each of these values represents the mean of 2—3 separate depositions/atomizations)

Sample no.	p_1 (mm)	p_2 (mm)	Cd added (p.p.b.)	Concn. found (p.p.b.)	Procedure II (p.p.b.)
1	17.0	44.5	20	12.4	10
2	30.0	60.0	5	5.0	5.8
3	26.2	56.2	4	3.5	3.5
4	14.0	32.2	2	1.5	1.6
5	2.5	3.7	2	4.2	3.7
6	35.0	52.4	4	5.1	4.7

agreement between the two procedures indicates that both give accurate results when applied to the analysis of urine for cadmium in the concentration range 1—10 p.p.b. No cadmium appears to be lost during the digestion step used in procedure II, nor were cadmium losses observed when standard solutions were carried through the same procedure. However, losses of cadmium of about 50 % were recently reported when precisely the same wet-ashing procedure was used for the determination of cadmium in rat organs [4].

The reproducibility obtained by using procedure II was found to be of the same order of magnitude as that of the electrochemical technique; the relative standard deviation was usually 10—20 %. In procedure II only a single standard solution is usually needed to calibrate the system. This may be considered an advantage of that technique, particularly for routine analysis.

The concentrations of cadmium given in Table 1 vary from 1 to 12 p.p.b. Although all samples were taken from workers suspected of cadmium exposure, it is difficult to decide, on the basis of the individual results, whether the persons in question have been exposed to cadmium. As pointed out by Friberg et al. [5], big differences in reported normal urinary concentrations of cadmium have sometimes been observed. The case is further complicated by the fact that cadmium exposure may occur without resulting in an increase in the urinary excretion of this metal. Even so, by treating the data on a group basis, it still appears possible to draw conclusions regarding cadmium exposure. Thus, the mean value of the results given in Table 1 is ca. 5 p.p.b., and the mean value for a similar group, representing 8 workers at the same factory, was found to be 4.0 p.p.b. In contrast to these values, the mean value for a control group of persons working in another part of the same factory was found to be 1.0 p.p.b. Urine samples were also analyzed for a control group of persons working at the Institute of Occupational Health; in this case a group mean value of 1.2 p.p.b. was obtained. The results for the control groups are in good agreement with the mean values for "normal" subjects reported by other workers, although recent results from Sweden indicate even lower cadmium values [5].

The results given above demonstrate that studies on cadmium exposure based on urinary excretion are best carried out on a group basis, instead of attempting to draw conclusions from individual data for urinary cadmium. In the present case, the group mean values indicate a significantly higher urinary excretion of cadmium for the workers than for the control groups. The values thus imply that the workers have been occupationally exposed to cadmium.

The authors wish to thank Dr. Tor Norseth for his interest in this work. The work was supported by a grant from Norges Teknisk-Naturvitenskapelige Forskningsråd, contract no. B.1520.3906.

REFERENCES

1 W. Lund and B. V. Larsen, Anal. Chim. Acta, 70 (1974) 299.
2 W. Lund and B. V. Larsen, Anal. Chim. Acta, 72 (1974) 57.
3 R. T. Ross and J. G. Gonzales, Anal. Chim. Acta, 70 (1974) 443.
4 T. L. M. Syversen and G. B. Syversen, Bull. Environ. Contam. Toxic., 13 (1975) 97.
5 L. Friberg, M. Piscator, G. F. Nordberg and T. Kjellstrøm, Cadmium in the Environment, CRC Press, Cleveland, Ohio, 2nd edn. 1974, p. 65.

Analytica Chimica Acta, 81 (1976) 325—336

MOLECULAR EMISSION CAVITY ANALYSIS: STIMULATION OF METAL HALIDE EMISSIONS

R. BELCHER, S. L. BOGDANSKI, I. H. B. RIX and A. TOWNSHEND

Chemistry Department, Birmingham University, P.O. Box 363, Birmingham, B15 2TT (England)

(Received 15th July 1975)

SUMMARY

Some metal halides (Mn, Co, Ni, Pb and possibly Fe) emit metal(I) halide spectra from the MECA cavity in hydrogen—nitrogen—air flames, in contrast to their behaviour in conventional aspiration flame systems. However, the emission intensity is too weak to provide sensitive analytical applications. Indium halides give intense emissions by either the MECA or aspiration method. Halogenated organic compounds give intense CH and C_2 emissions. Cadmium halides give only an intense atomic emission. Sensitive methods for halides, indium, cadmium and organic compounds are thus possible. Mercury (II) halides and metal fluorides give no measurable emission in the cavity method.

When solutions containing metal ions or compounds are aspirated into analytically used flames, the metal is generally converted into gaseous atoms and simple molecules such as oxides, hydroxides and hydrides. The emission spectra obtained from such flames are therefore usually restricted to atomic lines of relatively low energy, and bands from the molecular species. The atomic emissions are particularly prominent in the hot, inner cone of hydrocarbon flames, whereas molecular emissions are more evident in cooler regions of such flames, or when cooler flames are used.

Emissions from metal halide molecules have been observed when a large amount of halogen is introduced into a flame into which metals or their salts have been introduced. As early as 1863, Diacon [1] produced metal chloride emissions in a hydrogen—chlorine flame. Andrade [2] similarly produced emissions which appeared to arise from nickel, cobalt, iron and copper chlorides. More recently [3], SnCl and SnBr band emissions were observed in a hydrogen—nitrogen diffusion flame when the solutions investigated were 0.1 M in hydrochloric or hydrobromic acid. There are very few reports of metal halide emissions from flames other than those rich in hydrogen. However, Honma [4] published a method for the determination of chloride in sea water, based on CuCl emission in a fuel-lean hydrogen—oxygen flame.

Hydrogen diffusion flames are the coolest of the analytically used flames, but even in these, metal halide emissions are not readily obtained by aspirating metal halide solutions. With tin(II) chloride or bromide, for example, SnCl

or SnBr emission is observed only in a small region close to the base of the flame [3]. The major emitting species are SnH (red) in the interior of the flame, and SnO (blue) in the outer regions. Indium(III) halides are exceptions to this general pattern. Because of the great stability of the indium—halide bond in comparison with In—O and In—H bonds, appreciable indium(I) halide emissions are obtained in a nitrogen-diluted hydrogen flame [5]. Gilbert [5] and, later, Dagnall et al. [6] showed that sensitive determinations of chloride, bromide and iodide may be achieved by measurement of the emissions at 360, 376 and 410 nm, respectively.

The presence of halide ions frequently gives rise to enhanced flame emission from metals. The enhancement, however, arises from swifter volatilization of the analyte rather than from the production of metal halide emissions. This is exemplified by the Beilstein test for halides [7], in which copper-containing species are rapidly volatilized from a copper wire in a flame when halogens are present on the wire or in the flame. The emission observed, however, arises mainly from CuOH bands in the 535—555 nm region, CuO bands at 445—492 nm, and a CuH band centred at 429 nm. In a similar manner, certain non-halogens such as cyanide and thiocyanate ions, and organic compounds such as thiourea and 8-hydroxyquinoline, which also give rise to volatile copper species in the flame, also give a positive Beilstein test.

Molecular emission cavity analysis (MECA) is a technique in which, in its simplest form[8], the sample is deposited in a small cavity, which is introduced into a hydrogen flame in such a way that the flame flows almost vertically past the aperture, which is in line with the emission detection optics. Such a device stimulates molecular emissions within the cavity from sulphur compounds (S_2), phosphorus compounds (HPO), selenium and tellurium, compounds etc., which allows sensitive analytical measurements to be made.

It was recently found that copper(II) [9], tin(II) [9, 10] and indium(III) [11, 12] halides all gave metal(I) halide emissions in the cavity, with very little emission arising from oxy species. This was attributed to the interior of the cavity being a relatively cool zone, containing fewer active flame radicals than the outer flame, and therefore appearing similar to the region at the base of the hydrogen diffusion flame. The indium halide responses were particularly sensitive, allowing the determination of 2.5 ng of chloride or bromide, and 50 ng of iodide [11].

Because of the tendency of the MECA cavity to produce metal(I) halide emission, a study was undertaken of the behaviour of a range of metal halides by MECA and by the conventional aspiration technique, with fuel-rich hydrogen—nitrogen—air flames.

EXPERIMENTAL

The MECA spectroscopic equipment was the same as described previously for candoluminescence studies [13]. For investigating the MECA characteristics of metal halides, ca. 10 mg of powdered solid was placed in a

stainless steel cavity, and 0.5 μl of water was added. The non-cavity end of the steel rod was heated in a Bunsen flame until the solution in the cavity boiled; on cooling, the cavity was evenly covered with a thin coating of metal halide. The cavity was inserted into the holder, and rotated into the hydrogen—nitrogen—air flame (3.25, 8.25 and 4.0 l min^{-1}, respectively), and the emission was recorded. When such a large sample is used, the emission takes 1.5 min to reach maximal intensity, and remains fairly constant thereafter for 1.5 to 15 min, depending on the salt concerned. The spectra of the various emissions were scanned after constant intensity had been reached. The spectral slit width varied from 2 nm at 250 nm to 14 nm at 450 nm and 38 nm at 650 nm. With the flame conditions used, negligible incandescence of the cavity material occurred.

When the aspiration method was used, the spectra were recorded with an EEL 240 atomic absorption spectrophotometer, operated in the emission mode, with a slit width of 6 nm throughout the spectral region scanned, and a hydrogen—nitrogen—air flame (2.0, 5.0 and 3.5 l min^{-1}, respectively); 1000-p.p.m. solutions of the particular metal ion, as its halide, were aspirated.

RESULTS

Manganese(II)

The spectra of manganese chloride and bromide by the MECA method are shown in Fig. 1, and that of manganese iodide is shown in Fig. 2. The spectra show distinct similarities. The sharp emission at 403 nm from manganese atoms, and that at 589 nm from sodium impurity can also be obtained on aspiration of manganese salts. The spectrum of manganese iodide in an aspiration system is shown in Fig. 2; those of aspirated manganese(II) nitrate and acetate are almost identical to it. However, the band emission found between 450 and 550 nm in the MECA experiments is almost absent for the

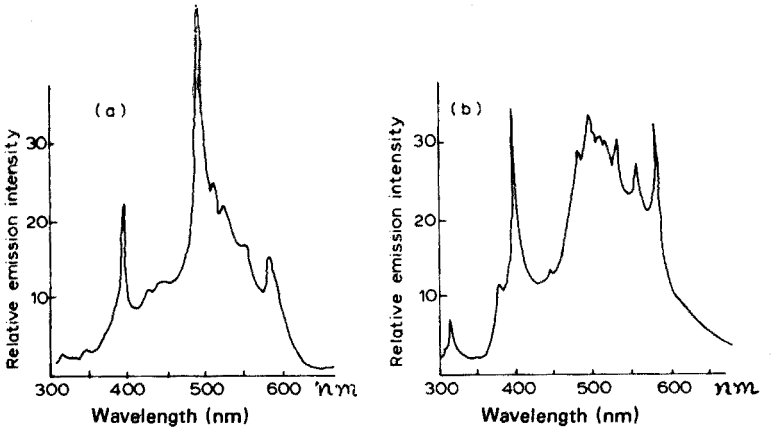

Fig. 1. MECA spectra of (a) $MnCl_2$, (b) $MnBr_2$.

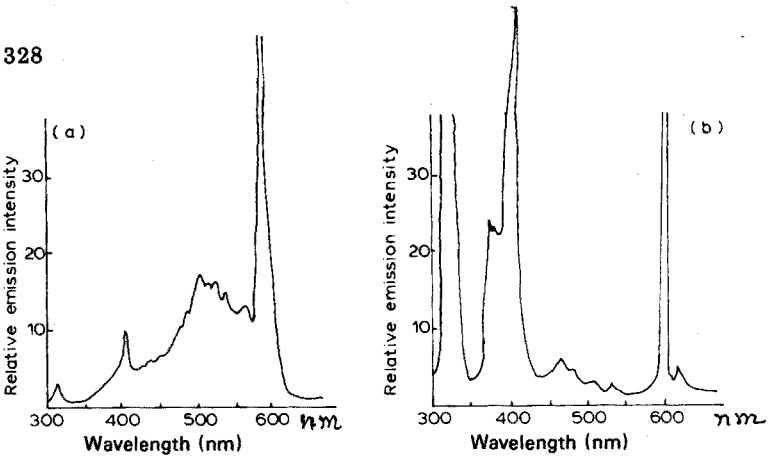

Fig. 2. Spectra of MnI_2 by (a) MECA, (b) aspiration.

aspiration method. The wavelengths of the major peaks in this region, for the chloride, bromide and iodide, are shown in Table 1, and would appear to arise from manganese(I) halide molecules. For example, Hayes [14] observed strong MnBr bands around 499 nm and 508 nm, and MnCl bands between 496 and 503 nm, in a high-frequency discharge. No other emitting manganese species, apart from MnH at 475 nm, have been observed in this region of the spectrum. Saha [15] observed bands between 520 and 570 nm when dry manganese(II) chloride was introduced into the oxidizing region of a Bunsen flame; the flame was pale yellowish-green. The MECA emission from all three halides was pale green.

Cobalt(II)

The spectra of cobalt(II) iodide obtained by the MECA and aspiration methods are compared in Fig. 3. The latter spectrum is almost identical with that obtained by aspiration of cobalt(II) chloride or nitrate solution. Cobalt(II iodide, bromide and chloride give pronounced band emissions between 360 and 570 nm. The wavelengths of the major peaks for the bromide and iodide

TABLE 1

Wavelengths of major MECA peaks for manganese(II) halides

Wavelength (nm)		
Chloride	Bromide	Iodide
435	450	472
445	495	480
500[a]	507[a]	495[a]
520	525	520
535	532	530
550	545[a]	562[a]

[a]Most intense peak.

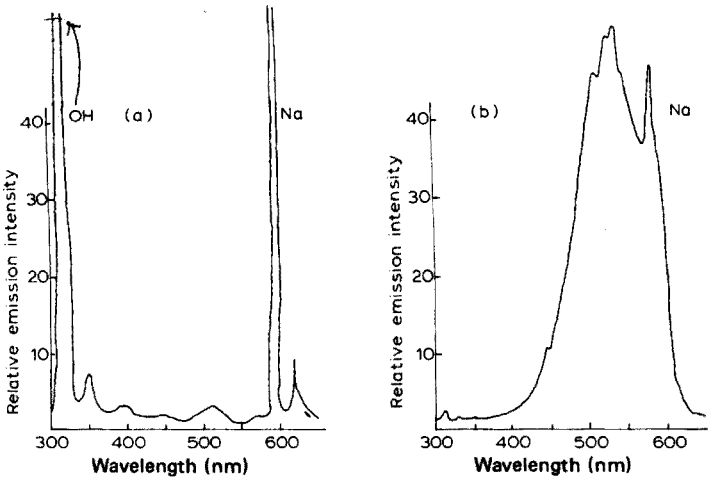

Fig. 3. Spectra of CoI_2 by (a) aspiration, (b) MECA.

are given in Table 2. The chloride emission was very weak. The emission at 345 nm (Fig. 3(a)) is from cobalt atoms. Previous reports of CoBr emission in a high-frequency discharge [16] give 564 nm and 553 nm as the strongest bands, with a series of peaks stretching to 434 nm. The emission is in the same spectral region as the MECA emission, but there is some discrepancy between peak wavelengths. The MECA emission from cobalt bromide was blue and was visually the most intense of all the metal halides investigated.

Nickel(II)

Nickel bromide in the MECA cavity gives a broad band emission between 300 and 600 nm (Fig. 4). The wavelengths of the major peaks are given in Table 2. The emission obtained on aspiration of nickel chloride solution is

TABLE 2

Wavelengths of major MECA peaks for cobalt(II) halides, nickel(II) bromide and iron(II) chloride

Wavelength (nm)					
$CoCl_2$	$CoBr_2$		CoI_2	$NiBr_2$	$FeCl_2$
	376	460	360	425	365[a]
	390	490[a]	510	440	382
	400	510	523	460	410
	420	540	535[a]	473[a]	448
ca. 500	425	550		500	470
	430	570		510	478
	440			550	500
					515[a]
					522
					535

[a]Most intense peak.

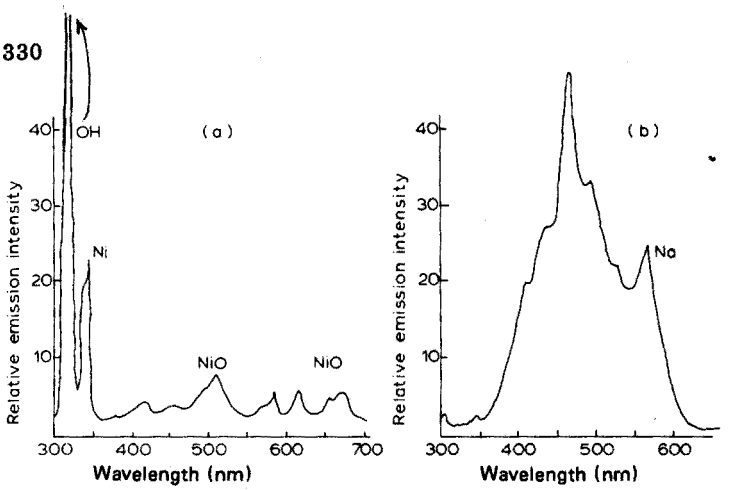

Fig. 4. Spectra of (a) $NiCl_2$ by aspiration; (b) $NiBr_2$ by MECA.

shown for comparison. Emission from nickel atoms is prominent in the latter, at 341 nm, but is very weak in the MECA spectrum. The MECA spectrum would appear to consist of NiO emissions, which may occur in the flame outside the cavity, and, possibly, NiBr emissions. NiO has been observed [17] to give several band emissions between 438 and 639 nm, with the strongest bands centred at 634, 613, 553 and 517 nm. NiBr bands have been observed in high-frequency discharges [18] at 411, 420, 435, 442, 459 and 466 nm. The small peak at 420 nm in the aspiration spectrum may arise from NiH [19]. This spectrum is very similar to that obtained by aspiration of nickel iodide or nitrate solution.

Nickel chloride gives only a very weak MECA emission, whereas nickel iodide gives a broad, featureless band between 400 and 700 nm.

Lead

Lead(II) chloride, bromide and iodide in the MECA cavity all give well structured band spectra between ca. 350 and 600 nm. The bands for chloride and bromide (Fig. 5) are symmetrical, with the bromide spectrum displaced to slightly longer wavelengths compared to that of the chloride. The iodide spectrum (Fig. 6) is not symmetrical and reaches its maximum at a longer wavelength than the bromide or chloride. The wavelengths of the emission peaks are given in Table 3; the variation of the wavelength with identity of the halogen indicates that at least some of the emission peaks arise from lead halide molecules. Lead chloride has been shown to give PbCl peaks in high-frequency discharges and in absorption [20, 21], in the region 436—536 nm; the peaks at 466, 485, 499 and 526 nm corresponding closely in wavelength to the most intense observed peaks. Similarly, absorption spectra of PbBr [21] show red-degraded bands in the region 448—532 nm, of which the 487 and 500-nm bands correspond closely in wavelength to the most intense observed peaks. Reported spectra of PbI have peaks at 556—622 nm, which correspond to the long-wavelength portion of the spectrum found.

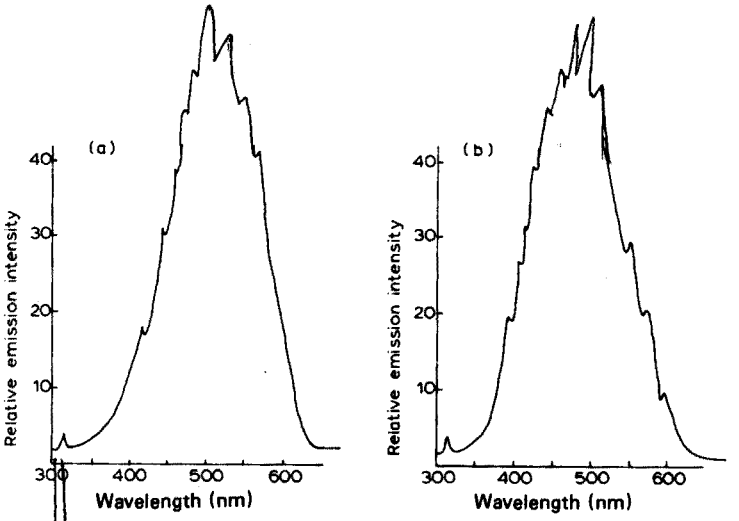

Fig. 5. MECA spectra of (a) $PbBr_2$, (b) $PbCl_2$.

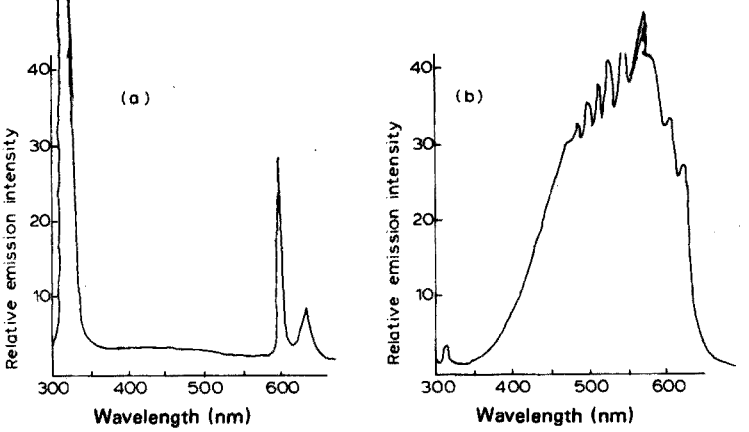

Fig. 6. Spectra of PbI_2 by (a) aspiration, (b) MECA.

TABLE 3

Wavelengths (nm) of major MECA peaks for lead(II) halides

Chloride			Bromide			Iodide		
355	448	535	335	452	535	330	412	485[a]
370	460	545	350	460	548	335	422	500[a]
375	470	567	360	467	557	345	430	522[a]
390	485[a]		365	475	567	352	435	527
415	500[a]		380	485		365	445	550
428	525		410	502[a]		375	467	560
435	530		437	527		405	470	577

[a]Most intense peaks.

However, many of the emission peaks, especially at shorter wavelengths can be attributed to PbO molecules in the flame outside the cavity, which give emissions from 332 nm to 591 nm [22]. The distorted shape of the lead iodide spectrum could thus arise from enhanced oxide production, causing the greater intensity at shorter wavelengths. As the PbI bond is significantly weaker than the PbCl and PbBr bonds (Table 4), dissociation of the lead-halide molecule is facilitated.

The spectra of lead iodide, acetate and nitrate obtained by the aspiration method show no emissions attributable to lead species in the region 300—600 nm.

Cadmium and mercury

In the MECA spectrum obtained from cadmium chloride (Fig. 7(b)), the only feature of note is the cadmium atom line at 326 nm. Cadmium, bromide and iodide behave similarly. The spectrum obtained by aspiration (Fig. 7(a)) shows the cadmium atom line, as a shoulder on the very intense OH peak at 306 nm which is almost absent from the MECA spectrum.

Mercury(II) chloride, bromide or iodide gave no emission in the MECA cavity

TABLE 4

Bond energies (in kcal mol^{-1}) of some metal halides [26]

Metal halide	InCl	InBr	NiCl	MnCl	NiBr	CuCl	FeCl	InI		
Bond energy	103	93	89	86	86	84	84(?)	80		
Metal halide	CuBr	MnBr	SnCl	PbCl	NiI	MnI	FeBr	PbBr	CdCl	CuI
Bond energy	79	75	75(?)	72	70	68	59	59	50	47(?)
Metal halide	SnBr	PbI	CdBr	CdI	HgCl	HgBr	HgI			
Bond energy	47	47	38	33	24	17	9			

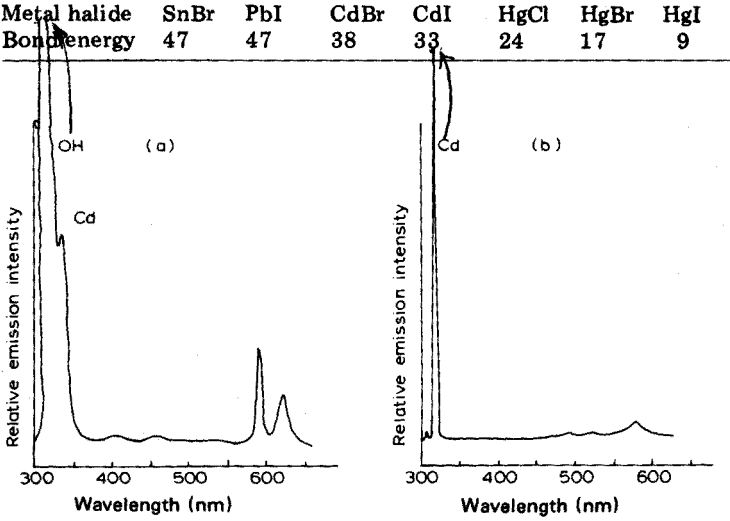

Fig. 7. Spectra of $CdCl_2$ by (a) aspiration, (b) MECA.

Indium and tin

Indium(III) chloride, bromide and iodide give similar emissions in the MECA and aspiration systems (Fig. 8). Indium chloride gives rise to InCl emissions at 364, 360, 355 and 350 nm. At longer wavelengths (368—400 nm) emissions ascribed to In_2 molecules are obtained. Indium bromide gives a well resolved spectrum centred at 376 nm, and indium iodide a band at 410 nm. The InI band is separated from the shorter wavelength In_2 emission, but the latter coincides almost exactly with the wavelength range of the InBr emission.

Tin(II) chloride and bromide give characteristic blue SnCl and green SnBr emissions in the MECA cavity [10], whereas tin(II) nitrate gives no emission. On aspiration, all the halides give mainly SnO emissions.

Iron

Iron(II) chloride gives a broad band emission centred at 515 nm, in the MECA spectrum. The wavelengths of the major peaks are given in Table 2; the peaks at 365 and 382 nm are probably iron atom and FeOH emissions [23], but those at 470, 478 and 500 nm correspond closely to FeCl emissions reported at 470, 477—481 and 496 nm [24]. Aspiration of iron(II) chloride and iodide solutions give spectra almost identical to each other, composed mainly of the atom lines between 347—373 nm and FeOH and FeO emissions.

Metal fluorides

The fluorides of cobalt(II), tin(II), copper(II), calcium and lead gave no visible MECA emission.

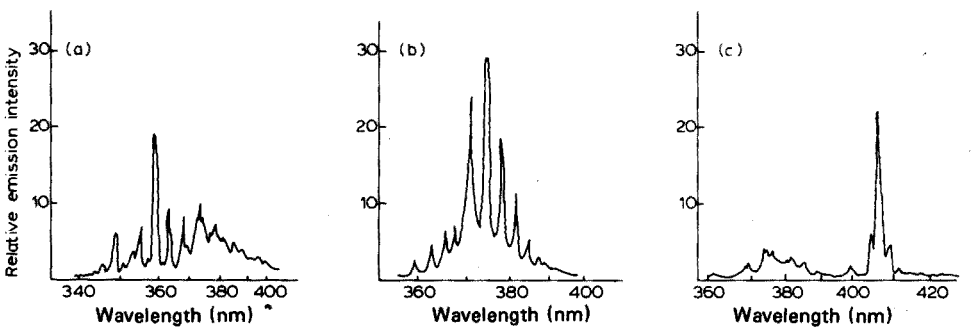

Fig. 8. Spectra of (a) $InCl_3$, (b) $InBr_3$ and (c) InI_3, by aspiration.

Organic chloro compounds

Many organic chloro compounds, such as carbon tetrachloride, give intense green MECA emissions, with major broad peaks centred at 431 (CH), 463 and 516 nm (C_2). Organic halides have previously been shown to give enhanced C_2 emissions relative to CH emissions in a hydrogen flame [25]. Non-halogenate oxygen-containing compounds give blue MECA emissions, (λ_{max} = 430 nm). This emission is given by all organic compounds if oxygen is introduced directly into the cavity and is primarily CH emission.

DISCUSSION

Many metal halides give characteristic emissions in the MECA cavity which are significantly different from those obtained by aspiration of aqueous solutions of metal halides into a hydrogen flame of similar composition. Under the experimental conditions used, the emissions are mostly weak, and require a large amount of sample; attempts are being made to increase the emission intensity. Until this is successful the emissions are unlikely to have any important general analytical applications. The emissions from indium, tin, cadmium and organic chloro compounds are exceptions to this statement, however, and should provide the basis for sensitive analytical methods for these species and for chlorine, bromine and iodine. A method for these halides, based on indium, has already been described briefly [11].

The identity of the emitting species is difficult to establish unequivocally for the transition metal halides, because the resolution of the spectrophotometers used was not high. However, the variations in the peak wavelengths and in the overall spectral band positions for different halides of a given metal indicate that the emissions arise at least in part from metal halide (MX) molecules. These assignments are borne out to a large extent by correlation with known spectra, where these are available, but are often confused by possible oxide emissions, which are known to occur outside the cavity. There can be little doubt, however, that the indium, tin and copper emissions arise almost entirely from metal halides.

Observations made previously with aspiration systems are of use in explaining the formation of excited metal halide molecules within the cavity. In aspiration systems, tin(II) halides, for example, give rise to tin(I) halide emission only in the region of the flame closest to the burner top, i.e. the low-temperature region containing the least oxygen and with only a small concentration of flame radicals. Thus the environment within the cavity would appear to be similar to the region at the base of the flame.

Under such conditions, the existence of metal halides in the vapour phase would be expected to depend on the metal—halide bond strength, and thus the resistance of the molecule to thermal breakdown, and also on the metal—hydride bond strength, and thus possible metal hydride formation at the expense of the metal halide population. The bond strengths

of relevant metal(I) halides are given in Table 4. Those of FeI and SnI are not known, but are expected to be less than the corresponding bromides. Metal hydride bond strengths are less than 67 kcal mol^{-1}. It is noteworthy that the species that give prominent halide spectra are those with relatively strong metal—halide bonds (i.e. those in Table 4 with bond strengths of $\geqslant$ 70 kcal mol^{-1}) and one or two others, such as SnBr and PbI; the most weakly bound halides, those of mercury and cadmium, gave no indication of metal halide emission. The emissions from the relatively weakly bound species such as SnBr and PbI may arise because of the relatively high volatility of their precursors ($PbCl_2$, $SnBr_2$), so that volatile emitting species are formed in the cavity before complete thermal breakdown occurs. Such decomposition would be retarded by the existence of an appreciable concentration of hydrogen halide molecules in the cavity resulting from the partial breakdown of the original metal halide (e.g. $PbCl_2(g) + H(g) \rightleftharpoons HCl(g) + PbCl(g)$).

That decomposition of the metal halides to the metal eventually takes place is shown by the metallic coating formed, particularly on the lip of the cavity when, for example, copper [9] or indium[11] halides have been used in the cavity. With such coated cavities, the metal halide emission can be regenerated after addition of 1 M hydrochloric acid.

Cadmium halides give only cadmium atom emission, an indication of the weakness of the cadmium—halide bond. The emission is very intense, considering the low temperature, and must be chemiluminescence. A more detailed investigation and analytical applications will be published later. Manganese also gives rise to a little atomic emission, and also some hydride emission.

The production of characteristic emissions (usually CH and C_2 bands) from organic compounds greatly extends the range of application of MECA. None of the emissions can be ascribed to halogen species, but the intensity of the emissions from organic halogen compounds should provide the basis of some very sensitive analytical procedures.

In conclusion, MECA provides a simple method of generating emissions from metal halide (MX) molecules in the gas phase. Although such emissions are of analytical utility only in a few instances, the technique should be of value in investigations of the emission spectra of the metal halides, without the need to resort to discharge tubes, vacuum systems, etc. The emissions from indium and tin halides, and from cadmium atoms, however, are sufficiently intense to provide sensitive methods for the determination of these metals, as well as halides.

This work has been carried out with the support of Procurement Executive, Ministry of Defence.

REFERENCES

1 E. Diacon, Compt. Rend., 56 (1863) 653.
2 E. N. da C. Andrade, Proc. Phys. Soc. London, 25 (1913) 230.
3 R. M. Dagnall, K. C. Thompson and T. S. West, Analyst (London), 93 (1968) 518.
4 M. Honma, Anal. Chem., 27 (1955) 1656.
5 P. T. Gilbert, Anal. Chem., 38 (1966) 1920.
6 R. M. Dagnall, K. C. Thompson and T. S. West, Analyst (London), 94 (1969) 643.
7 F. K. Beilstein, Ber. Deut. Chem. Ges., 5 (1872) 620.
8 R. Belcher, S. L. Bogdanski, S. A. Ghonaim and A. Townshend, Anal. Lett., 7 (1974) 133.
9 R. Belcher, S. L. Bogdanski, S. A. Ghonaim and A. Townshend, Nature (London), 248 (1974) 326.
10 S. A. Ghonaim, Proc. Soc. Anal. Chem., 11 (1974) 167.
11 R. Belcher, S. L. Bogdanski, Z. M. Kassir, D. A. Stiles and A. Townshend, Anal. Lett., 7 (1974) 751.
12 D. A. Stiles, Proc. Soc. Anal. Chem., 11 (1974) 141.
13 R. Belcher, K. P. Ranjitkar and A. Townshend, Analyst (London), 100 (1975) 415.
14 W. Hayes, Proc. Phys. Soc. London, 68 (1955) 1097.
15 B. Saha, Sci. Cult., 5 (1939) 197.
16 P. Mesnage, Doctoral Thesis, Paris, 1938, quoted in Ref. 23.
17 L. Malet and B. Rosen, Bull. Soc. Roy. Sci. Liege, 14 (1945) 382.
18 S. P. Reddy and P. T. Rao, Proc. Phys. Soc. London, 75 (1960) 275.
19 R. W. B. Pearse and A. G. Gaydon, Proc. Phys. Soc. London, 148 (1935) 312.
20 G. D. Rochester, Proc. Roy. Soc., 153 (1935) 407.
21 F. Morgan, Phys. Rev., 49 (1936) 47.
22 P. T. Rao, Ind. J. Phys., 23 (1949) 321.
23 R. W. B. Pearse and A. G. Gaydon, The Identification of Molecular Spectra, Chapman and Hall, London, 1965.
24 S. P. Reddy and P. T. Rao, J. Mol. Spectrosc., 4 (1960) 16.
25 R. S. Bramen, Anal. Chem., 38 (1966) 735.
26 R. C. Weast (Ed.), Handbook of Chemistry and Physics, The Chemical Rubber Co., Cleveland, U.S.A., 1974, p. F —183.

Analytica Chimica Acta, 81 (1976) 337—347

MULTIELEMENT PHOTON ACTIVATION ANALYSIS OF BIOLOGICAL MATERIALS

TOYOAKI KATO, NOBUYOSHI SATO* and NOBUO SUZUKI

Department of Chemistry, Faculty of Science, Tohoku University, Sendai (Japan)

(Received 9th June 1975)

SUMMARY

A non-destructive photon activation procedure with 30-MeV bremsstrahlung followed by high-resolution γ-spectrometry is proposed for multielement analysis of biological materials. The materials tested were the NBS SRM Orchard Leaves and Bovine Liver, Bowen's kale and Kentucky 1R1 tobacco standards. Simultaneous irradiation of the sample with synthetic multielement standards containing 25 elements showed that up to 12 elements can be determined in a single sample. The method is quite simple and gives good reproducible results. Agreement of the results with published data is excellent.

Of the elements commonly found in animal and plant tissues, a total of 18 minor and trace elements are essential in the life processes [1]. Some of the other elements, such as As, Cd, Hg, Sb and Pb, are known to be toxic, and special attention has been given to their levels from the environmental viewpoint. The remaining elements may also play significant biological roles in life systems. In studies of the rôles of these elements, multielement analysis has become increasingly attractive, for it can give an overall view of elemental patterns which may be very important in living matter. The impressive potential of activation analysis for this purpose has prompted a large volume of work on its application to the determination of many elements in a variety of biological materials. Thermal neutron activation followed by high-resolution γ-spectrometry has been successfully applied to the nondestructive determination of many elements in single samples. Nadkarni and Morrison [2] determined up to 35 elements in several biological materials, using two irradiations with different times according to the half-lives of the products to be measured. With instrumental neutron activation analysis, however, the high activities produced from abundant, readily activated elements such as manganese and sodium, often distort or mask lower activities from the elements of interest. Various schemes for the isolation of pure radioisotopes, and chemical group separations have therefore been proposed [3—9].

An alternative nuclear method which can meet various requirements for multielement work is photon activation analysis; several recent reviews of

*College of General Education, Iwate University, Morioka (Japan).

this method are available [10—13]. The yields of photonuclear reactions of various types have been measured by bremsstrahlung irradiations of numerous elements with energies up to 70 MeV [14, 15]. Useful compilations of the nuclear data [16—18], and γ-spectrum catalogues [19—21] for photon activation products are also available. Multielement photon activation analysis has been applied to geological samples [22—25], biological materials [26—28], and air particulate samples [29]. More recently, Chattopadhyay and Jervis [30] developed an instrumental method for simultaneous determination of 30 elements in market-garden soils with a 45-MeV electron linear accelerator. They also applied the method to several intercomparison standard materials.

The present paper describes the application of bremsstrahlung activation analysis to the nondestructive multielement analysis of biological standard reference materials. Emphasis is placed on the validity and versatility of the method. Because of experience gained in analysing geological materials [24], it was decided to combine 30-MeV bremsstrahlung activation and intact measurements with a lithium-drifted germanium detector for analysis of four round-robin standard samples to obtain maximum elemental information without chemical separations. Up to 12 elements could be determined by this method, and agreement of the present results with literature data was satisfactory.

EXPERIMENTAL

Samples and comparative standards

The standard reference materials SRM-1571 Orchard Leaves and SRM-1577 Bovine Liver (U.S. National Bureau of Standards [31]), the Bowen standard kale sample [32], and the standard reference tobacco 1R1 [33], were used. The 1R1 tobacco samples were taken from the same packet and the wrapping papers were rejected and the tobaccos were then powdered in an agate mortar. All samples were dried for 24 h at 90 °C before irradiation, as recommended by the suppliers. A portion (1 g) of the dried sample was placed in the stainless steel cavity of a lubricant press and compressed to a cylindrical pellet with a diameter of 13 mm.

The comparative standards used were synthetic multielement pellets containing the elements of interest distributed evenly in a matrix of cellulose. These standards were prepared by mixing 25 elements, mostly added as oxides, at appropriate concentration levels with cellulose powder. Portions (1 g) of this mixture was pelleted for irradiation. In preparing these standards, reagents with a chemical purity of 99.99% or better were used. Two kinds of standard with different elemental compositions were prepared: one for the plant materials and the other for Bovine Liver (Table 1).

TABLE 1

Concentration of elements in cellulose pellets used as multielement standards

For orchard leaves, kale and tobacco		*For bovine liver*	
Concentration	Element	Concentration	Element
4%	Ca	1%	Cl, K
2%	K	0.5%	Na
1%	Mg	0.1%	Ca, Mg
0.3%	Cl	500 p.p.m.	Cu, Fe, Zn
500 p.p.m.	Fe	50 p.p.m.	Ba, Mn, Ni, Rb, Sr
200 p.p.m.	Ba, Cu, Mn, Na, Ni, Rb, Sr, Zn	25 p.p.m.	As, Ce, Co, Cr, Cs, I, Mo, Pb, Sb, Ti, Tl, Zr
20 p.p.m.	As, Ce, Co, Cr, Cs, I, Mo, Pb, Sb, Ti, Tl, Zr		

Irradiation

Bremsstrahlung irradiations were done in the linear electron accelerator of Tohoku University. The accelerator was operated at 30 MeV, and the electron beam, the peak current being 90 mA, produced bremsstrahlung in a platinum converter with a thickness of 3 mm located 3 cm from the beam exit window. The average beam current in a typical operating condition was 70 μA at the position of the converter. The sample pellet and the comparative standards were stacked in a silica tube, the standards being placed in front of and behind the sample for simultaneous irradiation. The tube was placed in a water-cooled sample holder and aligned along the beam axis with the front face of the tube 10—15 cm from the photon-producing converter. A typical irradiation was performed for 2 h at a dose-rate of 10^6 R min^{-1}. The heat generated by the remaining electrons in the bremsstrahlung tended to cause chemical decomposition of biological samples, which therefore could not be positioned close to the converter. Under typical irradiation conditions with a 70-μA beam (on average) of 30-MeV electrons, however, no significant damage was observed for up to 2 h at a position 10 cm downstream from the converter.

Counting and evaluation

A 33-cm^3 lithium-drifted germanium detector (Ortec Model 8101-0525) was coupled to a 4096-channel pulse-height analyzer (Toshiba Electric Co. Ltd., Japan). The counting system had a resolution of 2.4 keV for the 1332-keV γ-line of ^{60}Co. Counting was done consecutively for increasing intervals over a period of one month or longer. For short-lived nuclides, ^{38}K and ^{34m}Cl, the counting time was progressively increased from 4 to 16 min. During this interval, a 50-mm thick Lucite plate was placed between the

sample and the detector to absorb positrons from a number of positron-emitting nuclides. For nuclides with intermediate half-lives, the counting times were 30—60 min, and, for long-lived nuclides, the counting times were 5—20 h. The γ-rays were characterized by means of the γ-spectra obtained by irradiating the pertinent pure elements, and from nuclear data listed in the Table of Isotopes [34]. In obtaining full-energy peak areas, the total peak counts were computed and the background contribution was subtracted; linear variation of background over the peak of interest was assumed. Decay curve analyses were made to check for interferences. The mean specific activity (in terms of the peak areas) for any specified γ-ray from the standards on both sides of the sample, was used for calculating the concentration of the required element.

Duplicate analyses were made for each material.

RESULTS AND DISCUSSION

Reaction products

At short decay times after irradiation, the γ-spectra of both the biological samples and the multielement standards were so strongly dominated by 511-keV annihilation radiation from the positron emitters that no γ-rays below that energy could be observed. The only products observed were those with high-energy γ-rays, e.g. 7.71-min ^{38}K and 32-min ^{34m}Cl. After a decay interval of 2—5 h, the products of major interest were ^{87m}Sr and those from (γ, p) reactions on iron (^{56}Mn), calcium (^{43}K) and magnesium (^{24}Na). Up to 10 d after irradiation, a comprehensive amount of spectral data was obtained. At this stage, 16 of the 25 elements in the comparative standard had been clearly identified. The principal products from these 16 elements are given in Table 2, along with half-lives, significant γ-rays and their intensities, time intervals best suited for measurements after irradiation, and practical detection limits. Apart from the γ-rays listed in Table 2, several γ-rays from additional elements were also observed, including the 279-keV peak of ^{203}Pb, the 1340-keV peak of ^{64}Cu and the 1378-keV peak of ^{57}Ni, but these were not used for abundance determinations because of the low peak-to-background ratios. The ^{47}Sc activity can be formed from titanium by the (γ, p) reaction, and the 160-keV peak of ^{47}Sc can be used for a sensitive determination of titanium [24]. In the present case, however, titanium could not be determined, because of the strong interference from calcium via the ^{48}Ca(γ, n)^{47}Ca β^- ^{47}Sc reaction. The practical detection limits listed in Table 2 were estimated from the spectral data for the synthetic multielement standard; these were measured at the time intervals shown in Table 2, and were calculated under the criterion for validation of the peaks, being the amounts needed to give a full-energy peak area corresponding to 3 times the standard deviation of the area under the peak of interest. These limits depend, of course, on the nature and strength of the background. For instance, the 279-keV peak of

TABLE 2

Principal photon activation products observed in synthetic standard

Element	Product nuclide	Process	Half-life	γ-ray observed (keV)	Photopeak intensity[a] (cpm/mg)	Optimal interval[b]	Practical detection limit (μg)
As	^{74}As	(γ, n)	17.9 d	596	$1.66 \cdot 10^3$	10—20 d	1.0
As	^{74}As	(γ, n)	17.9 d	634	$3.97 \cdot 10^2$	20 d	3.7
Ca	^{43}K	(γ, p)	22.4 h	374	$2.26 \cdot 10^2$	1—3 d	280
Ca	^{43}K	(γ, p)	22.4 h	619	$1.11 \cdot 10^2$	1—3 d	470
Ca	^{47}Ca	(γ, n)	4.53 d	1298	$6.35 \cdot 10^0$	10—20 d	330
Cl	^{34m}Cl	(γ, n)	32.0 min	2130	$2.98 \cdot 10^3$	30 min—1 h	280
Cl	^{34m}Cl	(γ, n)	32.0 min	3320	$4.87 \cdot 10^2$	30 min—1 h	810
Cs	^{132}Cs	(γ, n)	6.5 d	668	$1.04 \cdot 10^4$	10—20 d	0.4
Fe	^{56}Mn	(γ, p)	2.576 h	847	$1.01 \cdot 10^3$	2—5 h	140
I	^{126}I	(γ, n)	13 d	386	$3.64 \cdot 10^3$	10—20 d	0.8
K	^{38}K	(γ, n)	7.71 min	2170	$1.94 \cdot 10^4$	10—30 min	1700
Mg	^{24}Na	(γ, p)	15.0 h	1368	$8.88 \cdot 10^2$	1—3 d	110
Mn	^{54}Mn	(γ, n)	303 d	835	$8.77 \cdot 10^1$	20 d	4.6
Na	^{22}Na	(γ, n)	2.60 y	1275	$6.27 \cdot 10^0$	20 d	30
Rb	^{84}Rb	(γ, n)	33.0 d	880	$5.57 \cdot 10^2$	10—20 d	1.2
Sb	^{122}Sb	(γ, n)	2.80 d	564	$7.89 \cdot 10^3$	3—10 d	1.0
Sr	^{87m}Sr	(γ, n)	2.83 h	388	$3.46 \cdot 10^5$	2—10 h	1.2
Tl	^{202}Tl	(γ, n)	12.0 d	440	$2.92 \cdot 10^3$	10—20 d	0.8
Zn	^{67}Cu	(γ, p)	59 h	185	$5.86 \cdot 10^2$	2—3 d	30
Zn	^{65}Zn	(γ, n)	245 d	1115	$2.36 \cdot 10^1$	20 d	25
Zr	^{89}Zr	(γ, n)	78.4 h	913	$4.94 \cdot 10^3$	3—10 d	1.3

[a] At the end of 2-h irradiation with 30-MeV bremsstrahlung (10^6 R min^{-1}).
[b] Optimal time interval for measurement after irradiation.

^{203}Pb could be observed clearly in the spectra of Orchard Leaves (45 p.p.m. Pb); a practical detection limit of 7 μg Pb g^{-1} of sample was obtained for this material at a decay time of 9 d. However, in the spectrum of the comparative standard (20 μg Pb) at a comparable decay time, this peak was obscured by a much higher background level, so that lead could not be determined in any sample studied.

Elemental abundances

The elements identifiable in both sample and standard were determined quantitatively. Of the peaks of an element to be quantified, the most intense interference-free peak was selected. Twelve elements could be determined in Orchard Leaves, 11 in 1R1 tobacco, 10 in kale, and 9 in Bovine Liver; Cs, I, Tl and Zr could not be measured in these samples because they were present below the detection limit of the method. Some comments on the determinations of several of the elements are given below.

Arsenic was determined from the 596-keV peak of ^{74}As. The 634-keV ^{74}As peak could also be measured, but the results were then less precise, and this peak was used only for confirmation. To avoid the 593-keV ^{43}K peak, measurements were made 10 d or longer after irradiation. In Bovine Liver and kale samples, arsenic was present below the detection limit.

Calcium was determined either by the ^{44}Ca$(\gamma, p)^{43}$K or by the ^{48}Ca$(\gamma, n)^{47}$Ca reaction. Of the ^{43}K and ^{47}Ca peaks, the 374-keV and 619-keV peaks of ^{43}K and the 1298-keV peak of ^{47}Ca were preferred. As shown in Table 3 any peak provided reliable calcium values. Since animal tissues contain far less calcium than plant tissues, the ^{43}K and ^{47}Ca activities produced are lower; in Bovine Liver the 374-keV and 619-keV peaks of ^{43}K gave reliable values for calcium, and the 1298-keV ^{47}Ca peak was used only for confirmation.

Chlorine could be measured from the 2130-keV ^{34m}Cl peak; the 3320-keV peak was used only for confirmation because of its lower intensity.

In determinations of magnesium by the ^{25}Mg$(\gamma, p)^{24}$Na reaction, aluminum interferes through the ^{27}Al$(n, \alpha)^{24}$Na reaction. A separate irradiation of known amounts of magnesium and aluminum under identical conditions produced a ratio of ^{24}Na specific activities of 206:1. The ^{27}Al$(n, \alpha)^{24}$Na contribution to the total ^{24}Na activity could then be estimated as 0.08 % in the 1R1 tobacco sample which had the highest Al:Mg ratio [2] of the samples under study. Interferences from this source were therefore negligible.

The ^{54}Mn activity produced from iron by the ^{56}Fe$(\gamma, pn)^{54}$Mn reaction causes interference in the magnesium determination. When pure iron was irradiated with 30-MeV bremsstrahlung for 2 h, a ratio of $1.03 \cdot 10^{-3}$ was obtained for the 835-keV ^{54}Mn peak area to the 847-keV ^{56}Mn peak area at the end of irradiation. The ^{54}Mn activity arising from the ^{55}Mn$(\gamma, n)^{54}$Mn reaction for a given sample was therefore calculated by multiplying the count rate under the 847-keV peak by $1.03 \cdot 10^{-3}$, and then by subtracting this value from the count rate under the 835-keV peak corrected for decay to the end of irradiation. The ^{56}Fe$(\gamma, pn)^{54}$Mn contribution to the total ^{54}Mn activity was found to be 20 % for Bovine Liver, which had the highest Fe:Mn ratio of the samples studied. The corresponding contributions to Orchard Leaves, kale and 1R1 tobacco were 3.4, 7.5 and 1.9 %, respectively.

Zinc was measured at long decay times by the 1115-keV ^{65}Zn peak rather than by the 185-keV ^{67}Cu peak, because of the higher peak-to-background ratio.

There were some further possibilities of contributions by (γ, pn), (γ, α) and/or $(\gamma, \alpha n)$ reactions taking place on adjacent elements in the Periodic Table. However, detailed nuclear considerations based on the experimental yields of photonuclear reactions of various types [14, 15] showed that these secondary contributions did not produce serious interference problems in this study.

The results obtained are given in Tables 4—7.

TABLE 3

Calcium concentrations in Orchard Leaves, Bovine Liver, kale and tobacco determined from different photopeaks[a]

Photopeaks used	Orchard leaves (%)	Bovine liver (p.p.m.)	Bowen's kale (%)	1R1 tobacco (%)
^{43}K 374 keV	1.95 ± 0.01	139 ± 15	4.09 ± 0.05	2.70 ± 0.01
	2.04 ± 0.01	142 ± 20	4.16 ± 0.08	2.61 ± 0.01
^{43}K 619 keV	1.94 ± 0.01	130 ± 29	4.07 ± 0.07	2.69 ± 0.02
	2.02 ± 0.02	141 ± 34	4.15 ± 0.11	2.63 ± 0.02
^{47}Ca 1298 keV	1.90 ± 0.27	—	4.02 ± 0.08	2.58 ± 0.01
	1.93 ± 0.06	—	4.17 ± 0.10	2.56 ± 0.03
Average	1.93 ± 0.09	135 ± 16	4.06 ± 0.04	2.65 ± 0.01
	2.00 ± 0.02	141 ± 20	4.16 ± 0.06	2.60 ± 0.01

[a]Error limits are standard deviations based on counting statistics. The two results given for each sample at a particular photopeak were obtained on duplicate samples.

Reliability

As shown in Tables 4—7, duplicate samples provided reasonable reproducibility for each of the elements. When the values from duplicate analyses were averaged, the relative deviations from the means based on a total of 42 determinations were within ± 7 %.

In comparing the present results with those certified by NBS [31] or with other published data [4, 30, 35—38], the relative deviations of the means were within ± 6 % and ± 3 % for Orchard Leaves and Bovine Liver, respectively. The present values in kale are also quite compatible with the "best" values recommended by Bowen [32], except for sodium. The average relative deviation based on 10 elements was ± 2.7 %. For sodium in kale a value of 0.20 % was found compared to the "best" value of 0.25 % [32]. Bowen stated that the wide range (0.122—0.325 %) for sodium in kale is surprising, considering that this element can be determined by various analytical means; contamination during handling is probably responsible for this discrepancy. For 1R1 tobacco, the agreement between the present data and those reported by Nadkarni and Morrison [3] is excellent, the average relative deviation from the means being ± 4.6 % based on 11 elements determined here. For arsenic in 1R1 tobacco the present result (1.4 p.p.m.) is lower than that reported by Nadkarni and Morrison [3], but rather similar to the recent value [35] of 1.6 p.p.m. Nadkarni [35] indicated a slight scatter for arsenic determinations in 1R1 tobacco, which was attributed to the heterogeneous nature of this material.

TABLE 4

Elemental abundances of NBS standard reference material 1571, Orchard Leaves

Element (p.p.m.)	This work[a]	NBS[b]	Ref. 4[c]	Ref. 30	Others
As	11 ± 1 10 ± 1	11 ± 2	10	10.2 ± 1.0	10.7 ± 1.0 [37] 11.6 ± 1.3 [35]
Ca, %	1.93 ± 0.09 2.00 ± 0.02	2.09 ± 0.03	2.10	2.08 ± 0.01	
Cl	729 ± 197 705 ± 190	(700)	790	685 ± 32	
Fe	337 ± 123 326 ± 113	300 ± 20	290	290 ± 12	318 ± 27 [37]
K, %	1.45 ± 0.11 1.44 ± 0.11	1.47 ± 0.03	1.52		
Mg, %	0.605 ± 0.01 0.625 ± 0.01	0.62 ± 0.02	0.60	0.61 ± 0.01	
Mn	97 ± 5 92 ± 5	91 ± 4	86	88.2 ± 3.4	87.8 ± 5.9 [38]
Na	86 ± 18 88 ± 14	82 ± 6	77	79.3 ± 5.0	
Rb	12 ± 1 13 ± 1	12 ± 1	11		12.0 ± 1.1 [37]
Sb	3.3 ± 0.3 3.2 ± 0.3		3.0	3.15 ± 0.26	2.7 ± 0.3 [37]
Sr	35 ± 1 38 ± 1	(37)	40	36.2 ± 2.0	
Zn	29 ± 4 25 ± 4	25 ± 3	25	24.2 ± 1.5	23.3 ± 2.7 [38]

[a] Error limits are standard deviations based on counting statistics.
[b] Values in parentheses are NBS noncertified values.
[c] Average of duplicate analyses.

CONCLUSION

As demonstrated in Tables 4—7, up to 12 elements could be determined nondestructively in biological materials by the proposed method. The elements included essential minor elements such as Ca, Cl, K, Na and Mg, essential trace elements such as Fe, Mn and Zn, and possibly toxic elements such as As and Sb. The accuracy and precision of the method are good considering the number of elements determined. Instrumental neutron activation analysis is extremely sensitive for many elements, but is plagued often with very high matrix activities in biological specimens which interfere with measurements of the much lower activities from the elements of interest. Such difficulties are not inherent in photon activation analysis. The elemental abundances in Orchard Leaves, especially with regard to the elements determinable by this method, indicate that this material would be preferable to synthetic standards as the comparative standard in multi-

TABLE 5

Elemental abundances of NBS Standard Reference Material 1577, Bovine Liver

Element (p.p.m.)	This work[a]	NBS[b]	Ref. 2	Others
Ca	134 ± 16 141 ± 20	(123)	<0.02 %	
Cl	2690 ± 160 2680 ± 170	(2600)	0.275 %	
Fe	271 ± 24 278 ± 32	270 ± 20	262	
K, %	0.969 ± 0.096 0.969 ± 0.087	0.97 ± 0.06	0.96	
Mg	605 ± 18 588 ± 9	(605)	0.104 %	
Mn	9.7 ± 1.8 10.6 ± 2.5	10.3 ± 1.0	9.14	10.23 ± 0.43 [38]
Na, %	0.235 ± 0.004 0.240 ± 0.004	0.243 ± 0.013	0.24	
Rb	19.8 ± 1.5 18.1 ± 1.8	18.3 ± 1.0	20.1	
Zn	129 ± 13 133 ± 14	130 ± 10	116	121.9 [38] 127.9 ± 9.1 [37]

[a]Error limits are standard deviations based on counting statistics.
[b]Values in parentheses are NBS noncertified values.

element photon activation analysis. If irradiations with higher dose-rates were used, the sensitivities would be improved so that the method could be applied to the determination of more elements with lower detection limits. Especially when combined with simple radiochemical steps, photon activation analysis will offer the capability of determining traces of F, I, Pb and Ni that are of considerable environmental concern.

The authors express their appreciation to members of the linac and radioisotope groups at the Institute of Nuclear Science, Tohoku University, for their cooperation with the irradiations. The Orchard Leaves and Bovine Liver standards were kindly provided by Drs. P. D. LaFleur and G. J. Lutz, U.S. National Bureau of Standards. We also thank Professor H. J. M. Bowen, Reading University, England for the kale standard, and Professor W. D. Ehmann and members of the University of Kentucky Tobacco and Health Research Institute, Lexington, Ky., U.S.A. for the lRl tobacco sample.

Elemental abundances of Bowen's kale

Element (p.p.m.)	This work[a]	Bowen's "best" value	Ref. 2	Others
Ca, %	4.06 ± 0.04	4.09	4.43	
	4.16 ± 0.06			
Cl, %	0.343 ± 0.035	0.34	0.36	
	0.301 ± 0.029			
Fe	124 ± 64	118	103	
	124 ± 46			
K, %	2.45 ± 0.16	2.46	2.44	
	2.41 ± 0.25			
Mg, %	0.160 ± 0.002	0.16	0.16	
	0.163 ± 0.002			
Mn	15.7 ± 3.7	14.7	14.8	
	14.0 ± 3.6			
Na, %	0.197 ± 0.015	0.25	0.17	
	0.200 ± 0.014			
Rb	53.3 ± 3.8	52.2	59.6	
	53.1 ± 3.6			
Sr	90.9 ± 1.0	99	101	
	89.3 ± 0.9			
Zn	32.1 ± 3.7	33.2	31.7	29.8 ± 3.0 [37]
	36.2 ± 4.7			

[a]Error limits are standard deviations based on counting statistics.

TABLE 7

Elemental abundances of Kentucky tobacco IRI

Element (p.p.m.)	This work[a]	Ref. 2	Others
As	1.4 ± 0.1	2.05	1.62 ± 0.09 [35]
	1.4 ± 0.2		
Ca, %	2.65 ± 0.01	2.53	
	2.60 ± 0.01		
Cl, %	0.88 ± 0.07	0.87	
	0.85 ± 0.09		
Fe	460 ± 68	489	
	482 ± 73		
K, %	3.97 ± 0.25	3.96	
	3.99 ± 0.24		
Mg, %	0.462 ± 0.004	0.45	
	0.456 ± 0.003		
Mn	251 ± 17	213	
	230 ± 13		
Na	597 ± 37	401	
	575 ± 35		
Rb	15.3 ± 1.6	15.5	
	13.9 ± 1.6		
Sr	26.1 ± 0.5	25.6	
	28.7 ± 0.4		
Zn	34.3 ± 6.3	30.2	
	35.8 ± 5.0		

[a]Error limits are standard deviations based on counting statistics.

REFERENCES

1 E. J. Underwood, Trace Elements in Human and Animal Nutrition, Academic Press, New York, N.Y., 2nd edn., 1962.
2 R. A. Nadkarni and G. H. Morrison, Anal. Chem., 45 (1973) 1957.
3 K. Samsahl, P. O. Wester and O. Landström, Anal. Chem., 40 (1968) 181.
4 G. H. Morrison and N. M. Potter, Anal. Chem., 44 (1972) 839.
5 E. Steiness, O. R. Birkelund and O. Johansen, J. Radioanal. Chem., 9 (1971) 267.
6 J. A. Velandia and A. K. Perkons, J. Radioanal. Chem., 14 (1973) 171.
7 J. A. Velandia and A. K. Perkons, J. Radioanal. Chem., 20 (1974) 473.
8 J. A. Velandia and A. K. Perkons, J. Radioanal. Chem., 20 (1974) 715.
9 T. E. Henzler, R. J. Korda, P. A. Helmke, M. R. Anderson, M. M. Jimenez and L. A. Haskin, J. Radioanal. Chem., 20 (1974) 649.
10 C. Engelmann in J. M. A. Lenihan, S. J. Thomson and V. P. Guinn (Eds.), Advances in Activation Analysis, Vol. II, Academic Press, London, 1972, Ch. 1.
11 J. Hoste, J. Op de Beeck, R. Gijbels, F. Adams, P. Van den Winkel and D. De Soete, Instrumental and Radiochemical Activation Analysis, Butterworths, London, 1971, p. 87.
12 G. J. Lutz, Anal. Chem., 41 (1969) 424.
13 L. Kosta, M. Dermelj and J. Slunečko, Pure and Appl. Chem., 37 (1974) 251.
14 T. Kato and Y. Oka, Talanta, 19 (1972) 515.
15 T. Kato, J. Radioanal. Chem., 16 (1973) 307.
16 V. Galatanu and M. Grecescu, J. Radioanal. Chem., 10 (1972) 315.
17 T. Kato, Res. Rep. Lab. Nucl. Sci., Tohoku Univ., 5, No. 2 (1972) 137.
18 M. E. Toms, J. Radioanal. Chem., 20 (1974) 177.
19 C. A. Baker, G. J. Hunter and D. A. Wood, Rep. U.K. At. Energy Auth., AERE-R, 5547 (1967).
20 C. A. Baker and D. A. Wood, Rep. U.K. At. Energy Auth., AERE-R, 5818 (1968).
21 P. Anderson, J. S. Hislop and D. R. Williams, Rep. U.K. At. Energy Auth., AERE-R, 7823 (1974).
22 R. A. Schmitt, T. A. Linn, Jr. and H. Wakita, Radiochim. Acta, 13 (1970) 200.
23 J. S. Hislop and D. R. Williams, Rep. U.K. At. Energy Auth., AERE-R, 6910 (1971).
24 T. Kato, I. Morita and N. Sato, J. Radioanal. Chem., 18 (1973) 97.
25 N. Sato, T. Kato and N. Suzuki, Radiochim. Acta, 21 (1974) 63.
26 G. H. Anderson, F. M. Graber, V. P. Guinn, H. R. Lukens and D. M. Settle, Nuclear Activation Techniques in the Life Sciences, Amsterdam, IAEA, Vienna, 1967, p. 99.
27 J. S. Hislop and D. R. Williams, J. Radioanal. Chem., 16 (1973) 329.
28 R. D. Cooper, D. M. Kinekin and G. L. Brownell, Nuclear Activation Techniques in the Life Sciences, Amsterdam, IAEA, Vienna, 1967, p. 65.
29 N. K. Aras, W. H. Zoller, G. E. Gordon and G. J. Lutz, Anal. Chem., 45 (1973) 1481.
30 A. Chattopadhyay and R. E. Jervis, Anal. Chem., 46 (1974) 1630.
31 P. D. LaFleur, J. Radioanal. Chem., 19 (1974) 227.
32 H. J. M. Bowen, J. Radioanal. Chem., 19 (1974) 215.
33 W. O. Atkinson, Proc. Tobacco Health Conf., Lexington, Ky., 2 (1970) 28.
34 C. M. Lederer, J. M. Hollander and I. Perlman, Table of Isotopes, Wiley, New York, 6th edn., 1967.
35 R. A. Nadkarni, Radiochem. Radioanal. Lett., 19 (1974) 127.
36 E. Orvini, T. E. Gills and P. D. LaFleur, Anal. Chem., 46 (1974) 1294.
37 R. R. Becker, A. Veglia and E. R. Schmid, Radiochem. Radioanal. Lett., 19 (1974) 343.
38 V. Ravnik, M. Dermelj and L. Kosta, J. Radioanal. Chem., 20 (1974) 443.

Analytica Chimica Acta, 81 (1976) 349—360

PRECONCENTRATION OF TRACE METAL IONS BY COMBINED COMPLEXATION—ANION EXCHANGE
PART I. COBALT, ZINC AND CADMIUM WITH 2-(3'-SULFOBENZOYL)-PYRIDINE-2-PYRIDYLHYDRAZONE

JOHN E. GOING,* GARY WESENBERG and GEORGIANN ANDREJAT

Department of Chemistry, University of Wisconsin-Milwaukee, Milwaukee, Wisconsin 53201 (U.S.A.)

(Received 2nd July 1975)

SUMMARY

The ligand 2-(3'-sulfobenzoyl)pyridine-2-pyridylhydrazone forms anionic complexes with Fe, Co, Ni, Cu, Zn, Cd, Hg and Pd which demonstrate high affinities for anion-exchange resins. The behavior of Co, Zn and Cd was studied in detail, with respect to pH, flow rate, ligand/metal ratio, volume, concentration and percentage retention of the anionic complex on the Bio-Rad AG1-X2 resin. At optimal conditions, Co, Zn and Cd are quantitatively retained; Zn and Cd are removed completely by 2 M HNO_3 or 1 M H_2SO_4, and Co by 12 M HCl and 1 M HNO_3. Concentration enhancements up to 300-fold can be easily achieved. The complexes can be left on the columns for 48—96 h and still be quantitatively recovered. A ligand-loaded resin column can also be used to remove Co, Zn and Cd from solution. Batch experiments were used to determine distribution coefficients for the metal complexes.

Numerous recent publications have been concerned with novel methods of preconcentrating traces of metal ions from aqueous solutions, which are needed, for example, in the analysis of natural waters. With the advent of modern multi-element analysis techniques such as energy-dispersive x-ray fluorescence [1], high-energy beam particle bombardment [2, 3] and inductively coupled plasma emission spectroscopy [4], it is advantageous to preconcentrate metals as groups with similar properties. In many instances, it is also desirable that on-site sampling/preconcentration be performed, thus avoiding the transportation of large volumes of sample. Some of the newer techniques include the use of naturally occurring chelating polymers [5], extraction chromatography [6—9], and chelating resins [10—17]. Conventional ion-exchange resins have not shown the selectivity or efficiency of these other techniques.

The chelating resins are of particular interest. The ability to use a chemically bonded chelating group introduces a high degree of selectivity

*Present address: Midwest Research Institute, 425 Volker Boulevard, Kansas City, Missouri. (Address for reprints.)

into the choice of metal ions sampled. Ligands such as 8-hydroxyquinoline [17], iminodiacetate [10, 14, 15] and dithiocarbamate [11—13] have been attached to various solid supports. Such procedures, however, usually require the synthesis of special resins and do not take advantage of the readily available and well characterized ion-exchange resins.

This study is directed toward demonstrating that selective and highly efficient separations of traces of metal ions are possible with conventional anion-exchange resins. The principal problem is that of generating a metal complex for which the resin has a very high affinity. In fact, very few examples of the isolation of metal chelates by anion-exchange resins have been reported. Distribution coefficients have been reported for the metal complexes of EDTA [18], oxalic acid [19] and citric acid [19, 20] although no applications for trace isolations have been attempted. While the chloro complexes have been used to isolate and separate various transition metals, the acidity that is required is impractical for trace analysis.

In a study of the solvent extraction of the metal complexes of 2-benzoylpyridine-2-pyridylhydrazone, BPPH [21], it became necessary to determine the formation constants accurately. For this purpose, the sulfonated form of the ligand, BPPH—S, was prepared [22].

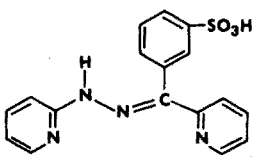

The transition metal complexes of BPPH—S, in basic solution, generally have at net charge of —2 because of the peripherally located sulfonate groups. Anion-exchange resins were found to have a very high affinity for these metal complexes; this appears to be the first reported example of the isolation of a metal complex based on a charged group totally removed from the complexation sites. Studies of the isolation of the cobalt, zinc and cadmium BPPH—S complexes by conventional anion-exchange resins are reported in this paper.

EXPERIMENTAL

Reagents

2-(3′-Sulfobenzoyl)pyridine-2-pyridylhydrazone, BPPH—S, was synthesized as described previously [22]. A $2.00 \cdot 10^{-3}$ M stock solution was prepared at a pH of 3.0 by the addition of (1 + 9) perchloric acid.

Metal ion solutions (0.100 mM) were prepared by dilution from stock solutions and spiked with ^{57}Co, ^{65}Zn, ^{109}Cd or ^{203}Hg.

The anion-exchange resin used was Bio-Rad AG 1-X2, 100—200 mesh.

After removal of the fines, the resin was treated with 1 M HCl and NaOH several times and left in the OH^--form before use.

Equipment and techniques

γ-Emission was counted with a Picker-Nuclear Spectroscaler Model III A with a 1.75 × 1.75-in. NaI well-type scintillation counter.

Atomic absorption analyses were done with an Instrumentation Laboratory Model 151 spectrometer equipped with background correction. An air—acetylene flame with a Boling burner was used. All instrument settings were as recommended by the manufacturer.

An all-glass column following the design of Pankow and Janauer [23] was used for the column experiments. The system was modified by attaching the column to a 3-way stopcock by a 5/20 ground-glass joint shortened to 5/12. The column was 1 × 6 cm and was generally filled with 3 ml of wet resin (OH^--form). The 3-way stopcock allowed the complex to be loaded onto the bottom of the column by ascending flow. For elution studies, descending flow was used to elute the metal through the bottom of the column; this approach served to minimize the elution volume.

Percentage recoveries were measured by counting an aliquot of the eluted solution and comparing to the activity of the same quantity of metal not passed through the column.

Distribution coefficients were determined by a batch technique. Weighed amounts of resin were added to known volumes of the complex and gently stirred until equilibrium was attained. Aliquots were counted before the addition of the resin and at equilibrium. The D value was computed from the following formula.

$$D = \frac{(A_i - A_f) \times \text{ml}}{A_f \times \text{g}}$$

where A_i and A_f are the activities in c.p.m. of the solution initially and at equilibrium; ml the volume of the solution; and g the weight of the resin. Averages of 2—4 measurements were used.

The time required to reach equilibrium was determined by withdrawing small aliquots periodically and measuring the remaining activity.

Breakthrough curves were determined by collecting 10—25-ml fractions of eluate and counting or by ultraviolet spectrophotometry.

Procedures

Zinc and cadmium. For each 100 ml of solution to be analyzed up to 1 l, add 10 ml of BPPH—S, assuming a maximum total heavy metal level of $2 \cdot 10^{-6}$ M. Add 1 ml of (1 + 1) ammonia solution for each 100 ml of solution and check that the pH is greater than 10. Pass the solution through an anion-exchange column containing 3 ml of wet resin (OH^--form) at a flow

rate of 10 ml min^{-1} cm^{-2}. Wash all of the solution onto the column with a few ml of pH 10 water. Adjust the stopcock for elution and pass 2 M HNO_3 or 1 M H_2SO_4 down the column. With the apparatus described, all the zinc and cadmium will appear in the first 10 ml of eluate.

Cobalt. The procedure for the isolation of cobalt is basically the same except for the elution. The cobalt is eluted by first passing 5 ml of 12 M HCl through the column, and then eluting with 1 M HNO_3. The cobalt is eluted in 25 ml of acid with the apparatus described.

Cobalt, zinc and cadmium. Zn and Cd along with Co can be eluted by the procedure given for cobalt alone. The recoveries of each will be ca. 98 % for Co, 98 % for Zn and 94 % for Cd, however.

RESULTS AND DISCUSSION

The ligand, referred to as HL—S, has been shown to form bis complexes with Co, Zn, Cd and Hg [22]. The complexes of Zn, Cd and Hg exist as $M(HL—S)_2^0$ in slightly acidic solution. In basic solution the imino proton is titrated from both complexed ligands, yielding the "deprotonated complexes" $M(L—S)_2^{2-}$ having a net charge of −2. The charge is actually located on the peripheral sulfonate groups. The complex as $M(HL—S)_2^0$ is in fact a diprotic acid with pK values of 8.14 and 9.66 for Zn, 8.89 and 10.23 for Cd and 7.52 and 9.01 for Hg [22]. The cobalt complex undergoes spontaneous oxidation and deprotonation in slightly acidic solution and consequently the pK values are not determinable [22, 24]. The resulting cobalt(III) complex has a net charge of −1 rather than −2.

The anionic deprotonated divalent complexes are suitable for retention by anion-exchange resins, being preferred over monovalent anions. Interaction between the aromatic matrix of the resin and the aromatic portions of the complex will increase the affinity. In fact, it has been reported that a styrene—divinylbenzene resin alone has a high affinity for the phenyl- and naphthyl-monosulfonic acids [25]. Similarly, Dowex-2 has been shown to have a very high affinity for naphthalene sulfonate [26]. However, the large size of the complex would probably limit its uptake because of a sieving action [27]. To guard against this, a low-crosslinked resin with large pores was used.

Column experiments

In the initial study the elution volumes of the metal ions from the glass column were determined. It was known [22] that strong acid was effective in dissociating the complexes and releasing the free metal ions. After the resin had been loaded by ascending flow, various strong acids were tested as eluants by descending flow. The elution curves were determined by collecting

and counting 2-ml aliquots of the acid at a flow rate of 5 ml min^{-1}. As shown in Fig. 1, cadmium (and similarly zinc) was removed from the column by 10 ml of 2 M HNO_3. Similar results were obtained with 1 M H_2SO_4. The cobalt complex was not completely removed by these acids owing to its inertness; the addition of 5 ml of 12 M HCl to the column destroyed the complex and formed $CoCl_4^{2-}$, which could then be eluted with 20 ml of 1 M HNO_3. In subsequent experiments in which percent recovery was determined, elution volumes of 25 ml were collected for counting. Under the conditions optimized for cobalt elution, Zn and Cd were recovered at 98 and 94 % respectively.

The solution pH affects the extent of complexation which in turn determines the percentage of metal retained by the column. Since the elution is quantitative, the percentage recovery determined is essentially a measure of percentage retention. Figure 2 shows that, as expected, zinc and cadmium are totally retained above pH 9 while cobalt is effectively retained between pH 5 and 11. This is in agreement with spectrophotometric studies of formation [22]. The flow rates and ligand/metal ratios were well within the limits subsequently determined.

The flow rate of the solution of the complex through the column affects the percentage recovery. When the column was packed with 3 ml of wet resin, flow rates up to 15—18 ml min^{-1} cm^{-2} were possible (Table 1), but all subsequent studies were run at 10 ml min^{-1} cm^{-2}. Consequently, samples of 500 ml could be easily processed in about 1 h. For elution, flow rates of up to 15 ml min^{-1} cm^{-2} could be employed (Table 1). In practice, flow rates of only 5 ml min^{-1} cm^{-2} were used.

The complexation reaction obviously requires a sufficient excess of ligand.

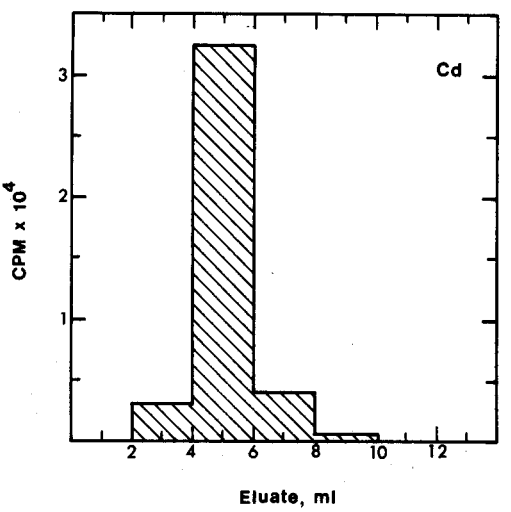

Fig. 1. Elution profile of cadmium with 2 M HNO_3.

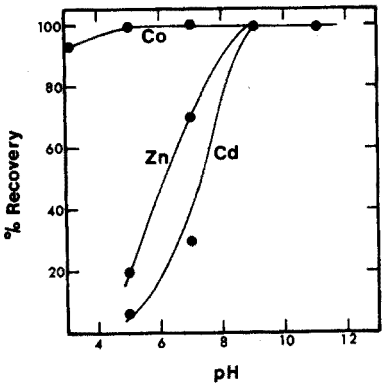

Fig. 2. Percentage recovery of Co, Zn and Cd as a function of pH.

TABLE 1

Recovery of Co, Zn and Cd vs. loading and elution flow rates
(Conditions: 0.1 μmol metal, 20 μmol BPPH—S; volume 250 ml, pH 11 for Zn and Cd, 5 for Co)

Co		Zn		Cd	
v[a]	% R	v	% R	v	% R
Effect of loading flow rate					
2	98	5	>99	5	>99
5	98	13	>99	8	>99
17	98	26	>99	12	>99
31	92			28	96
Effect of elution flow rate[b]					
3	>99	5	>99	1	>99
7	>99	8	>99	5	>99
16	98	11	>99	19	>99
30	94	24	>99		

[a] v = flow rate, ml $min^{-1} cm^{-2}$.
[b] For a loading flow rate of 10 ml min^{-1} cm^{-2}.

At least a 20-fold molar excess was necessary (Table 2), and a 200-fold excess was normally used.

Concentration from large volumes

The volume of samples that could be passed through the column while maintaining quantitative recovery, was determined. With 0.1 μmol of metal and 20 μmol of ligand, the volume was varied from 0.10 to 3 l. The recovery was excellent for zinc and cadmium at all volumes but slightly lower for cobal

TABLE 2

Recovery of Co, Zn and Cd vs. ligand/metal ratio
(Conditions: 0.1 μmol metal; volume 250 ml; pH 11 for Zn and Cd, 5 for Co; loading, 10 ml min^{-1} cm^{-2}, eluting 5 ml min^{-1} cm^{-2})

Co		Zn		Cd	
L/M	% R	L/M	% R	L/M	% R
20	95	20	>99	20	>99
200	>99	200	>99	200	>99
2000	>99	2000	>99	2000	>99

TABLE 3

Recovery of Co, Zn and Cd vs. aqueous volume
(Conditions: 0.1 μmol metal, 20 μmol BPPH—S; pH 11 for Zn and Cd, 5 for Co; loading, 10 ml min^{-1} cm^{-2}; eluting, 5 ml min^{-1} cm^{-2})

Co		Zn		Cd	
Volume (ml)	% R	Volume (ml)	% R	Volume (ml)	% R
100	99	100	>99	100	>99
250	99	250	>99	250	>99
500	97	500	>99	500	>99
1000	99	1000	>99	1000	>99
3000	96	3000	>99	3000	>99

at high volumes (Table 3). With the recommended elution volumes, the increases in concentration are 10—300-fold for zinc and cadmium and 4—267-fold for cobalt.

The percentage recoveries were determined with decreasing metal concentrations at a constant volume of 250 ml. In all cases the ligand was 0.2 mM. No attempt was made to determine an upper limit of recoverability or capacity of the column. Good recoveries were found for as little as 25 p.p.t. (parts per trillion) zinc, 45 p.p.t. cadmium and 66 p.p.t. cobalt (Table 4); this corresponds to 6.5, 11.2 and 16.5 ng, respectively. It should be emphasized that these recoveries were measured radiochemically, and do not necessarily indicate what level can be readily measured.

An artificial sea water sample of 250 ml was prepared as a 0.55 M NaCl solution and spiked with 0.1 μmol cadmium. With 20 μmol of ligand present, more than 99 % of the cadmium was recovered. In the absence of the ligand, 13 % of the cadmium was recovered; this was presumably retained as a chloro complex.

In the analysis of sea water, it is usually essential to separate the trace metal ions from the bulk salts. Should neutron activation analysis be used, it is particularly important to remove sodium chloride. Of the original 136

TABLE 4

Recovery of Co, Zn and Cd vs. concentration
(Conditions: 20 μmol BPPH—S; volume 250 ml, pH 11 for Zn and Cd, 5 for Co; loading, 10 ml min^{-1}, eluting 5 ml min^{-1})

Co		Zn		Cd	
p.p.b.	% R	p.p.b.	% R	p.p.b.	% R
60.0	99	65.4	>99	450	>99
30.0	99	26.2	>99	45.0	>99
15.0	99	6.54	>99	4.50	>99
12.0	97	0.26	>99	2.25	>99
6.0	99	0.026	>99	0.45	>99
0.60	95			0.045	>99
0.060	96				

mmol of sodium in the solution, 27 μmol (0.027 %) was found in the cadmium-containing acid eluate. Thus a decontamination factor of 3700 was achieved while the cadmium concentration was increased 25-fold.

It was envisioned that this technique would be quite useful for field sampling [14]. A solution, up to several liters, could be passed through a small column, which could then be returned to the laboratory and stripped of the metals for analysis by the appropriate technique. Consequently, the stability of the complexes when isolated on a column was tested for up to 96 h. The results (Table 5) indicate that the complex can be left on the column for 48—96 h before elution with negligible loss. Field sampling should therefore be quite feasible.

Ligand-loaded resins

Since the ligand is a monovalent anion above pH 6 [22], it is also strongly retained by the anion-exchange resin. If a solution of Zn, Cd or Co at the appropriate pH were passed through such a column, the metals should be complexed and removed from solution. This is very similar to the systems based on chemically bonded chelating groups, and is an example of reactive ion exchange, as defined by Janauer et al. [28]. The approach is attractive in

TABLE 5

Recovery of Co, Zn and Cd vs. time of complex on resin
(0.1 μmol of metal; other conditions as for Table 4)

	% Recovery		
	Co	Zn	Cd
48 h	94	>99	99
96 h	—	>99	98

that it is experimentally much simpler. A solution of 100 ml containing 0.1 μmol metal was adjusted to pH 11 for zinc and cadmium or 6 for cobalt and passed through a ligand-loaded column. The results (Table 6) indicate the reasonable success of this approach; a 10 % ligand-loaded column corresponds to a gross ligand/metal ratio of 2400 for 0.1 μmol metal. The recoveries for the batch-loaded resins were generally higher than those for the flow-loaded resins. With the flow-loaded columns, the distribution of the ligand was heterogeneous, the ligand being retained by the first 1—2 cm of the column, and this short "column" was inadequate for complete recovery. The batch-loaded columns, with the ligand distributed evenly over the whole column, were more effective. It was not determined whether film or bead diffusion or the rate of complexation were most critical.

It is of interest that cobalt is in fact retained so completely. It has been shown that cobalt undergoes oxidation on complexation with loss of both imino protons. The complex is formed as $Co(L—S)_2^{1-}$ by a somewhat slow reaction, complete formation taking 4—5 min at pH 5 [29]. Nevertheless, cobalt was effectively retained by the ligand-loaded column, though the residence time of the solution in the column would be only 15—20 s. Evidently, complexation is quite rapid although the subsequent oxidation and loss of protons may be slower.

Capacity

Capacity is difficult to define in the usual manner, for both the ligand and metal concentrations will have an effect. Initially, the breakthrough point for $2 \cdot 10^{-4}$ M BPPH—S was found to be about 1500 ml on a 3-ml wet resin column. With the requirement of a ligand/metal ratio of 100 for quantitative recovery, the breakthrough curve for $2 \cdot 10^{-6}$ M zinc was determined with the same column; breakthrough was about 1 % at 1100 ml and rose rapidly at about 1500 ml. This is a loading of about 2 μmol of zinc or only about 0.17 % of the resin sites; most of the remaining exchange sites are occupied

TABLE 6

Recovery by ligand-loaded columns
(Conditions: 0.1 μmol metal; volume 250 ml; resin, 3 ml loaded to 10% capacity; elution at 5 ml min^{-1} cm^{-2})

	Flow-loaded[a]	Batch-loaded[b]
Co	—	95 (10 ml min^{-1})
Zn	—	99 (10 ml min^{-1})
Cd	90 (10 ml min^{-1})	99 (10 ml min^{-1})
	89 (20 ml min^{-1})	94 (20 ml min^{-1})

[a]Resin prepared by passing ligand solution through the column.
[b]Resin loaded by batch procedure, and then placed in the column.

by excess ligand, so that capacity with respect to the metal ion is lower than would be expected.

The capacity of a 3-ml 10 % ligand-loaded resin column was also determined; a solution of $1 \cdot 10^{-4}$ M zinc at pH 10.5 was passed through at 2 ml min^{-1} cm^{-2}. Breakthrough of about 1 % occurred at 425 ml, and rose rapidly after 500 ml. The capacity was about 40 μmol of zinc, corresponding to a 6:1 ratio of ligand to metal on the resin or to 33 % of the ligand being used for complexation. This is significantly more efficient than the pre-complexation—anion exchange technique and is under further investigation.

Studies with Fe, Ni, Hg, Pd and Cu

Preliminary studies with iron were hampered by the lack of a suitable isotope. Total recoveries were generally about 80 % in the pH range 5—10, probably because of incomplete elution resulting from the high stability of the complex. About 80 % of the retained iron was removed by 30 ml of 3 M H_2SO_4. Initial studies with atomic absorption indicated that nickel behaves similarly to zinc and cadmium; recoveries exceeded 99 % under the conditions optimized for the latter metals. The results obtained with mercury were anomalous: in the absence of ligand, mercury was about 60 % retained throughout the pH range 4—12 on a resin in the OH^--form and about 90—99 % retained with the resin in the Cl^--form. With the ligand, retention was greater than 90 % from pH 6—10, being 99 % at pH 6.5. Elution was incomplete with the strong acid eluants HCl, NHO_3 and H_2SO_4. The best eluent was 9 M HNO_3.

Qualitative batch experiments indicated that copper is removed from solution as the anionic complex above about pH 10; copper would in fact be expected to behave like Zn and Cd. Palladium was effectively isolated in the range pH 1—12. Studies with ligands similar to BPPH—S have indicated that the complexes are stable from pH 9 to molar acidities [30]. Further studies with palladium are warranted.

Batch experiments

By use of a batch technique, the distribution coefficients, D, were determined for cobalt, zinc and cadmium (Table 7). The values are high for zinc and cadmium; the lower value for cobalt is probably a consequence of the lower net charge of that complex. The generally large values are probably due to interaction of the aromatic resin matrix with the aromatic portions of the complexed ligands. Uncomplexed ligand is also removed by the anion-exchange resin although no distribution coefficient was measured.

The results in Table 7 also list the percentage of metal removed from 100 ml of solution with 1 g of resin. For small volumes of solution, the batch procedure can be experimentally simpler to perform and is commonly

TABLE 7

Distribution coefficients of the Co, Zn and Cd complexes
(Conditions: 0.2 μmol metal, 40 μmol BPPH—S; volume 100 ml; resin, 1 g of dry OH^--form; pH 11 for Zn and Cd, 5 for Co; equilibration time, 2 h. Each result is the average of 2—4 results)

Metal	Log *D*	% Removed
Co	3.5	97.1
Zn	5.1	99.9
Cd	5.0	99.9

used [10, 13, 16]. Studies of the rate of uptake of the complexes by the resin under the same experimental conditions, showed that zinc and cadmium are more than 99 % removed in less than 20 min and that cobalt is more than 98 % removed in 30 min.

A batch experiment with a 4 % ligand-loaded resin was performed. The rate of uptake of 0.1 μmole of cadmium in 100 ml by 1.00 g of ligand-loaded resin was measured. As before, more than 99 % of the cadmium was removed from solution in less than 20 min; zinc and cobalt should behave similarly. Interestingly, the resin had been loaded with ligand 10 days before its use.

CONCLUSIONS

The possibility of using conventional anion-exchange resins for the isolation of trace metal ion as anionic chelate complexes has been demonstrated. The procedure compares well with the use of chelating resins. For cobalt, zinc and cadmium, the procedure gives quantitative retention of the complexes and quantitative elution with strong acids. Concentration enhancements of up to 300-fold are possible.

The optimal flow rates employed, 10 ml min^{-1} cm^{-2}, are 2—3 times faster than those used with chelating resins such as Chelex-100 [14, 15]; likewise the rate of uptake in the batch technique was as fast or faster than that of Chelex-100 [10, 15].

In comparison with most chelating resins this system has considerably greater selectivity. Riley and Taylor [14] report, for example, that Chelex-100 will complex about 24 different elements. The ligands, 8-hydroxyquinoline and the dithiocarbamates, are also not highly selective. Such lack of selectivity can sometimes be a serious disadvantage. The ligand used in this study is selective towards only 8—10 transition metal ions. With the development of additional ligands for use, e.g., 2-(3'-sulfobenzoyl)pyridine ketoxime [31], different sets of selectivities will be available.

The technique described is well suited to on-site sampling, as samples can be collected and concentrated, and the loaded resins stored for 2—4 days before analysis.

The use of ligand-loaded resin seems promising. When a column was used,

the recovery of cobalt, zinc and cadmium was equal to that attained by the pre-complexation—anion exchange approach, whereas the capacity of the ligand-loaded resin column was about 20 times better; in the batch technique, the rate of uptake was equally fast. For field work, either the pre-loaded column or the batch technique has an advantage in that the only sample treatment, other than possibly filtration, is a simple pH adjustment; and the resin can be loaded with the ligand at least 10 days prior to use.

This paper was presented in part at the 1975 Pittsburgh Conference on Applied Spectroscopy and Analytical Chemistry.

REFERENCES

1 D. E. Leyden, Amer. Lab., Nov. (1974) 24.
2 P. J. Clark, G. F. Neal and R. O. Allen, Anal. Chem., 47 (1975) 650.
3 C. H. Lochmuller, J. Galbraith, R. Walter and J. Joyce, Anal. Lett., 5 (1972) 943.
4 V. A. Fassel and R. N. Kniseley, Anal. Chem., 1110A (1974).
5 R. A. A. Muzzarelli, Natural Chelating Polymers, Pergamon Press, Oxford, 1973.
6 T. Braun and A. B. Farag, Anal. Chim. Acta, 72 (1974) 133.
7 G. Erdtmann and G. Aboulwafa, Zeit. Anal. Chem., 270 (1974) 1.
8 Y. Sekizuka, T. Kozima, T. Yang and K. Uemo, Talanta, 20 (1973) 979.
9 J. J. Topping and W. A. MacCrehan, Talanta, 21 (1974) 1281.
10 C. W. Blout, D. E. Leyden, T. L. Thomas and S. M. Guill, Anal. Chem., 45 (1973) 1045.
11 J. F. Dingman, K. M. Gross, E. A. Milano and S. Siggia, Anal. Chem., 46 (1974) 774.
12 D. M. Hercules, L. E. Cox, S. Onisiek, G. D. Nichols and J. C. Carver, Anal. Chem., 45 (1973) 1973.
13 D. E. Leyden, G. H. Luttrell and W. K. Nonidex, Pittsburgh Conference on Analytical Chemistry and Applied Spectroscopy, 1974, paper 61.
14 D. E. Leyden, T. A. Patterson and J. J. Alberts, Anal. Chem., 47 (1975) 733.
15 J. P. Riley and D. Taylor, Anal. Chim. Acta, 40 (1968) 479.
16 R. G. Smith, Jr., Anal. Chem., 46 (1974) 607.
17 K. F. Sugawara, H. H. Weetall and G. D. Schucker, Anal. Chem., 46 (1974) 489.
18 F. Nelson, R. A. Day, Jr. and K. A. Kraus, J. Inorg. Nucl. Chem., 151 (1960) 140.
19 W. R. Bandi, E. G. Buyok, L. L. Lewis and L. M. Melnick, Anal. Chem., 33 (1961) 1275.
20 F. Nelson and K. A. Kraus, J. Amer. Chem. Soc., 77 (1955) 801.
21 J. E. Going, D. Berge and G. Daigneault, in preparation.
22 J. E. Going and C. Sykora, Anal. Chim. Acta, 70 (1974) 127.
23 J. F. Pankow and G. E. Janauer, Anal. Chim. Acta, 69 (1974) 97.
24 J. E. Going and R. T. Pflaum, Anal. Chem., 42 (1970) 1098.
25 M. W. Scoggins and J. W. Miller, Anal. Chem., 40 (1968) 1155.
26 S. Peterson, Ann. N.Y. Acad. Sci., 57 (1953) 144.
27 F. Helfferich, Ion Exchange, McGraw—Hill, New York, 1962, Chap. 5.
28 G. E. Janauer, G. O. Ramseyer and J. W. Lin, Anal. Chim. Acta, 73 (1974) 311.
29 J. E. Going, Doctoral Dissertation, University of Iowa, 1968, Univ. Microfilms, Ann Arbor, Mich., 69-8738.
30 G. S. Vasilikiotic, T. Kouimtzis, C. Apostolopoulou and A. Voulgaropoulos, Anal. Chim. Acta, 70 (1974) 319.
31 J. Thompson and J. Going, unpublished results.

Analytica Chimica Acta, 81 (1976) 361—370

AUTOMATISCH-FLUORIMETRISCHE BESTIMMUNG VON METANEPHRIN UND NORMETANEPHRIN — VERGLEICH VERSCHIEDENER OXIDATIONSVERFAHREN

G. SCHWEDT

Institut für Arbeitsphysiologie an der Universität Dortmund, 46 Dortmund, Ardeystrasse 67 (German Federal Republic)

(Eingegangen den 7. Juli 1975)

ZUSAMMENFASSUNG

Es wurden die Möglichkeiten zur automatisch-fluorimetrischen Bestimmung der O-Methyl-Katecholamine Metanephrin und Normetanephrin nach verschiedenen Verfahren der Oxidation und Stabilisierung untersucht und die einzelnen Parameter der Methoden optimiert. Die Oxidation mit Kaliumhexacyanoferrat(III) und anschliessender Stabilisierung der Fluorophore durch Ascorbinsäure zeigte die günstigsten Ergebnisse. Durch die Wahl unterschiedlicher Oxidation-pH-Werte, Pumpengeschwindigkeiten des Analysenautomaten oder Fluoreszenzbedingungen kann eine differenzierte Bestimmung der Amine durchgeführt werden.

SUMMARY

Automatic fluorimetric determinations of the O-methylcatecholamines, metanephrine and normetanephrine, by different methods of oxidation and stabilization are compared. Optimal experimental parameters for each method are described. Oxidation with hexacyanoferrate(III) and final stabilization of the fluorophore with ascorbic acid yields the best results. Differential determinations of the amines are possible if the oxidation pH values, pumping rates and excitation—emission wavelengths are selected appropriately.

Die O-Methyl-Katecholamin-Metaboliten Metanephrin und Normetanephrin lassen sich in ähnlicher Weise wie Dopamin mit Natriumperjodat zu fluoreszierenden Verbindungen oxidieren [1, 2]. Für die automatisch-fluorimetrische Bestimmung von Dopamin wurde von Wisser und Stamm [3] eine Analyseneinheit für einen Autoanalyzer beschrieben. Der Einsatz dieses Systems für die Bestimmung von Metanephrin und Normetanephrin wurde untersucht, wobei ausser Perjodat auch Jod als Oxidationsmittel Verwendung fand.

Die automatisch-fluorimetrische Bestimmung der Katecholamine Adrenalin und Noradrenalin als Trihydroxyindole wurde bereits öfter beschrieben [z.B. 4, 5]. Für die O-methylierten Amine haben bisher nur Zuspan et al. [6] eine automatische Methode angegeben, die auf der

Oxidation mit Kaliumhexacyanoferrat(III) in Anwesenheit von Zinkionen zu Trihydroxyindolen beruht. Für dieses Oxidationsverfahren wurde eine zweite Analyseneinheit eingesetzt, die in der Routineanalyse zur differenzierten Bestimmung der Katecholamine [5] verwendet wird.

EXPERIMENTELLER TEIL

Geräte

Der Analysenautomat besteht aus dem Probengeber, an welchem die Saugzeiten eingestellt werden (Saugzeit für die Probe: 30 s, für die Spüllösung 60 s), der Pumpe, deren Geschwindigkeit sich in Stufen regeln lässt, der eigentlichen analytischen Einheit, in welcher die Durchmischungsvorgänge stattfinden, sowie dem Fluorimeter mit Kompensations-Schreiber (Abb. 1).

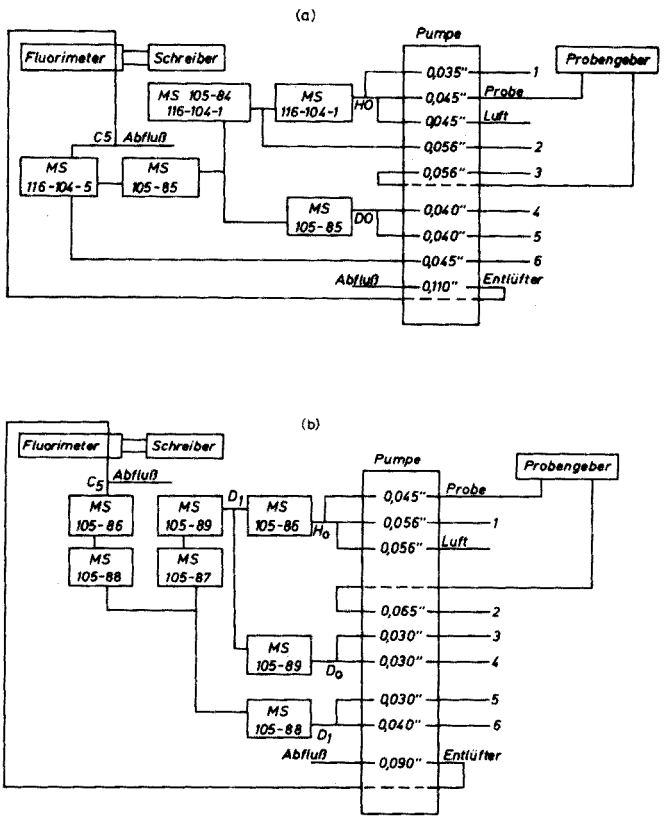

Abb. 1. Fliessschema des Analysenautomaten. (a) Perjodatverfahren: 1, 3, Puffer; 2, $NaJO_4$; 4, Na_2SO_3; 5, NaOH; 6, Ascorbinsäure. Jodverfahren: 1, 3, Puffer; 2, Jod; 4, NaOH; 5, Na_2SO_3 (bzw. Ascorbinsäure); 6, Essigsäure. (b) Kaliumhexacyanoferrat(III)—Verfahren: 1, 3, Zn/Puffer; 2, H_2O; 4, $K_3Fe(CN)_6$; 5, Ascorbinsäure; 6, NaOH.

Probengeber: Automatischer Probengeber SD 3, Modell 1512 (Erba Science).

Pumpe: Micro-Pump MP-13/GJ-4 (Isamatec).

Analyseneinheit I (Jod/Perjodat—Oxidation; Abb. 1a): zusammengestellt aus Einzelteilen der Fa. Elkay Products. Pumpenschläuche (aus Polyäthylen): i.d. 0,035—0,040—0,045—0,056—0,110 (2,79) in. (mm). Verbindungsschlauch: 1/16 in. i.d., 1/8 in. o.d. × 1/32 in. Wandstärke. Mischspiralen: (5 mm o.d. mit 4 mm Ausgang) MS 105-84: 14 Schleifen, 3,4 mm i.d., MS 105-84: 28 Schleifen, 3,4 mm i.d., MS 116-104-1: 14 Schleifen, 2,4 mm i.d., MS 116-104-5: 28 Schleifen, 2,4 mm i.d. Zwischenstücke: C 5: "T" Debubbler; D 0: "h Connector"; H 0: "Cactus" (1/8 in. i.d., 1/4 in. o.d.)

Die Glasteile sind untereinander bzw. mit den Schläuchen durch Schlauchstücke und "Nipples" verbunden: N 5 für Schläuche mit i.d. 0,045 in. oder kleiner, N 6 für Schläuche mit i.d. 0,051 in oder grösser.

Analyseneinheit II. (Kaliumhexacyanoferrat (III)-Oxidation): fertig bezogen von der Fa. Technicon, siehe Abb. 1 b.

Fluorimeter. Aminco—Bowman Spectrophotofluorometer mit Durchflussküvette aus Quarzglas mit Entlüfter (Volumen 0,45 ml).

Chemikalien und Pufferlösungen

DL-Metanephrine hydrochloride und DL-Normetanephrine hydrochloride (Calbiochem). Alle Chemikalien z.A. (Merck).
0,8 M Citrat/Acetate—Puffer [2]: pH 3,5; 4,0; 4,5; 5,0; 5,5; 6,0. 2,0 M Citronensäure mit 2,0 Natriumacetatlösung auf den gewünschten pH-Wert einstellen, mit dest. Wasser auf 0,8 M verdünnen; bei höheren pH-Werten zusätzlich 1 M NaOH verwenden.
Boratpuffer: pH 8,0; 8,6; 9,2 (nach Sörensen)
Acetatpuffer, 0,2 M: pH 2; 3; 4; 5; 6; 6, 7
Phosphatpuffer, 0,5 M: pH 6,5; 7,0; 7,5; aus Kaliumdihydrogenphosphat, pH-Wert mit verd. Natronlauge einstellen.

Methodik

Zur Optimierung der chemischen Parameter (Konzentrationen der Lösungen) wurde jeweils in Anlehnung an die manuellen Verfahren von bestimmten Ausgangskonzentrationen ausgegangen. Dann wurde zuerst die optimale Konzentration des Oxidationsmittels festgestellt. In weiteren Schritten erfolgte die Optimierung der übrigen Lösungen, wobei die jeweils vorher ermittelte optimale Konzentration einer Lösung eingesetzt wurde. Nach der Optimierung der chemischen Parameter wurden die Einflüsse der

fluorimetrischen Einstellungen und der Pumpengeschwindigkeit des Analysenautomaten auf die Fluoreszenzausbeute gemessen.

Perjodatoxidation. In Anlehnung an Anton und Sayre [2] wurden folgende Ausgangsbedingungen gewählt: 0,1 % Natriumperjodatlösung; 0,8 M Citrat/Acetat–Puffer pH 5,0; 2 M Natronlauge; 0,1 % Ascorbinsäure; 5 % Natriumsulfitlösung. Die Ermittlung der optimalen Konzentrationen erfolgte nacheinander in der Reihenfolge Natriumperjodat, Natronlauge, Natriumsulfit, Ascorbinsäure. Taniguchi et al. [1] haben über die unterschiedliche pH-Abhängigkeit der Perjodatoxidation für Metanephrin und Normetanephrin berichtet. Mit dem beschriebenen Analysenautomaten wurde diese Abhängigkeit von pH 3,5 bis 6,0 untersucht.

Jodoxidation. Für die fluorimetrische Bestimmung von Metanephrin und Normetanephrin nach der Oxidation mit Jod werden in der Literatur zwei verschiedene Möglichkeiten der Reduktion und Stabilisierung beschrieben: Bertler et al. [7] setzen eine alkalische Ascorbatlösung ein. Von anderen Autoren [z.B. 8] wird eine alkalische Sulfitlösung verwendet. In beiden Fällen schliesst sich eine weitere Stabilisierung der Fluorophore durch Ansäuern der Lösung mit Essigsäure an.

(a) Ausgangsbedingungen für Ascorbatverfahren. 0,5 M Phosphatpuffer pH 7,0; 0,01 M Jod; 1 % Ascorbinsäure; 5 M Natronlauge; 10 M Essigsäure. Reihenfolge der Optimierung: Jod, Essigsäure, Ascorbinsäure, Natronlauge.

(b) Ausgangsbedingungen für Sulfitverfahren: Boratpuffer pH 8,6; 0,01 M Jod; 5 % Natriumsulfitlösung; 2 M Natronlauge; 10 M Essigsäure. Reihenfolge der Optimierung: Jod, Natriumsulfit, Natronlauge, Essigsäure, pH-Wert der Oxidation.

Kaliumhexacyanoferrat(III)–Verfahren. Smith und Weil-Malherbe [9] sowie Brunjes et al. [10] setzten Kaliumhexacyanoferrat(III) zur Oxidation von Metanephrin und Normetanephrin in Anwesenheit von Zinkionen ein. Wie bei der Oxidation der Katecholamine erfolgt die Reduktion und Stabilisierung mit Ascorbinsäure im Alkalischen. Ausgangsbedingungen: 0,5 % Zinksulfat-7-hydrat in 0,2 M Acetatpuffer pH 6,0; 0,25 % Kaliumhexacyanoferrat (III); 0,5 % Ascorbinsäure; 5 M Natronlauge. Reihenfolge der Optimierung: Kaliumhexacyanoferrat(III), Zink, Ascorbinsäure, Natronlauge, pH-Wert der Oxidation.

ERGEBNISSE UND DISKUSSION

Perjodatoxidation

Abbildung 2 zeigt die Abhängigkeiten der Fluoreszenzintensitäten von den chemischen Parametern (Konzentrationen der Lösungen) sowie vom pH-Wert der Oxidation und der Pumpengeschwindigkeit des Analysenautomaten

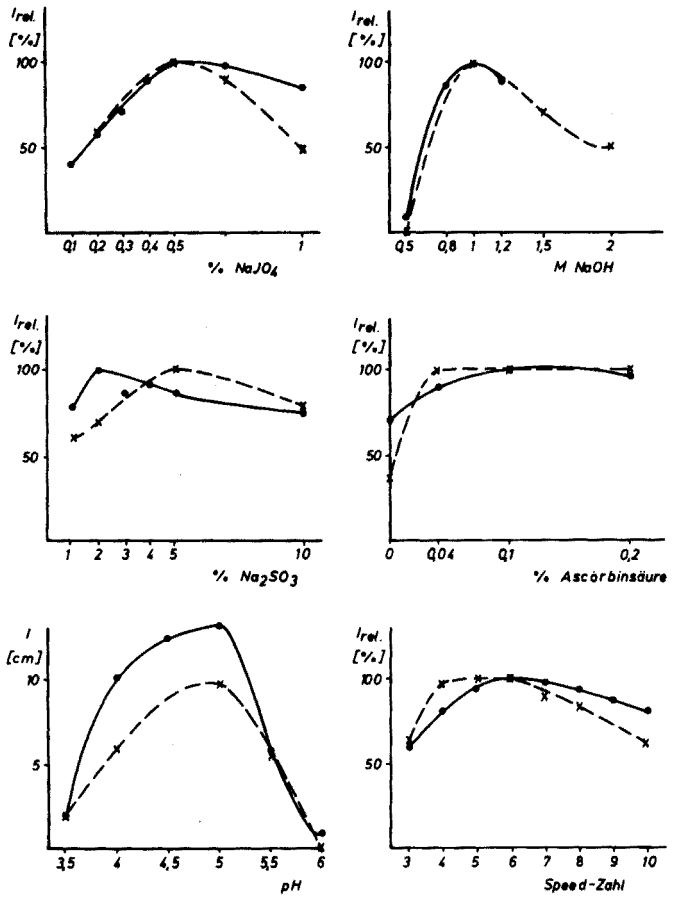

Abb. 2. Perjodatverfahren. Abhängigkeiten der Fluoreszenzausbeute von den Konzentrationen der Lösungen, dem pH-Wert der Oxidation und der Pumpengeschwindigkeit des Analysenautomaten. (Empfindlichkeit S = 1, je 500 ng Amin/ml.). (•) Metanephrin. (x) Normetanephrin.

(speed-Zahl). Die sich daraus ergebenden optimalen Bedingungen sind in Tab. 1 zusammengestellt. Differenzierungsmöglichkeiten für die Bestimmung von Metanephrin und Normetanephrin bestehen in den unterschiedlichen Abhängigkeiten der Oxidation vom pH-Wert (Tab. 2). Der Verlauf der pH-Abhängigkeit bei der Perjodatoxidation entspricht im wesentlichen den Ergebnissen von Taniguchi et al. [1].

Jodoxidation

Wird bei der Oxidation mit Jod die Reduktion und Stabilisierung der Fluorophore mit Ascorbinsäure durchgeführt, so ist die Empfindlichkeit des Verfahrens durch den sehr hohen Chemikalienblindwert herabgesetzt. Die

TABELLE 1

Optimale Analysenbedingungen
(MN: Metanephrin, NMN: Normetanephrin)

Perjodatverfahren	MN	NMN	gemeinsame analyse
Fluorimetrie (A/F)[a]	390/510	390/510	
$NaJO_4$ [%]	0,5	0,5	0,5
NaOH [M]	1,0	1,0	1,0
Na_2SO_3 [%]	2	5	5
Ascorbinsäure [%]	> 0,05	> 0,1	0,1
pH-Wert	5,0	5,0	5,0
Speed-Zahl	4—6	6	6
Jod/Sulfitverfahren			
Fluorimetrie (A/F)	400/520	380/480	
Jod [M]	0,02	0,05	0,02
Na_2SO_3 [%]	10	15	10
NaOH [M]	2	3	3
Essigsäure [M]	8	10	10
pH-Wert	7,0	7,0	7,0
Jod/Ascorbatverfahren			
Fluorimetrie (A/F)	400/520	380/480	
Jod [M]	0,001	0,005	0,005
Essigsäure [M]	8—10	10	10
Ascorbinsäure [%]	2	2	2
NaOH [M]	3	7	5
pH-Wert	6,5	7,0	7,0
Kaliumhexacyanoferrat-(III)-Verfahren			
Fluorimetrie (A/F)	400/520	400/500	
$K_3[Fe(CN)_6]$ [%]	0,1	0,1	0,1
$ZnSO_4$ [%]	1	0,5	0,5
Ascorbinsäure [%]	0,1	0,5	0,5
NaOH [M]	1	5	5
pH-Wert	3	5	4

[a] Anregung (A) und Fluoreszenz (F): nm.

höchste Empfindlichkeitsstufe des Fluorimeters kann nicht mehr eingestellt werden. Bei der Verwendung von Sulfit tritt diese Erscheinung nicht auf. Die Fluoreszenzintensitäten für Normetanephrin sind im Verhältnis zu denen von Metanephrin extrem niedrig, wie die absoluten Messwerte bei der pH-Abhängigkeit der Oxidation (Abb. 3) zeigen. Die übrigen Abhängigkeiten sind ebenfalls in Abb. 3 dargestellt.

Die optimalen Parameter für das Jod/Sulfit-Verfahren sind aus Tab. 1 zu entnehmen, die einzelnen Abhängigkeiten sind in Abb. 4 dargestellt.

Erfolgt die Oxidation mit Jod bei pH 8,6, so wird die Bestimmung von

TABELLE 2

Differenzierungsmöglichkeiten

Parameter	Perjodat	Jod/Sulfit	$K_3Fe(CN)_6$
pH-Wert der Oxidation	4,0 und 5,5	7,0 und 8,6	3 und 5
Speed-Zahl	—	5 und 8	10 und 6
Fluorimetrie A/F	—	380/480 und 420/520	400/500 und 420/540

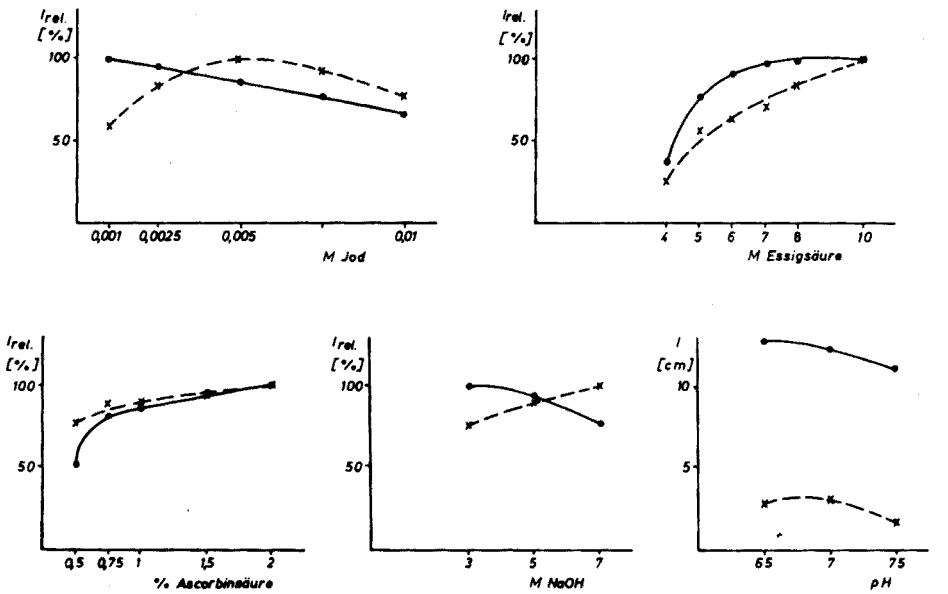

Abb. 3. Jod/Ascorbatverfahren. Abhängigkeiten der Fluoreszenzausbeute von den Konzentrationen der Lösungen und dem pH-Wert der Oxidation. (Empfindlichkeit S = 1, je 500 ng Amin/ml.). (•) Metanephrin. (x) Normetanephrin.

Metanephrin kaum noch durch Normetanephrin gestört. Das pH-Maximum der Oxidation liegt für beide Amine bei 7 (Abb. 4). Von Laverty und Taylor [8] werden jedoch andere optimale Werte angegeben: für Metanephrin pH 9,1, für Normetanephrin pH 8,6. Diese im manuellen Verfahren ermittelten Maxima konnten mit dem Analysenautomaten nicht bestätigt werden.

Mit steigender speed-Zahl nimmt die Fluoreszenzausbeute für Metanephrin zu, die für Normetanephrin fällt von speed 5 auf 6 stark ab (Abb. 4). Diese Ergebnisse deuten auf unterschiedliche optimale Reaktionszeiten für die einzelnen Reaktionsschritte wie Oxidation-, Reduktions- (bzw. Tautomerisierungs-) Zeit und Zeit zwischen dem Ansäuern und dem Messen der Probe hin. Für Metanephrin sind diese Zeiten kürzer, wie auch Laverty und Taylor [8] gefunden haben.

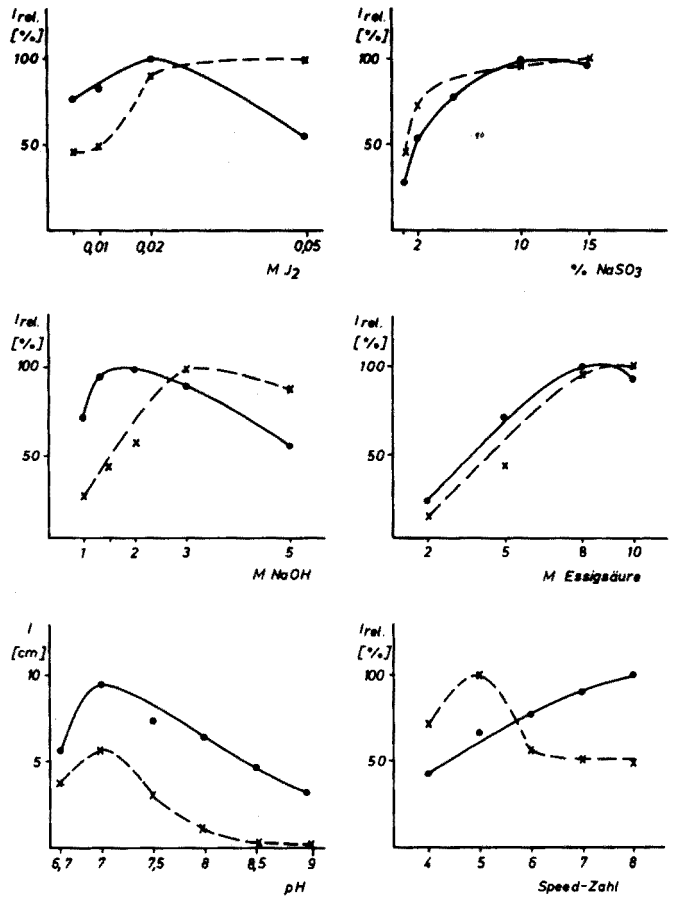

Abb. 4. Jod/Sulfitverfahren. Abhängigkeiten der Fluoreszenzausbeute von den Konzentrationen der Lösungen, dem pH-Wert der Oxidation und der Pumpengeschwindigkeit des Analysenautomaten. (Empfindlichkeit S = 1, je 500 ng Amin/ml.) (•) Metanephrin. (x) Normetanephrin.

Kaliumhexacyanoferrat(III)—Oxidation

Bei diesem Verfahren ergibt sich eine starke Abhängigkeit der Fluoreszenzintensitäten vom pH-Wert der Oxidation (Abb. 5). Auch eine unterschiedliche Alkalinität der zu messenden Lösung ermöglicht eine Differenzierung zwischen Metanephrin und Normetanephrin (Abb. 5). Bei der Änderung der Pumpengeschwindigkeit wird für Normetanephrin ein Ansteigen der Fluroeszenzintensität beobachtet, das durch die Verkürzung der Reaktionszeiten hervorgerufen wird. Der geringe Anstieg für Metanephrin ist auf das grössere Probevolumen mit steigender Speed-Zahl zurückzuführen.

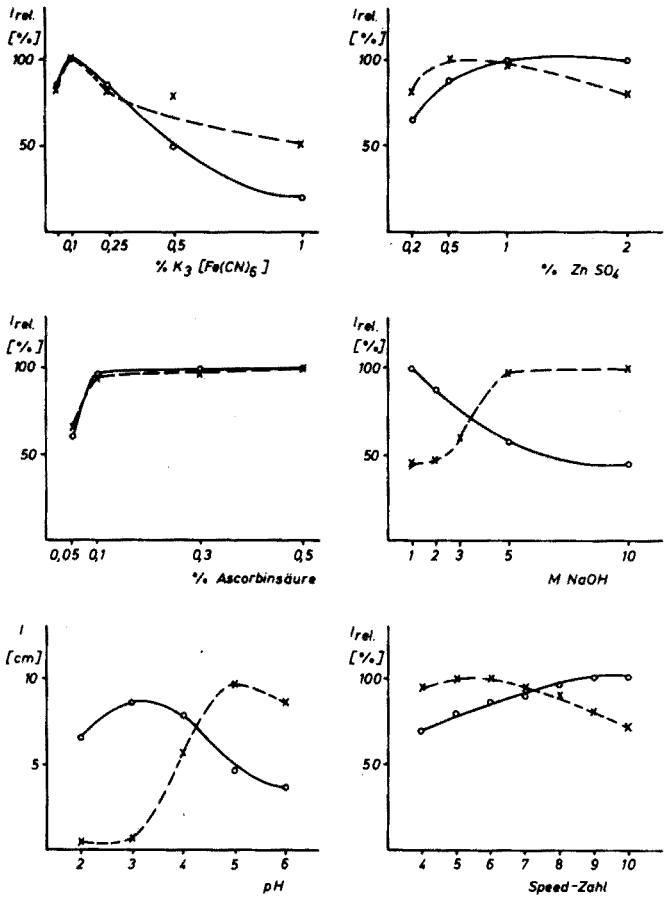

Abb. 5. Kaliumhexacyanoferrat(III)—Verfahren. Abhängigkeiten der Fluoreszenzausbeute von den Konzentrationen der Lösungen, dem pH-Wert der Oxidation und der Pumpengeschwindigkeit des Analysenautomaten. (Empfindlichkeit S = 3, je 500 ng Amin/ml.) (•) Metanephrin. (x) Normetanephrin.

Vergleich der Methoden

Der Vergleich der vier verschiedenen Methoden zur fluorimetrischen Bestimmung von Normetanephrin und Metanephrin mit den beschriebenen Analysenautomaten zeigt, dass beim Jod/Sulfit-Verfahren und Kaliumhexacyanoferrat(III)—Verfahren die günstigsten Differenzierungsmöglichkeiten (Tab. 2) erzielt werden können. Für die differenzierte Bestimmung empfiehlt es sich, die Bedingungen einmal so zu wählen, dass sich annähernd gleiche Fluoreszenzintensitäten für beide Amine ergeben. Bei der zweiten Messung soll die Fluoreszenzausbeute eines Amins bedeutend höher als die des anderen liegen. Diese Bedingungen sind am besten durch die Oxidation bei verschiedenen pH-Werten erfüllt. Aber auch durch die

Änderung physikalischer Einstellungen (Pumpengeschwindigkeit, Fluorimetereinstellungen) ohne das Auswechseln von Lösungen kann eine Differenzierung durchgeführt werden (Tab. 2).

Die höchsten Empfindlichkeiten werden mit der Kaliumhexacyanoferrat (III)—Oxidation erreicht, wie sich durch den Vergleich der absoluten Messwerte (unter Berücksichtigung der Fluorimeterempfindlichkeiten) aus den pH-Abhängigkeiten der einzelnen Verfahren (Abb. 2 bis 5) ergibt.

Die Bestimmungsgrenze liegt bei diesem Verfahren bei etwa 5—10 ng Amin je ml Lösung. Die Linearität ist bis mindestens 1 μg/ml gewährleistet. Für die Reproduzierbarkeit in der Serie kann ein Variationskoeffizient von weniger als 10 % angegeben werden. An einer Abtrennung von Metanephrin und Normetanephrin aus Urin zur automatisch-fluorimetrischen Bestimmung nach diesem Verfahren wird gearbeitet.

LITERATUR

1 K. Taniguchi, Y. Kakimoto und M. D. Armstrong, J. Lab. Clin. Med., 64 (1964) 469.
2 A. H. Anton und D. F. Sayre, J. Pharm. Exp. Ther., 153 (1966) 15.
2 H. Wisser und D. Stamm, Z. Klin. Chem. Klin. Biochem., 7 (1969) 631.
4 B. Andersson, S. Hovmöller, C.-G. Karlsson und S. Svensson, Clin. Chim. Acta, 51 (1974) 13.
5 H. Wisser und D. Stamm, Z. Anal. Chem., 252 (1970) 98.
6 F. P. Zuspan, M. A. Cooley und M. Abbott, Advances in Automated Analysis, Technicon International Congress, Vol. 1, 1969, p. 355.
7 A. Bertler, A. Carlsson und E. Rosengren, Clin. Chim. Acta, 4 (1959) 456.
8 R. Laverty und K. M. Taylor, Anal. Biochem., 22 (1968) 269.
9 E. R. B. Smith und H. Weil-Malherbe, J. Lab. Clin. Med., 60 (1962) 212.
10 S. Brunjes, D. Wybenga und V. J. Johns, Clin. Chem., 10 (1964) 1.

Analytica Chimica Acta, 81 (1976) 371—386

FLOW INJECTION ANALYSIS
PART III. COMPARISON OF CONTINUOUS FLOW SPECTROPHOTOMETRY AND POTENTIOMETRY FOR THE RAPID DETERMINATION OF THE TOTAL NITROGEN CONTENT IN PLANT DIGESTS

J. W. B. STEWART*, J. RŮŽIČKA*, H. BERGAMIN FILHO** and E. A. ZAGATTO
Centro de Energia Nuclear na Agricultura (CENA), C.P. 96, 13400 Piracicaba, S.P. (Brasil)
(Received 4th August 1975)

SUMMARY

The Berthelot reaction for the determination of ammonia by formation of indophenol blue, has been adapted to continuous flow spectrophotometry and the effects of acidity, temperature, ethanol content and sampling rate have been investigated; optimal conditions are described for the determination of nitrogen in Kjeldahl digests. Comparison of results obtained by this method, the air-gap electrode and classical distillation show no statistical difference at the 1 % level, but the flow injection technique can be run at a much higher sampling rate (110—180 samples per h) than any other method and uses as little as 0.3 ml of digest per analysis.

In the previous papers of this series [1, 2] the principle of Flow Injection Analysis was described, and the method was applied to the determination of phosphate in plant digests. It was found that a relatively simple chemical reaction such as formation of phosphomolybdenum blue and its spectrophotometry, can be easily accommodated by this new technique, which allowed phosphate analyses to be done at a rate of 250 samples per hour on a routine basis.

In contrast to conventional continuous flow analyses, as represented by the AutoAnalyzer concept, the new approach is based on rapid injection of the sample solution into a carrier stream of a reagent. The injected samples thus form a well defined zone which is then transported towards a detector. During this transport the sample solution is mixed with the carrier stream and reacts with its components to form a species which is quantitatively measured in a flow-through detector. As long as the chemical reactions are fast enough, the carrier stream does not need to be segmented by air, because the carry-over can effectively be prevented by keeping the conduits

*UNDP/IAEA Experts in Soil Science and Radiochemistry respectively. Assigned to UN Project BRA/71/556 during 1975. Present address J.W.B.S., Department of Soil Science, University of Saskatchewan, Saskatoon, Canada, and J.R., Chemistry Department A, The Technical University of Denmark, Building 207, 2800 Lyngby, Denmark.
**Professor Adjunto, ESALQ.

of the analyser short and by creating a turbulent flow. The turbulence of the carrier stream was so effective in the phosphate determination where the carrier was pumped at a rate of 20 ml min^{-1} through a tube of internal diameter 0.95 mm (length 230 cm) that the carry-over amounted to less than 1 % even at sampling rates of 420 analyses per hour. Thus the practical value of the Flow Injection Method was established and shown to have great promise with simple chemical reactions. In order to extend the possibilities of the method, it was decided to investigate a more complicated analytical procedure based on sequential addition of reagents, and involving a slower reaction and therefore requiring a more complicated manifold.

The Berthelot reaction [3] is frequently used for determination of ammonia which is oxidized by hypochlorite to form chloramine which then reacts with phenol to form an indophenol dye:

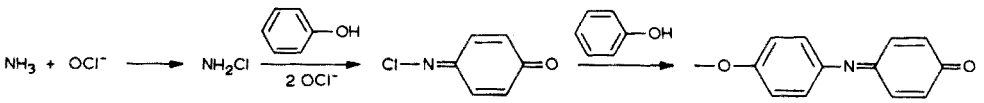

The indophenol dye is then measured spectrophotometrically at 620 nm. The formation and intensity of the colour depends on the sequence of a addition of the reagents [4], as well as on time, temperature, the pH of the solution and its redox potential, as indophenol is both an acid—base and a redox indicator [5, 6]. Therefore, although formerly employed in manual procedures, the Berthelot reaction is most successfully used in automated systems, which allow close control of reaction conditions.

The present AutoAnalyzer procedures [7—12] based on the work of Ferrari [13] are widely applied for the determination of the total nitrogen content in plant materials [7], food [8, 10], fertilizers [11], soils, waste water, etc. after Kjeldahl digestion of the sample material. It was therefore decided to adapt the Berthelot reaction to the Flow Injection system. At the same time, as an alternative approach, the use of potentiometric measurement of gaseous ammonia with the air-gap electrode [14] was investigated. These developments, the resulting methods, and their comparison with the classical distillation titration method are the subject of the present work.

The choice of the digestion method was considered from the viewpoint of requirement of this Institute, where up to 40000 plant and soil samples should be analysed annually for nitrogen. The possibility of automated continuous digestion was however, rejected, as it is wasteful on acid consumption and its output rate is rather low. Moreover, it requires a relatively uniform type of sample material and does not allow the analysis of soil samples. Instead, a manual digestion procedure [15] was selected, as it is suitable for various types of sample materials and provides a solution suitable for the determination of nitrogen, phosphorus, potassium, and most mineral ions. It is believed that, with the aid of programmed block digestion systems, this digestion procedure will have an output compatible with that of the flow injection method.

EXPERIMENTAL

Instrumentation

Samples were injected manually by means of disposable 1-ml plastic syringes through a valve located on a plastic tube through which the carrier stream of a reagent was pumped. The valve had a dead volume less than 3 μl, and the samples were forced through it at maximum, yet convenient, speed. This approach, in comparison with the previously described technique [12] based on hypodermic needle and rubber septum, was simpler to use and greatly facilitated the sampling.

The spectrophotometric apparatus consisted of a peristaltic pump model 8511, 60 r.p.m. (Polymetron, Hombrechtikon, Switzerland), a spectrophotometer model 25, with a digital readout, connected to a recorder model 24 25 ACC (both Beckman Inc., Fullerton) and flow-through cuvette (Helma type 178, light path 10 mm, volume 0.08 ml). The dual-beam mode was used with an aqueous saturated potassium chloride solution serving as a blank.

For potentiometric measurements, a digital pH Meter (model 64, Radiometer A/S, Copenhagen, Denmark) connected to a recorder (model RE571, Servogor, Goertz Electro, Vienna, Austria) was used. The air-gap electrode [14—16] was used to monitor the ammonia gas. The flow-through cell was made by drilling inlet, outlet and ventilation holes (all 1.0 mm diameter) into the Perspex microvessel supplied with the electrode. The inlet hole sloped down towards the bottom of the cell, its orifice being situated 2 mm above it, while the outlet hole was exactly level with the floor of the cell, thus allowing only a very thin layer of the measured solution to be present in the cell at any time. As a larger volume is pumped out of the cell than into it, a ventilation hole allowing free influx of air was drilled; the hole was situated as high as possible above the cell floor. The sensitivity and speed of response can be regulated by choosing the distance between the electrode surface and measured solution. In the present measurements the width of the air gap was 4 mm. The electrolyte employed in the electrode was 0.1 M ammonium chloride.

The manifold was made entirely of polyethylene and tygon tubing with noncollapsible walls; Y-shaped and straight connectors were made from drilled Perspex blocks, and mixing coils by winding the required lengths of plastic tube on a suitable support. All components of the manifold were conveniently fixed on a baseplate by plastic blocks (Lego A/S, Billund, Denmark).

Computations

All calibration curves were drawn and then calculated by either linear or parabolic regression analysis with a Hewlett-Packard Electronic Calculator Model 9801A. The nitrogen content in the sample material was then computed from the weighted mean of bracketing standards.

Reagents

For the alkaline phenol solution, 50 g of phenol, 120 g of sodium hydroxide and 330 ml of ethanol were dissolved and diluted to 1 l with distilled water.

Alkaline hypochlorite was made by dissolving 20 g of sodium hydroxide and 20 g of sodium tetraborate decahydrate in 800 ml of household bleach solution (containing 4 % of active chlorine) and diluting to 1 l with distilled water.

Nitrogen standards were all prepared in 1 M H_2SO_4 by appropriate dilution from a standard stock containing 452.9 mg of ammonium sulphate in 200.0 ml of 1 M H_2SO_4. Thus the standard stock, with regard to the amount of sample taken for digestion and subsequent dilution (see below) corresponded to 8.0 % nitrogen in the assayed plant material.

The digestion mixture was prepared by mixing 350 ml of hydrogen peroxide, 0.42 g of selenium powder and 14 g of lithium sulphate monohydrate in a 1-l flat-bottomed boiling flask; 420 ml of 18 M H_2SO_4 was added carefully with swirling and cooling.

All the above reagents were stable for at least a week if stored in a refrigerator.

Plant material

The plant material consisted of foliar samples taken from leguminous and non-leguminous trees in the Reserve Ducke of Campina Forests in the Rio Negro region of Amazonia near to Manaus, and from bean samples (*Phaseolus vulgaris* L.) taken from field experiments in the Piracicaba region of São Paulo State. All foliar material was dried at 65 °C for 48 h, and then ground to pass a 0.5-mm sieve with a Wiley mill.

The digestion and analytical procedures

The samples (300 mg) of plant material were digested as described by Parkinson and Allen [15] and brought to a final volume of 50.0 ml, of which 0.30 ml was injected for each determination. The individual steps comprised: 1) weighing the dry, finely ground sample into a 100-ml long-necked Kjeldahl flask; 2) adding 4.4 ml of the digestion solution; 3) heating gently until the initial reaction subsidized, and then more strongly until the hydrogen peroxide was driven off and the sulphuric acid refluxed; 4) digestion until all trace of yellow colour disappeared, followed by heating for another 20 min; 5) careful cooling and dilution to 50.0 ml with distilled water (or 0.5 M H_2SO_4, should the final acidity of digest be lower than that); and 6) injection of 0.30 ml of the diluted digest for analysis.

The distillation titration procedure used for comparison was identical with that described by Bremner [17].

RESULTS AND DISCUSSION

Spectrophotometric determination

The blue colour of indophenol formed by ammonia, hypochlorite and phenol in alkaline medium has been employed since its discovery in 1859 in numerous analytical procedures [4—13] which, however, still differ very much from each other. The most obvious discrepancy is in the order at which reagents are added to the ammonia solution. While the manual methods usually follow the reaction sequence [4] shown in eqn. (1), in the automated methods [7—14] the alkaline phenol is invariably added before the sodium hypochlorite solution. Various species have been suggested to catalyze the reaction, amongst which manganese(II) [18] and acetone [19] are the most effective, the latter allowing full colour development to be attained at room temperature in 20 min. The AutoAnalyzer methods are more rapid because the ractions do not need to be brought to completion, yet a relatively complicated manifold consisting of a number of mixing coils, a time delay coil [7—14] and even an elevated temperature bath have been used to assist the colour development [7—13].

In order to recheck the previous observations and adapt the method for the flow injection method, a preliminary study was undertaken from which it was learned that:

a) the addition of ethanol considerably speeds up development of the colour and improves its stability;

b) the two absorption maxima (at 358 and 620 nm) in the spectrum can vary in their proportion depending on pH, redox potential and the sequence of reagent addition, thus forming blue to emerald colours;

c) if alkaline phenol is added first, the automated procedure is less sensitive to the acidity of the sample solution.

Based on these observations, reagent solutions were chosen and two manifolds designed, identical in construction (Fig. 1), but of different line lengths. The short manifold (140 and 350 cm line and coil length) was used in preliminary studies and for analysis of samples of reasonably uniform composition, as it allowed a higher sampling rate, but had a nonlinear response. The long manifold (170 and 550 cm line and coil length) gave a strictly linear response even at low nitrogen contents, but had to be operated at lower sampling rates.

The calibration curves were influenced by the line length, temperature, ethanol content and the acidity of the sample. In order to minimize this last factor, a series of experiments was designed in which the content of sodium hydroxide in both the phenol and hypochlorite solutions was varied along with sample acidity. With the short manifold, peaks were recorded for samples containing ammonium sulphate in amounts corresponding to 3.0 % N in the digested sample (corresponding to 300 mg of plant material in a final volume of 50.0 ml). High contents of sodium hydroxide, together with sodium

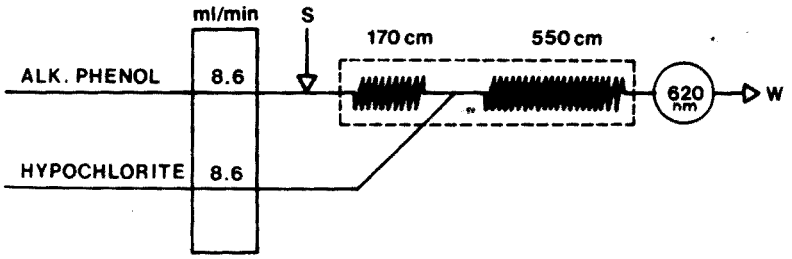

Fig. 1. Flow diagram for spectrophotometry of ammonia by flow injection. S is the point of sample injection (0.3 or 0.5 ml), W is waste and i.d. of tubing 0.95 mm. The dotted line encloses the part of the manifold immersed in the water bath. The long manifold had a total line length of 720 cm of which 170 cm were between S and the stream junction, while 550 cm were between the stream junction and the flow-through cell. The first coil comprised about 90 % of the respective line length and the second one about 80 %. The short manifold had a total line length of 490 cm (140 cm and 350 cm) distributed in the same manner.

tetraborate, extended the range of permissible variation of sample acidities (Fig. 2) so that even doubling the amount of digestion mixture, or reducing the amount of plant material, did not influence the calibration as a result of the change of the acidity of the digest to be assayed (Curve d).

As both temperature and ethanol content affect the rate of formation of

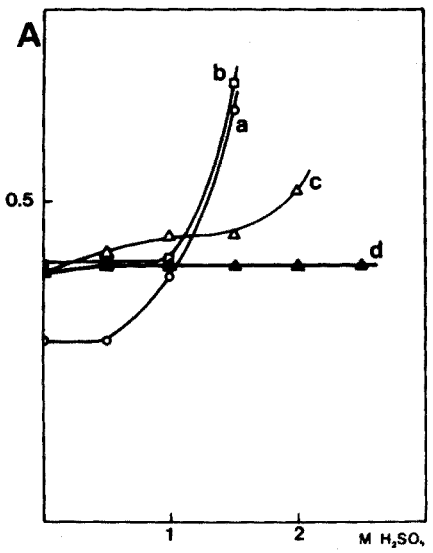

Fig. 2. Influence of sample acidity and reagent composition on the peak height, registered in a short manifold for a 3 % N content. The sodium hydroxide contents (g^{-1}) in the hypochlorite and alkaline phenol solutions were (a) 0, 80; (b) 0, 120 (c) 10, 120; and (d) 20, 120 (24 °C).

the indophenol colour, their influence on the calibration curve was studied in detail (Figs. 3 and 4). In both cases the short manifold was used and the compositions of the hypochlorite and alkaline phenol solutions were the same as stated under Reagents — except when the ethanol content was varied. Obviously both these factors must be kept constant to give reproducible results during any particular run. In the absence of a thermostated bath, the mixing coils were immersed in a stirred water bath which slowed down but did not prevent a rise in temperature in the coil caused by the slow accumulation of neutralization heat. Thus during each run (Figs. 5 and 6) the temperature increase caused a gradual change in the slope of the calibration curve. This effect was corrected by means of a computer programme for continuous weighting of the mean of the calibration curves. Obviously, the use of thermostated bath is preferable, but is unnecessary as a means of increasing the reaction rate, which can be much more effectively and conveniently controlled by variation of ethanol content.

The influence of time can be seen by comparing the recordings (Figs. 5 and 6) of two sets of routine analyses, bracketed by a series of standards, all injections being affected in triplicate. The recording (Fig. 5) obtained with the short manifold and injected volumes of 0.5 ml differs from the recording obtained with the long manifold and injected volumes of 0.3 ml (Fig. 6) in several respects. The response to ammonia concentration in the short manifold is not linear, so that this manifold is suitable only for materials

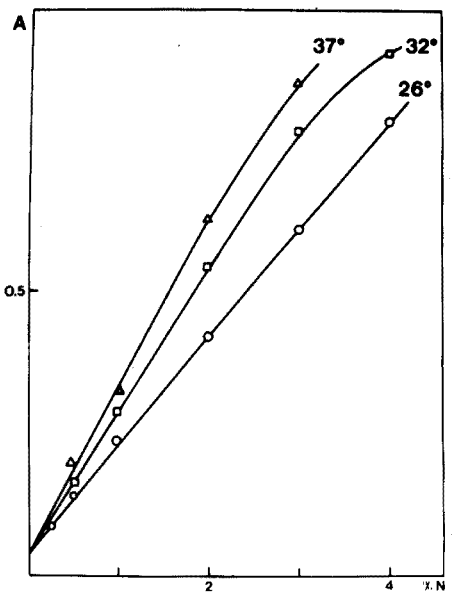

Fig. 3. The influence of temperature on the slope of calibration curve obtained with the short manifold and alkaline phenol with 20 % ethanol content.

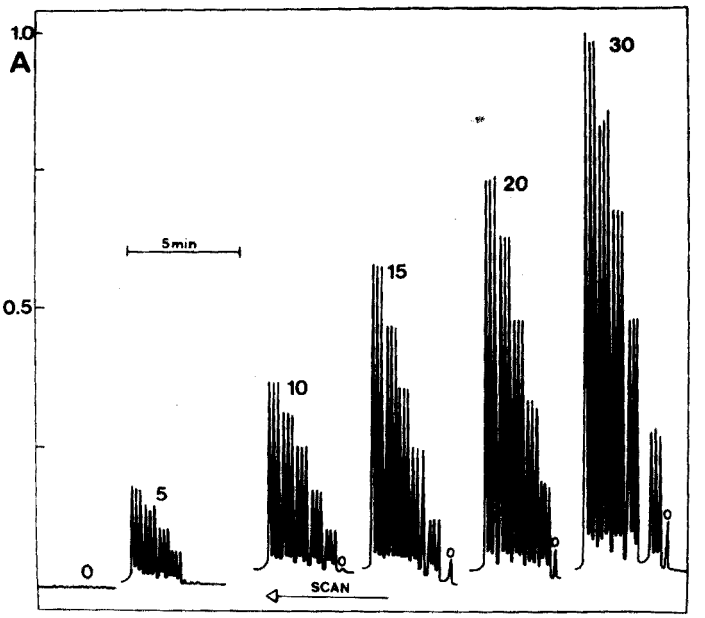

Fig. 4. The influence of ethanol content (5—30 %) in the alkaline phenol solution on the peak heights for 1, 2, 3, 4 and 5 % N content, obtained with a short manifold. All samples except the blank were injected in triplicate (23—23.2 °C).

with quite similar nitrogen contents, situated in the upper part of the calibration curve. With the longer manifold, not only strict linearity but also higher sensitivity is achieved; materials with lower nitrogen contents were therefore analysed with this manifold and small injected volumes (0.3 ml), as the absorbance was nearly twice as high as in the shorter line. However, the sampling rate in the longer manifold was approximately 30 % slower because of the line length and widening sample zone.

The maximum sampling rates for the short and long manifolds can be evaluated from the rise and fall curves, recorded at high paper speeds (Figs. 7 and 8). In the short manifold, with the larger injected volume, the sample zone is better preserved and the half-wash time, obtained from the fall part of the curve is 2.5 s; the first readout R_1 is obtained 18 s after the sample has been injected (S_1). Then, if the second sample (S_2) is injected immediately after R_1, it will reach a maximum for readout R_2 when less than 1 % of the colour of the first sample is left in the flow cell. In practice, the carry-over will be less than 1 %, as the injection of the second sample into the line will momentarily increase the flow rate in the system and thus facilitate the washout of the cell. Therefore, if only one sample is to be in the line at a time, the sampling frequency is limited by the period between S_1 and R_1 which for the short manifold gives a sampling rate in excess of 180 analyses per hour.

For the long manifold with a 47 % longer analytical line and smaller

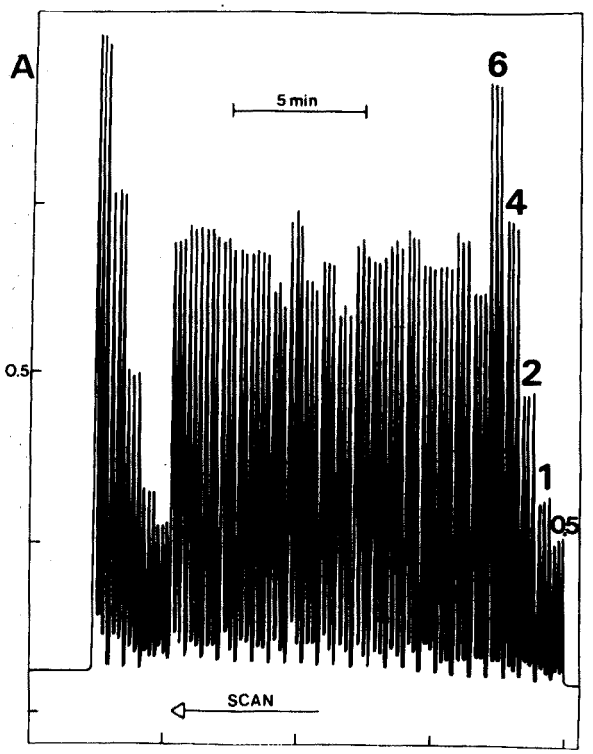

Fig. 5. Routine run of bean digests at a sampling rate of 180 analyses per hour in the short manifold (average standard deviation 0.75 %). Injected volume 0.5 ml, all samples injected in triplicate, from right to left: 0.5, 1.0, 2.0, 4.0 and 6.0 % N standards, followed by 19 samples and the same sequence of standards (temperature rising from 23.5 to 25.3 °C during the run).

injected volumes of 0.3 ml, the flow pattern is different, the response curve is nearly Gaussian in shape, and therefore the fall part of the curve should not be evaluated in the term of half-wash time. Nevertheless, it can be seen from Fig. 8 that 20 s after the curve has reached the maximum (R), less than 1 % of the colour from sample S_1 remains in the flow cell. The time between S and R is 24 s. Thus even when the next injection is effected immediately after the first readout, the carry-over is much less than 1 %. If another 4 s is allowed to elapse between R and S_2, to ensure a reliable readout, samples can be injected every 28th s, corresponding to a sampling rate in excess of 120 analyses per hour with a carry-over close to zero.

Potentiometric determination with the gas electrode

The theory of operation and the construction of the air-gap electrode have been described previously [16] and its application as a sensor in flow injection was reported in the first paper of this series [1]. In contrast to the

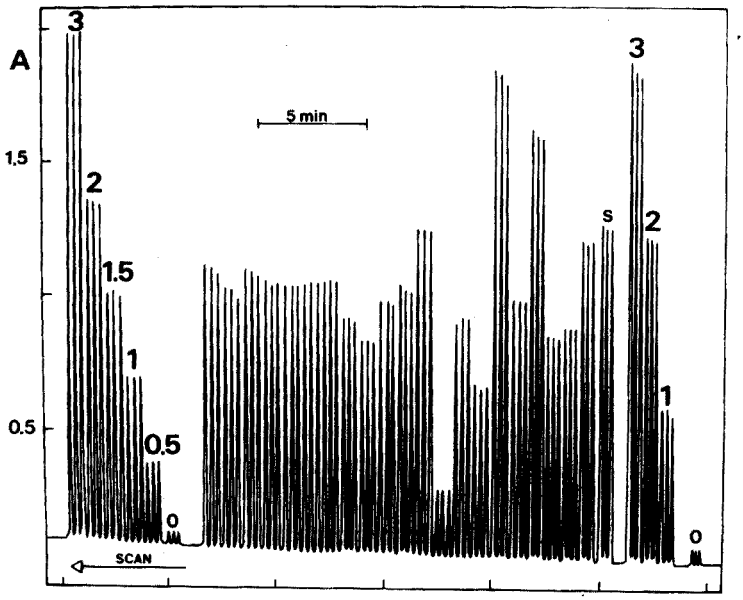

Fig. 6. Routine run of various digested plant materials at an average sampling rate of 110 analyses per hour in the long manifold (results in Table 1). Injected volume 0.3 ml, all samples injected in triplicate, from right to left: Blank, 1.0, 2.0, 3.0 % N standard, 2 % intercomparison standard, followed by 21 samples and blank, 0.5, 1.0, 1.5, 2.0 and 3.0 % N standard (temperature rising from 23.0 °C to 25.2 °C during the run).

spectrophotometric determination of ammonia, the electrode measurement is highly selective and employs very simple chemistry (Fig. 9). The injection of the acid digest into a carrier stream of sodium hydroxide causes the evolution of ammonia gas which diffuses across the air gap and reaches the surface of the glass electrode where the change of pH caused in a thin layer of electrolyte can be continuously recorded. Thus, for the determination of ammonia in the the Kjeldahl digests, the only parameter to be investigated was the concentration of the sodium hydroxide in the carrier stream, which should be sufficient to neutralize the acid in the digest to make the pH of the solution higher than 11.2 [14, 16]. Should the concentration of sodium hydroxide and line length not be sufficient, a valley on top of the peak would be recorded (Fig. 10) similar to that observed in the flow-injection analysis of phosphate [2]. The samples are injected always at the same potential (S_1, S_2) which is chosen so that the readout potential (R) is at least 90 mV (1.5 pH unit) away from the background point (B). In actual analysis, when 1.0 M sodium hydroxide is used in the carrier stream, the flow pattern is more favourable, resulting in a potential difference of 120 mV between R and B with a time interval of 30 s. A sampling rate of about 100 analyses per hour is possible with a carry-over of 1 %. For routine analyses, when 0.4 ml of digest was injected, 1.0 M sodium hydroxid was used. The long line length (490 cm) was used to allow as much as possible of the neutralization heat to be absorbed by a water bath in which the mixing

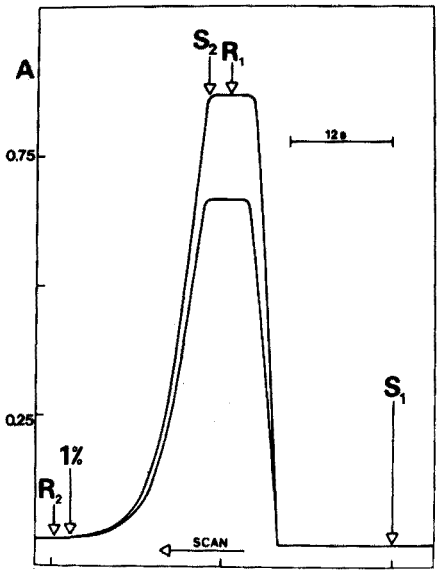

Fig. 7. Flow patterns in a short manifold for 0.5 ml of 4.0 and 6.0 % N samples, S_1, S_2 sample injections, R_1, R_2 readouts, half-wash time 2.5 s. Maximum sampling rate for carry-over less than 1 % is 180 samples per h. For details see text.

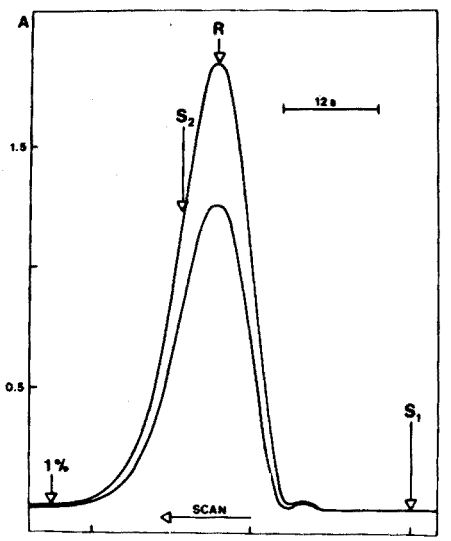

Fig. 8. Flow patterns in a long manifold with 0.3 ml of 2.0 and 3.0 % N samples. S_1, S_2 sample injections, R readout. Maximum sampling rate 120 samples per h. For details see text.

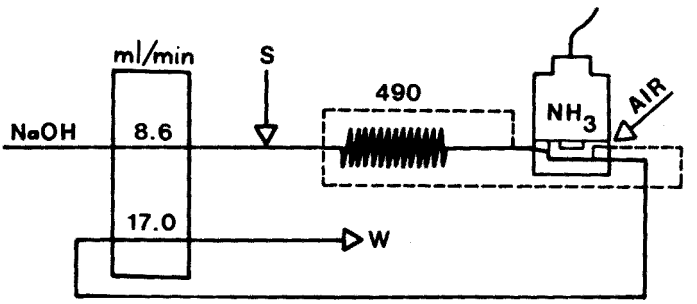

Fig. 9. Flow diagram for the potentiometric determination of ammonia with the air-gap electrode. S is the point of sample injection (0.4 ml), W is waste. Tubing 1.05 mm i.d. The dotted line encloses the part of the manifold immersed in the water bath. The line length was 490 cm of which about 90 % was accommodated on the coil.

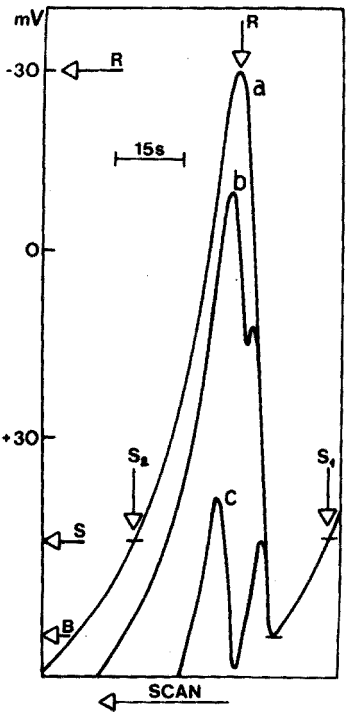

Fig. 10. The influence of acidity of the sample on the form and height of the peak obtained in the manifold shown in Fig. 9. S_1, S_2 injection points, R is readout, B is background point. The molarity of H_2SO_4 in the sample: (a) 0.15 M; (b) 0.75 M; (c) 1.5 M. Carrier stream 0.25 M NaOH.

coil and the flowthrough chamber of the air-gap electrode were immersed. This, however, was not sufficient to prevent a temperature rise of 2—3 °C during a routine run of one hundred analyses. This rise and changes of room temperature, caused significant changes in the electrode potential and the position of the calibration curve. As the slope of the calibration line remained essentially the same, the routine runs were bracketed by series of standards and a recalibration with one standard was done after each series of twenty injections. Obviously, thermostating of both mixing coil and electrode system would substantially improve the performance of the system.

Comparison of flow injection methods with the distillation—titration procedure

The classical Kjeldahl procedure, viz. distillation of ammonia into a solution of boric acid followed by titration, is inherently very precise, but time-consuming. Even microdistillation [17] which is most frequently employed today, requires as much as 2—3 min of attended operation. When additional operations and the titrations are accounted for, it is unlikely that more than 15 samples can be analyzed per hour; moreover, replicate samples usually have to be digested for statistical accuracy. AutoAnalyzer methods based on a sample rate of 30 samples per h are preferable, because duplicate or triplicate analyses can be made on the same acid digest at higher working loads. Therefore the contribution of Flow Injection analysis, with a four times higher output, also should be evaluated in the terms of the improved reliability of the analytical data.

In order to compare all three methods, 21 plant samples with different nitrogen contents were digested, and suitable aliquots of each digest were analyzed. The same series of standard solutions was used to calibrate the instrument for both Flow Injection spectrophotometry and potentiometry, while one of these standards was also used to calibrate the distillation—titration procedure. The recording of analyses by Flow Injection spectrophotometry is shown in Fig. 6, while all results are summarized in Table 1.

As there is no statistical difference (at the 1 % level) between the results obtained by the three methods, Flow Injection spectrophotometry is the method of choice, because it has high productivity and utilizes the generally accepted technique of colour measurement. Moreover, a very small volume of the digest is required, which is important if the same plant material has to be analyzed for other elements. Provided that the reagents are prepared as specified, the results will be highly reliable. The gas sensor is based on extremely simple chemistry and its high selectivity makes it suitable for the determination of ammonia in other samples, e.g. soil extracts, fertilizers, waste waters, etc., but it requires a knowledge of electrode operation and the sensor is not widely available commercially.

TABLE 1

Comparison of methods of determining Kjeldahl-nitrogen in plant digests

Sample Foliar material taken from	Distn. Titn.	Flow injection			
		Photometry		Electrode	
	% N	% N	*s*	% N	*s*
Eschweilera mata-mata	1.99	1.94	0.36	2.23	2.41
Virola surinamensis (Rol.) Warb	1.43	1.44	0.24	1.51	2.30
Aldina heterophylla Benth.	1.40	1.38	0.60	1.48	0.23
Pithecolobium sp.	2.62	2.55	0.55	2.57	1.86
Phaseolus vulgaris L.	1.56	1.57	0.22	1.64	0.99
Pithecolobium racemosum Ducke	2.88	2.89	0.96	3.04	0.82
Eperua schomburgkiana Benth.	1.08	1.06	1.15	1.10	0.82
Phaseolus vulgaris L.	1.46	1.43	1.45	1.42	1.94
Pradosia glycyphloea Kuln.	0.46	0.47	0.15	0.39	3.56
Parkia oppositifolia Spreng. ex Benth.	1.94	1.94	0.11	1.83	1.04
Copaifera sp.	1.62	1.60	1.32	1.74	1.98
Carapa guianensis Aubl.	1.49	1.51	0.99	1.32	2.96
Phaseolus vulgaris L.	1.27	1.28	0.49	1.25	2.16
Phaseolus vulgaris L.	1.39	1.40	0.65	1.41	0.60
Phaseolus vulgaris L.	1.63	1.61	0.21	1.58	0.23
Phaseolus vulgaris L.	1.62	1.59	0.09	1.58	0.99
Phaseolus vulgaris L.	1.63	1.56	1.66	1.58	1.21
Phaseolus vulgaris L.	1.63	1.57	0.96	1.52	1.36
Phaseolus vulgaris L.	1.66	1.63	1.10	1.59	0.61
Phaseolus vulgaris L.	1.54	1.51	2.09	1.43	1.43
Phaseolus vulgaris L.	1.77	1.63	1.50	1.68	0.60
Mean	1.62	1.60	0.75	1.61	1.43
Regression coef. for calibration curve N (N)		0.9995(9)		0.9974(15)	
Relationship between means relative to m % dist.—titr.	100	98.5		99.5	

CONCLUSION

Flow injection analysis of Kjeldahl digests can be done at a rate up to 180 samples per hour with a standard deviation of 0.75 %. The results obtained are identical to those reached by the classical distillation titration technique. It thus might appear that the main assets of the new technique are the high sampling rate and the small sample volumes. But it should be emphasized that the simplicity of experimental arrangement, as shown in the flow diagrams, is equally important. From a practical view point, two additional aspects should be stressed: owing to the very low carry-over, samples with widely different nitrogen contents can be analysed successively and, because of the shortness of the analytical line the result is available less than 30 s after the sample has been injected. Except for the spectrophotometer, there is no "warm up" period, so that the system can be switched on for instant operation and short series of samples can be rapidly analysed. The disadvantage of the new method, namely, the necessity of manual injection, still has to be overcome.

The feasibility of adding a second reagent to a carrier stream already containing the injected sample, considerably increases the range of methods potentially suitable for Flow Injection analysis. Moreover, the line length employed in the present case accommodates the sample for a longer time, thus allowing the use of slower chemical reactions. Much practical and theoretical work remains to be done in this respect, in order to establish the relationships between reaction rates, flow rates and line lengths.

Further parts of this series will describe the possibilities of sample splitting and of multiple analyses, for instance, simultaneous determination of phosphate and nitrogen in the same plant digest.

The authors wish to express their gratitude to Jan Schaefer Jr. for the donation of the Lego building set and to A. Růžicková for preparation of the diagrams.

REFERENCES

1 J. Růžička and E. H. Hansen, Anal. Chim. Acta, 78 (1975) 145.
2 J. Růžička and J. W. B. Stewart, Anal. Chim. Acta, 79 (1975) 79.
3 M. P. E. Berthelot, Report de Chimie Appliqué, 284 (1859).
4 W. T. Boletter, C. J. Bushman and P. W. Tidwell, Anal. Chem., 33 (1961) 592.
5 E. D. Noble, Anal. Chem., 27 (1955) 1413.
6 P. G. Scheurer and F. Smith, Anal. Chem., 27 (1955) 1616.
7 M. H. Werner and J. Benton Jones, Soil Sci. and Plant Anal., 1 (1970) 109.
8 C. W. Gherke, F. E. Kaiser and J. P. Ussary, J. Ass. Offic. Anal. Chem., 51 (1968) 200.
9 H. P. Moore and R. E. Kelly, Technicon Symposia, Advan. Auto. Anal. Chem., (1970) p. 47.
10 H. G. Lento and D. E. Daugherty, Technicon Symposia, Advan. Auto Anal. Chem., (1970) p. 75.
11 C. W. Gherke, L. L. Wall Sr., J. S. Killingley and K. Inata, Technicon Symposia, Advan. Auto Anal. Chem., p. 39 (1970).

12 Technicon AutoAnalyser II, Industrial method 218-72A, Technicon Tarrytown, NY.
13 A. Ferrari, Ann. N.Y. Acad. Sci. 87(2), 792 (1960).
14 J. Růžička and E. H. Hansen, Anal. Chim. Acta, 69 (1974) 129.
15 J. A. Parkinson and S. E. Allen, Commun. Soil Sci. Plant Anal. 6 (1975) 1.
16 E. H. Hansen and J. Růžička, Anal. Chim. Acta, 72 (1974) 353.
17 J. M. Bremner, in C. A. Black et al. (Eds.), Methods of Soil Analyses Part 2, Amer. Soc. Agron. p. 1149, (1965).
18 J. A. Russell, J. Biol. Chem., 156 (1944) 457.
19 A. B. Crowther and R. S. Large, Analyst (London), 81 (1956) 64.

Analytica Chimica Acta, 81 (1976) 387—396

FLOW INJECTION ANALYSIS
PART IV. STREAM SAMPLE SPLITTING AND ITS APPLICATION TO THE CONTINUOUS SPECTROPHOTOMETRIC DETERMINATION OF CHLORIDE IN BRACKISH WATERS

J. RŮŽIČKA*, J. W. B. STEWART* and E. A. ZAGATTO
Centro de Energia Nuclear na Agricultura (CENA) C.P. 96, 13400 Piracicaba, S.P. (Brasil)
(Received 4th August 1975)

SUMMARY

The rapid determination of chloride in water samples based on spectrophotometric measurement of iron(III)thiocyanate has been adapted to Flow Injection Analysis. The simple manifold allows a routine sampling rate of 300 samples/hour, and evidence is presented that 500 samples/hour are possible. For increased accuracy in the measurement of samples of widely varying chloride content, the sample is split in the reagent stream so that the relevant absorbance of the split sample zones varies from 1:2 to 1:10 allowing expansion of the analytical range without loss of accuracy.

The Amazon River has the largest drainage basin and the greatest discharge volume of all the rivers of the world, supplying approximately 1/5 of all the river water discharged into the oceans [1]. The effect of this vast volume of water on the ocean environment in the vicinity of the mouth of the river and around Marajó island has recently been studied [2]. Presently, this Institute (CENA) has a programme in which salinity, river and ocean flow patterns and sea water contamination of estuarine areas are being studied by analysis of water samples taken at different seasons and tides at specific locations at or near the Amazon River estuary. One of the most useful chemical analysis in this study is the determination of the concentration of chloride in river, estuarine and sea water samples.

The need for a simple rapid automated colorimetric method with a sensitivity ranging from 0 to 40 meq Cl^- l^{-1}, to measure chloride in the numerous water samples collected monthly, focussed attention on the spectrophotometric method originally suggested by Utsumi [3], studied in detail by Zall et al. [4] and automated by Skeggs and Hochstrasser [5, 6]. In the latter approach, which is one of the most frequently used methods in clinical and industrial laboratories, the colour of an iron(III) thiocyanate

*UNDP/IAEA Experts in Radiochemistry and Soil Science respectively assigned to UN Project BRA/71/556 during 1975. Present address: J. R., Chemistry Department A, The Technical University of Denmark, Building 207, 2800 Lyngby, Denmark, and J. W. B. S., Department of Soil Science, University of Saskatchewan, Saskatoon, Canada.

complex formed as shown below, is measured at 480 nm. It has been noted that the absorbance of the red complex varies directly with the amount of chloride present but that the response is non-linear [5].

$$Hg(SCN)_2 + 2Cl^- \rightarrow HgCl_2 + 2\,(SCN)^-$$

$$3\,(SCN)^- + Fe^{3+} \rightarrow Fe(SCN)_3$$

It was therefore decided to adapt this method for Flow Injection Analysis [7] which from past experience with other types of analysis [7,8] allows a higher sampling rate with a simple uncomplicated system.

EXPERIMENTAL

Instrumentation

Injection of the sample was done manually as previously described [9], by means of disposable 1-ml plastic syringes, through a valve located on a plastic tube through which a reagent was pumped. The valve had a dead volume of 3 μl and the samples were forced through at maximum yet convenient speed.

The apparatus used consisted of a peristaltic pump (model 8511, 60 r.p.m., Polymetron, Hombrechtikon, Switzerland), a spectrophotometer model 25, with digital readout, connected to a recorder Model 24 25 ACC (both Beckman Inc., Fullerton) and a flow-through cuvette (Helma type 178, light path 10 mm, volume 0.08 ml). The dual-beam mode was used with a chloride colour reagent solution serving as a blank.

The manifold was made entirely of polyethylene and tygon tubing of the non-collapsible wall type. Straight and Y-shaped connectors were made from drilled perspex blocks, and mixing coils by winding the required lengths of plastic tube around a suitable support. All components of the manifold were conveniently fixed on a base plate by plastic blocks (Lego A/S, Billund, Denmark).

Computations

All calibration curves were drawn and then calculated by means of parabolic regression analyses with a Hewlett-Packard Electronic Calculator Model 9601A.

Reagents and materials

For the chloride colour reagent 0.626 g of mercury(II) thiocyanate, 30.3 g of iron(III) nitrate, 4.72 g of 14 M nitric acid and 150 ml of ethanol were dissolved in water and diluted to 1 l.

Chloride standards were made from sodium chloride in water; the 100 meq $Cl^-\ l^{-1}$ standard was made by dissolving 5.85 g of NaCl in 1 l of water.

All water samples were collected in Nansen bottles at different depths from the surface at various locations around the Island of Marajó at the mouth of the Amazon River. All samples were filtered through 5-μm filter paper to remove suspended colloidal particles before analysis.

RESULTS AND DISCUSSION

Based on previous experience with the flow injection analysis [8, 9] it was decided to investigate the following parameters: (a) the volume of sample injected into the reagent stream; and (b) the time of reaction and the effects of line length and carrier flow rate, in order to establish the optimal sampling frequency. Further, as the amount of chloride in the samples covered a wide concentration range, sample splitting in the flowing stream was attempted. These parameters were investigated with the manifolds shown in Fig. 1.

The sample volume was optimized in a series of experiments carried out with a simple manifold (Fig. 1 upper), where A was a 287-cm plastic tube (1.0 mm i.d.); the flow rate was 17 ml min^{-1}. Injection volumes were varied from 0.1 to 1.0 ml. The results (Fig. 2) showed that, as is characteristic for the chloride method [5], the response is non-linear, but that there is an increase in linearity and sensitivity with injected sample volume. Above 0.6 ml, the response is distorted because of insufficient mixing of the sample plug with the carrier stream of the reagent. (Note the form of the curve — Fig. 2 — when a 1.0-ml sample volume is used showing a distinct trough effect). On the basis of this evidence plus consideration of the ease of manual injection, a 0.4-ml sample volume was used in all subsequent experiments.

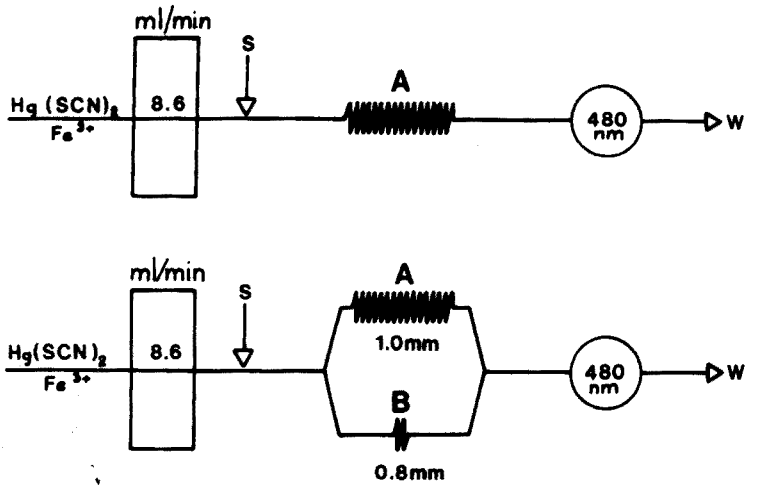

Fig. 1. Flow diagrams for spectrophotometry of chloride. S is the point of sample injection, W is waste. Unless otherwise stated in the text the i.d. of all tubing was 1.0 mm and the pumping rate 8.6 ml min^{-1}. The upper diagram shows the simple manifold whereas the lower diagram shows the branched manifold used to split the sample. For coil lengths A and B, see text.

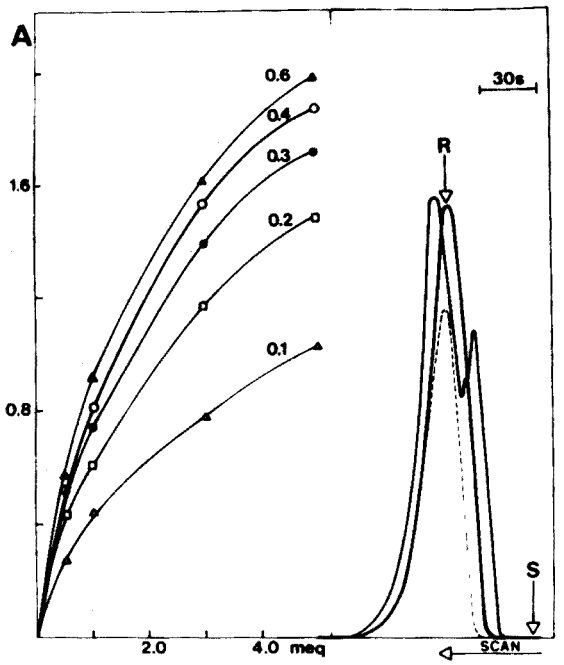

Fig. 2. The influence of sample volume (0.1—0.6 ml) on the calibration curve for chloride (0.5—5.0 meq $Cl^- l^{-1}$) obtained with the simple manifold, where A was 287 cm and the flow rate was 17 ml min^{-1}. The actual peaks for an injection volume of 0.2 ml (dotted line) 0.4 ml (marked R) and 1.0 ml (showing trough) of the 3 meq $Cl^- l^{-1}$ standard are shown, together with point of injection S and readout R.

Effects of line length and flow rate

The line length together with the flow rate influences the residence time of the sample in the analyzer. At a constant flow rate, typical hyperbolic curves are obtained (Fig. 3) for 1.0, 2.0 and 5.0 meq $Cl^- l^{-1}$ standards. The ascending part of the curve reflects the build-up of the colour caused by the increased residence time and therefore in the reaction time from injection to measurement. The descending part of the curve reflects the dilution of the colour formed in the carrier stream as the sample zone moves along the line. At a fast flow rate of 17.0 ml min^{-1}, maximum sensitivity is obtained at line lengths between 300 and 500 cm (corresponding to a coil length A of 150—350 cm — Fig. 1 upper). As there is not much difference beyond this line length, and as the sample colour is fully developed with the shortest line length, the choice of line length will be determined by the sampling rate. For this purpose, the rise and fall curves of individual peaks (see Fig. 4) were studied and the result for each line length was plotted in the same graph

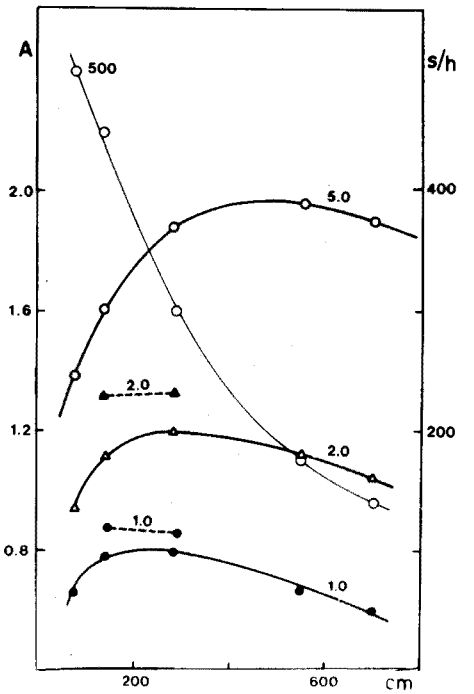

Fig. 3. The influence of line length on the sensitivity of the chloride determination (1.0, 2.0 and 5.0 meq $Cl^- l^{-1}$) obtained with the simple manifold; A varied from 75 to 700 cm with a pumping speed of 17 ml min^{-1} from which the corresponding sampling rates (thin continuous line) were calculated. The broken lines (2.0 and 1.0 meq $Cl^- l^{-1}$) were obtained with a slower pumping speed (8.6 ml min^{-1}).

(thin line, Fig. 3). It can be seen that the shortest line length (85 cm) would allow a sampling rate of 500 samples/h (computed for a sample carry-over of less than 1 %) and that the sampling rate decreases with the line length.

For manual injection, however, the maximum convenient sampling rate is about 200 samples/h (corresponding to a line length of 500 cm). The same output, with better economy of reagents, can be obtained by reducing the flow rate to 8.6 ml min^{-1} and the line length by half (Fig. 3, broken lines).

The sampling rate, carry-over and reproducibility of the chloride measurement were studied at high (17 ml min^{-1}) as well as low (8.6 ml min^{-1}) reagent carrier stream flow rates with a line length of 287 cm in both cases. The recording obtained is shown in Fig. 4. By injecting, in triplicate, samples in the range 0.2—5.0 meq $Cl^- l^{-1}$ at a high pumping rate (Fig. 4a) and a low pumping rate (Fig. 4b), calibration curves were obtained with regression coefficients of 0.989 and 0.992, and average standard deviations of 1.56 % and 1.40 %, respectively. From the curves (Fig. 4) recorded at a higher chart speed, obtained by injecting 5.0 meq (a) and 4.0 meq $Cl^- l^{-1}$ (b) standards, the maximum sampling rate for a carry-over of 1 % or less was obtained by comparing the time intervals elapsing between sample injection S_1, readout R

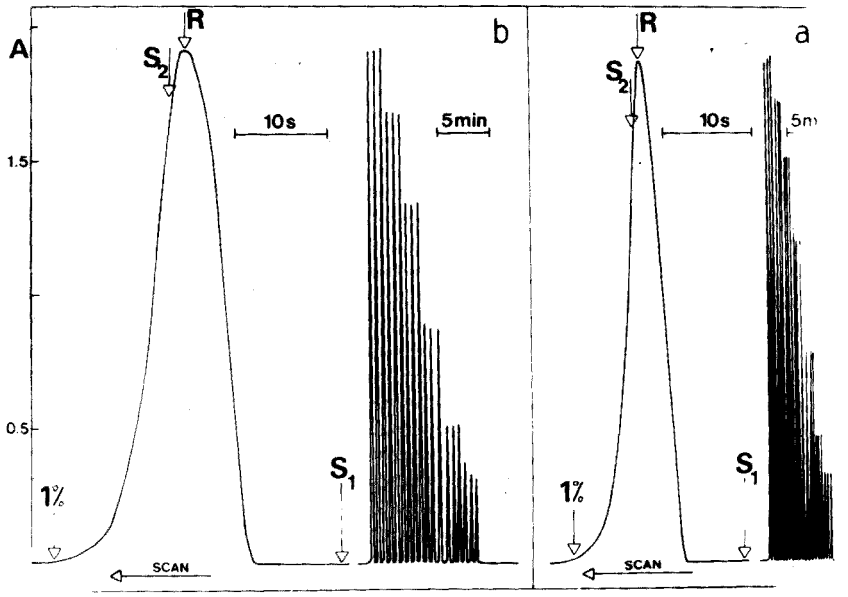

Fig. 4. Flow patterns in a simple manifold at a high (a) and low (b) pumping rate. S_1 and S_2 are the points of injection, R is the readout and 1 % marks the time at which 1 % of the maximum absorbance colour is left in the flow cell. Corresponding calibration curves (a) 0.2, 0.5, 1.0, 2.0, 3.0, 4.0 and 5.0 meq $Cl^- l^{-1}$, and (b) 0.2—4.0 meq $Cl^- l^{-1}$, are shown.

and the time when the colour left in the flow cell is 1 % of the maximum absorbance. At both flow rates, the interval between S_1 and R is longer than that between R and 1 % so that the carry-over would be negligible even if the next sample were injected immediately after the readout R. Allowing a safety margin of 1—2 s for reliable readout, a maximum sampling rate of 300 samples/h was obtained for the fast flow rate, and 200 samples/h for the slow flow rate. Several samples of brackish waters were analysed at the slow flow rate (Table 1), but it was often necessary to dilute samples which had chloride contents higher than 4.0 meq $Cl^- l^{-1}$. Therefore, to avoid this dilution and repetition of analysis, stream sample splitting was devised.

Stream splitting

Sample splitting was effected by the manifold shown in Fig. 1 (lower). Different branch lengths A and B and different tube internal diameters (1.00 mm and 0.82 mm) were employed to allow precision splitting of the sample stream. The splitting was arranged so that the respective absorbances of the split sample zones, re-routed through the same flow cell ranged from 1:2 to 1:10 (Fig. 5, b—f). For comparison, extreme cases are shown, i.e., when branch B was blocked (A = 95 cm, peak a), and when branch A was blocked (B = 11 cm, peak g). By imposing 1 % as the highest acceptable

TABLE 1

Chloride concentration in water samples determined by (a) single peak, and (b) split peak methods

Sample	Single peak meq $Cl^- l^{-1}$	Split peak[a] meq $Cl^- l^{-1}$	
		First peak	Second peak
1	1.18	1.32	1.30
2	0.68	0.67	0.72
3	0.27	0.30	~ 0.30
4	9.20	—	8.85
5	4.45	4.35	4.30
6	~ 0.10	0.15	~ 0.10
7	8.40	—	8.62
8	0.15	0.18	~ 0.15
9	0.28	0.31	~ 0.35
10	4.15	4.20	4.08
11	~ 0.10	0.15	~ 0.15
12	5.15	5.00	5.12
13	6.30	—	6.09
14	0.23	0.20	~ 0.20
15	~ 0.10	0.07	~ 0.15
	m = 2.716	m = 2.694	

[a]In the split peak method, values less than 4.0 meq $Cl^- l^{-1}$ were read off the first peak graph and values above 4.0 meq $Cl^- l^{-1}$ were read off the second peak. Values above 5 meq $Cl^- l^{-1}$ were off-scale for the first peak. Values used for comparison with the single peak method are underlined.

[b]The symbol ~ is used to designate a relative standard deviation of more than 10 % between the three replicates in any analysis. The average relative standard deviations computed from these results were: single peak 1.36 %; double peak for < 4 meq $Cl^- l^-$, 4.23 %; double peak for > 4 meq $Cl^- l^{-1}$, 1.08 %.

carry-over, the maximum sampling rate was estimated by comparing the time between S, R_1, R_2 and 1 % time marks. As both R_1 and R_2 for a particular sample originate from the sample plug of the same composition, the carry-over within the split peak need not be considered; the contribution of the first peak to the second is always included in the respective calibration line. If 1:2 splitting (Fig. 5, peak b) is taken as an example, it can be seen that the time lag between S_1 and R_1 is 6 s, between S_1 and R_2 20 s, and between S_1 and 1 % 40 s. Thus in order to have a carry-over of 1 % or less, the next sample S_2 can be injected, at the earliest, 10 s before the 1 % time mark, which leaves a time interval of 30 s between S_1 and S_2. This indicates a sampling frequency of 120 samples/h. In practice, however, a slightly higher sampling rate can be obtained, because the injection of the second sample at time S_2 momentarily increases the flow rate, improving the washout of the flow cell and decreasing the interval between S_1 and 1 %.

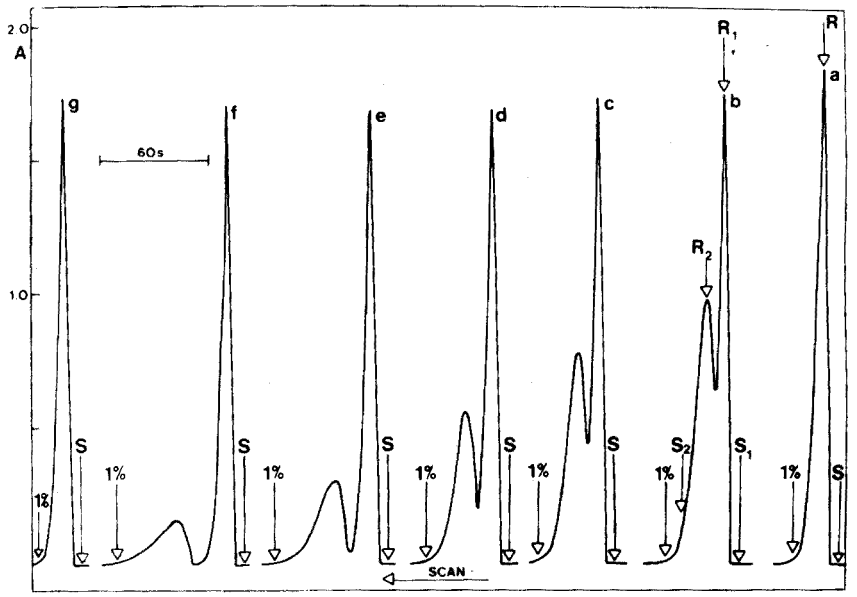

Fig. 5. Stream sample splitting with the branched manifold and a 4.0 meq Cl^- l^{-1} standard. A slow pumping rate was used with different B branch lengths and A constant at 95 cm. The length of B was (b) 22 cm, (c) 16.5 cm, (d) 11 cm, (e) 5.5 cm, (f) 2.8 cm. In (a) B was blocked and in (g) A was blocked with B 11 cm. S, S_1 and S_2 are points of injection, R, R_1 and R_2 are readouts and 1 % is the time at which 1 % of the maximum absorbance colour is left in the flow cell.

Thus the maximum sampling rate obtained with a split stream, which is then re-routed through the same flow cell, depends on the relative lengths and diameters of the branches A and B of the manifold. These in turn determine the proportion of the sample split. It was observed (Fig. 5) that for 1:2 splitting a rate of 120 samples/h is obtained (b); for 1:3 splitting the rate is 110 (c); for 1:4—100 (d); for 1:6—70; and for 1:10—60 samples/h. An unsplit sample with the short line blocked (B) could be run at a rate of 200 samples/h (a), and an unsplit sample with the long branch (A) blocked at a rate of 240 samples/h. In all these experiments the line A was kept constant and the length of branch B was varied. Obviously by changing the line length A, the time lag between R_1 and R_2 can also be varied and shortening of A would lead to an increase in sampling rate, which might be desirable if division of the sample in the ratio of 1:6 and 1:10 is required.

Analysis of water samples

The analysis of water samples was carried out in two ways: either the simple manifold was used to give a single readout peak, or the split stream gave two readout peaks. These two approaches were compared by analysing

identical samples (Table 1); the reproducibility of splitting could also be evaluated, because some of the samples fell within the range where both R_1 and R_2 could be used for evaluation. Comparison of these results showed that they were statistically identical (at the 1 % level) and that the reproducibility of splitting was excellent. Part of the sample output from the split peak method, and a calibration graph, are shown in Fig. 6. The reproducibility of splitting any one sample was very good.

CONCLUSIONS

The results described demonstrate not only that Flow Injection Analysis can be adapted to the determination of chloride in water samples at faster sampling rates than any previously reported, but, more important, that the sample can be split in the carrier stream in a reproducible manner after injection.

It was confirmed that the line length is the most important parameter to be investigated in adapting any method for Flow Injection Analysis. Its choice affects the reproducibility and sensitivity of the determination, and also allows a specific sampling rate to be selected and thus a flow rate which offers the best economy of reagents. The highest sampling rate of 500 analyses per hour achieved here is about five times higher than those of

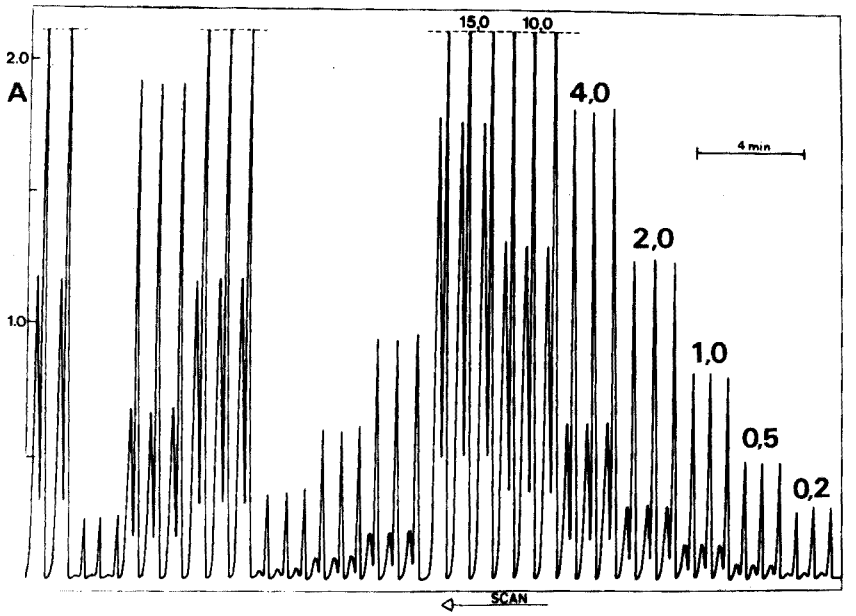

Fig. 6. Calibration graph (0.2—15.0 meq Cl^- l^{-1}) and part of a routine water analysis output obtained with the branched manifold (A, 95 cm and B, 11 cm) and a flow rate of 8.6 ml min^{-1}. All samples (0.4 ml) injected in triplicate.

analogous industrial methods [6]. Thus, taking into consideration the sampling rates achieved in phosphate and nitrogen determination, it might be postulated that many other AutoAnalyser methods could be adapted for the Flow Injection Analysis method with similar gains in speed.

Splitting of the sample in the stream and re-routing it through the same flow cell was used here to give expansion of the analytical range without loss of reproducibility. The same approach, however, can probably serve yet another purpose. For instance, in analyses based on reaction rate measurements, e.g. the determination of enzyme activities, the length of lines and branches may be arranged in such a way that two point rate measurements may be made. Another important facet of reproducible stream splitting is the possibility of simultaneously determining two components by means of two flow-through cells and one recorder.

The authors wish to thank Professor Eneas Salati, Head, Division of Environmental Sciences, CENA, for drawing attention to the problem, for scientific discussion and cooperation, and to A. Růžičková for preparation of the diagrams.

REFERENCES

1 R. J. Gibbs, Geochim. Cosmochim. Acta, 36 (1972) 1061.
2 Marinha do Brasil, Projeto Atlas Oceanografico, 3 (1973).
3 S. Utsumi, J. Chem. Soc. Jap. Pure Chem. Sect., 73 (1952) 835.
4 D. M. Zall, D. Fisher and M. Q. Garner, Anal. Chem., 28 (1956) 1665.
5 L. T. Skeggs and H. Hochstrasser. Clin. Chem., 10 (1964) 918.
6 Technicon Instruments Corporation, Tarrytown, N.Y. Technicon method SE4-0005 FD4, 1974.
7 J. Růžička and E. Hansen. Anal. Chim. Acta, 78 (1975) 145.
8 J. Růžička and J. W. B. Stewart. Anal. Chim. Acta, 79 (1975) 79.

Analytica Chimica Acta, 81 (1976) 397—407

SYSTEMATIC ERRORS IN VACUUM AND INERT GAS FUSION ANALYSIS FOR OXYGEN IN METALS

A. COLOMBO

Chemistry Division, Joint Nuclear Research Centre, Euratom, Ispra Establishment, Ispra-Varese (Italy)

(Received 20th May 1975)

SUMMARY

Determinations of oxygen in metals by conventional vacuum or inert gas fusion are usually based on the assumption that oxygen is extracted from the melt wholly as carbon monoxyde. A qualitative thermodynamic approach is used to demonstrate that whilst this is true for most metals in the Periodic Table, a significant number of them can yield oxygen partially as gaseous species other than carbon monoxide, so that systematic errors are obtained. Practical suggestions are made to overcome this inconvenience. Vacuum fusion and neutron activation results on different metals are given.

In the conventional vacuum and inert gas fusion methods for the determination of oxygen in metals, the sample is fused in vacuum or in an inert gas stream in a heated graphite crucible with or without a dissolving metal bath or flux, and the oxygen present in various chemical forms is extracted by the well known carbon reduction reaction. The oxygen content is then calculated on the assumption that oxygen has been evolved wholly as carbon monoxide. This is true for most metals; but it is obvious that if the oxygen has been partially evolved as some chemical species other than carbon monoxide, then the analysis will be subject to error.

The problem is not new: Frohberg and Leygraf [1] proved the occurrence of carbon dioxide in the vacuum fusion analysis of copper; Paesold et al. [2] indicated that carbon dioxide is formed in vacuum fusion analyses of easily reducible oxides like CuO and Fe_2O_3, suggested that oxygen is evolved as gaseous suboxides where their occurrence is possible, e.g. in the analysis of silica and alumina. However, recent discussions at a meeting on copper analysis between vacuum and inert gas fusion users, has shown that the point is rather unclear and often neglected. The problem is also barely mentioned in a recent book [3]. It seems useful therefore to establish the theoretical background to the question and to present supporting results obtained during the application of the vacuum fusion method to various metals and compounds.

THEORY

Oxygen is contained in a solid metal as a solution which is in equilibrium with the lowest stable oxide of the oxygen solubility limit has been reached. Because of its relatively low content, oxygen usually goes wholly into solution when the metal is fused either alone or with the help of a dissolving medium. Therefore, in the case of vacuum or inert gas fusion analyses, non-ideal solutions of oxygen in the multi-component homogeneous melt contained in the graphite crucible must be considered, as must the activities of all the components of the melt. For lack of data, this is very difficult to do in most cases.

However, for practical purposes, if one assumes that for any oxygen level, ideal solutions of the lowest stable oxides are present in the melt, then four reaction mechanisms may be postulated; these can account for the errors mentioned above, and provide at least a rough guide for evaluating the possibility of such errors.

The well known carbon reduction can be written as*

$$\frac{1}{m}\mathrm{Me}_n\mathrm{O}_m + \mathrm{C} \rightarrow \frac{n}{m}\mathrm{Me} + (\mathrm{CO}) \qquad (1)$$

the equilibrium constant of which is given by

$$K_1 = \frac{P_{\mathrm{CO}} X_{\mathrm{Me}}^{n/m}}{X_{\mathrm{Ox}}^{1/m} X_{\mathrm{C}}}$$

where Ox refers to $\mathrm{Me}_n\mathrm{O}_m$, P is the partial pressure of a gaseous reactant over the melt, and X is the mole fraction of a solute in the melt.

The other four possible reactions occurring within the melt are as follows.

(A) At the working temperature the metal oxide decomposes. On the assumptions made, the chemical reaction which determines the pressure of oxygen over the melt is

$$\frac{2}{m}\mathrm{Me}_n\mathrm{O}_m \rightarrow \frac{2n}{m}\mathrm{Me} + (\mathrm{O}_2);\ K_2 = \frac{P_{\mathrm{O}_2} X_{\mathrm{Me}}^{2n/m}}{X_{\mathrm{Ox}}^{2/m}} \qquad (2)$$

which combined with reaction (1) gives the equilibrium ratio of oxygen to carbon monoxide over the melt

$$\frac{P_{\mathrm{O}_2}}{P_{\mathrm{CO}}} = \frac{K_2 X_{\mathrm{Ox}}^{1/m}}{K_1 X_{\mathrm{C}} X_{\mathrm{Me}}^{n/m}} \qquad (2')$$

(B) At the working temperature the metal oxide is reduced by carbon monoxide to give carbon dioxide. The equilibrium ratio of carbon dioxide to carbon monoxide over the melt is then determined by

---

*Elements or compounds in the gaseous state are indicated by parentheses; other reactants are in solution.

$$\frac{1}{m}Me_nO_m + (CO) \rightarrow \frac{n}{m}Me + (CO_2); K_3 = \frac{P_{CO_2} X_{Me}^{n/m}}{P_{CO} X_{Ox}^{1/m}} \quad (3)$$

from which

$$\frac{P_{CO_2}}{P_{CO}} = K_3 \cdot \frac{X_{Ox}^{1/m}}{X_{Me}^{n/m}} \quad (3')$$

(C) At the working temperature the metal oxide is volatile

$$Me_nO_m \rightarrow (Me_nO_m); K_4 = \frac{P_{Ox}}{X_{Ox}} \quad (4)$$

Combination of reactions (1) and (4) gives the equilibrium ratio of gaseous Me_nO_m to carbon monoxide over the melt

$$\frac{P_{Ox}}{P_{CO}} = \frac{K_4 X_{Me}^{n/m} X_{Ox}^{(m-1)/m}}{K_1 X_C} \quad (4')$$

(D) At the working temperature, the metal oxide gives a suboxide which is stable only in the gaseous state

$$\frac{1}{m-n}Me_nO_m + C \rightarrow \frac{n}{m-n}(MeO) + (CO); K_5 = \frac{P_{MeO}^{n/(m-n)} P_{CO}}{X_{Ox}^{1/(m-n)} X_C} \quad (5)$$

$$\frac{1}{m-n}Me_nO_m + Me \rightarrow \frac{m}{m-n}(MeO); K_6 = \frac{P_{MeO}^{m/(m-n)}}{X_{Ox}^{1/(m-n)} X_{Me}} \quad (6)$$

$$(MeO) + C \rightarrow Me + (CO); K_7 = \frac{K_5}{K_6} = \frac{P_{CO} X_{Me}}{P_{MeO} X_C} \quad (7)$$

Combination of reactions (5) and (6) or (7) gives the equilibrium ratio of the gaseous suboxide to carbon monoxide over the melt:

$$\frac{P_{MeO}}{P_{CO}} = \frac{K_6 X_{Me}}{K_5 X_C} = \frac{X_{Me}}{K_7 X_C} \quad (5')$$

If X_{Ox} represents the initial mole fraction of the oxide in the melt (which is directly related to the oxygen content of the sample), then eqns. (2')—(5') make it possible to estimate how much oxygen is extracted from the melt as chemical species other than carbon monoxide, provided that the various K and X values are known. It is known that for reactions involving gases and ideal solutions, the standard free energy change equals that involving gases and pure condensed substances [4]; therefore the K values can be calculated by means of the standard free energy changes which would occur if the substances participating in the reactions were pure or gaseous, and these data are readily available [5—7]. The X_C values can be estimated reasonably from the solubility data for carbon in metals [8—10]; the X_{Ox} and X_{Me} values are calculated on the basis of how much oxygen is supposed to be in the metal and how much metal is in the melt. Except for the value given by

eqn. (5′) which is constant, it should be noted that the initial ratios calculated in this way are the highest that can be obtained during degassing of a sample. In practice, X_{Ox} gradually diminishes until it becomes vanishingly small, and X_{Me} and X_C remain ideally unchanged (as the metal here is considered as non-volatile and X_{Me} is always large compared to X_{Ox}, and the carbon consumed is replaced by more carbon dissolved from the crucible).

The alkaline earth metals, Hg, Cd, Zn, Mg, As, Se, Te and Po, have rather high vapour pressures and so cannot be analyzed directly by vacuum or inert gas fusion, but application of the above equations to the other metals of the Periodic Table (up to plutonium and including the rare earth elements) allows the following conclusions to be reached.

(a) The only oxides which could decompose according to reaction (2) under practical fusion conditions are Au_2O_3, Ag_2O and those of the noble metals of the platinum group (in order of increasing stability). However, application of eqn. (2′) shows that when these oxides are contained at any practical oxygen level (considered as an oxygen content lower than 10000 p.p.m.) in the corresponding metals, the ratio of oxygen to carbon monoxide is always very low; thus extraction as gaseous oxygen should be irrelevant compared with that as carbon monoxide.

(b) The oxides which could be reduced, as in reaction (3), by carbon monoxide are Au_2O_3, Ag_2O, oxides of the Pt group, Tl_2O, ReO_3, Bi_2O_3, Cu_2O, PbO, NiO, Sb_2O_3, CoO, GeO_2, SnO_2, In_2O_3, WO_2, FeO, MoO_2 and Ga_2O_3 (roughly in order of increasing stability). Equation (3′) shows that when these oxides are present in the corresponding metals, the ratio of carbon dioxide to carbon monoxide is low for gallium and iron when the oxygen level is less than about 10000 p.p.m.; thus below this level, extraction as carbon dioxide can be considered negligible in comparison with extraction as carbon monoxide. The ratio is also low for cobalt and molybdenum at oxygen levels below 1000 p.p.m.; for nickel and tungsten at levels below 100 p.p.m.; and for In, Pb, Sn, Ge and Cu at levels below 10 p.p.m. For the other metals the ratio is high even at oxygen levels below 10 p.p.m. Therefore, depending on their oxygen content, partial extraction of oxygen as carbon dioxide can be expected from these metals, with the practical exception of iron and gallium.

(c) Oxides which could volatilize (reaction 4) are OsO_4, Sb_2O_3, PbO, B_2O_3, and to a lesser extent TiO and VO (in the order of decreasing volatility). No exact data have been found, but it seems from the literature that Tl_2O and In_2O_3 are also volatile. The application of eqn (4′) shows, nevertheless, that the ratio of gaseous oxide to carbon monoxide for all the oxides mentioned is very low when they are present at any practical oxygen level in the corresponding metals; this may also be true for Tl_2O and In_2O_3. Accordingly, the extraction of oxygen as a gaseous oxide should be irrelevant compared with that as carbon monoxide.

(d) Oxides which could form stable gaseous suboxides are Al_2O_3, GeO_2, SiO_2 and SnO_2, which give AlO, GeO, SiO and SnO, respectively. Equation (5′) shows that the ratio of gaseous suboxide to carbon monoxide can be

relatively high in the analysis of germanium, tin, and especially silicon. Consequently, oxygen may be extracted from these metals as both a gaseous suboxide and carbon monoxide.

These predictions are made on the basis of calculations which take into account fusion conditions such as those mentioned in the relevant literature or which would be approximately utilizable for a determination of oxygen in metals. The conditions were as follows: 1250 °C without bath or flux for Au, Ag, Tl, Bi, Pb, Sb, In, Ga; 1500 °C without bath or flux for Pd, Cu, Ni, Co, Ge, Sn, Fe, Si; 1500 °C with a platinum bath for silicon; 1500 °C with a platinum-tin bath for copper; and 1900 °C with a platinum bath for the metals of the platinum group excluding palladium and for Re, W, Mo, B, Ti, V, Al.*

The use of "absolutely correct" fusion conditions would be of little significance, as the conclusions reached are qualitative in nature and must be considered as only explanatory and indicative of possible behaviour. Not only were ideal laws used, but the extrapolations to high temperatures sometimes made in calculating the K values may not be wholly valid; moreover, in some cases there is uncertainty in the literature either about the chemical formulae of the lowest stable oxides or about the carbon solubilities. For instance, germanium and tin are expected to give considerable amounts of gaseous suboxide mainly because their carbon solubilities have been estimated as exceedingly small [8, 9]; if their carbon solubilities were even as high as the low value given for silicon (X_C in silicon at 1500 °C $\simeq 5 \cdot 10^{-4}$ [9]), the calculated amount of gaseous suboxide would become small. The qualitative nature of this thermodynamic approach together with the lack of data on the solubility of carbides in platinum, are in fact the main reasons why the formation of carbides in the melt has not been taken into account for stable carbide formers, such as W, Mo, B, Ti, V, Al and Si.

If an oxide does not dissolve in the melt but is only dispersed in it, ($X_{Ox} = 1$ which represents the most unfavourable case), then on the basis of the equations given, an increased ratio of carbon dioxide to carbon monoxide would be expected, though the other ratios should remain very low or unchanged.

On the basis of the stability of the lowest oxides, no metal other than those mentioned under (a) should give oxygen as the chemical species other than carbon monoxide when analyzed under practical vacuum or inert gas fusion conditions, even if its oxide is insoluble in the melt. A possible exception could be technetium, for which the necessary data, although scarce, seem to indicate the occurrence of large amounts of carbon dioxide.

A more in-depth examination of the problem allows other conclusions to be reached. Although the ratios so far calculated do not take kinetic factors and their implications into account, they are "equilibrium" ratios; it is assumed that there is a homogeneous distribution of the components in the

*For the metals of the Pt group and for Re, W, Mo, B, Ti, V, Al a concentration of either 1% or 10% weight of sample metal in the bath was assumed. For Si and Cu see Table 1.

melt, and that the amount of carbon present equals its solubility. If such conditions are not fulfilled, the ratios may alter. X_C must be considered as the carbon dissolved "within" the melt; at the boundary between the melt and the crucible, X_C can be assumed to be unity, and the effect of reactions at the boundary should be to decrease the ratios, with the exception of CO_2/CO (eqns. 2′—5′).

If the working conditions are such that several samples can be degassed in the same crucible, the later samples will drop into a larger oxygen-free melt; the dilution should diminish X_{Ox} in the melt and consequently the ratio CO_2/CO (eqn. 3′). However, the ratio of gaseous suboxide to carbon monoxide should either remain unchanged when no bath metal is used ($X_{Me} \simeq 1$ and X_C constant) or increase when a bath metal is used (X_C constant and X_{Me} increases, cf. eqn. 5′).

After the extracted oxygen-bearing gases have left the melt, they come in contact with the hot walls of the graphite crucible where they tend to form carbon monoxide, depending on their quantity, the temperature, the contact time, and the surface area and volume of the crucible, i.e. depending on the working conditions and the instrument used.

For all the reasons given above, the actual ratios could be substantially different from those calculated: it must be emphasized again that the theory given should be considered mainly from the standpoint of the explanations which it provides. However, ideal solutions of oxides behave qualitatively like actual oxygen solutions; for example the lower the oxide content of an ideal metal-oxide solution, the higher is its stability (eqns. 1—6), and the same tendency is invariably shown by actual oxygen-metal solutions. Accordingly, there is no doubt that the theory supplies qualitatively correct results. The results suggest a list of metals which should be tested under various fusion conditions and possibly by an independent method of analysis, before an oxygen content determined on the basis of the carbon monoxide extracted can be accepted without reservation.

Apart from the use of instruments which can measure both the carbon monoxide and at least the carbon dioxide which may be evolved from these metals, a practical device which should help in obtaining only carbon monoxide is the enclosure of samples in graphite capsules which are then firmly closed and dropped into the hot crucible of the instrument: under these conditions the oxygen-bearing gases evolved from the metal are forced to react with the carbon of the capsule to give carbon monoxide [1]. With the inert gas fusion method, especially, the same goal could be achieved by placing hot (ca. 1000 °C) carbon granules in the line carrying the gases from the furnace to the analyzer.

Another possibility would be to use a fusion bath metal which gave an oxide reducible under the fusion conditions but more stable than the oxides of the metals being analyzed; in the melt, the less stable oxide must be converted to the most stable one. Of the metals usually employed as bath materials, viz. Pd, Pt, Fe, Co, Ni and Sn, iron should be the most satisfactory

from this standpoint (see (b)). Unfortunately, the introduction of a sample with a low solubility for carbon into a carbon-rich bath like that of iron, can ruin the bath because of graphite precipitation [10]. Therefore, less carbon-rich baths like Fe/Sn or perhaps galium should be used for metals having a low carbon solubility (Au, Ag, Tl, Bi, Cu, Pb, Sb, Ge, Sn, In; not Si, the oxide of which is very stable). No data for the solubility of carbon in gallium seem to be available, but it is probably small by analogy with aluminium.

As an example of the calculations made, Table 1 presents the percentage of the oxygen extracted as carbon monoxide from three different metals, computed on the basis of various fusion parameters.

EXPERIMENTAL RESULTS

Table 2 presents the results obtained on different materials and Table 3 summarizes the working conditions employed. The results were not obtained expressly for the present work, but were accumulated over a period of years, by the fortuitous application of the vacuum fusion method to the metals under discussion. The theory has been developed to explain the abnormal results.

The vacuum fusion values are divided into two groups: those obtained by the conventional technique, which consists of degassing the sample after it has been dropped into the crucible of the instrument with or without a bath metal; and those obtained by the graphite capsule technique [12] which may well serve as a reference. Whenever possible, the vacuum fusion results were verified by an independent neutron activation method of analysis.

Two commercial vacuum fusion instruments were employed: the Feichtinger St Re 0583 (H. Feichtinger, Schaffhausen, Switzerland) [13] and the Heraeus VH 6 (W. C. Heraeus GmbH, Hanau/Main, Germany) [14]. Both instruments accumulate the analyzed samples in unlidded graphite crucibles; for the determination of the extracted gases, both use gas chromatographs with an argon or helium carrier gas, a molecular sieve column and thermal conductivity detection). The molecular sieve column allows the elution, and thus the detection, of only hydrogen, oxygen, nitrogen, methane and carbon monoxide, so that any other oxygen-bearing gas possibly evolved from the melt is not measured.

The vacuum fusion results shown in Table 2 are based only on the carbon monoxide evolved and require comment. At the oxygen levels encountered, the results by the conventional technique for Cu1, Ni, Mo, W, Ti agree with those obtained by the graphite capsule technique or by activation analysis. For Cu2, Cu3, Cu4 and NiO, only the results by the graphite capsule technique agree with those obtained by activation analysis or with the theoretical value; the results for the conventional method show that some oxygen has not been accounted for. However, the results for CuO show that the graphite capsules may sometimes fail: this oxide probably begins to be reduced or decomposed to Cu_2O at a temperature well below that of the

TABLE 1

Calculated percentages of oxygen extracted as carbon monoxide

System[a]	*0 in metal (p.p.m. weight)*	X_{Ox}	P_{CO_2}/P_{CO}	*% 0 as CO in gas*
$Cu—Cu_2O$	1000	$3.97 \cdot 10^{-3}$	$6.85 \cdot 10^{-1}$	42.2
1500 °C — no bath	200	$7.94 \cdot 10^{-4}$	$1.37 \cdot 10^{-1}$	78.5
$X_{Cu} \simeq 1$[b]	100	$3.97 \cdot 10^{-4}$	$6.85 \cdot 10^{-2}$	87.9
$K_3 \simeq 1.73 \cdot 10^2$	10	$3.97 \cdot 10^{-5}$	$6.85 \cdot 10^{-3}$	98.6
$Cu—Cu_2O$	1000	$2.48 \cdot 10^{-4}$	$1.27 \cdot 10^{-1}$	79.8
1500 °C — Pt/Sn(20%) bath[c]	200	$4.97 \cdot 10^{-5}$	$5.67 \cdot 10^{-2}$	89.8
$X_{Cu} \simeq 0.125$	100	$2.48 \cdot 10^{-5}$	$4.01 \cdot 10^{-2}$	92.6
$X_{Sn} \simeq 0.254$				
$X_{Pt} \simeq 0.619$				
$K_3 \simeq 4.06$				
Ni—NiO	1000	$3.23 \cdot 10^{-3}$	$1.32 \cdot 10^{-1}$	79.0
1500 °C — no bath	300	$9.69 \cdot 10^{-4}$	$3.98 \cdot 10^{-2}$	92.6
$X_{Ni} \cdot \simeq 0.88$[b]	100	$3.23 \cdot 10^{-4}$	$1.32 \cdot 10^{-2}$	97.4
$K_3 \simeq 3.61 \cdot 10^1$	10	$3.23 \cdot 10^{-5}$	$1.32 \cdot 10^{-3}$	99.7
System[a]	*0 in metal*	X_{Ox}	P_{SiO}/P_{Co}	*% 0 as CO in gas*
$Si—SiO_2$				
1500 °C — no bath				
$X_{Si} \simeq 1$	Independent	Independent	$2.43 \cdot 10^2$	0.4
$X_C \simeq 5 \cdot 10^{-4}$				
$K_6/K_5 \simeq 1.21 \cdot 10^{-1}$				
$Si—SiO_2$				
1500 °C — Pt bath or flux[d]				
$X_{Si} \simeq 0.62$				
$X_{Pt} \simeq 0.32$	Independent	Independent	1.25	44.4
$X_C \simeq 0.06$				
$K_6/K_5 \simeq 1.21 \cdot 10^{-1}$				

[a] X_C values from refs. 8—10; K values from ref. 6.

[b] In a graphite crucible, copper does not dissolve carbon to a great extent [8]: $X_C \simeq 2.6 \cdot 10^{-5}$, but nickel dissolves large amounts of carbon [9]: $X_C \simeq 0.12$.

[c] Corresponds to a melt composed of 5 parts of Cu in 95 parts of a bath initially made of 80% Pt and 20% Sn. The calculations were made on the assumption that Cu_2O is wholly transformed into the more stable SnO_2, which, on the basis of ideal laws, is reasonably correct. On the basis of earlier data [10], it was assumed that the C content of the melt exceeds 0.01 % weight: with such an amount of C a very low ratio of gaseous suboxide to carbon monoxide is expected.

[d] Corresponds to a melt composed of 40 parts of Si, 140 parts of Pt, and 1.7 parts of C; the amount of C was estimated from the solubility of carbon in Pt.

TABLE 2

Results obtained on different materials (expressed as p.p.m. of oxygen unless otherwise indicated). In columns 2—4, the numbers in parentheses indicate the standard deviation and the number of determinations involved

Sample[a]	Heraeus[b, c]		Feichtinger[b, c]		N.a.a.[d] or theor.
	Conventional $S \simeq 14.5$ cm^2 $V \simeq 4.5$ cm^3	Graphite capsule	Conventional $S \simeq 37$ cm^2 $V \simeq 19$ cm^3	Graphite capsule	
Cu 1			2.8 (1.0, 12)		2.3 (3)
Cu 2		72.8 (5.1, 12)	62.3 (1.9, 4)	73.6 (2.4, 4)	71.2 (4)
Cu 3			150.1 (2.5, 4)	202.6 (4.5, 4)	187.0 (1)
Cu 4				136.0 (4.0, 18)	140.0 (5)
CuO				12.26 % (1, 3)	20.12 % (theor.)
Ni			325.2 (8.1, 4)	331.7 (46, 3)	
NiO			15.05 % (1.6, 6)	20.84 % (0.9, 6)	21.42 % (theor.)
Mo			12.8 (1.8, 6)		10.9 (1)
W			5.6 (1.5, 7)		3.6 (3)
Ti			823 (30, 8)		850.5 (3)
Zr			1173 (29, 18)		1188 (5)
Si 1		9625 (1190, 2)	1710 (385, 2)	8815 (155, 2)	
Si 2		2800 (220, 2)	405 (12, 2)	2890 (20, 2)	
SiC 1	2760 (340, 2)	5285 (50, 2)	5240 (55, 2)	5115 (95, 2)	5255 (1)
SiC 2	1765 (40, 2)	3825 (7, 2)	4065 (135, 2)	3885 (15, 2)	4670 (1)
Si_3N_4		7085 (465, 2)	7580 (855, 5)		

[a]Cu, Ni, Mo, W, Ti and Zr: massive samples, unalloyed, surface polished before analysis. Cu2: copper deoxidized with P. CuO and NiO: powdered samples, calcined at 800 °C before analysis.
Si, SiC and Si_3N_4; powdered samples, analyzed on "as received" basis.
[b]S and V indicate the inner surface area and the inner volume of the crucible used in the conventional technique.
[c]Although of little statistical significance, the standard deviation (s) is also given for a small number of determinations (n), to obtain a more thorough comparison of the results.
[d]The numbers in parentheses indicate the numbers of laboratories participating in the neutron activation analyses.

TABLE 3

Summary of the vacuum fusion working conditions

Sample	Working conditions[a]	Remarks
Cu	Conventional: 1550 °C — Pt/Sn(20 %) bath Capsule: 1450 °C	Both techniques: samples (0.9—1 g Cu1 and Cu4; 0.4—0.5 g Cu2 and Cu3) not fluxed
CuO	Capsule: 1450 °C — Pt/Cu flux	Samples (0.3—0.8 mg) wrapped in about 65 mg of Pt foil and sealed into the capsules together with 0.5—1 g of pre-degassed copper. Copper added to fuse the whole content of the capsule at the operating temperature
Ni	Conventional[b]: 1800 °C — Pt bath (2 detn) 1500 °C — Ni bath (2 detn) Capsule: 1550 °C	Both techniques: samples (about 0.15 g conventional; 0.15—0.45 g capsule) not fluxed
NiO	Conventional[b]: 1800 °C — Pt flux (2 detn) 1650 °C — Ni bath + Pt flux (2 detn) 1550 °C — Pt/Sn(20 %) bath + Pt flux (2 detn) Capsule: 1450 °C—Pt/Cu flux	Conventional: samples (0.3—0.8 mg) wrapped in about 65 mg of Pt foil Capsule: as CuO
Mo, W	Conventional: 1900 °C — Pt bath	Samples (about 0.5 g Mo; 0.9 g W) not fluxed
Ti, Zr	Conventional: 1900 °C — Pt bath + Pt flux	Samples (about 0.17 g) wrapped in Pt foil at a weight ratio of Pt/sample of about 3
Si	Conventional: 1500 °C — Pt flux Capsule: 1500 °C — Pt flux	Conventional: samples (30—50 mg) wrapped in about 130 mg of Pt/foil. Capsule: Samples (15—30 mg Heraeus; 30—50 Feichtinger) sealed into the capsule after having been wrapped in about 130 mg of Pt foil
SiC	Conventional: 1800 °C — Pt flux (Feichtinger) 1700 °C with some surges to 1850—1900 °C to speed the degassing — Pt flux (Heraeus) Capsule: 1800 °C — Pt flux (Feichtinger) 1700 °C with some surges to 1850—1900 °C to speed the degassing — Pt flux (Heraeus)	Both techniques: as Si, except for sample weight (30—50 mg everywhere)
Si_3N_4	Conventional: samples introduced at 1500 °C to avoid sprays of material; temperature slowly increased to the working value of 1850 °C — Pt flux Capsule: 1800 °C with some surges to 1900 °C to speed the degassing — Pt flux	Both techniques: as Si, except for sample weight (6—10 mg everywhere)

[a]Bath technique: the sample is dropped in the crucible which contains a degassed bath metal. Flux technique: the sample is dropped in the crucible or sealed into the capsule together with a flux metal at the weight ratio flux/sample indicated.
Unless otherwise indicated the temperature of introduction into the crucible corresponds to the working temperature.
[b]Because of their consistency, the results are grouped together in Table 2.

complete conversion of oxygen and carbon dioxide to carbon monoxide, during the unavoidable progressive heating of the capsule in the crucible.

Silicon and silicon compounds behave differently. At least with the Feichtinger instrument, the conventional technique applied to silicon compounds showed no sign of failure compared with the graphite capsule technique or activation analysis; the low values obtained conventionally with the Heraeus instrument are probably due largely to the smaller heating element. For silicon, the results are also low with the conventional Feichtinger method: this could be explained by the fact that X_{Si} is high in silicon but low in the silicon compounds, and the effect would be to increase the P_{SiO}/P_{CO} ratio (eqn. 5′). Zirconium is included in the Table only as a representative of the metals which should not give trouble.

It seems worth mentioning that replicate analyses by the conventional technique of massive samples of palladium and platinum have never shown evolution of molecular oxygen from the melt.

The results presented appear to be in good qualitative agreement with theory, but it must be emphasized that the results obtained conventionally were sometimes dependent on the instrument and on the working conditions used. The pumping speed, carrier flow rate, temperature and dimensions of the crucible, etc., can influence to some extent the efficiency of the reaction with the crucible walls, i.e. the conversion to carbon monoxide of the equilibrium gases which have left the melt.

The author thanks Messrs. E. Rodari and R. Vivian, Chemistry Division, JRC Ispra, who performed the vacuum fusion analyses. Most of the results as well as the neutron activation results, were obtained during a programme on the assay of oxygen in non-ferrous metals (Eurisotop Office, Brussels) coordinated by Dr. J. Pauwels, whose permission to use the neutron activation results is gratefully acknowledged.

REFERENCES

1 M. G. Frohberg and H. Leygraf, Critical Investigation for Oxygen Analysis of Copper by the Vacuum Fusion Method, Balzers High Vacuum Report, No. 8, January, 1967.
2 G. Paesold, K. Müller and R. Kieffer, Z. Anal. Chem., 232 (1967) 31.
3 L. M. Meluick, L. L. Lewis and B. D. Holt, Determination of Gaseous Elements in Metals, J. Wiley, New York, 1974.
4 J. D. Fast, Interaction of Metals and Gases, Philips, Eindhoven, 1965.
5 O. Kubaschewski and E. Ll. Evans, Metallurgical Thermochemistry, Pergamon, Oxford, 1958.
6 Z. M. Turovtseva and L. L. Kunin, Analysis of Gases in Metals, Consultants Bureau, New York, 1961.
7 C. J. Smithellis, Metals Reference Book, Butterworths, London, 1962.
8 M. Hansen, Constitution of Binary Alloys, McGraw-Hill, 2nd ed., 1958.
9 P. E. Rodney, Constitution of Binary Alloys, 1st Supplement, McGraw-Hill, 1965.
10 F. A. Shunk, Constitution of Binary Alloys, 2nd Supplement, McGraw-Hill, 1969.
11 R. W. Ashley and T. H. Longhurst, AECL 3743, November, 1970.
12 A. Colombo, R. Vivian and E. Rodari, Anal. Chim. Acta, 62 (1972) 472.
13 H. Feichtinger, H. Bächtold and W. Schuhknecht, Schweiz. Arch., 12 (1959) 426.
14 R. Lesser and H. Gruber, Z. Metallk., 51 (1960) 495.

Analytica Chimica Acta, 81 (1976) 409—411

Short communication

COMPARATIVE ANALYSIS FOR BORON IN STEEL BY ION MICROPROBE MASS ANALYZER AND THE NUCLEAR TRACK TECHNIQUE

B. STEPHEN CARPENTER and ROBERT L. MYKLEBUST

Analytical Chemistry Division, National Bureau of Standards, Washington, D.C. 20234 (U.S.A.)

(Received 11th June 1975)

This work describes the analytical capabilities of the NBS Ion Microprobe Mass Analyzer for determining trace concentrations of boron in a steel matrix. In addition, the boron concentration values obtained in this way are compared with those obtained by the Nuclear Track Technique, in which the boron concentration and distribution are determined by counting the alpha tracks produced by the nuclear reaction $^{10}B(n, \alpha)^{7}Li$ in plastic solid-state recorders [1]. Both methods are surface, or limited depth, microtechniques that perform analyses through interaction with individual atoms; thus, comparison of the results from both methods is useful in revealing the spatial homogeneity of the boron in the steels.

Experimental

National Bureau of Standards Standard Reference Material (SRM) steels 661, 662, 663, 664, and 665, were used. The certified boron concentrations in these steels range from 1.3 to 111.0 p.p.m.

The steel SRM's in the form of rods, 3.2 mm in diameter and 51 mm long, were cut, mounted with epoxy resin in 2.54-cm rings, metallographically polished and carbon-coated for ion microprobe mass analysis. The instrument used for this study bombards the specimen with a focused beam (ca. 2 μm diameter) of high-energy ions. A mass analyser permits the selection of a single ionic species in the primary ion beam. Those ions impinging on the specimen cause atoms at the specimen surface to be removed by sputtering. A fraction of the sputtered atoms leaves the specimen surface as ions which are separated for analysis in a double-focusing mass spectrometer [2]. The analysis was performed with two different gases for the incident ion beam; $^{16}O_2^+$ and $^{14}N_2^+$. In both cases, the ion-accelerating voltage was 20 kV. The ion beams were focused in such a way that the beam was scanned over an area of 120 μm × 80 μm on the sample surface. After a mass scan of the steel (from mass 1 to 150) to check for possible interferences in the $^{11}B^+$ region, the secondary mass analyzer was set on the $^{11}B^+$ peak and the surface was

ion-etched for 30 min with either $^{16}O_2^+$ or $^{14}N_2^+$ to remove any possible surface contamination. Counts at the $^{11}B^+$ peak position were then collected over 20-s intervals many times in order to obtain adequate counting statistics. During the counting period, the sample current was also recorded. This procedure was repeated over different areas of the surface of each steel with both the $^{16}O_2^+$ and $^{14}N_2^+$ ion beams.

For analysis by the nuclear track technique, pieces of the steel rods were mounted in epoxy resin, polished and fixed to cellulose acetate butyrate (CAB) detectors. Then the combination of epoxy mount and CAB detector was placed in a polyethylene bag and heat-sealed under vacuum. The combination was then irradiated in the National Bureau of Standards Research Reactor, for 10 s in a thermal flux of $1.33 \cdot 10^{13}$ ncm^{-2} s^{-1}, along with a standard of known boron concentration. After irradiation, the detectors were separated from the mounted samples and chemically etched in 6.5 M NaOH at 70 °C for 8 min, then rinsed with water and air-dried. The alpha tracks from the nuclear reaction $^{10}B(n, \alpha)^7Li$ produced in the CAB detectors during irradiation were then counted in the etched detector with the aid of an optical microscope [1]. In order to determine the boron concentration in each of the five steels, their track densities were compared with the track density obtained from the standard (SRM 612) whose boron concentration was known.

Results and Discussion

Figure 1 was constructed from a least-squares analysis of the results obtained from the two independent analyses of the steels. These results show the linear relationship that can be obtained with between the two techniques. Although it was possible to obtain this linear relationship, severe boron inhomogeneity was observed in SRM 664 by both procedures. The white regions in the scanning ion micrograph shown in Fig. 2(a) indicate a typical boron distribution. A similar distribution of clusters of tracks was observed by α-track micro-mapping of SRM 664 (Fig. 2b). The remainder of the steels, SRM 661, 662, 663, and 665, showed a more uniform and homogeneous boron distribution. In addition to the scanning ion micrograph, a mass scan of a boron inclusion was made; in addition to boron, the principal constituents were Nb, Zr, Mo, V, Cr, and Ti.

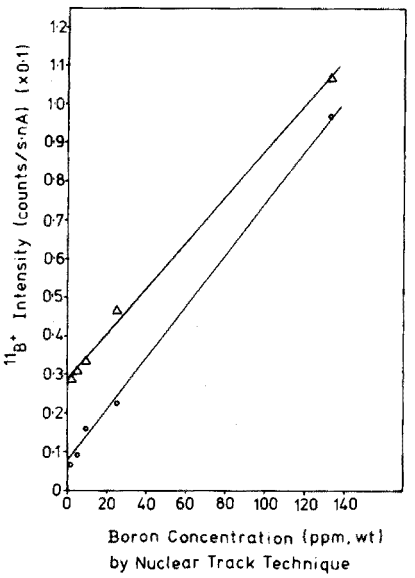

Fig. 1. Intensities of the $^{11}B^+$ signal obtained by the ion microprobe mass analyzer as a function of the boron concentration determined by the nuclear track technique. (△)$^{14}N_2^+$ source. (○)$^{16}O_2^+$ source.

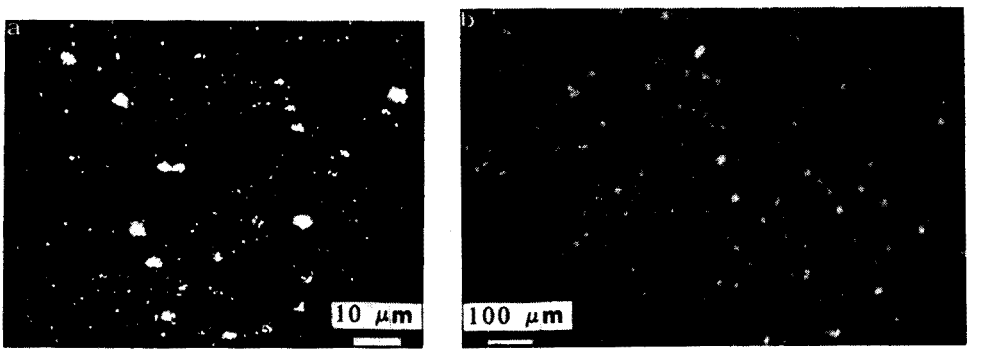

Fig. 2. Boron distributions in microscopic regions of SRM 664, by (a) the ion microprobe mass analyzer, and (b) the nuclear track technique.

REFERENCES

1 B. S. Carpenter, Microscope, 20 (1972) 175.
2 C. F. Robinson, Microprobe Analysis, in C. A. Anderson, (Ed.) Wiley, New York, 1973 p. 507.

Analytica Chimica Acta, 81 (1976) 413—417

Short communication

A MODULAR SYSTEM FOR ELECTROPLATING ALPHA NUCLIDES

R. L. FOREMAN, G. J. PARKS, JR. and V. F. HODGE

Mt. Soledad Laboratory for Marine Radioactivity Studies, Scripps Institution of Oceanography, La Jolla, California 92037 (U.S.A.)

(Received 7th July 1975)

Because of increased interest in the behavior of α-emitting nuclides, such as plutonium, in the marine environment, 12 α-counters were installed at the Mt. Soledad Laboratory of Scripps Institution of Oceanography. Thus, a system for electroplating large numbers of samples was required. Because of the very low activity levels of most environmental samples, cross-contamination had to be completely eliminated. Further, experience has shown that electrodeposition with constant cell current gives excellent and reproducible recoveries [1]. Therefore, a modular system was devised to plate eight samples simultaneously in semidisposable cells each having an independent, constant-current power source.

Plating cell

Cross-contamination was controlled by insuring that all parts of the plating cell (Fig. 1) that came in contact with the sample were either disposable or easily cleaned in hot 8 M nitric acid. Disposable liquid scintillation vials of linear polyethylene (Amersham-Searle no. 3327) [1] were found to be suitable containers, and the design was centered around these vials although the basic concept could be modified to accept samples of larger volume.

The bottom of each vial is quickly and neatly pared off with a "hot-wire" cutter. The length from vial neck to the cut is kept uniform to facilitate reproducible placement of the anode 4 mm from the planchet (cathode). Plutonium, americium, polonium, and uranium are normally plated onto 0.75 in. stainless steel planchets. This size matches the diameter of the sealing lip on the vials. A stainless steel contact provides electrical connection between the banana plug and the planchet and helps insure that, when the plastic vial cap that has had a hole drilled in it is slipped over the contact and tightened, the planchet will be flat against the vial lip assuring a liquid-tight seal. The cell cover (Teflon) serves as the anode holder and is vented to allow any generated gases to escape. Because the vials are cut to uniform length, the anode to cathode distance need be set only once.

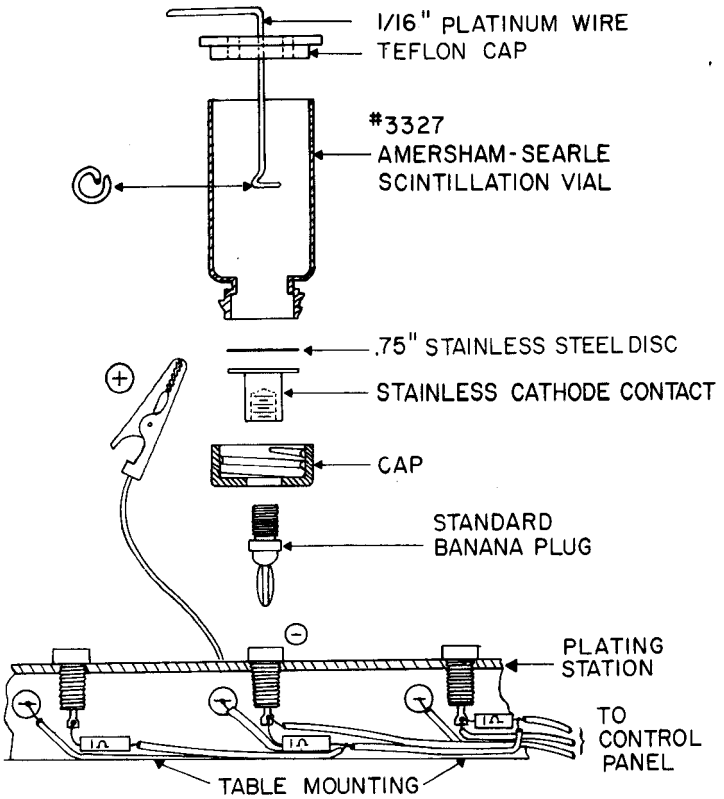

Fig. 1. Details of plating cell assembly (after Talvitie [1]).

Plating Station

The plating station (Fig. 1) is constructed of 1 in. × 1 in. × 1/8 in. anodized aluminum channel. Pairs of female banana plugs are set perpendicular to each other on 2-in. centers along the length of channel. (An eight-station assembly is about 17 in. long). A 2-in. wide lucite strip above the channel has 1.1-in. holes centered above each pair of plugs and serves to guide the cells into their sockets and support them vertically. The anodes are connected by a short lead with an alligator clip on one end. The power leads and current-sense resistors are routed under the channel into a 17-lead cable that plugs into the constant-current power supply. The cable is about 4 ft. long so that the plating station can be placed inside a hood during the plating operation.

Circuit function

Figure 2 shows details of one element of the power supply which supplies

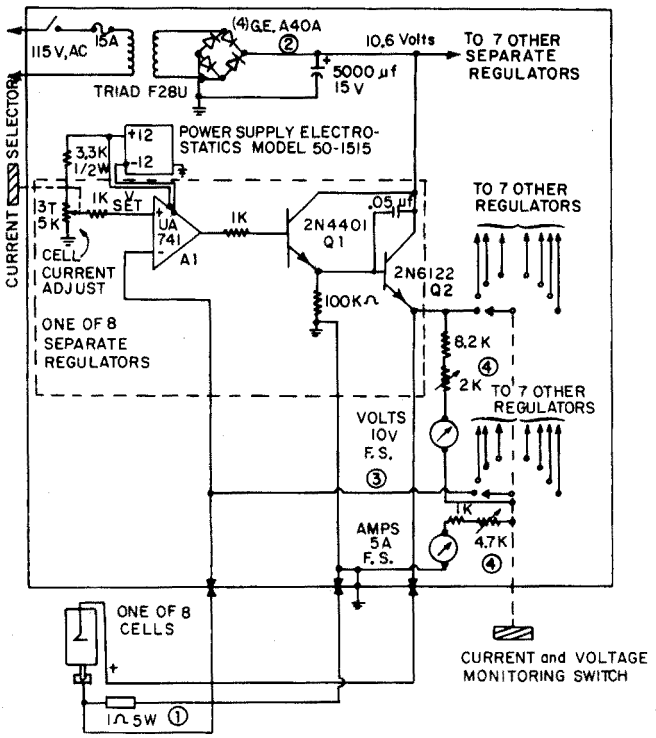

Fig. 2. Eight-channel constant current supply. (1) Reference resistor placed at cell to eliminate line IR drop error. $I_{cell} = V_{set}/R_{ref}$. (2) F28U rated at 25 A at 7.5 V. Voltage limitation of $\sim$ 8 V ($10.6 - V_{ce}$) may necessitate cell conductivity adjustment by carrier addition, i.e., NH_4OH. (3) 1-mA meters were used resulting in 0.1 % metering loss error. Lower current meters may be used to reduce error. (4) Trimming potentiometers were used to calibrate meters. Note: All resistors are 1/4 W carbon composition unless otherwise noted. I_{cell} regulation = ±2 % for a change in R_{cell} of 60 % at I_{cell} = 1 A. I_{cell} maximum = 1.6 A with 8 cells operating.

and independently regulates current for eight separate cells. Transistors Q_1 and Q_2 are inside a feed-back loop closed by the cell and 1-ohm reference resistor. Current flows through the reference resistor, which is in series with the cell, producing a voltage proportional to the cell current. An op-amp (A_1) senses the voltage and compares it to a pre-set voltage, controlled by a 3/4-turn variable resistor on the front panel. In operation, the cell current, normally 1-1.1 A, is set by the front panel control while viewing the current meter. Upon a change in cell conductivity, an error voltage is produced at the op-amp input equal to the set voltage minus the reference voltage. The op-amp output voltage then changes in a direction to return the error voltage to zero which is the balance state for the current desired. R_{ref} is physically located at the cell to eliminate error from supply wire voltage drop. A sense wire is returned to the power supply from R_{ref} which carries currents in the μA

range. The metering arrangement was chosen because it simplifies the switching necessary for current and voltage monitoring. The error associated with monitoring (with 1-mA meters) can be neglected. If cell potentials larger than 8 V are required, the power transformer has to be changed. The power supply for the op-amps was an Electrostatics Model 50-1515.

Hot-wire cutter accessory

The hot-wire cutter (Fig. 3) cleanly cuts the bottoms off the vials and maintains a uniform length between the vial lip and cut. A 0.020-in. piano wire is stretched between two ceramic insulators on an aluminum bar. This bar in turn is pivoted from a 1-in. thick block of PVC with a U-shaped slot cut in it to cradle the vials. An adjustable stop is mounted behind the vial holder to set the length precisely. Two power leads are connected to the ends of the taut wire and lead to a low-voltage a.c. power supply in the small chassis box beneath.

Operation

The required number of vials are first cut to length with the hot-wire cutter. The cells are then assembled with new stainless steel planchets that

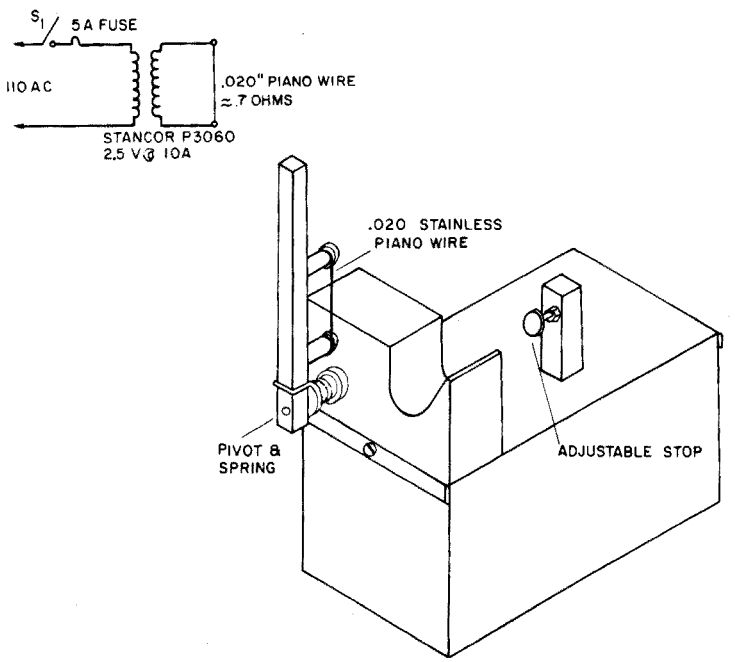

Fig. 3. Accessory for cutting off plastic vials at uniform lengths.

have been thoroughly cleaned with acetone. (Note: Only one set of the plastic vial caps with holes are needed as they do not come in contact with the samples and are easily washed between platings.) The assembled cells are then placed in a rack and filled with the sample solutions. A final check of pH is made on each sample and pH is adjusted as required. The cell caps (anodes) are pressed onto the vials, and the complete cells then transferred to the plating station. The alligator clips are attached to the platinum anode wires taking care that the clips are not over one of the vent holes as corrosive gases are evolved. After all the cells are connected, the plating station is transferred to a fume hood and the current for each cell is set as required [2].

Conclusion

The modular plating system streamlines the preparation of large numbers of samples and improves the reproducibility of the electrodeposition process. This approach was found to be relatively economical and one which could be easily expanded as the need arises. The design was kept simple and functional and appears to be quite reliable after one year of operation (approximately 1200 samples).

This work was supported by the U.S. Atomic Energy Commission and the U.S. Office of Naval Research.

REFERENCES

1 N. A. Talvitie, Anal. Chem., 44 (1972) 280.
2 V. F. Hodge and M. E. Gurney, Anal. Chem., (1975) in press.

Analytic Chimica Acta, 81 (1976) 419—422

Short communication

SOLVENT EXTRACTION OF PHOSPHONIUM SALTS AND THEIR ANALYTICAL APPLICATIONS PART VI — SEPARATION AND SPECTROPHOTOMETRIC DETERMINATION OF HEXACYANOFERRATE(III)*

PASCHOAL SENISE and RUTH LEME DE OLIVEIRA
Instituto de Química da Universidade de São Paulo, São Paulo (Brazil)
(Received 11th June 1975)

Systematic studies of the extractability of phosphonium salts of metal cyano complexes showed that hexacyanoferrate(III) can be extracted efficiently into butanol and pentanol from solutions containing either triphenyl-n-propylphosphonium or triphenylisopropylphosphonium ions, whereas hexacyanoferrate(II) is extracted only very slightly or not at all. These results gave the basis of a method for the determination of hexacyanoferrate(III) and its separation from cyanoferrate(II). Hexacyanoferrate(III) is usually determined via its oxidizing power, and the procedures available (mostly titrimetric) are suitable only for relatively large amounts. Semimicro and microanalytical methods are scarce and apparently subject to many more limitations [2, 3] than the spectrophotometric method described below.

Experimental

Apparatus. A Zeiss PMQ II spectrophotometer and 10-mm Corex stoppered cells were used.

Standard hexacyanoferrate(III) solution. A stock aqueous solution of potassium hexacyanoferrate(III) containing 0.98 mg $Fe(CN)_6^{3-}$ ml^{-1} was standardized iodimetrically in the presence of zinc(II) [4]. Working solutions obtained by dilution of the stock solution were kept in darkness, and were stable for several months.

Working conditions. Preliminary experiments with various solvents showed that butanol and pentanol were the most efficient and selective extractants. Traces of cyanoferrate(II) were removed from the aqueous phase by butanols; pentan-l-ol was therefore chosen. Triphenyl-n- propyl- and triphenylisopropylphosphonium gave the same results; the former was chosen because of the higher solubility of the corresponding chloride.

These experiments were performed under different pH conditions; the best results were obtained in the pH range 1.5—2.5 when 0.5 M sulfuric acid

* Ref. 1.

was used. The use of hydrochloric acid was avoided because large amounts of chloride interfered and led to low results. The volume of the aqueous solution could vary from 1 to 3 ml without affecting the results, provided the phosphonium ion concentration was kept constant.

Spectral characteristics and calibration curve. The absorption spectrum of the yellow extract showed a well-defined maximum at 420 nm (Fig. 1, curve a). The system obeyed Beer's law up to 200 μg ml^{-1} and a Ringbom plot showed the optimum concentration of hexacyanoferrate(III) to be 40—160 μg ml^{-1} in the final dilution.

The yellow extract was stable when kept in darkness; absorbance values were reproducible for at least 7 days.

Extraction efficiency. The distribution coefficient was estimated by extracting 2.0 ml of the aqueous solution (pH 2) with 2.0 ml of pentan-l-ol. Over the range 100—1000 μg, 97.5% of the hexacyanoferrate(III) was extracted in a single pass, and considerably smaller amounts were also extracted quantitatively.

Sensitivity improvement. The sensitivity of the method was increased about ten times when the extracted hexacyanoferrate(III) was allowed to react directly in the organic phase with iron(II) ions, by homogenizing with ethyleneglycol. The absorption spectrum of the blue colored medium showed maximum absorbance at 720 nm (Fig. 1, curve b). Beer's law applied up to 18 μg ml^{-1}, and a Ringbom plot showed the optimum concentration range

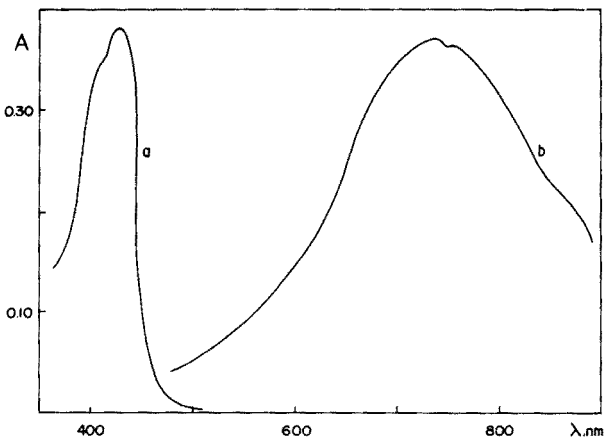

Fig. 1. Absorption spectra: (a) hexacyanoferrate (III) in pentan-l-ol after extraction from aqueous solutions containing triphenyl-n-propylphosphonium ions (76.4 μg $Fe(CN)_6^{3-}$ ml^{-1}); (b) hexacyanoferrate(III) pentan-l-ol plus ethyleneglycol after extraction from aqueous solution containing triphenyl-n-propylphosphonium and further addition of iron(II) sulfate to the organic extract (9.5 μg $Fe(CN)_6^{3-}$ml^{-1}).

to be 4—18 $\mu g\ ml^{-1}$. in the final dilution (20—90 $\mu g\ ml^{-1}$ in the original aqueous solution). The color stability was considerably lower than in the absence of iron(II), and decreased with increased concentration of hexacyanoferrate(III). However, the absorbances of solutions containing the largest amount of hexacyanoferrate(III) studied were reproducible for 1.5 h.

The effect of hexacyanoferrate(II). Hexacyanoferrate(II) in acidic medium is easily oxidized to hexacyanoferrate(III), which appeared in the organic phase obtained by shaking aqueous solutions containing relatively large amounts of hexacyanoferrate(II) acidified with sulfuric acid (pH 1.5—2.5), with pentan-1-ol; the amount of hexacyanoferrate(III) in the organic layer increased with increased time of standing of the aqueous acidic solution of hexacyanoferrate(II) before extraction. These experiments were run with 10000 $\mu g\ Fe(CN)_6^{4-}$, and solutions were kept under diffuse light. Exposure to ordinary light accelerated the oxidation. Therefore hexacyanoferrate(II) although not extracted, might affect the determination of hexacyanoferrate—(III) by the proposed method. Thorium(IV) ions were therefore added to the aqueous solution to precipitate the hexacyanoferrate(II) and allow the normal extraction of hexacyanoferrate(III). In experiments with up to 20000 μg of hexacyanoferrate(II), no interference was observed in the determination of 20 μg of hexacyanoferrate(III).

Precision study. Twenty independent determinations with 20 μg of hexacyanoferrate(III) in the aqueous phase were carried out to evaluate the precision of the method. The standard deviation calculated from the absorbances obtained was 0.0011, corresponding to 0.09 μg at the 95 % confidence level.

Interference study. The influence of different amounts of other anions was studied by performing experiments with 20 μg of hexacyanoferrate(III). The following ions did not interfere within the limits of the precision study when present in the amount given in parentheses: acetate, SO_4^{2-} (10000 μg); Br^-, I^-, BrO_3^-, AsO_4^{3-}, HPO_4^{2-} (4000 μg); MnO_4^-, SCN^-, ClO_4^- (3000 μg); ReO_4^{2-} (1500 μg). The tolerance for Cl^- and NO_3^- (3000 μg), IO_4^- (2000 μg), ClO_3^- and MoO_4^{2-} (1000 μg) was within ± 1.5 %. With MnO_4^-, the result reported was obtained after dropwise addition of 2 % sodium thiocyanate to give complete decolorization.

The following cations did not interfere within the limits of the precision study: Mg^{2+}, Ca^{2+}, Sr^{2+}, Pb^{2+}(2000 μg); Ba^{2+}, Cr^{3+}, Fe^{3+}, Al^{3+} (1000 μg).

Procedure. To an aliquot of the sample solution (not more than 3.00 ml) in a glass-stoppered test tube add a 2 % solution of thorium sulfate carefully and dropwise until precipitation is complete. Add 0.1 ml of 0.5 M sulfuric acid and 0.5 ml of 10 % triphenyl-n-propyl phosphonium chloride solution followed by 1.5 ml of pentan-1-ol. Shake vigorously for 30 s, centrifuge, and

transfer the organic layer to a 5- ml volumetric flask with an extraction pipet [5]. Repeat the extraction with 0.8 ml of solvent after adding 0.1 ml of 10 % phosphonium chloride solution. Rinse with about 0.8 ml of solvent and add to the total organic extract 0.1 ml of 5 % iron(II) sulfate solution in 0.05 M sulfuric acid. Make up to the mark with ethylene glycol. Keep in the dark. Read the absorbance at 720 nm. If cyanoferrate(II) is known to be absent, omit the addition of thorium sulfate.

Discussion

The main feature of this method is the marked difference in behavior between hexacyanoferrate(II) and (III) which allows the quantitative separation of small amounts of the latter from large amounts of the former.

Financial support from Fundacão de Amparo à Pesquisa do Estado de São Paulo, FAPESP, and The Ford Foundation is acknowledged. One of the authors (R.L.O.) is indebted to these institutions for fellowships and to Instituto Adolpho Lutz, Secretaria da Saúde Pública e Assistência Social, São Paulo, for leave of absence.

REFERENCES

1 Part V. P. Senise and L. R. M. Pitombo, Talanta, 11 (1964) 1185.
2 A. I. Kuper, Gigiena i Sanit., 12 (1947) 11; Chem. Abstr., 43 (1949) 1506 i.
3 N. S. Frumina, Inst. Geokhim. i Anal. Khim., 11 (1960) 120; Chem. Abstr., 55 (1961) 8154 d.
4 A. I. Vogel, Quantitative Inorganic Analysis, Longmans and Green, London, 3rd edn., 1961, p. 371.
5 J. K. Carlton, Anal. Chem., 22 (1950) 1072.

Analytica Chimica Acta, 81 (1976) 423—427

Short communication

GEL FILTRATION OF METHYL-SUBSTITUTED POLYNUCLEAR AROMATIC HYDROCARBONS*

M. E. SNOOK

Tobacco Laboratory, ARS, USDA, Athens, Georgia 30604 (U.S.A.)

(Received 9th May 1975)

Considerable interest has been shown recently in gel filtration chromatography (g.f.c) to isolate polynuclear aromatic hydrocarbons (PAH) [1—11] from such sources as polluted water, petroleum, coal tars, and cigarette smoke condensate; the PAH were separated effectively from aliphatic hydrocarbons and other interfering materials [1—8]. The separation and order of elution of individual PAH depended on the solvent and type of gel used. For example, with gels of the Bio-Beads SX-series, acetone [3, 9], methyl ethyl ketone [9], or benzene [11] eluted the PAH in order of increasing ring number, contrary to the principles of gel permeation chromatography. However, with tetrahydrofuran (THF) as the eluting solvent [6, 9] the larger molecules were eluted first, as expected in gel permeation chromatography. Neither methanol [9] nor acetonitrile [12] separates individual PAH on Bio-Beads.

Generally, PAH standards are used to calibrate the gels to determine the start of PAH elution, but with Bio-Beads SX-12 the use of unsubstituted-PAH standards can lead to erroneous results, because methyl-substituted PAH are eluted before their parent PAH. Consequently, quantitative isolation of a total PAH fraction would not be achieved. More significantly, methyl groups appear to increase the carcinogenicity of some PAH [13], and the total biological activity of such a fraction would be missed. Thus, the quantitative recovery of methyl-substituted PAH is important in all analytical methods for the isolation and identification of PAH in the environment.

Experimental

Gel filtration chromatography. Four 1.25 × 109-cm Chromatronix LC columns were connected in series and packed with Bio-Beads SX-12 (Bio-Rad Laboratories, Richmond, California) in benzene. The total length of the wet gel bed was 400 cm (about 200 g of dry beads).

About 0.1—0.5 mg of each PAH standard (Table 1), dissolved in 1 ml of

*Presented in part at the 26th Southeastern Regional Meeting of ACS, October, 1974, Norfolk, Virginia.

TABLE 1

Gel filtration elution of standard PAH

PAH	Percent distribution of PAH[a]													
	Fraction number													
	36	37	38	39	40	41	42	43	44	45	46	47	48	49
2,3,6-Trimethylnaphthalene	3.1	21.9	35.9	31.7	6.4	0.9								
2,6-Dimethylnaphthalene		11.7	45.3	30.0	12.8	0.3								
1,4-Dimethylnaphthalene		0.1	10.1	43.3	29.1	13.3	3.9	0.3						
2-Ethylnaphthalene	1.7	26.1	50.0	17.8	4.3	0.1								
1-Methylnaphthalene				23.3	32.7	27.9	15.5	0.6						
Naphthalene				2.3	14.2	35.6	44.5	3.4						
Acenaphthene					4.8	65.3	27.1	2.2	0.7					
Acenaphthylene					0.1	24.2	51.2	14.5	9.9					
2-Methylfluorene			7.2	53.8	31.3	6.8	0.8							
Fluorene				11.8	35.3	35.3	15.6	2.1						
3,6-Dimethylphenanthrene	0.2	4.4	19.5	42.9	21.8	8.6	2.3	0.4						
2-Methylphenanthrene			1.2	17.3	21.9	29.7	17.1	5.3	0.5					
Phenanthrene				0.4	5.7	21.5	35.6	27.0	8.3	1.5				
1-Methylpyrene					1.6	8.3	23.1	31.5	19.9	9.9	5.0	0.7		
Pyrene						0.5	6.1	20.3	27.4	26.4	14.5	4.9		
3-Methylchrysene				11.5	24.9	31.3	22.9	8.9	0.8					
Chrysene					1.9	12.0	29.8	34.1	16.6	5.1				
Benzo(a)pyrene								1.2	10.7	26.2	35.7	20.2	5.9	
Dibenz(a,h)pyrene									4.0	10.5	30.0	38.5	14.6	2.4

[a]Based on total g.c. peak area count of each PAH, assuming unitary detector response.

benzene, was placed on the columns with a 1.0-ml loop injection valve. Benzene was pumped (Chromatronix CMP-3 pump) at a constant flow of 120 ml h^{-1} ; 8-ml fractions were collected, evaporated to dryness with a stream of dry nitrogen and analyzed by gas chromatography (g.c.). The percentage distribution of individual PAH calculated for consecutive g.f.c. fractions (Table 1) was based on total g.c. peak area counts. A PAH-containing neutral subfraction (F-20) of cigarette smoke condensate (CSC) was obtained as described previously [12]. A sample (0.5 g) of F-20 was separated by the above g.f.c. system and analyzed by g.c., u.v. spectroscopy, and g.c.-mass spectrometric methods (Table 2).

Gas chromatography. A Hewlett-Packard Model 5750 gas chromatograph was used with a 15-ft., × 0.125-in. o.d. stainless steel column packed with 5 % Dexsil 300 GC on 100—120 mesh Chromosorb W-AW (temperature program: 100—325 °C at 8° min^{-1}; He flow, 48 ml min^{-1}; injector, 290 °C; flame detector, 350 °C). The percentage calculations of the selected PAH found were based on g.c. peak areas of volatiles, determined by a Varian Model 485 electronic integrator.

Results and discussion

Table 1 shows that in this Bio-Beads SX-12/benzene system the order of elution of the methyl-substituted naphthalenes was trimethyl-, dimethyl-,

TABLE 2

Gel filtration elution of selected PAH in a cigarette smoke fraction

	Percent of PAH found[a]									
	Fraction number									
PAH	38[b]	39[b]	40[c]	41[c]	42[b]	43[c]	44[b]	45[c]	46[c]	47[b]
1-Methylnaphthalene	1.7	1.3	4.6	6.5	3.9	1.0				
2-Methylnaphthalene	1.2	2.5	5.8	7.0	2.0	0.3				
Naphthalene		1.1	1.8	3.6	6.9	1.1				
Acenaphthene		0.4	0.6	1.3	1.6	0.9	0.2			
Acenaphthylene				1.5	3.7	3.6	4.0	0.3		
2-Methylfluorene	2.0	4.6	5.1	3.1	1.0	0.6				
1-+4-Methylfluorene	1.0	3.4	3.9	2.4	0.9	0.5				
Fluorene	0.6	1.6	5.4	8.5	10.1	3.8	0.8			
1-Methylphenanthrene		1.0	1.5	2.4	6.1	3.3	0.8			
Phenanthrene			0.8	2.6	17.3	29.4	15.5	6.8		
2-Methylpyrene		0.7	0.8	0.9	1.6	2.6	3.6	2.7	1.0	
Pyrene					1.1	2.9	14.4	21.4	33.5	18.3
Other volatiles	93.5	83.4	69.7	39.8	43.8	50.0	40.7	68.8	65.5	81.7

[a]Based on total peak area.count of g.c. volatiles, assuming unitary detector response.
[b]Identified by g.c. parameters.
[c]Identified by g.c., u.v. spectra, and g.c.—m.s. methods.

and monomethyl-naphthalene. The elution trends of methyl-substituted fluorenes, phenanthrenes, pyrenes, and chrysenes are the same. The methyl effect on elution apparently holds, regardless of ring size or ring configuration. An earlier report noted that methyl- and ethyl-substituted benzene, naphthalene, and anthracene eluted before the parent PAH [6]. However, this was observed with Bio-Beads SX-8 in THF, where the parent PAH eluted in order of decreasing ring number. Such elution, which is consistent with theory, is the reverse of that from the SX-12/benzene system.

Elution of the parent PAH in order of increasing ring number indicates that an adsorption mechanism, possibly involving the formation of π-complexes between the PAH and the benzene rings of the polystyrene gel, may be taking place. The addition of three methyl groups to naphthalene increases its longest dimension [2] from 10.1 Å to 11.5 Å and decreases its elution volume. However, a similar increase in molecular dimension of 10.1 Å to 11.0 Å for naphthalene compared to phenanthrene does not result in a shortened elution volume through dimensional increase, but a slightly greater elution volume from ring number increase (Table 1). This suggests that the methyl groups are not causing a greater retention—permeation effect because of increased molecular size, but are interfering with an adsorption mechanism between the PAH and the polystyrene gel, resulting in earlier elution of the methylated PAH. This concept is further supported by the fact that chrysene elutes before pyrene (Table 1). The relatively localized and dense π-electron system of pyrene apparently interacts more strongly with the gel than the relatively extended π-system of chrysene. The early elution of the saturated acenaphthene relative to the unsaturated, electron-richer acenaphthylene also agrees with this adsorption mechanism.

This methyl effect was also observed for a PAH-enriched fraction of cigarette smoke condensate (CSC), which was separated by g.f.c. The contents of selected, easily quantified parent and monomethyl-PAH in the separated g.f.c. fractions are shown in Table 2. The data confirmed that methyl-PAH eluted before the parent compounds, even in such a highly complex mixture as that isolated from CSC. Dimethyl- and trimethyl-PAH eluted before the monomethyl compounds, but they appeared as shoulders on g.c. peaks or in combination with other PAH in a peak, so that only their identities, and not their proportions, could be determined. These results have been applied in the preparation of a highly-enriched PAH fraction of CSC to obtain more definitive bioassay results.

REFERENCES

1 J. G. Kendrickson and J. C. Moore, J. Polym. Sci., 4 (1966) 167.
2 T. Edstrom and B. A. Petro, J. Polym. Sci., C21 (1968) 171.
3 R. L. Stedman, R. L. Miller, L. Lakritz and W. J. Chamberlain, Chem. Ind., (1968) 394.
4 H. H. Oelert, D. R. Latham and W. E. Haines, in K. H. Altgelt and L. Segal, (Eds.), Proc. ACS Symp. on Gel Permeation Chromatography, Houston, Texas., 1970, Dekker, New York, (1971), p. 549.

5 H. J. Klimisch and L. Stadler, J. Chromatogr., 67 (1972) 1975.
6 H. J. Klimisch and D. Reese, J. Chromatogr., 67 (1972) 299.
7 H. J. Coleman, J. E. Dooley, D. E. Hirsch and C. J. Thompson, Anal Chem., 45 (1973) 1724.
8 H. J. Klimisch, Z. Anal. Chem., 264 (1973) 275.
9 H. J. Klimisch and D. Reese, J. Chromatogr., 80 (1973) 266.
10 M. Popl, M. Stejskal and J. Mostecky, Anal. Chem., 46 (1974) 1581.
11 M. E. Snook, W. J. Chamberlain, R. F. Severson and O. T. Chortyk, Anal. Chem., 47 (1975) 1155.
12 A. P. Swain, J. E. Cooper, R. L. Stedman and F. G. Bock, Beitr. Tabakforsch., 5 (1969) 97.
13 D. Hoffmann, W. E. Bondinell and E. L. Wynder, Science, 183 (1974) 215.

Analytica Chimica Acta, 81 (1976) 429—431

Short communication

ANALYSIS OF ORGANIC AMINES AND ACIDS FOR WATER

M. CONCEIÇÃO P. LIMA and M. SPIRO

Department of Chemistry, Imperial College of Science and Technology, London SW7 2AY (England)

(Received 2nd August 1975)

The purity of non-aqueous solvents used in physicochemical research is best assessed by specific analyses for the most likely contaminants [1], of which the most pervasive are electrolytes (easily monitored by conductivity) and water. The basic principles of the Karl Fischer method are well known [2], but details of the appropriate procedure must be defined carefully, especially when very small water contents, often found in purified non-aqueous solvents, are being determined. The situation for 1,2-diaminoethane and acetic acid is described here; the results obtained with Karl Fischer reagent containing 2-methoxyethanol [3], were similar to those obtained with solutions containing methanol. End-points were detected electrochemically by the dead-stop method.

Amines such as 1,2-diaminoethane cannot be titrated directly nor in methanolic solution [2(a)]; they can be titrated satisfactorily if first dissolved in an excess of anhydrous acetic acid. Since no information concerning the excess necessary or other experimental details were available, several series of titrations were carried out. The points on line A in Fig. 1 show the volumes of the reagent required to titrate 50 cm^3 of glacial acetic acid containing different known volumes of distilled 1,2-diaminoethane. A fresh sample of acetic acid was used for each point on line A; the intercept represents the water content of the acetic acid (0.27 cm^3 of reagent/50 cm^3, i.e., 0.0024 wt % H_2O); the slope represents the water content of the amine (0.16 cm^3 reagent cm^{-3}, i.e. 0.083 wt % H_2O). A different set of titrations gave the points on line B in Fig. 1; a mixture of 50 cm^3 of acetic acid and 2 cm^3 of 1,2-diaminoethane was titrated with the reagent and then used as solvent, further aliquots of 1,2-diaminoethane being added and titrated in turn. Line B passes through the origin and possesses the same slope as line A; this rules out the possibility that the extra reagent required for subsequent samples of 1,2-diaminoethane was due to water formed by the reaction

$$CH_3COOH + H_2N(CH_2)_2NH_2 \rightleftharpoons CH_3CONH(CH_2)_2NH_2 + H_2O \qquad (1)$$

Two tests were made to check that side-reactions such as (1) were absent. A mixture of 50 cm^3 of glacial acetic acid and 2 cm^3 of 1,2-diamino-ethane was left to stand for 2.25 h before being titrated with Karl Fischer

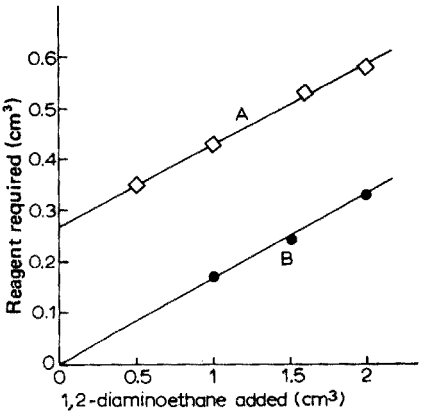

Fig. 1. Volumes of Karl Fischer reagent (2.15 $cm^3 \equiv 10$ mg H_2O) required to titrate various amounts of distilled 1,2-diaminoethane in 50 cm^3 of glacial acetic acid.

reagent. The resulting titration value was only 5 % greater than normal. In another experiment, 50 cm^3 of acetic acid and 2 cm^3 of 1,2-diaminoethane were mixed, titrated with the reagent to the end-point, and allowed to stand for 1 h; ca. 20 % of the previous titre was then required to reach the end-point again. The extra water may have arisen from esterification between the acetic acid and the alcohol in the reagent. The titrations should therefore be carried out fairly quickly.

Another series of titrations of type A was carried out with an older supply of glacial acetic acid which had absorbed water, and with undistilled 1,2-diaminoethane. The intercept (0.82 cm^3 reagent/50 cm^3, i.e. 0.0074 wt % H_2O) and slope (1.03 cm^3 reagent cm^{-3}, i.e. 0.54 wt % H_2O) were greater than in Fig. 1. Some larger volumes of 1,2-diaminoethane than in Fig. 1. were used; the point corresponding to 6 cm^3 of 1,2-diaminoethane fell well above the line obtained for 2—5 cm^3. With 10 cm^3 of 1,2-diaminoethane no end-point was obtained, even after 20 cm^3 of the reagent had been added. With large volumes of the amine the solution became very hot and amide was probably formed according to eqn. (1). A similar phenomenon occurred when the experiment was scaled down: a mixture of 10 cm^3 of acetic acid + 2 cm^3 of 1,2-diaminoethane also became hot, and a white solid was formed. It would appear that the excess of acetic acid to 1,2-diaminoethane must be at least 10:1 (v/v) to avoid formation of water by eqn. (1).

The large excess of glacial acetic acid required contains more water than an aliquot of distilled 1,2-diaminoethane; attempts were therefore made to substitute smaller amounts of stronger acids. These all proved unsatisfactory: sulphuric acid caused charring, picric acid in methanol produced a precipitate with the reagent, and phosphoric acid in methanol gave a precipitate on the addition of 1,2-diaminoethane.

To check the intercepts of type A titration plots, attempts were made to

analyse directly the acetic acid employed, but glacial acetic acid, by itself, could not be titrated with the reagent; the addition of just one drop of reagent immediately produced a small stable current indicative of zero water content, although the acid was known to contain water. Nor could the acid be diluted with methanol and then titrated; Mitchell and Smith [2(b)] who included acetic acid in a list of organic materials to be analysed in this way, mentioned the existence of a slow esterification reaction, but regarded the interference by the water produced as negligible when the titration was not prolonged. Even very rapid addition of Karl Fischer reagent led in our experiments to a water content that was too high by ca. 25 %; with slow addition, it became impossible to ascertain the end-point. It is essential for the esterification reaction to be inhibited by adding a base such as 1,2-diaminoethane or pyridine [4]. With a mixture of 10 cm^3 of methanol + 10 cm^3 of pyridine as solvent for 50 cm^3 of acetic acid, reproducible and stable end-points were obtained; the water contents agreed within 1.6 % with those derived from the intercepts of plots of type A and were therefore independent of the base employed. Mitchell and Smith [2(b)] advocated the addition of pyridine to the methanol when only traces of water are present in the acid, but it appears to be vital even with rather larger concentrations of water.

Experimental

1,2-Diaminoethane (Jefferson Chemicals U.K.) was distilled over calcium hydride in a stream of nitrogen. Glacial acetic acid (AnalaR), Karl Fischer reagent and improved [3] reagent, and the standard solution of water in methanol were supplied by B.D.H. Ltd.

Dead-stop end-points were obtained with platinum foil electrodes, 0.5 cm^2 in area and 5 mm apart, polarized by a Farnell L30B power supply and a voltage divider, and detected on a shunted ammeter (50 μA). The solution was stirred during titration, and moisture kept out, by passing very dry nitrogen generated by electrically heating liquid nitrogen in a dewar vessel at a controlled rate [5].

We thank the Instituto de Alta Cultura, Lisbon, for the award of an overseas grant to M.C.P.L.

REFERENCES

1 M. Carmo Santos and M. Spiro, J. Phys. Chem., 76 (1972) 712.
2 J. Mitchell, Jr. and D. M. Smith, Aquametry, Interscience, New York, 1948, (a) pp. 126—128, (b) pp. 104—106.
3 E. D. Peters and J. L. Jungnickel, Anal. Chem., 27 (1955) 450.
4 E. G. Almy, W. C. Griffin and C. S. Wilcox, Ind. Eng. Chem. Anal. Ed., 12 (1940) 392.
5 J. H. Robertson, J. Sci. Instrum., 40 (1963) 506.

Analytica Chimica Acta, 81 (1976) 433—436

Short communication

CONDUCTOMETRIC TITRATIONS OF ORGANIC ACIDS IN 2-ETHOXYETHANOL

BARBARA J. BARKER, GARY A. SCHWARTZ and MONICA E. NAINES
Department of Chemistry, Hope College, Holland, Michigan 49423 (U.S.A.)
(Received 9th June 1975)

Alcohols have received much attention as media for acid-base determinations, but there have been few reports [1] of the use of 2-ethoxyethanol (cellosolve), although the cellosolves are excellent solvents for organic compounds.

Potentiometric end-points are used frequently for acid—base titrations, but are not well-defined in some solvents, such as the cellosolves. These limitations can be overcome through conductometric titrations which are often used successfully in analyses for relatively weak acids and bases. Since studies of conductometric titrations in 2-ethoxyethanol have not been reported, the present study was undertaken to evaluate the usefulness of such methods.

Experimental

Reagents. "Distilled-in-glass" 2-ethoxyethanol was obtained from Burdick and Jackson Chemical Co. (Muskegon, MI.) Benzoic, *p*-nitrobenzoic, phthalic and salicyclic acids and *p*-phenylphenol (Baker Analyzed reagent); anthranilic and picric acids, *p*-ethoxyphenol, 2,4-dinitrophenol (Eastman chemicals) and barbital (Fisher reagent) were recrystallized from acetone—water. Oxalic (Fisher reagent), succinic (Matheson, Coleman and Bell reagent), adipic (Baker Analyzed reagent), *o*-nitrobenzoic and *p*-hydroxybenzoic acids (Eastman chemicals) were recrystallized from water. *p*-Chlorobenzoic acid and 1,3-diphenylguanidine (Eastman chemicals) were recrystallized from acetone—ether and toluene, respectively. Distilled acetone and deionized water were used in the recrystallizations. The acids and diphenylguanidine were recrystallized several times, ground finely and dried in vacuo before use.

Apparatus and procedures. An RC-18 Industrial Instruments conductivity bridge and Sargent model S-29870 conductance cells were used. The electrodes were adjusted to obtain a cell constant of ca. 0.15 cm^{-1}. Titrations were performed at about 25 °C.

The accurately weighed acid samples, dissolved in 50.0 ml of ethoxyethanol, were titrated with 0.10 M diphenylguanidine, from a 10-ml burette graduated

in 0.05-ml divisions. After each addition of titrant the solutions were stirred and resistance readings (at 1000 Hz) were obtained. The resistance values were verified after further magnetic stirring. Some titrations were performed under nitrogen, but resistances were the same as when nitrogen was not used.

Results and discussion

Both monoprotic and diprotic carboxylic acids and phenols were titrated in ethoxyethanol. Although tetramethyl- and tetrabutylammonium hydroxide and potassium methoxide have been used as titrants in previous conductometric titrations in non- aqueous solvents [2—6], diphenylguanidine was chosen for the present study since it is a conveniently recrystallized, stable, soluble primary standard.

Figures 1 and 2 show the titration curves of the acids investigated. The conductance curves have been displaced both horizontally and vertically in order that typical results for all acids may be presented clearly. Volume corrections were applied to all the conductance data used. The results for duplicate titrations in ethoxyethanol are presented in Table 1; the precision is comparable to that generally obtained from titration of organic acids in non-aqueous solvents [6].

Distinct end-points were obtained for the relatively strong picric acid and 2,4-dinitrophenol (Fig. 1). As expected, replacement of the electron-withdrawing nitro groups with the electron-releasing phenyl and ethoxy groups reduced the strength of the acids. For *p*-phenyl- and *p*-ethoxyphenol there were no differences in slope before and after the end-points. Satisfactory recoveries were obtained for barbital and for benzoic acid and its chloro- and nitro- derivatives; no results were obtained for the weaker anthranilic acid

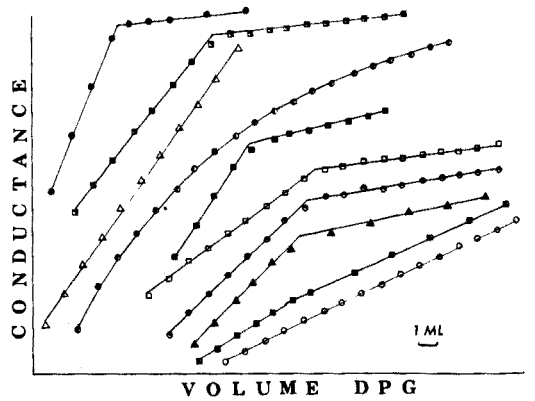

Fig. 1. Conductometric titration curves of organic acids in ethoxyethanol with diphenylguanidine. (●) Picric acid; (▪) 2,4-dinitrophenol; (△) *p*-phenylphenol; (◐) anthranilic acid; (▪) *p*-chlorobenzoic acid; (□) *p*-nitrobenzoic acid; (●) *o*-nitrobenzoic acid; (▲) benzoic acid; (▪) barbital; (○) *p*-ethoxyphenol.

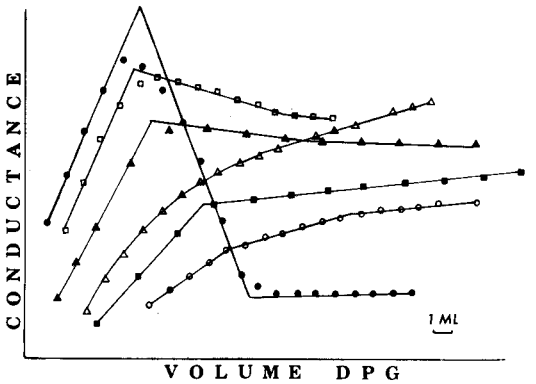

Fig. 2. Conductometric titration curves of organic acids in ethoxyethanol with diphenylguanidine. (●) Oxalic acid; (□) succinic acid; (▲) phthalic acid; (△) *p*-hydroxybenzoic acid; (■) salicylic acid; (○) adipic acid.

TABLE 1

Conductometric titrations of organic acids in ethoxyethanol with diphenylguanidine

Acid	Millimoles taken	% Recovery	Acid	Millimoles taken	% Recovery
Benzoic acid	0.8800	99.3	Picric acid	0.6865	98.2
	1.040	100.1		0.6695	99.0
p-Chlorobenzoic	0.7421	99.0	Barbital	0.6699	101.0
acid	0.6859	100.0		0.4104	99.0
p-Nitrobenzoic	0.9987	100.0	Adipic acid[a]	0.8594	97.0, 97.0
acid	1.004	100.1		0.7588	99.2, 99.1
o-Nitrobenzoic	1.002	99.3	Phthalic acid[a]	0.7301	98.5, 102.0
acid	1.005	98.5		0.6675	99.0, 99.1
2,4-Dinitrophenol	0.9978	99.7			
	0.9994	100.9			

[a]Recoveries determined from each of the two equivalence points.

because of curvature in the titration plot. Benzoic acid could not be determined successfully by conductometric titrations in pyridine, methanol, or dimethylformamide [2].

Several diprotic acids were titrated to determine if multiple end-points could be detected in ethoxyethanol. Two distinct end-points were obtained for oxalic, succinic, and adipic acids (Fig. 2), but recoveries calculated from the graphical end-points were satisfactory only for adipic acid; the calculated recoveries were low for oxalic and succinic acids. Unlike the titration plots in ethoxyethanol, "N-shaped" and "chair-shaped" titration curves were obtained for oxalic, succinic, and adipic acids in pyridine, methanol, tert-butanol, and dimethylformamide [2, 3, 5]. The second equivalence point for phthalic acid was more distinct in tert.-butanol [5] than in ethoxyethanol, but satisfactory recoveries were obtained in ethoxyethanol.

Only one end-point was found for salicylic acid in cellosolve; the results calculated from this point were low. Fairly distinct end-points were obtained from the titrations of salicylic acid in tetramethylguanidine and dimethylformamide [2, 6]. As in other solvents [2, 5], satisfactory recovery was not obtained for the difunctional *p*-hydroxybenzoic acid in ethoxyethanol.

The present investigation has shown that, although there are limitations in the use of 2-ethoxyethanol in conductometric titrations, a variety of organic acids can be determined successfully in this solvent.

Grateful acknowledgement is made to the National Science Foundation for partial support of this investigation, by the award of a Research Participant scholarship to G. A. S.

REFERENCES

1 A. E. Ruehle, Ind. Eng. Chem., Anal. Ed., 10 (1938) 130.
2 N. van Meurs and E. A. M. F. Dahmen, Anal. Chim. Acta, 19 (1958) 64.
3 N. van Meurs and E. A. M. F. Dahmen, Anal. Chim. Acta, 21 (1959) 10.
4 N. van Meurs and E. A. M. F. Dahmen, Anal. Chim. Acta, 21 (1959) 443.
5 L. W. Marple and G. J. Scheppers, Anal. Chem., 38 (1966) 553.
6 M. L. Anderson and R. N. Hammer, Anal. Chem., 40 (1968) 940.

Analytica Chimica Acta, 81 (1976) 437—438

Short communication

IODIMETRIC DETERMINATION OF HYDRAZINE AND HYDROQUINONE WITH THALLIUM(III) SOLUTIONS

D. N. SHARMA, P. D. SHARMA and Y. K. GUPTA
Department of Chemistry, University of Rajasthan, Jaipur (India)
(Received 5th July 1975)

Thallium(III) solutions can be used in titrations of hydrogen peroxide, sulphite, thiosulphate, thiourea, and ascorbic acid, by iodimetric titration of the excess of Tl(III) or by direct titration in presence of *p*-ethoxychrysoidine indicator [1, 2]. This communication extends the range of application to hydrazine and hydroquinone. Both these compounds can be titrated readily with strong oxidants [3], usually in acidic media, but iodimetric titrations are better done in hydrogencarbonate solutions [3], which are also appropriate for thallium(III) titrations.

Experimental

Reagents. Thallium(III) perchlorate or sulphate solution (0.1 M) was prepared and standardized as described [1]. Aqueous hydrazine sulphate (B.D.H. AnalaR) solutions were prepared by direct weighing. Hydroquinone solutions were prepared in 1 % sulphuric acid by warming; after 24 h, the clear solution was standardized by cerium(IV) titration [4].

Procedure. To the sample solution, add 15—20 ml of a saturated solution of sodium hydrogencarbonate, some fresh starch solution and 5 ml of 0.05 M potassium iodide solution. Titrate with 0.1 M thallium(III) solution to the blue end-point. Shake vigorously and, near the end-point, add the titrant in small amounts at intervals of 10—15 s.

Hydrazine (6.50—45.5 mg) and hydroquinone (10.1—40.5 mg) could be titrated with errors which did not exceed 0.2 %.

Discussion

The reactions of thallium(III) with hydrazine [4] and hydroquinone [5] are fast, but not instantaneous. However, when iodide is present, iodine is instantaneously liberated by thallium(III), and oxidizes the hydrazine or hydroquinone in hydrogencarbonate medium. Hydrazine is oxidized quantitatively to nitrogen by iodine [3]. The oxidation of hydroquinone is an equilibrium reaction [3] but goes to completion under the above

conditions [4]. In these reactions, thallium(I) iodide is precipitated and takes up iodine to form readily dissociated $TlI \cdot I_2$ [5]. Vigorous swirling is therefore necessary for complete reaction during the titrations. The advantage of using thallium(III) is that its solutions are stable to light and atmospheric oxygen for months.

REFERENCES

1 P. D. Sharma and Y. K. Gupta, Talanta, 20 (1973) 903; 21 (1974) 168.
2 D. Gupta, P. D. Sharma and Y. K. Gupta, Talanta, 22 (1975).
3 See, e.g., I. M. Kolthoff and R. Belcher, Volumetric Analysis, Vol. 3, Interscience, New York, 1957.
4 B. M. Thakuria and Y. K. Gupta, J. Chem. Soc. Dalton (1975).
5 H. G. S. Sengar and Y. K. Gupta, J. Indian Chem. Soc., 43 (1966) 223.

Analytica Chimica Acta, 81 (1976) 439—443

Book reviews

G. F. Kirkbright and M. Sargent, *Atomic Absorption and Fluorescence Spectroscopy*, Academic Press, London, 1974, pp. ix + 798, £17.00.

During the development of any branch of science, there comes a time when it is necessary to bring together all the important aspects of the subject, to give a comprehensive account of the status quo. For atomic absorption and fluorescence spectroscopy, the time is ripe, and the need is admirably filled by the present text. The very rapid and considerable advances that have been made, especially in the last decade, in this most popular area of analytical chemistry is evidenced by the size of the book. It is, therefore, especially convenient to have these advances collected and rationalized in a single text.

The book begins with a brief discussion of historical aspects, fundamentals, and a comparison of atomic emission, absorption and fluorescence techniques. There follows chapters on spectroscopic theory, atomic absorption and fluorescence measurements, spectral light sources, flames, and non-flame absorption cells. Devices for wavelength selection are dealt with, and there is a detailed description of instrumental aspects. In a number of these sections, there is a great deal of theoretical treatment, sufficient for all but the most specialized spectroscopists. This is clearly presented, and will considerably aid the analytical chemist in his understanding of the basic aspects of atomic spectroscopy.

The practice and applications of the techniques receive their fair share of the text. One chapter deals with wavelength selection, instrumental optimization, calibration, sensitivity, precision and accuracy, as well as sample pretreatment processes. Interference effects are considered in a separate chapter, which is followed by details pertinent to the determination of each element in turn. A typical section gives detail of spectral lines, with appropriate sensitivity and detection limits, notes on analytical conditions, and on particular applications, all fully referenced. The final chapter deals with indirect determinations, isotopic analysis, laser excitation, and flame temperature measurement by a.a.s. and a.f.s. There is a comprehensive subject index, and each chapter is extensively referenced.

There are few criticisms. Perhaps the biggest is the presentation: the book is printed on thick paper, making it unwieldy; and the large type-face and ungenerous margins give the impression of overfilling each page. This may be partly in the interests of economy, but surely a slightly smaller type-face would have brought equal economy with greater aesthetic satisfaction.

Nevertheless, this is a clear, comprehensive, up-to-date account of a.a.s. and a.f.s. which can be recommended unreservedly to all who are concerned in analytical atomic spectroscopy. Although the price is high, it will soon

repay the investment, and will remain the standard reference book on the subject for some years to come.

A. Townshend

Max Pestemer, *Correlation Tables for the Structural Determination of Organic Compounds by Ultraviolet Light Absorptiometry*, Verlag Chemie, Weinheim, 1975, vi + 157 pp., price DM 98,—.

This book contains spectral data (ν_{max}, λ_{max}, and log ϵ values) from the ultraviolet and visible absorption region of ca. 2300 organic compounds. In order to facilitate the use of this information for the recognition of the chromophoric parts of unidentified molecules, the compounds are grouped primarily according to their "unsaturation numbers" (R). Within each group of compounds having the same value of R, the number and kind of hetero-atoms, taken alphabetically, serve as a further basis for subdivision, and finally the compounds within each subdivision are arranged in order of decreasing frequency of their lowest electronic transitions. The effect of this method of ordering is to group together compounds possessing similar chromophoric systems, irrespective of the number and type of saturated aliphatic substituents. As a further aid to rapid retrieval of information from the tables, a structural formula is shown for each of the compounds listed. The selection of examples for inclusion in the tables is reasonably representative of the major classes of organic compounds.

The tables will no doubt serve a useful purpose in the spectroscopic identification of organic compounds, being complementary to existing sources of information on electronic spectra such as Landolt—Bornstein, the DMS UV Atlas, and "Organic Electronic Spectral Data". They are much less comprehensive than the last-named work but this will no doubt prove to be an advantage in certain circumstances, as also will the novel system of ordering. The book is well produced and the price, though high, is considerably less than would have to be paid for a comparable amount of information elsewhere.

D. Leaver

Robert V. Dilts, *Analytical Chemistry, Methods of Separation*, Van Nostrand, New York, 1974, pp. ix + 592, price £7.50.

As the teaching of analytical chemistry moves away from the classical format, and attempts are made to include basic instrumental and chromatographic techniques at an early stage, so the need grows for text books in sympathy with these aims. The present book fulfils this need well, with the

exception of general instrumental methods. It retains the classical concepts of equilibria, and shows how these are applied to acid-base reactions, solubility, and complex formation, and their analytical uses. These concepts are also applied to partition processes (solvent extraction and the various chromatographic processes), this section occupying more than half of the book. A brief chapter on statistics is also included.

Overall, the treatment is clear, accurate and comprehensive. Particularly praiseworthy are the details of useful applications of the techniques described (a feature so often missing from books of this type), the practically and theoretically relevant experiments, and the numerical problems (with answers) at the end of the chapter. The inclusion of descriptions of the single-pan balance, phase-separating paper, pH meters, chromatographic syringes, EDTA equilibria, and masking, as well as all the chromatographic information is also creditable.

Nevertheless, there are several criticisms. The main one concerns the organization of the first chapters. The book begins abruptly with a description of the balance. The next chapter describes what appears at that stage to be a random selection of analytically useful equipment. The third chapter is a curious blend of laboratory operations (gravimetry, titrimetry, extraction and chromatography, operating instructions for one particular pH meter and spectrophotometer) and some theoretical discussion such as precipitation, including that from homogeneous solution, and the theory of light absorption. It later becomes apparent that much of this information is relevant to the practical exercises. How much more logical if the book had begun with an introduction outlining the practice and relevance of analysis, before discussion of detailed aspects, and how much better if the theory and applications preceded the description of the apparatus and procedures. There are a number of other, minor deficiencies, but they do not detract from a text at this level, apart from the absence of redox titrations. There are relatively few typographical errors; typical ones are "flourescence" (p. 358), bacteriocide (p. 437), Purmutit (p. 451), coions (p. 458), cloride (p. 465), and there are just a few oddities, such as the valueless birds-eye views of piles of powders in chapters 8, 9 and 12, "on, and on, and on" (p. 17) and the truism (p. 31) that "cylindrical separating funnels are called cylindrical separating funnels". The text does not deal with instrumentation, other than that concerned with chromatography, and the few items mentioned above.

In summary, this is a well-produced book, which will be useful for students in the initial stages of their undergraduate training.

A. Townshend

Sun-Tak Hwang and Karl Kammermeyer, *Membranes in Separations*, (*Techniques of Chemistry, Volume VII.* Series Editor: Arnold Weissberger.) John Wiley and Sons, New York, 1975, xxii + 559 pp., price £17.50.

This volume is the seventh in a series devoted to the wider concept of techniques in chemistry. With its predecessors being devoted to physical methods of chemistry, organic solvents, photochroism, elucidation of organic structures, electroorganic synthesis and investigations of rates and mechanisms of reactions, respectively, the leader cannot be led into thinking that this latest volume is going to be concerned with separations in the analytical sense. Indeed, only the final chapter of 14 pages is devoted to analytical chemistry per se. Thus, reviewing from the end of the book, this chapter is seen as a brief, somewhat patchy introduction to ion-selective electrodes and gas sensors followed by 50 lines devoted to separations by ultrafiltration, dialysis and electrodialysis. In the reference list the name of a well-known author although correct on the first citation is twice mis-spelt.

The book, however, is not to be cast aside for its limited usefulness and interest to analytical chemists, for its stated purpose "is to provide a unified treatise of all membrane separation processes." The task is tackled in 18 chapters covering classification, fundamentals, transport, diffusion, equilibria, transfer coefficients, membrane preparation, pervaporation, liquid phase separations, electromembrane processes, various applications and engineering aspects. These provide useful discussion on the subject but have a tendency to drift into the review-type approach whereby core information must be sought elsewhere.

The largest single chapter covers the 98 pages devoted to engineering aspects of membrane separation wherein the authors discuss the interplay of materials, equipment and process design. Such considerations together with the chapters on separations in the liquid phase and electromembrane processes occupy two-fifths of the book. The overall treatment gives prominence to the comparatively recent nature of much of the development of membrane technology but with an underlying realization that membrane science has a long history that is scanned in a most interesting prologue in the form of a personal letter by Karl Sollner. Biological membranes are considered to be adequately covered by other books, but the multidisciplinary nature of the science and technology of artificial membranes has left the author with a big enough challenge which despite the shortcomings of the analytical chapter has been valiantly met to produce a book that can be a source of inspiration for further development of the subject.

J. D. R. Thomas

O. I. Mamayer, *Temperature—Salinity Analysis of World Ocean Waters*, Elsevier Scientific Publishing Co., Amsterdam, 1975, x + 374 pp., price Dfl. 105.00.

This book, which is a revised and updated translation of a monograph first published in Russia in 1970, is concerned with the theory and application of the analysis of temperature (T) and salinity (S) data to oceanographic research. Analysis of T—S data has proved an important tool for the identification of water masses and for studying the processes of salinity and heat exchange which occur in them. It is, however, a topic which despite its great value has only received cursory attention in most textbooks of physical oceanography. The present volume which gives a comprehensive account of the subject will be welcomed both by physical oceanographers and by those chemists who are concerned with oceanic processes. Its coverage is well summarized by the chapter headings which include: the equation of state of sea water; fundamentals of the thermodynamics of sea water; the T—S diagram and its properties; analytical theories of T—S curves; method of T—S analysis and waters of the World Ocean. The book is likely to be only of limited value to the average marine chemist, and those who require practical details of the determination of salinity and in situ temperature will be disappointed as measurement of these vital parameters is scarcely mentioned. There is unfortunately no discussion of the general reliability of T and S measurements. Another very curious omission is the page numbers of all the references in the bibliography.

The book is clearly written and well illustrated and measures up to the high standards set by the earlier volumes in the Elsevier Oceanography Series.

J. P. Riley

ANALYTICA CHIMICA ACTA, VOL. 81 (1976)

AUTHOR INDEX

ANALYTICA CHIMICA ACTA, VOL. 81 (1976)

SUBJECT INDEX

EXTRACTION CHROMATOGRAPHY

edited by **T. BRAUN**, Institute of Inorganic and Analytical Chemistry, L. Eötvös University, Budapest, Hungary, and **G. GHERSINI**, Centro Informazioni Studi Esperienze, Segrate-Milano, Italy

JOURNAL OF CHROMATOGRAPHY LIBRARY, Vol. 2

1975. 584 pages. US $54.25/Dfl. 130.00. ISBN 0-444-99878-0

The purpose of this book is to provide analytical chemists and radiochemists, especially those interested in separations, with a broad survey of the role that extraction chromatography can and should play in chemical analysis.

This volume is the result of the collective work of many specialists, each responsible for a chapter in which a definite aspect of column extraction chromatography is thoroughly presented and discussed. Subjects presented include the basic and technical aspects of the method, the organic stationary phases and supports, the separation of elements with particular reference to radiochemical problems, the separation of lanthanides, actinides and fission products, radiotoxicological separations and the preconcentration of trace elements in various materials prior to their determination.

The book should prove invaluable to chemists working in various fields, as well as to students, physicists and research workers in biology and medicine.

CONTENTS: Theoretical aspects of extraction chromatography *(S. Siekierski).* Correlation between extraction chromatography and liquid-liquid extraction *(I. Akaza).* Techniques in column extraction chromatography *(P. Markl, E.R. Schmid).* Stationary phases in extraction chromatography *(G. Ghersini).* Inert supports in column extraction chromatography *(G.S. Katykhin).* Extraction chromatography of metallic and non-metallic ions *(I. Stronski).* Extraction chromatography of actinides *(W. Müller).* Extraction chromatography of lanthanides *(S. Siekierski, I. Fidelis).* Extraction chromatography of fission products *(M. Bonnevie-Svedsen, K. Joon).* Use of extraction chromatography in radiotoxicology *(C. Testa).* Chelating agents as stationary phase in extraction chromatography *(F. Šebesta).* Use of extraction chromatography for trace metal preconcentration and separation *(I.P. Alimarin, T.A. Bolshova).* Use of cellular plastics in extraction chromatography *(T. Braun, A.B. Farag).* Laminar techniques as an aid in planning column extraction chromatographic separations *(G. Ghersini, E. Cerrai).* Bibliography of extraction chromatography *(W. Drent, H. Eschrich).* Author index. Subject index.

ELSEVIER SCIENTIFIC PUBLISHING COMPANY
P.O. Box 211, Amsterdam, The Netherlands

Distributed in the U.S.A. and Canada by:
AMERICAN ELSEVIER PUBLISHING COMPANY, INC.,
52 Vanderbilt Ave., New York, N.Y. 10017
Prices are subject to change without prior notice

1692 E

Developments in Inorganic Nitrogen Chemistry, Volume 2

edited by CHARLES B. COLBURN, *Department of Chemistry, School of Arts and Sciences, Auburn University, Alabama, U.S.A.*

1973. 238 pages. US$41.75/Dfl. 100.00. ISBN 0-444-40962-9

Contents:

Elsevier

P.O. BOX 211

AMSTERDAM - THE NETHERLANDS

A 1097E

(Continued from page 4 of cover)

Printed in The Netherlands

VOL. 81 NO. 2 ANALYTICA CHIMICA ACTA FEBRUARY 1976

CONTENTS

Short communications

(Continued on inside page of cover)